Aus dem

Institut für Prophylaxe und Epidemiologie der Kreislaufkrankheiten (IPEK)

Klinikum der Ludwig-Maximilians-Universität München

The rhythm of the Plaque:
Circadian oscillation in the advanced atherosclerotic lesion

Dissertation

zum Erwerb des Doctor of Philosophy (Ph.D.)

an der Medizinischen Fakultät der

Ludwig-Maximilians-Universität München

vorgelegt von

Celia Borja Almarcha

aus

Algemesí (Spanien)

Jahr

2023

Erstes Gutachten:	Prof. Dr. Dr. med Oliver Soehnlein
Zweites Gutachten:	Prof. Dr. Ralf Zimmer
Drittes Gutachten:	Prof. Dr. Maria del Sagrario Robles Martinez
Viertes Gutachten:	Prof. Dr. Christoph Scheiermann

Dekan:	Prof. Dr. med. Thomas Gudermann

Tag der mündlichen Prüfung: 28.09.2023

Abstract

The organisms show changes at the level of the biological functions performed by different organs throughout the day, with the objective to adapt to the daily changes in the planet and increase their adaptation to the surroundings. These changes can be observed in different organs, which exhibit different degree of variation across the day. Circadian changes can also be detected in the atherosclerotic plaque, which has clear temporal compartmentalization of several biological functions. The oscillation of biological functions which have an important impact in the development of the atherosclerotic plaque or in its stability can be used as pharmacological targets. The possibility of targeting a specific biological process with the aim of reducing the plaque development or increase the plaque stability at its peak of maximum activity could be potentially used for the design of targeted interventional approaches with increased effectivity. Furthermore, due to the facts that different organs and tissues can be differentially influenced by the circadian rhythms opens the possibility of targeting a process in its peak in the atherosclerotic plaque, with the aim to limit the impact of the treatment in the rest of the organism and therefore reducing the side effects.

Here, we studied the oscillation of different biological processes at the transcriptome and proteome level, complementing this high-throughput data with histopathology and molecular data in order to create an exhaustive description of the oscillation of biological processes in the plaque of a murine model. Furthermore, we compared the oscillation of the protein-coding genes (PCG) in the atherosclerotic plaque with the oscillatory patterns of 11 additional organs (adrenal gland, colon, ileum, liver, spleen, kidney, muscle, white adipose tissue, heart, lung and aorta) to describe molecular functions that would oscillate in an antiphase manner when comparing the plaque with the rest of the organs. Lastly, we have translated our discoveries to human samples, in an effort to describe therapeutic approaches to be targeted with chronopharmacology.

The fact that this project combines the discovery of new targets and the enhancement of the effectivity of the existing drugs that target atherosclerosis makes it of extreme importance for the clinic management of the atherosclerotic disease.

Table of content

List of figures

Abbreviations

ACTH	Adrenocorticotropic hormone	**ER**	Endoplasmic Reticulum
BCA	Brachiocephalic artery	**ERAD**	Endoplasmic-Reticulum-associated protein degradation
BM	Bone marrow	**FBS**	fetal bovine serum
BM	Bone marrow	**FC/fc**	Fold change
BMAL1	Brain and muscle ARNT-like 1	**FDA**	Food and Drug Administration
BrdU	Bromdesoxyuridin	**FSC**	forward scattered
BSA	bovine serum albumin	**G-CSF**	Granulocyte Colony Stimulating factor
CCL-	C-Cmotif chemokine ligand-	**GM-CSF**	Granulocyte/Macrophage colony stimulating factor
CCR-	C-C chemokine receptor-	**h**	hours
CD	cluster of differentiation	**H&E**	hematoxylin and eosin staining
CLR	C-type lectin receptor	**HBSS**	Hanks' Balanced Salt Solution
CRY	Cryptochrome	**HDL**	High-density lipoprotein
CSF	Colony Stimulating Factor	**HFD**	high fat diet
CVD	Cardiovascular disease	**HIF**	Hypoxia-inducible factors
CXCL-	Chemokine (C-X-C motif) ligand-	**ICAM1**	Intercellular adhesion molecule-1
CXCR-	C-X-C motif chemokine receptor-	**IFN-**	Interferon-
DAMP	Damage-associated molecular pattern	**Ig**	Immunoglobulin
DAPI	4´6-Diamidin-2-phenylindol	**IL-**	Interleukin-
DEG	Differentially expressed gene	**LDL**	Low density lipoprotein
DNA	Deoxyribonucleic acid	**M-CSF**	Macrophage colony-stimulating factor
EC	Endothelial cells	**MAC**	Membrane attack complex
ECM	Extracellular matrix	**MHC**	Major histocompatibility complex
EDTA	Ethylenediaminetetraacetic acid	**mL**	mililiter

MMPs	Matrix metalloproteinases	**SCN**	Suprachiasmatic nucleus
MPTP	Mitochondrial premeability transition pore	**scRNA-seq**	Single-cell RNA Seq
mRNA	messenger RNA	**SMC**	Smooth muscle cell
mTOR	Mammalian target of rapamycin	**SSC**	Side scattered
NF-kB	Nuclear factor-kappa B	**T eff**	Effector T cells
NLR	NOD-like receptor	**TG**	triglycerides
°C	Degree Celsius	**TGF-β**	Transforming growth factor beta
oxLDL	oxidized LDL	**Th**	Helper T cells
p.adj value	P adjusted value	**TLRs**	Toll-like receptors
PAMP	pathogen-associated molecular pattern	**TNF**	Tumor necrosis factor
PBS	Phosphate-buffered saline	**Treg**	Regulatory T cells
PCGs	Protein-coding genes	**TUNEL**	Terminal deoxynucleotidyl transferase dUTP nick end labeling
PCR	Polymerase chain reaction	**VCAM1**	Vascular cell adhesion molecule 1
PER	Period circadian protein	**VEGFs**	Vascular endothelial growth factors
PFA	paraformaldehyd	**VLDL**	Very-low density lipoprotein
PRR	Pattern recognition receptor	**VSMC**	Vascular smooth muscle cell
PSEA	Phase set enrichment analysis	**W**	Weeks
PSGL-1	P-selectin glycoprotein ligand-1	**WAT**	White adipose tissue
RNA	Ribonucleic acid	**ZT**	Zeitgeber time
RNS	Reactive nitrogen species	**μL**	microliter
ROR	Retinoid-related orphan receptor	**scRNA-seq**	Single-cell RNA Seq
ROS	reactive oxygen species	**°C**	Degree Celsius
rpm	Revolutions per minute		
RPMI	Roswell Park Memorial Institute		
rRNA	Ribosomic RNA		

1.Introduction

1.1 Atherosclerosis

1.1.1 Definition and importance in healthcare

Atherosclerosis is the main cause of cardiovascular events in industrialized countries. Atherosclerotic cardiovascular disease is the cause of ischemic heart disease and ischemic stroke, which are the leading causes of death in the world, causing more than 54 million deaths in 2013[1].

Even though the disease can be developing for ages without showing any symptoms, advanced lesions can stop the blood flow, creating ischemia in the tissues. Furthermore, smaller lesions that don´t impede the blood flow can break and detach from the vessel wall, creating a thrombus and blocking the supply of blood to the organs, which are depleted of oxygen and nutrients.

In the last decades, we have seen a strong decline in the mortality rates due to the causes of atherosclerosis because of better access to healthcare[2], but there is an increase prevalence and incidence of atherosclerosis worldwide[3,4].

The fact that heart attack is the leading cause of death worldwide makes the study of its causes an extremely important issue due to the costs for the health system, the mortality associated and the high probability of developing chronic sequelae, as heart failure or cerebrovascular disease. The study of atherosclerosis development, which is the primary cause of heart attack, as well as the factors that cause unstable atherosclerosis lesions, are of vital importance to understand how to minimise these fatalities, as well as being able to provide efficient solutions that minimise treatment costs[1].

Despite the number of deaths that atherosclerosis causes every year world-wide, there is still not definitive treatment available that allows the disappearance of the disease and the actual treatments can only target side-effects as stabilising the plaque or reduce the rate of enlargement, which makes the establishment of new treatments an imperious necessity.

1.1.2 Plaque development

The atherosclerosis disease starts in patients with high concentration of cholesterol in plasma with the accumulation low-density lipoproteins (LDL) in the wall of medium and large arteries[5].

Arteries are composed by three different layers, from inner to outer: the tunica intima, the tunica media and the adventitia (**Figure** *1*). The inner layer, which is in direct contact with the blood, is also called intima, and it is formed by a monolayer of endothelial cells. The medium layer is formed by smooth muscle cells and elastic fibres and it´s the responsible one for the contraction and relaxation of the arteries. The outer layer is composed by fibrotic connective tissue.
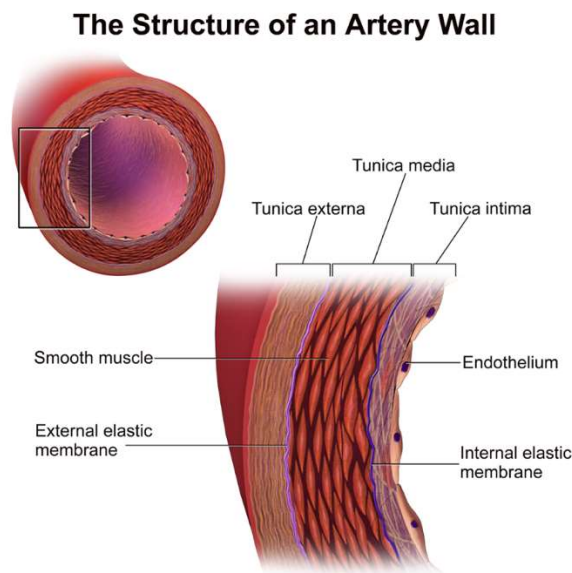
Figure 1. Structure of a large arterial wall (from Blausen.com staff (2014). "Medical gallery of Blausen Medical 2014". WikiJournal of Medicine).

The disease starts with the accumulation of LDL in the intima layer, which is facilitated by the activation of the endothelial cells that form the intima. These lipoproteins are in charge of transporting cholesterol to cells, but due to its small size, the LDL will extravasate from the blood circulation and accumulate in the intima[6]. This accumulation predominantly happens in regions where the blood flow is disturbed, as can be in bifurcations or curved areas. The disturbed blood flow causes shear stress on endothelial cells, which will change their transcriptome and start expressing receptors and adhesion molecules to recruit inflammatory cells to the intima. This change of expression, which turns the endothelial cells into proinflammatory and procoagulant, it´s commonly referred as activation of endothelial cells. The endothelium starts expressing adhesion molecules, as E-selectin and P-selectin, intercellular adhesion molecule-1 (ICAM1) and vascular cell adhesion molecule-1 (VCAM1)[7].

The different receptors and adhesion molecules will attract leukocytes, lymphocytes, platelets but also cytokines from the blood flow. This cellular migration goes along with the increased permeability of the endothelium, that allows the accumulation of more lipids in the intima layer[8]. These lipoproteins contribute to the increase of the inflammation process, enhancing the recruitment of other immune cells. Besides, lipoproteins are immobilized by extracellular matrix proteins, as proteoglycans and undergo chemical modifications, as glycation or oxidation, altering the composition of the lipoproteins[9].

1.1.2.1 Key cells in atherosclerosis development

Both leukocytes and stromal cells have critical roles in the development of the atherosclerotic plaque and the crosstalk between different populations are going to modulate the development of the plaque.

1.1.2.1.1 Immune cells

Several cellular types of the innate and adaptive immune system contribute differently to the atherosclerotic disease.

Monocytes are the most abundantly recruited leucocytes. They are attracted to the inflammatory site by the chemokine CCL5 and CCL2, which are ligands of the receptors CCR1, CCR5 and CCR2, abundantly expressed in monocytes[10]. Monocytes express O-glycosylated carbohydrate ligands (such as P-selectin glycoprotein ligand-1, PSGL-1) on their surfaces, which will interact with P-selectin from the endothelium, capturing the monocyte. After this first interaction, the monocyte will firmly anchor to the endothelium by CCL2 and IL-8 and the extravasation through the intima will be performed by the integrin lymphocyte function-associated antigen-1 (LFA-1), macrophage-1-antigen (Mac-1) and ICAM1 and ICAM2[7]. LFA-1 acts as a receptor of ICAM1 and ICAM2, which are abundantly expressed by the endothelium, while Mac-1 is necessary for the crawling and the extravasation[11].

Once migrated into the intima, monocytes differentiate into macrophages, a process that it´s initiated as a response to the macrophage-colony stimulating factor (M-CSF) and granulocyte-macrophage colony stimulating factor (GM-CSF), which are produced by the activated endothelial cells to keep the proinflammatory stimuli[12]. Macrophages are traditionally classified into M1 and M2 subsets. M1 macrophages (or also Ly6^{hi}) are a pro-inflammatory group, situated in areas of the plaque with high lipid content while M2 subset (Ly6^{lo}) is more associated with a more resolutive and less inflammatory character, placed in less fatty areas. The stimuli that will differentiate a monocyte into a M1 or M2 macrophage are also different; while M1 macrophages need the intervention of IFNγ, M2 macrophages are the product of the

differentiation started by IL-4 or IL-13[13]. Nevertheless, the heterogeneity of the macrophages in the plaque suggests that this classification is too rigid to include all the subsets of macrophages[14], and recent published studies describe different and new subsets[15,16]. Regardless of the subtype, the maximum reduction of atherosclerotic lesion is achieved when the recruitment of the both types into the plaque is blocked[10].

Besides extravasation from the blood, the origin of the plaque macrophages can also be because of the proliferation of plaque macrophages. Recent studies show that the proliferation of the plaque macrophages can be orchestrated by the activation of type 1 scavenger receptor class A (MSR1). The importance of the proliferation in the total amount of plaque macrophages is very important in advanced lesions[17].

After differentiation, macrophages start expressing different scavenger receptors, that mediate the phagocytosis of lipoproteins that are accumulated in the intima. Scavenger receptors are a family of transmembrane proteins that mediate the uptake of lipoproteins and also modified lipoproteins[18]. In addition to scavenger receptors, macrophages express other receptors that internalise lipoproteins, as LDLR[19], but scavenger receptors are not affected by the negative feedback loop activated by the high concentration of cholesterol in the cytoplasm of the cell, which gives them a more deciding role in the fate of the macrophage[12]. In addition to these receptors, macrophages can also uptake cholesterol in a uncontrolled way through pinocytosis[20].

The uptake of lipids through different means increases the accumulation of intracellular cholesterol and oxidized lipids, which accumulate into big vesicles in the cytoplasm. These lipid-loaded macrophages don´t go out of the atherosclerotic plaque after having cleared lipids, instead, they stay in the intima layer. This lack of immigration from the plaque has been correlated with the accumulation of oxidized LDL (oxLDL) in the cell[21], which also causes endoplasmic reticulum (ER) stress[22]. The prolonged ER stress will reduce the survival signalling of the cell and increase the pro-apoptotic signals. Furthermore, as result of the ER stress signalling, the foam cells will produce pro-inflammatory pathways, contributing to the accumulation of more leukocytes[23]. The dead foam cells will accumulate into the plaque, creating a necrotic core composed by lipids and cellular debris[24].

But not all the biological functions driven by macrophages are pro-atherogenic. The M2 macrophage type produces anti-inflammatory factors (IL-10 and TGF-ß) and has a higher expression of phagocyte receptors. On the contrary to M1 macrophages, which have a higher increased expression of glycolysis, M2 macrophages have a higher activity of fatty acid

oxidation and oxidative phosphorylation, which makes lipids to be their main source of energy. Furthermore, M2 macrophages have effective efferocytosis and cholesterol handling, which keeps them from turning pro-apoptotic and pro-inflammatory. Lastly, M2 macrophages also promote tissue repair by synthesizing several extracellular matrix proteins (collagen type VI, fibronectin)[25].

Neutrophils are the most abundant white blood cells in the blood in humans and they extravasate from the circulation into the plaque as a product of the interaction of different cytokines with their ligands (CCR1, CCR2, CCR5 and CXCR2)[26]. Once in the plaque, they contribute to the pro-inflammatory signalling through different processes, such as the release of chemokines that enhance monocyte migration and recruitment[27]. Furthermore, neutrophils release highly toxic compounds when activated. Their immunological powers lies in the granulocytes stored in their cytoplasm, which are full of toxic molecules necessary for fighting pathogens, as myeloperoxidase, azurocidin or α-defensins[28]. Neutrophils also contribute to the plaque formation. They display phagocytosis functions, that cause the accumulation of oxidised lipoproteins in their cytoplasm and lead to their apoptosis, contributing to the formation of the necrotic core. Furthermore, some of the proteins stored in the granulocytes, as α-defensins, increase the radical production of reactive oxygen species (ROS) by different cell types, which is also combined with the ROS production by the neutrophils. The presence of ROS in the plaque increases the accumulation of oxidized lipids[27,29] which will have an impact in the phagocytosis of the macrophages. Lastly, they interact with other leukocytes, as natural killer cells, macrophages, dendritic cells, and T and B lymphocytes, increasing the inflammation[30].

Mast cells are not as abundant as neutrophils or macrophages, but also play an important role in inflammation. Their activation through the Fc epsilonRI (FcεRI) by antigen-specific IgE causes the releasement of histamine, proteases, cytokines and chemotactic factors[31]. This activation has as result the activation of LAT (linker for activation of T-cells), which will cause the histamine release and pro-inflammatory cytokine production[32]. The presence of mast cells in the plaque has been linked to psychological stress[33] and it is associated with the development of unstable plaques[34,35].

Innate cells, as monocytes or neutrophils, sense the molecules that indicate an "invasion" or a "problem" (pathogen-associated molecular patterns, PAMPs or damage associated molecular pattern molecules, DAMPs). This recognition is done by pathogen or pattern-recognition receptors (PRRs). There are different types of PRRs, among which we can

find intracellular nucleotide-binding domain, leucine rich repeat containing receptors (NLRs), Toll-like receptors (TLRs) and C-type lectin receptors (CLRs)[36].

NLRs recognise PAMPs/DAMPs from phagocyted vesicles or from intracellular infections. Some NLRs can activate NF-kB signalling via RIP2, while others activate the inflammasome[37]. In the case of toll-like receptor, after detecting different PAMPs, they activate several signalling pathways that end up with the production of interferon alpha and beta and inflammatory cytokines[38]. All TLRs, except TLR3, activate a MyD88-dependent pathway, which leads to the NF-kB activation and the activation of interferon regulatory factors (IRFs), which are responsible for the expression of Type-I INFs[39]. An alternative pathway is activated only by TLR3 and TLR4. TLR3 is expressed on myeloid dendritic cells and macrophages and mediates the inflammatory response of the innate immune system. TLR4 reacts to the presence of different PAMPs and stimulates the biosynthesis of mediators of inflammation, as TNF-alpha and IL6, required for the activation of the adaptive immune response[40]. Toll-like receptors can also modulate TRIF-dependent programmed cell death, that causes the apoptotic death of different cell types. Besides apoptosis, the activation of TRIF can lead to RIP3-dependent necroptosis and in case the caspase activity is not available[41].

C-type lectin receptors bind carbohydrates or C-type lectin-like domains and some activate NF-kB or TLR to trigger phagocytosis, dendritic cell maturation, chemotaxis, inflammasome activation of cytokine production[42]. Different CLRs as CD209, CLEC7A, CLEC6A have been extensively characterized. CD209 is preferentially expressed in dendritic cells[42], while CLEC7A is a CLR expressed in myeloid cells that triggers direct immune responses, as phagocytosis or production of various cytokines and chemokines (TNF, CXCL2, IL-1b, IL-2, IL-10, IL-12)[43]. CLEC6A (known also as Dectin-2) activation, on the contrary, leads to the production of cytokines as TNF and interleukin 6 (IL-6)[44].

Besides the activation of NF-kB by PRR, this pathway can also be activated by the PAMPs themselves. During infection, the activation of alpha-protein kinase 1 (ALPK1) leads to the translocation of NF-kB and expression of proinflammatory genes[45].

After the "threaten" has been sensed by NLRs or TLRs, the innate immune system responds to minimize and neutralize the danger. Phagocytosis is one of the most important responses and is being conducted by monocytes, macrophages, dendritic cells, eosinophils and neutrophils[46]. The process, starts with the recognition of the particle by Fc gamma receptors (FCGRs), that bind to the Fc portion of immunoglobulin G. After their activation, they provoke the reorganisation of the cytoskeleton and membrane in order to internalize the particles in a

phagosome[47]. Once inside the phagocyte, the particles will be destroyed by the production of reactive oxygen and nitrogen species (ROS and RNS)[48].

Immune cells are not the only components in the innate immune system that have key roles in the plaque. The terminal pathway of the complement, which is the last step upon activation of the complement, consists in the creation of the membrane attack complex (MAC) by several components of the complement (C5b, C6, C7, C8 and C9). MAC will form a pore in the attacked cell, which causes the lysis of the cell[49]. Both mRNA and proteins from the complement pathway have been found in human plaques, which indicates a localized production instead of a extravasation from the plasma[49] and its abundance is higher in vulnerable and unstable plaques[50].

The **adaptive immune system** also plays an important role in plaque development. The adaptive branch of the immune system is activated when antigen-presenting cells (like dendritic cells, macrophages or also B cells) activate **T cells**. There are different types of T cells when considering their activation process. CD4$^+$ T cells (or T helper cells, also known as Th) by presenting processed fragments using MHC class II. CD8$^+$ T cells (also known as cytotoxic T cell or killer T cell) get activated instead by fragments presented by any nucleated cell by MHC class I complexes[51].

In order to activate T-cells, besides the recognition of antigens bound to MHC class I and MHC class II by the T-cell receptor (TCR), a second costimulatory signal, which can be detected by costimulatory receptors, as CD28, CTLA4, ICOS… is necessary[52]. These signals can lead to different processes in T-cells, for example, the costimulation by CD28 can activate PI3K/Akt, which end promoting cytokine transcription, survival, cell-cycle entry and growth[53].

T cells account for about 20% of all the leukocytes present in healthy aorta, being IFNγ-producing T helper (Th1) the most abundant subtype[54] and they exhibit pro-atherogenic roles[55]. On the contrary, other subtypes of T cells, as regulatory T cells (Treg) Th cells have anti-atherogenic functions, even though they can switch to a more pro-atherogenic function. They recruitment is made by chemokines and their receptors, as CCR5, CXCR3 and CXCR6[56]. T helper cells become either effector T cells (Teff) or regulatory T cells (Treg) after interacting with antigenic peptides from apolipoprotein B (ApoB) which are presented by antigen-presenting cells in the plaque. Treg cells will show a more anti-inflammatory paper, with the secretion of IL-10 and TGF-ß, which enhance plaque stabilization and have anti-inflammatory properties[56]. On the other side, T eff cells can exhibit either pro-atherogenic roles (increased inflammation with IL-21, IL-2, IL-3, TNF and IFNγ production) or atheroprotective roles

(reduction of VCAM-1 expression and the recruitment of macrophages into the plaque)[56]. Cytotoxic T cells activate Fas-FasL pathway, which induces apoptosis. The death of different populations inside the plaque has different effects in its stability, accelerating the necrotic core expansion but also contributing to plaque erosion and unstable plaque development when the population of endothelial cells is targeted[57].

B cells are also present in the healthy aorta, representing approximately 20% of all the leukocytes and they have an important role in atherosclerosis. B cells specific receptors (BCRs) can bind self and foreign antigens, which results in the activation of the cell. Normally, this activation is initiated by T helper cells, but some antigens can active B cells by themselves[58]. In order to prevent overactivation of b-cells, its activation is regulated by several proteins, as CD22, which controls not only the activation of the BCR, but also its survival[59,60]. The activation leads to changes in the biological processes, due to the activation of the NF-kB pathway, the MAPK/ERK pathway and the PI3K pathway, that are all related to cell survival, differentiation, and proliferation[54,61]. After activation, B cells produce different antibodies, some of them (IgM and IgG) can be abundantly found in plaques in human and mouse, which react with modified LDL particles and also with apoptotic cells, with still unclear results[62]. Besides antibodies, B cells produce different cytokines with a relevant role in the atherosclerotic development. B cells are a source of TNF, which regulates T cells response, but they also produce IL-6 and IL-10, aside of IFN-y. Lastly, a subset of B-cells can produce GM-CSF, which has a direct impact in macrophages.

1.1.2.1.2 Stromal cells

Leukocytes are not the only players in the atherosclerotic plaque. Either in the healthy aorta or in the development of the disease, smooth muscle cells and endothelial cells have key roles.

Vascular smooth muscle cells (VSMC) are located in the media layer of the healthy aortas and they contract involuntarily, controlling the volume of blood and the blood pressure along the arteries[63]. Furthermore, they produce and remodel the extracellular matrix, secreting different proteins as fibronectin[64] and collagen[65]. On the contrary of skeletal and heart muscle cells, smooth muscle cells exhibit a very high degree of plasticity and can easily change their phenotype[66]. In the first steps of the plaque development, VSMC migrate from the media to the intima, start losing the capability of contraction, show a low proliferation rate and even reduce the expression of common VSMC markers, as α-smooth muscle actin (ACTA-2), smooth muscle myosin heavy chains (MYH11) and smooth muscle 22α[67]. With the progressive development of the plaque, these features, especially the loss of contraction and the increased

proliferation rate, become more pronounced. This combination of phenotypic changes is called synthetic phenotype and includes dedifferentiation of the cells[68]. VSMC in the intima start expressing markers that are commonly associated to other cellular types, as CD68 and Mac-2[69]. Synthetic VSMCs contribute to the pool of phagocytic cells, even though they don't exhibit such a strong phagocytic capability as monocyte-derived macrophages[70]. Despite the reduced activity, VSMCs need to be taken into consideration when explaining the sources of macrophages in the plaque, since different studies have shown that between 30 and 40% of the macrophages are from VSMC origin[71-73]. VSMCs become loaded of lipids from the environment through scavenger receptors and end up contributing to the pool of foam cells[74].

Endothelial cells (ECs) are the first players in the development of atherosclerosis disease. ECs create a monolayer along all blood vessels and control the blood supply of almost all tissues[75]. Besides regulating the pass of nutrients and oxygen, they also control the migration of cells from the blood flow to the tissues[76]. This type of cells has proliferating activity, and adult endothelial cells can divide until creating a monolayer if neighbour cells have been damaged. Furthermore, their proliferation also occurs when new capillaries need to be created[77]. The creation of a new capillary starts with the sprouting of an endothelial cell. The cells response to several signals from the tissue, one of the most powerful ones is vascular endothelial growth factor (VEGF), that can be produced as response to a lack of oxygen through the increase of the transcriptional factor hypoxia-inducible factor-1 (HIF-1)[78]. VEGF also induces migration of endothelial cells[77] .

In response to turbulent flow, high-lipid content, or pro-inflammatory signals, as IL-1B, the endothelial cells activate and this activation leads to change in their behaviour. The cells start expressing pro-inflammatory molecules, such as TNF, IL-4, interferon-γ and IL-1, that attract immune cells and adhesion molecules that will help these immune cells to extravasate[79,80]. Activated endothelial cells can adapt mesenchymal cell features (processed known as endothelial-to-mesenchymal transition, EndMT), exhibiting features more commonly seen in fibroblasts or even VSMC[81].

Endothelial cells also contribute to the creation and remodelling of the extracellular matrix together with VSMC and are capable of producing fibronectin[64], collagen and laminin[82].

Fibroblasts regulate many key functions crucial for the stability of the plaque, as inflammation and extracellular matrix production and remodelling[83]. They are capable of producing all the proteins that form the extracellular matrix, either if they are structural proteins, adhesive proteins, glycosaminoglycans or proteoglycans[84]. The origin of these cells is very variable since

there are studies that suggest that fibroblast can originate from adventitial mesenchymal stem cells, from VSMC or from EC[85]. Fibroblasts are one of the first cellular types involved in the formation of the atherosclerotic lesion after becoming activated. After their activation, they secrete different cytokines and growth factors that have an important impact in the other cell populations, such as VEGF, TGF-ß, PDGF and MCP1, among others[86].

1.1.2.2 Advanced lesion

The plaque slowly develops into a more complex entity, with the accumulation of leukocytes that come attracted by the proinflammatory molecules, the migration of vascular smooth muscle cells from the media but also the proliferation of these cellular types. Several structures can be recognized in an advanced atherosclerotic plaque, as can be seen in **Figure 2**. Normally, the plaque possesses a necrotic core, which is composed by debris from dead cells and crystals of oxidized fats. The necrotic core is surrounded by a fibrous cap, which is composed by connective tissue and separates the necrotic core from the endothelial layer. Around the necrotic core, in the area delimited by the fibrous cap, we can find different immune cells, attracted to the plaque by pro-inflammatory signals[87].
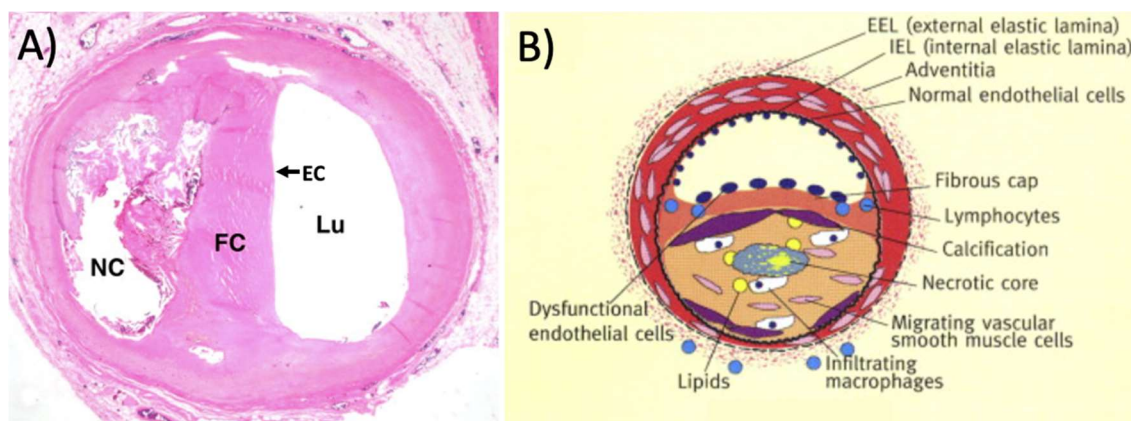
Figure 2. Morphology of the advanced atherosclerotic plaque. A) Histologic section of a human stable plaque with well defined structures (Lu: lumen, NC: necrotic core, FC: fibrous cap, EC: endothelial layer). B) Schematic representation of a stable advanced atherosclerotic plaque. Pictures adapted from Seidman et al. 2014[88].

The apoptosis and accumulation of different cellular types causes the instability of the plaque, due to the reduction in the production of ECM[89] and its breakdown to allow migration of leukocytes to the lesion area[90] and also due to the secretion of pro-inflammatory molecules[22]. The apoptotic process can be initiated by different factors, either extrinsic or intrinsic. Extrinsic

factors can be presence of TNFα, FasL or TRAIL, that join to their membrane receptors and start a cascade that finishes with the activation of Caspase 8[91]. In case of an inhibition of Caspase-8, which is not uncommon in an oxidative environment as the plaque, the necrotic death would replace the apoptotic process[92]. The recognition of pathogen associated molecular patterns (PAMPs) can also be an apoptosis trigger with the activation of Caspase-9[36]. On the other side, the intrinsic pathway can be initiated by several intracellular signals, such as absence of growth factors, hormones and/or cytokines that can lead to stop pro-survival pathways. Furthermore, the intrinsic pathway can also be activated as a response to radiation, toxins, hypoxia, infections or free radicals, as well as prolonged ER[92,93]. The activation of the intrinsic pathway has as a result the opening of a pore in the mitochondrial membrane (MPTP), that allows the release into the cytoplasm of pro-apoptotic effectors, as cytochrome c, Smac/DIABLO and the serine protease HtrA2/Omi[93]. Cytochrome c activates APAF, creating the apoptosome, which will activate the initiator Caspase-9[94]. Either extrinsic or intrinsic signals will activate the effector caspases (3, 6 and 7), which will fragment DNA and start the apoptotic process[92].

While the apoptosis and posterior clearance of dead macrophages (efferocytosis) is considered to be beneficial in the early stages of atherosclerosis due to the fact that limits the cellularity and plaque expansion[92], this is not completely true in advanced lesions. The negative aspect of macrophages apoptosis in advanced lesion is related to the incomplete efferocytosis, which can be due to the reduction of the signals that healthy macrophages use to detect apoptotic cells to clear them ("find me" signals like lysophosphatidylcholine, ATP/UTP, CX3CL1 or fractalkine and "eat me" signals like phosphatidylserine or calreticulin[95])[96]. Incomplete efferocytosis enhances the pro-inflammatory signals[97] in the plaque and increases the debris accumulation in the necrotic core[98]. Furthermore, the apoptotic cells increase the thrombogenicity of the plaque in the event of a plaque rupture[99].

Apoptosis is not the only form of cell death present in the plaque. Necroptosis, known also as programmed necroptosis of caspase-independent cell death, differs from passive necrosis, which is characterized by swelling, cytoplasmic granulation and final membrane rupture[100]. Necroptosis is also started by extrinsic stimuli (TNFα, FASL, TRAIL or even oxidized LDL[101]) but the inhibition of the Caspase-8 allows the formation of a complex between RIP3 and RIP1, which induce mitochondrial fragmentation and cell death[102]. Apoptosis and necroptosis are not separated pathways and it is common that apoptotic cells that failed to be cleared, go through a necrosis process[103].

Opposite to cell death, many cells in the plaque proliferate, being VSMC and macrophages the cellular types with the highest proliferative rate[104]. In fact, the contribution of proliferation to the cellularity of the plaque has been described as a key event in the plaque development, outnumbering the quantity of cells in the plaque that migrate into the plaque in the case of macrophages[17]. The proliferation of macrophages is associated with granulocyte-macrophage colony-stimulating factor (GM-CSF) and macrophage colony-stimulating factor (M-CSF), which show elevated levels in atherosclerotic plaques[105]. Furthermore, the presence of oxidized LDL (oxLDL) positively regulates macrophage[106], EC[107] and VSMC proliferation[108], despite the fact that its effect in EC is still under discussion[107]. The effect of proliferation in the atherosclerotic plaque is also under discussion. On the one side, proliferation of VSMC is seen as beneficial due to the fact that a stable and thick fibrous cap would be more resistant against erosion and plaque rupture[109]. On the other side, the swift from a contractile phenotype to a synthetic phenotype with proliferating capabilities in the case of VSMC is associated with reduced contractile capabilities and their ability to become foam cells might end up with the apoptosis of the cell, contributing to the increase of the necrotic core[67]. Furthermore, the proliferation of cells inside the plaque might increase the cellularity and therefore, promoting the growth of the plaque. In fact, the administration of antiproliferative drugs is associated with a reduction in the progression of the atherosclerotic plaque[110].

Besides cell death and proliferation, other processes that affect the plaque stability, as neovascularization or crystallization can occur in the advanced lesion[111].

Neovascularization is triggered by the lack of oxygen in the deepest areas of the plaque. The cells in these areas release angiogenic factors, like VEGF, to promote the sprouting from nearby blood vessels. Different cell types are affected by the hypoxic conditions, but it is believed that the population of macrophages are an important source of pro-angiogenic factors due to their high oxygen consumption, necessary for the cholesterol uptake and further processing[111]. The expression of VEGF is controlled by HIF (Hypoxia-Inducible Factor), which is composed by a dimerization of two proteins (HIF-1α and HIF-1β). In hypoxia, the two subunits dimerize and start the transcription of many genes, such as several vascular endothelial factors, Flt-1 (which is the gene coding for VEGFR1), angiopoietin-2 and NO synthase[112]. The VEGF family is composed by different homolog genes (Vegfa, Vegfb, Vegfd and Pgf) and the receptors (Flt1, Kdr, Flt4)[113]. VEGFA (Flt1) is the most known homolog and has different functions in the plaque. VEGFA is a potent angiogenic, but besides that, it is an endothelial mitogen that helps re-endothelialization and also promotes monocyte migration. VEGFB exhibits less angiogenic activity, but can stimulate the uptake of lipids by endothelial cells[114].

Other factors are involved in the stabilization of the blood vessels (angiopoietin-1) or enhance SMC proliferation and angiogenesis development (NO synthase[115]).

The vascularization enhances the plaque growth due to the increase of transmigrated cells and also the availability of nutrients and oxygen[114]. This growth, together with intraplaque haemorrhages, caused by the high vessel density and their fragile walls, increase the instability of the plaque[116].

Another process that critically affects the plaque stability is the cholesterol crystallization. Even though, the cholesterol is in liquid state at body temperature, it can transform into cholesterol crystals due to changes into the cholesterol concentration, pH and pressure. The environmental conditions inside of the necrotic core of large plaques are adequate for this change to occur and the creation of crystals can tear up the fibrous cap, enhancing the plaque rupture[117].

All these different processes contribute in different ways to the remodelling of the plaque. The weakening of the fibrous cap by cell death, lack of extracellular matrix production, expansion of the necrotic core or increase of the extravasation of leukocytes creates unstable plaques, which will develop into plaque rupture. The fibrous cap, formed to encapsulate the necrotic core, is threatened by two main processes: first, it is formed by abnormal VSMC, that will end up dying and second, it must bear the expansion of the necrotic core and the plaque due to the permanent transmigration of cells and the continued cell death[118,119]. The erosion of the fibrous cap, especially in the shoulders of the plaque[120], which are the areas between the fibrous cap and the intima area without plaque, is very critical. In these areas the fibrous cap doesn't have a thick expansion, it ends up tearing, which allows the exit of the collagen and the lipid core into the lumen, creating a thrombus[8,121]. The features of the plaque makes it very thrombogenic, specially due to the production by activated macrophages of tissue factor (also called factor III or CD142), an important initiator of the coagulation pathway [122].

Sometimes, the rupture of the plaque is not complete, and only part of the arterial endothelium (smooth muscle cells from the fibrous cap, foam cells and lipids from the extracellular matrix) are freed into the lumen[120].

The rupture of the cap is asymptomatic and the consequent thrombosis occurs spontaneously, even though it can be triggered by emotional or physical stress or circadian rhythms[123]. For a long time, it has been known the relationship of the circadian rhythms with the probability of plaque rupture, concentrating in the morning hours (between 6 am and 12 pm) most of the heart attacks and strokes[124,125].

1.2 Circadian regulation

In nature, the ability to predict changes in the environment with the finality to prepare for them and take advantage of the new situations can be key for the survival of an organism. Many key factors in the wild (availability of food, light, presence of predators…) are dependent on the light-darkness cycles, therefore the possibility to predict these 24-hour cycles would give organisms a higher advantage. Organisms living in the surface or the planet, ranging from multicellular to unicellular organisms, have evolved to predict these light changes to maximize their fitness over their competitors´[126].

Many biological functions in animals oscillate in a 24h-fasion, as it can be blood pressure, sleeping cycles, feeding cycles, hormone release, metabolism…[126-128] And different cycles can also be found in other beings, as in plants. In fact, the first documented circadian studies were conducted in the 18th Century in plants. Jean-Jacques d'Ortous de Mairan studied the 24h pattern of the leaves´ movement in *Mimosa pudica.* He also proved that this oscillation is maintained even in darkness, which settled down the basis to think of an intrinsic regulation in the organisms[129].

Circadian rhythms describe an approximately 24-hour oscillation cycle that continues either in constant light or constant darkness. If the rhythm shows a circadian oscillation, but it's not being kept in constant darkness, then it is considered to be driven by external cues (or "zeitgeber", time-giver)[130].

Focusing on mammals, circadian system has a hierarchical organization and it is centralized by an oscillator localized in the hypothalamus, called the suprachiasmatic nucleus (SCN), which controls all the peripheral clocks. Furthermore, at the cellular level, mammal cells possess molecular clocks that control the expression of an important proportion of the transcriptome[131].

1.2.1 The Suprachiasmatic Nucleus (SCN)

The SCN is a small are in the hypothalamus which is in charge of adjusting the different clocks in the organism to external cues. The SCN acts as a general pacemaker that translates the external factors, mainly the presence of light, into molecular signals that will synchronize all the peripheral clocks in the body[132].

The SCN is composed by two regions: the core region, that receives signals about the presence of light from the retinohypothalamic tract and the shell, that receives the information from the core region[133]. The shell region of the SCN sends this information to different areas of the brain that will control the sleep-wake cycle, feeding-fasting cycle or body temperature[134], as can be seen in **Figure 3**.
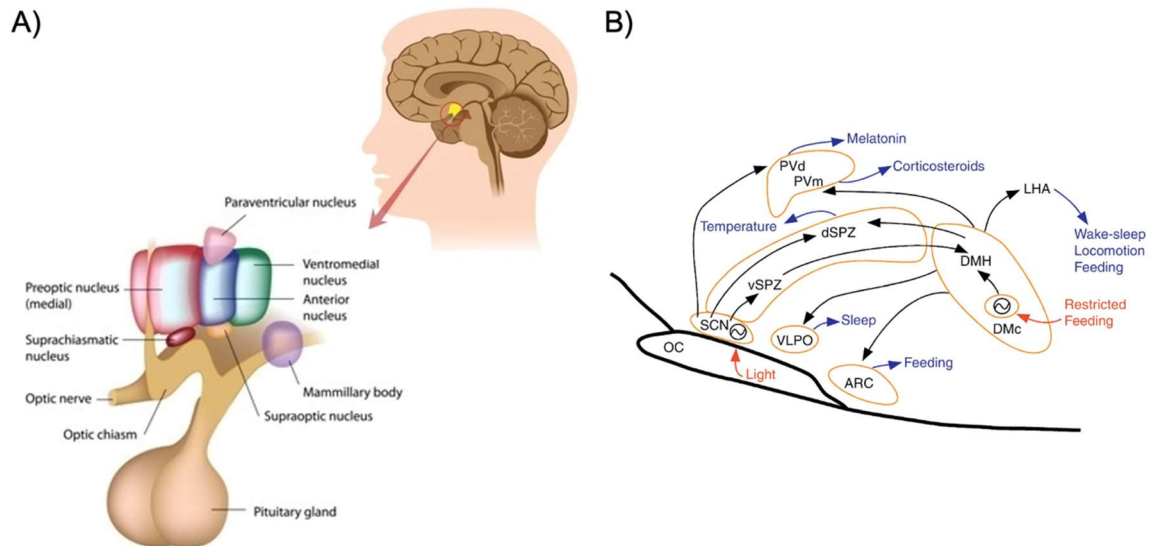
Figure 3. Anatomic situation of the SCN and the other nucleus that control the peripheral clocks. A) Anatomic localization of the SCN together with other adjacent structures, as the optic nerve and the pituitary gland. Adapted from Alila Medical Media (https://alilamedicalimages.photoshelter.com/index). **B)** Schematic representation of the different areas of the brain that are directly connected with the SCN and that will receive information from the shell region of the SCN and control several biological functions through the activation of peripheral clocks. Abbreviations used: SCN (suprachiasmatic nucleus), PV (paraventricular nucleus), (SPZ) subparaventricular zone, vSPZ (ventral subparaventricular zone), DMH (dorsomedial nucleus of the hypothalamus), DMc (compart part of the dorsomedial nucleus of the hypothalamus), ARC (arcuate hypothalamic nucleus), OC (optic chiasm), VLPO (ventrolateral preoptic nucleus). Adapted from Saper, 2013[134].

These areas of the brain, after being activated by the SCN, will send the information by different mechanisms, that imply the nervous system and hormonal changes to the peripheral clocks in the organisms [135]. The synchrony of the peripheral clocks is orchestrated by the hypothalamic-pituitary-adrenal axis and the autonomic nervous system.

On the one side, the hypothalamus controls the secretions of the pituitary gland, which, among others, secretes the adrenocorticotropic hormone (ACTH)[136]. When the ACTH reaches the adrenal gland, it will stimulate two different areas: the zona fasciculata and the zona reticularis, which will produce corticosteroids and androgens respectively.

On the other side, the autonomic nervous system can also regulate the peripheral clocks by direct innervation of the peripheral organs, through the release of catecholamines (norepinephrine and epinephrine)[137]. Moreover, the nervous system also influences the release of corticosteroids, either by stimulating the adrenal gland to produce it but also by increasing the sensitivity of the adrenal gland to ACTH[138].

1.2.2 The molecular clock

It is known that all the cells in the organism possess a molecular clock that coordinates the expression of specific biological functions along the day[139].

The molecular circadian clock of each cell is composed by three transcription/translation feedback loops. The first feedback loop is generated by two transcriptional factors, CLOCK and BMAL1. CLOCK and BMAL1 create a dimer, that recruits the necessary proteins to start the transcription of their target genes.

Among the genes controlled by CLOCK-BMAL1 we find *Per* and *Cry*. PER and CRY (which are present in different isoforms: CRY1, CRY2, PER1, PER2 AND PER3) also dimerize and translocate into the nucleus of the cell in order to stop their own transcription, interacting directly with CLOCK-BMAL1.

The second feedback loop comprehends other CLOCK-BMAL1´s targets, a family of proteins know as REV-ERBs. REV-ERBα and REV-ERBβ will compete with RORs (RORα, RORβ and RORγ) on the control of the transcription of BMAL1. The two REV-ERB exert a negative regulation of the transcription of BMAL1, which completes a Feedback loop that regulates its amount[140], while the RORs will enhance the expression of BMAL1. Moreover, REV-ERBs will have an important role in the circadian control of the metabolism[141].

The last feedback loop is associated to all the rest of the genes that will create the rhythmicity in several biological processes. This loop is created by DBP, a protein encoded by the gene *Dbp*, whose transcription is controlled by BMAL1-CLOCK and NFIL3, a protein coded by the gene *Nfil3*, whose transcription is controlled by RORs. The dimer created by DBP-NFIL3 will activate

the transcription of *Rora/b* genes. The schematic representation of these three feedback loops is displayed in **Figure 4.**

These three feedback loops (DBP-NFIL3, CLOCK-BMAL1 and the transcriptional factors RORs/REV-ERB) will regulate the expression of many processes, as metabolism, autophagy, cell division, differentiation[142]. Furthermore, other products of these pathways, as Per and Cry will mediate also the expression and repression of different genes. This is the case of the repression of glucocorticoid receptor by CRY1 and CRY2[143], the regulation of core proliferating genes as *c-Myc* and *CyclinD* by PER2[144] or the interaction of CRY1 with central enzymes of metabolic pathways, as CBS[145].

CLOCK-BMAL1 directly regulate the expression of an important part of the transcriptome. There are genome-wide association studies in which it has been proved that CLOCK-BMAL1 directly regulate more than the 15% of the transcriptome[146]. Furthermore, the fact that most of these analyses are done in standard conditions, with genes not being expressed, makes the researches think that the total number of genes under CLOCK-BMAL1 control can reach up to the 50% of the transcriptome[147]. But, in order to trustworthily assess the impact of CLOCK-BMAL1 in the transcriptome regulation, we also have to consider the different layers of regulation that are ruled by DBP-NFIL3 and REV-ERB/RORs. Due to complex regulations, it is difficult to estimate the number of genes under control of the molecular clock, but there are publications that estimate that the number of genes with circadian patterns of transcription (and would potentially be regulated with the molecular clock) is very large, reaching more than 80% of protein-coding genes in some cell types[148].
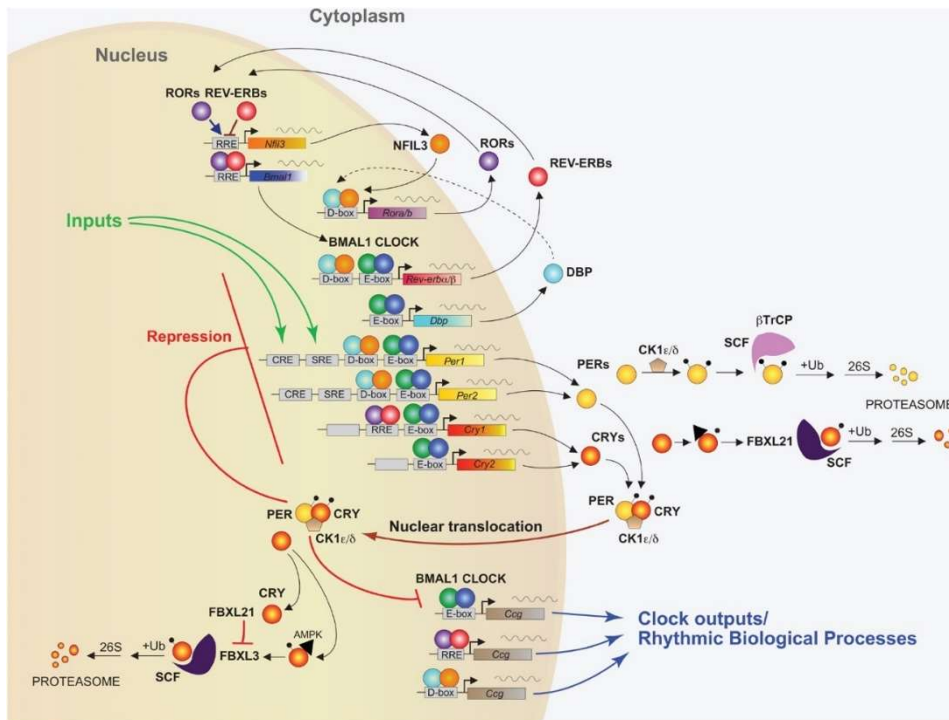
Figure 4. Molecular circadian clock. Representation of the molecular circadian clock in mammals. In the image, the three feedback loops (BMAL1-CLOCK and CRY-PER; BMAL1-CLOCK and REV-ERBs/RORs; NFIL3/DBP) explained in the text are represented. Furthermore, the clock outputs, that comprehend rhythmic regulation of several biological processes such as proliferation, metabolism or transcription, among others, are also represented. Image adapted from K H Cox and J S Takahashi, 2019[140].

1.2.3 Circadian rhythms in atherosclerosis

As it has been highlighted before, many genes from different biological processes are under the control of the molecular clock and therefore show oscillations in their expression.

Gene expression and translation are one of the cellular functions that oscillate over day[142]. The processing and degradation of RNA and also the translation are, for example, under circadian control, which gives circadian rhythmicity to the transcription and translation of genes that are not under the direct control of the molecular clock. Furthermore, splicing factors also show a circadian rhythm in their expression[149].

In the case of proliferation and cell division, different genes from the circadian clock control the expression of important checkpoints during the cell cycle (as p21, p16 or CDK1) [142].

Opposite to cell division, apoptosis is also regulated by clock genes. Tumor necrosis factor α (TNFα), which is a strong inducer of apoptosis but also an activator of cell-survival mechanisms dependent of NF-kB[150], is under regulation of CRY1 and CRY2[151]. Furthermore, NF-kB, which is activate downstream of TNFα and is also regulated indirectly by CRY1/2. In case of the intrinsic apoptotic pathway, TP53, which controls the expression of the death-related genes that will lead to the apoptotic process (*Bax*, *Bak1*, *Bnip3*), interacts with proteins of the core of the molecular clock (BMAL1, CRY and PER)[151].

Considering specific organelle, there are several examples of pathways that oscillate in a specific cellular compartment that are worth mentioning. The endoplasmic-stress response to unfolded proteins is highly regulated by CLOCK and PER, the response to oxidative stress and hypoxia in the mitochondria is connected to the circadian clock, the amount of autophagic vesicles in the lysosomes also shows oscillation over the day[142].

These molecular processes, especially the oscillation of cell proliferation and cell death, are going to have a strong impact in the stability and composition of the atherosclerotic plaque. Besides these cellular processes, there are many physiological processes related to atherosclerosis development and plaque stability that are influenced by circadian rhythms, as it can be blood pressure or leukocyte transmigration into the plaque.

Blood pressure and heart rate oscillate in a circadian fashion. There´s a peak in the early morning in the blood pressure values, associated with a more "awake" or "alert" state and it has the lowest values during the sleeping period. This modulation of pressure is important up to the point of associating an absence of nocturnal dipping of blood pressure with hypertension and higher risk of cardiovascular events[152]. In case of heart rate, the highest values are also found at around 10 am [153].

In terms of the key cellular players in the plaque development, the number of circulating leukocytes varies during the day, being higher during the resting period (ZT1-ZT12 in mice) with a peak round 5 hours after the start of the light period (ZT5)[154]. This increase is caused by the egress into the blood of the leukocytes produced in the bone marrow mostly at the beginning of the resting phase and the fact that their transmigration into peripheral tissues takes place at the end of the resting phase. On the contrary, the homing to the bone marrow (BM) shows an increase in the active period, with a peak at ZT13[155].

The expression of the chemokine C-C motif ligand 2 (known as CCL2 or MCP-1), which attracts monocytes, T cells, B cells, natural killers, basophils, macrophages, dendritic cells, neutrophils and myeloid-derived suppressor cells to inflammation sites[156], is under circadian control. The

receptor of this chemokine (CCR2) is expressed in inflammatory (Ly6C^{hi}) monocytes, hematopoietic stem cells (HSCs) and a subset of natural killer cells and it mediates the migration from the bone marrow towards inflamed tissues following increasing concentrations of CCL2, which is expressed to all nucleated cells in response to inflammation[157]. There is higher amount of CCL2 in plasma in ZT1 versus ZT13, which has been shown to get immobilized on endothelial cells of the atherosclerosis plaque, provoking a peak of leukocytes migrating into the lesion at the end of the activity phase (ZT17)[158].

ICAM-1 (Intracellular Adhesion Molecule 1) and VCAM-1 (Vascular Cell Adhesion Molecule 1) are most important adhesion molecules that allow the migration of the leukocytes towards the tissue and they exhibit a circadian expression, peaking in the evening in vascular beds in murine models[159]. The ligands of these adhesion molecules (the integrins CD18 and CD11 in the case of ICAM-1 and VLA4 in case of VCAM) are expressed in leukocytes[160] and control the migration from the blood to the tissue. Alongside, the endothelium also produces chemokines that act as attractant signals to the inflammation side, targeting different receptors in monocytes (CCR2, CCR5 and CX3CR1)[161] and in neutrophils (CCR1, CCR5)[26]. The rolling of leukocytes in the inflamed endothelium is controlled by selectins, such as P-selectin, which is expressed in the endothelium when inflamed and binds P-selectin glycoprotein ligand 1 (PSGL-1), expressed in leukocytes[162].

Lastly, the amount of circulating lipids also has a circadian oscillation, highly impacted by the feeding times. Cholesterol, triglycerides and LDL proteins show oscillation in the plasma, with a peak at ZT18 (corresponding to highest activity)[163] . The biosynthesis of lipids by the liver also shows oscillation, with a peak in the middle of the resting period[163].

Even though we're starting to elucidate the influence that the circadian clock has in some aspects of this recruitment, as in the expression of integrins in leukocytes and the adhesion molecules in the endothelium[159,164] or in the attraction of the leukocytes [158,165], there's still a lot of missing information about the mechanisms that are controlled by circadian variation and their influence in the stability of the atherosclerotic plaque, as the death of smooth muscle cells and macrophages, the action of metalloproteinases (MMPs) that destroy the extracellular matrix or the proliferation of macrophages.

The importance of the timing of these events lies in the epidemiological studies that show an increased number of adverse cardiovascular events in the morning times. This observation was already done by Muller in 1985, when he studied in 2999 patients the time of the day in which they had an elevation of creatine kinase MB (myocardial infarction marker). He described a 3-

fold increase in the frequency of infarctions in the morning hours (with a peak at 9 am) when compared with evening hours (with a trough at 11 pm)[166]. More recent studies can be found in Thosar et al[167], where the epidemiological studies show an increase in the morning hours (from 8am to 12pm) of sudden cardiac death and ischemic stroke, besides myocardial infarction.

Even though the plaque rupture is asymptomatic and can happen before a cardiovascular event[123], there´s evidence of a higher incidence of cardiovascular events in the morning hours in humans that might be related to the circadian oscillations of biological processes in the atherosclerotic plaque. To study the oscillation of these processes in order to be able to fund therapeutic targets to reduce the probability or even avoid the rupture of the plaque is of vital importance for the atherosclerotic treatment.

1.3 Chronopharmacology

As we have already mentioned, many genes and processes show oscillation in their expression, with a percentage changing from one organ to the other, but with an average oscillation of 7.34% in protein coding genes (data calculated from Mure et al[148]). This percentage oscillates enormously among the different organs of the body and can have effects in the absorption, distribution and metabolism of drug compounds.

Chronopharmacology, defined as "the study of how the effects of drugs vary with biological timing and endogenous periodicities"[168] studies the concepts of pharmacodynamics and pharmacokinetics in the context of circadian variation, with the goal to maximize the efficacy of a therapy by applying it at the most convenient time.

The creation of new pharmacological treatments needs to take into consideration the variability of gene expression along the day. Many genes exhibit daily variability in their expression and numerous studies highlight the relationship between the time of administration of a drug and its effectiveness. In fact, up to 82.2% of proteins that are targets for existing drugs show circadian variation in their genes[148] and the influence doesn't stop in the main targets of the drugs; the gastric and intestinal absorption, as well as the xenobiotic detoxification by the liver are believed to show circadian variation[169,170].

Besides this variation in the cell transcriptome that creates differences in terms of cellular performance, the half-life of the drug has also to be considered, since its administration can be uncoupled to the time of the day in which the protein that targets display its biggest activity.

The two branches of pharmacology (pharmacokinetics and pharmacodynamic) describe processes of crucial importance to assess the therapeutic potential of a drug and in these processes, we can find numerous examples of circadian regulation.

1.3.1 Chronopharmacokinetics

Pharmacokinetics studies the modifications that the organism performs to the drug. The processes that the drug goes through in the organism (absorption, distribution and metabolization) are highly conditioned by the circadian oscillations. A representation of the different biological processes that control pharmacokinetics and are under the circadian clock can be found in **Figure 6**.

In terms of absorption, this accounts with a very high impact in the drug that are orally taken. Gastric mobility is higher during the day than at night in the case of humans and this is a valid statement also for gut mobility. The higher mobility increases the speed of absorption and posterior pass to the blood[171].

The metabolization, done in the liver or in the kidney, is also a process in which the circadian clock has a high effect. In the liver, cytochromes are a family of proteins in charge of the xenobiotic detoxification. Out of the 10 most important drug-metabolizing cytochromes, 6 have shown circadian expression[172]. Furthermore, there´s evidence than the circadian clock influences the three phases of xenobiotic detoxification (modification, conjugation and excretion) and that this control is exerted by circadian-controlled transcription factors instead of being a direct control by BMAL1[169].

In the kidney, different parameters that control the elimination of the drug from the blood, such as renal blood flow, show circadian oscillation, with a peak in the active phase[173,174].

Lastly, despite not being part of the digestive or excretory systems, the different cardiac output during the day (up to 30% higher in the morning versus night) is going to determine also the extent of the tissue irrigation and therefore, the amount of drug that is in contact with the tissue[175].

All these described processes are going to have a tremendous impact in determining the levels of a drug in the organism and should be taken into consideration when designing a therapeutic process.
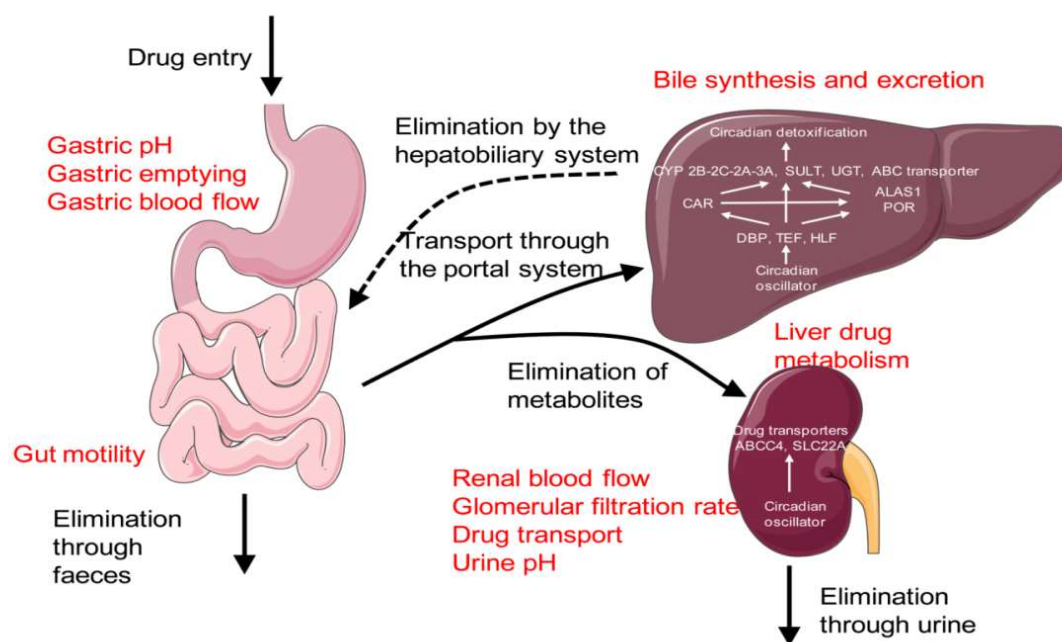
Figure 5. Influence of circadian rhythms in digestion and excretion. Illustration of the main processes that influence pharmacokinetics. The processes that show circadian oscillation are highlighted in red. Image adapted from Ahuja et al. 2021[176].

1.3.2 Chronopharmacodynamics

Pharmacodynamics comprehends the study of the effects that the drug causes in the organism. The drugs produce effects by interacting directly with receptors and enzymes, interacting with cell surface proteins that will start downstream signalling or by interacting with soluble molecules, like cytokines[177].

The important percentage of genes that have an oscillatory rhythm over the day in the organism leads to the thought that there are differences of expression in the drug targets. In fact, 82.2% of genes identified as druggable targets by the FDA show oscillation in non-human primates[148].

The optimal timing for a drug can be extremely important in the case of drugs with a very short life, since the drug can be already metabolized and eliminated before the peak of abundance of its target and this has been shown in meta-analysis of clinical trials that evaluated the impact of the time of dose in the efficacy or toxicity. This scenario also applies to drugs that target specific proteins that are part of the core molecular clock pathway, such as REV-ERBs, CRY and RORs which are being tested to decrease atherosclerotic plaque[178], to reduce

inflammation[178] or to enhance circadian rhythmicity with the aim to reduce the effects of metabolic disease[179]. In the case of cardiovascular diseases, many drugs used in clinical practice, such as acebutolol, hydrochlorothiazide, amlodipine or captopril show evidence for chronopharmacodynamics[180]. Nevertheless, a small percentage of prescribed drugs have a recommendation on time dosage[181].

Choosing the correct time of dosage becomes even more complex when comparing the oscillatory patterns in different organs. As it has been seen in RNA-Seq from primates and mice[147,148] there are big differences in terms of oscillating genes in the different tissues of the organism. This can be used as a therapeutic approach to enhance the drug effect in a specific organ, which can reduce the side effects of the medication and allow a more targeted approach.

1.4 Research objective

The objective of this doctoral thesis are 1) to describe the circadian oscillation of key biological processes that have a direct impact on the stability and development of the advanced atherosclerotic plaque in a murine model, 2) to describe the changes in the circadian clock and in the oscillating transcriptome that a long term of western diet feeding has in different organs, 3) to identify differences of oscillation among key organs and the atherosclerotic plaque in molecular pathways that could be used as drug targets in the treatment of advanced atherosclerosis and 4) to translate the oscillating profile of an atherosclerotic plaque from a murine model into clinical human samples.

To meet these objectives, several high-throughput techniques (RNA-Seq, proteomics, single-cell transcriptomics) together with immunohistochemistry, histology and flow cytometry were applied in different organs (brachiocephalic artery, blood, aortic arch, descendent aorta, lung, liver, spleen, colon, ileum, heart, white adipose tissue, tibia muscle, adrenal gland, kidney, human carotids).

2. Materials and Methods

2.1 Mice housing and harvesting

2.1.1 Mice

8 weeks old Apoe$^{-/-}$ were used in order to study the circadian oscillations in the mouse plaque. The origin of the mice was mixed, coming either from a provider (The Jackson Laboratory) or were bred in our own animal facility. All the animals were genotyped as explained in the **Section 2.1.1.1** by Olga Schengel. As control group for the Apoe$^{-/-}$ mice, C57BL/6J mice were used. The origin of these mice is also mixed, partially coming from the Jackson Laboratory and partially from the breeding in our animal facility.

The mice were kept in a 12-hour light/12-hour dark cycle, being 7am (ZT1) the moment in which the lights would turn on and 7 pm (ZT12) the moment in which the lights would turn off. The mice were kept at a temperature between of 20-22 degrees in 45-60% humidity.

In order to mimic advanced atherosclerotic lesions, Apoe$^{-/-}$ mice were fed for 16W with a high-fat diet (HFD), which contains 21% fat and 0.15% cholesterol (sniff, Soest).

All animal experiments had been approved by the local ethical committee for animal experimentation (Regierung von Oberbayern and LANUV).

2.1.1.1 Genotyping of the mice

Apoe$^{-/-}$ mice were genotyped in order to control their genetic background. The procedure was performed by Olga Schengel and was done as described.

A tail biopsy was obtained from each mouse and it was digested overnight with 250µL tissue lysis buffer with proteinase k (0.2 mg/ml, Qiagen). DNA was then isolated using QIAxtractor kit (Qiagen) and performing the protocol offered by the manufacturer.

A PCR reagent mix was prepared with the following elements

Reagent	Brand	Concentration
Green Gotaq Flexi buffer	Promega	1x
25 mM Mgcl2	Sigma-Aldrich	1.5 mM
dNTPs	Sigma-Aldrich	0.2mM
Forward Primer	Sigma-Aldrich	0.5µM

Reverse Primer	Sigma-Aldrich	0.5 µM
GoTaq DNA polymerase	Promega	0.05 U/µL
Genomic DNA	Promega	200 ng

To detect the genetically modified mice, which don´t express Apoe$^{-/-}$, the following forward and reverse primers were used:

Name	Sequence
Apoe **wildtype forward**	5' GCC TAG CCG AGG GAG AGC CG 3'
Apoe **wildtype reverse**	5' TGT GAC TTG GGA GCT CTG CAG C 3'
Apoe **mutant reverse**	5' GCC GCC CCG ACT GCA TCT 3'

The program used in the cycler was the following one

Step	Temperature	Time
1	94°C	5 min
2	94 °C	30 seconds
3	60°C	30 seconds
4	72 °C	30 seconds
5	Repeat 35x steps 2-4	
6	72 °C	5 min
7	21 °C	5 min

After the cycling, the PCR products were run in an electrophoresis gel using QIAxcel Advanced System (Qiagen).

2.1.1.2 BrdU injection

To study the proliferation in the plaque and in other organs, an assay with BrdU was performed. Following the instructions of the manufacturer (BD biosciences), 100 µL of BrdU solution (10mg/mL) were injected in mice 2 hours before harvesting peritoneally. After injection, mice were allowed to rest until harvest time with access to food and water ab libitum.

2.1.2 Circadian harvesting

To collect mice tissues every 4 hours during 24h interval and avoiding the increase of variability, a set of mice that had been littered and kept together was harvested during a continuous 24h-interval.

Mice were kept in their normal housing conditions until the moment of the sacrifice. The mice that were sacrificed from 7pm to 7am were killed in conditions of semi-darkness without any direct light to avoid the disruption of their circadian cycle.

Mice were killed after having been anesthetized with 6-8 mg/kg xylacine plus 90-120 mg/kg ketamine. When they were unconscious, the mice were bled using heart puncture.

When the mouse was dead by exsanguination, 20 ml PBS was used to flush the body of the animal, in order to eliminate as much blood from the tissues as possible.

2.1.2.1 Organ harvesting and processing

The following organs and tissues were harvested from the mice:

Blood: As much blood as possible was extracted through a heart puncture using needles previously coated with EDTA. The blood was kept in tubes containing EDTA to avoid coagulation of the blood. Afterwards, 100 µL of total blood was separated in order to perform cellular counts of the main populations in the blood.

To remove the red blood cells, the 100 µL of total blood were lysed with 3 ml of lysis buffer for 4 minutes at room temperature, following the addition 10mL of Hanks buffer to stop the lysis. The next step would be to centrifugate the mix and resuspend the cells in staining solution for flow cytometry (**Section 2.3.1.1**).

The rest of the blood was used to collect plasma. The blood was spun down at 3000xg for 10 minutes at 4°C and the supernatant was taken carefully. The plasma samples were kept at -80°C to avoid protein degradation.

Organs for RNA-Seq: The organs that were going to be processed for bulk RNA-Seq (lung, liver, spleen, BCA, colon, ileum, heart, adrenal gland, kidney, white adipose tissue, tibia muscle, aorta) were harvested and put in a 2ml Eppendorf containing 1 ml Qiazol (Qiagen) and two magnetic beads. Before putting the organ in Qiazol, the piece was weighted in order to be able to correct by weight when performing the RNA-isolation. Afterwards, the tissue was homogenized using a tissue homogenizer (TissueLyser, Qiagen) for 2 minutes at maximum speed. For the more fibrous tissues (spleen, intestines, aorta), the organs were chopped with scissors to create small fragments and facilitate the homogenization. The process was performed as soon as possible to stop the degradation of the tissue. Furthermore, the holder of the tissue homogenizer had been kept in -80°C to avoid the increase of temperature in the samples due to the friction of the magnetic beads. Further processing of these samples is explained in **Section 2.6.2**.

BCA for Histology. In order to facilitate the sectioning of the BCA, it was embedded in a liver piece of liver, making sure that the BCA would lay plain and without wrinkles. Afterwards, it was put on Tissue-Tek OCT Compound (A.Hartestein) and kept at -80 °C until further processing.

BCA for flow cytometry. The BCA together with the arch were used for flow cytometry. The two arteries were collected in a tub with 300 µL of digestion buffer. The aorta was chopped into small pieces and it was digested for 1 hour at 37°C, shaking the tubes every 15 minutes to help in the digestion. The digestion was stopped with 1 ml Hanks buffer and it was filtered using a 70µm strainer (Corning) while centrifuging at 300xg for 5 minutes. Afterwards, the precipitated sample was resuspended with antibody staining mix (**Section 2.3.1.2**)

Arch for proteomics. The arch was separated from the descendant aorta and the BCA during the harvest and was put immediately into an Eppendorf. Afterwards, it was quickly frozen

using liquid nitrogen in order to preserve the tissue and was kept in -80 °C until further processing.

Organs for flow cytometry. The lung, liver, kidney were harvested and processed for flow cytometry. For the lung and the kidney, the organ was put in an Eppendorf with 500 µL of digestion buffer. The organ was minced in small pieces in order to facilitate digestion. The tube with the minced organ was put 50 minutes at 37°C with constant agitation (300-350 rpm). The digested organ was transferred to a 15mL tube through 50 µm strainer and it was centrifugated for 5 minutes at 300xg at 4°C. The pellet was resuspended with 200 µL Hanks buffer.

In the case of the liver, the biggest lobe was smashed through a 70 µm strainer in a 50mL tube. 5mL of HBSS were used to facilitate the pass through the strainer. The smashed tissue was centrifuged 5 minutes at 300xg at room temperature. The pellet was resuspended in 5 mL of 36% Percoll-HBSS solution and transferred to a 15mL tube. The tube was centrifuged at 800g for 20 minutes with no break and an acceleration of 1. The smashed tissue layered in three different phases: the hepatocytes on top, an aqueous phase and in the pellet the leukocytes. The two upper layers were carefully removed and the pellet was washed with 3ml HBSS to remove the leftovers of Percoll. The pellet was resuspended in 200 µL Hanks buffer. After digestion, the single-cell suspension was stained as explained in Section **2.3.1.2**.

2.2 Small molecule measurement

The plasma acquired during the experiments was used in order to measure the abundance of important lipids and proteins related to the project. The plasma was kept in -80°C from the harvesting moment until the measurement, when it was thawed in ice to avoid strong temperature changes.

2.2.1 Cholesterol and triglyceride

The plasma triglycerides and cholesterol were measured using a commercial kit (CHOD-PAP from Roche/Hitachi, Ref: 11875540 216 and GPO-PAP from Roche/Hitachi, Ref:04657594) and following the specific instructions from the manufacturer. The samples coming from mice that

had been fed for 16 weeks with high fat diet were diluted in a 1:20 factor for cholesterol measurements and in a 1:5 factor for triglyceride measurement to avoid the saturation of the reaction. Duplicates from all the samples and the standard samples were prepared to increase the accuracy. The final value for each sample was the average of the two measurements. The absorbance measurement was performed at 505-510 nm using a Tecan reader Infinite 200 Pro.

2.2.2 Cytokine measurement

A customized panel of several cytokines (LEGENDplex, BioLegend) was acquired to detect soluble analytes in plasma samples and study their oscillation throughout the day. The assay consists in the detection of the specific analytes, that will attach to a bead coated with antibodies for each analyte. The detection of each analyte is made by the size of each bead, that changes between analytes.

For the analysis, plasma samples were diluted 1:2 ratio for the customized panel to avoid saturation of the reaction. Each sample was measured twice to increase the accuracy of the measurement. The final value for each sample was the average of the two measurements.

The following analytes were measured in plasma samples following the indications of the manufacturer.

Analytes detected			
BAFF	CCL5	CXCL9	CXCL10

The quantification of the abundance of the analytes was performed using the Cytometer Aurora (Cytek).

2.3 Flow cytometry

Flow cytometry is a laser-based measurement that allows the characterization and quantification of the cellular populations that are present in a sample.

The methodology used by the technic consists in staining specific cellular markers that are present in the outer membrane of the cells, such as receptors or other membrane proteins,

that characterize the cellular population or populations that has specific interest for the study. The markers are normally conjugated with fluorescent particles that absorb light and afterwards emit it in a different wavelength.

The procedure starts with a single cell suspension that is stained with the antibodies that mark the populations of interest. When the staining is performed, the cellular suspension goes through a capillary that forces the cell to form a line (**Figure 6**). This capillary is excited with a laser (or with several lasers) and the fluorescent marker is excited, emitting at a specific wavelength. The emission wavelength is detected and this information, together with measurements about the cell size (forward scattered light, FSC) and granularity (side scattered light, SSC) is used to characterize individual cells and assign them to a specific population.

The instrument used to perform the Flow Cytometry were a LSR-Fortessa (BD Biosciences) and a Cytek Aurora (16UV-16V-14B-10YG-8R).
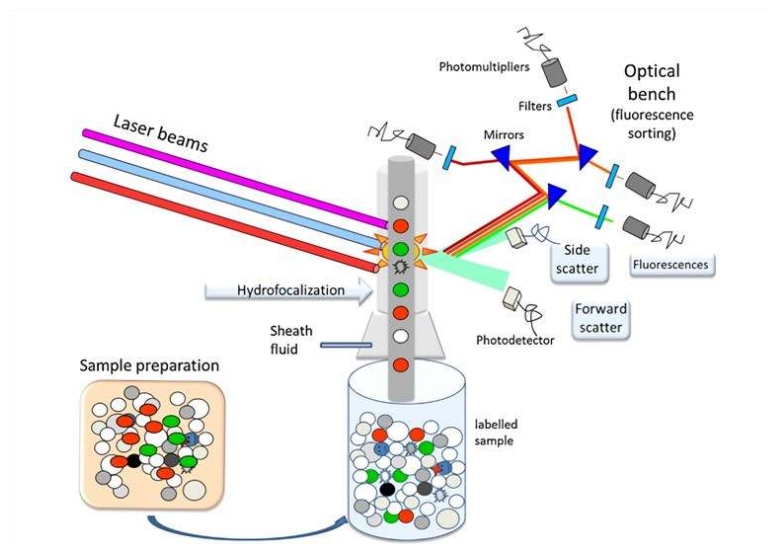
Figure 6. Scheme of the functioning of a Flow Cytometer. The sample, that has been stained, is suctioned and disposed in a one-cell line. Each individual cell hits the laser beams and emits fluorescent signal, that will be detected with different filters. Image obtained from Creative Biolabs (https://www.antibody-creativebiolabs.com/flow-cytometry.htm).

2.3.1 Staining protocol

2.3.1.1 Blood counts

The cell suspension was stained with 50 μL of the mix described in **Table 1**.

Table 1. Cellular markers used for the detection of populations in the blood.

Cell marker	Fluorophore	Clone	Company	Dilution
CD45	BV605	30-F11	eBioscience	1:100
CD11b	PerCP	M1/70	eBioscience	1:100
CD115	PE	AFS98	eBioscience	1:100
Ly6C	APC	HK1.4	Invitrogen	1:100
Ly6G	UV395	18A	BD Horizon	1:100
B220	APCy7	RA3-6B2	eBioscience	1:100
CD3	FITC	145-2C11	eBioscience	1:100

The cell suspension was incubated with the staining mix for 20 minutes on ice and in darkness. After staining, a washing step was performed in order to remove the antibodies that weren´t attached to the cell surfaces. The washing step was performed with 200 μL of HANKS and a posterior centrifugation for 5 minutes at 300 x g. The supernatant was removed and the cells were finally suspended in 400μL, ready to perform the flow cytometry analysis.

In order to normalize the amounts of cells among samples, 10μL counting beads (CountBright) were used and were added prior to the flow cytometry measurement.

2.3.1.2 BCA, kidney, lung and liver counts

The BCA, kidney, lung and liver from mice injected with BrdU (explained in **Section 2.1.1.2**) until obtaining a single-cell suspension (explained in **Section 2.1.2.1**), the single-cell solutions of different organs (lung, liver, kidney, bone marrow, BCA and blood) were stained with cell surface antigens (**Table 2**) solved in 50μL of annexin staining buffer (BioLegend). The cells were incubated with the antibodies for 15 minutes on ice and washed afterwards with 1 mL of staining buffer. The cells were permeabilized with 100μL BD Cytofix/Cytoperm Buffer for 30 minutes on ice. After the permeabilization, intracellular markers indicated in **Table 3** together with anti-BrdU antibody was added. The solutions of single cells were read in the Flow Cytometer.

Table 2. Surface markers used to detect different populations in the BCA, kidney, lung and liver

Cell marker	Fluorophore	Clone	Company	Dilution
CD45	BV605	30-F11	eBioscience	1:100
CD31	PECY7	MEC13.3	BioLegend	1:100

Table 3. Intracellular markers used to detect different populations and biological processes in the BCA, kidney, lung and liver

Cell marker	Fluorophore	Clone	Company	Dilution
Anti-BrdU	APC	Polyclonal	BD Biosciences	Indicated by manufacturer
Ki67	BUV-737	16A8		1/100
SMA	FITC	1A5	Sigma	1/500
anA5	Percp-Cy5.5	Polyclonal	Biolegend	1/100

2.3.2 Gating strategy

To perform the counts of the main cellular populations in blood and plaque, the following gating strategies were used. First, the single cells were isolated using FSC and SSC, in order to remove the droplets and debris. From the pool of single cells, the cells were classified according to the following table

Table 4. Gating strategies in blood and digested tissues (BCA, liver, lung and kidney)

	Blood	BCA, liver, lung, kidney
Leukocytes	CD45$^+$	
Stromal cells	NA	CD45$^-$
Classical Monocytes	CD45$^+$, CD11B$^+$, CD115$^+$, Ly6C^{hi}	NA
Non-Classical Monocytes	CD45$^+$, CD11B$^+$, CD115$^+$, Ly6C^{lo}	NA
Neutrophils	CD45$^+$, CD11B$^+$, CD115$^+$, Ly6C^{int}, Ly6G$^+$	NA

T cells	CD45$^+$, CD11B$^-$, B220$^-$, CD3$^+$	NA
B cells	CD45$^+$, CD11B$^-$, B220$^+$, CD3$^-$	NA

2.3.3 Analysis

The Analysis was performed with the software FlowJo version 10.1 (BD Biosciences).

2.4 Histology

The BCAs were cut using a cryostat (Leica), obtaining sections of 4 μm that were used afterwards for the staining.

2.4.1 Haematoxylin-eosin (H&E) staining

Haematoxylin and eosin staining were used to analyse the composition of the plaques in the BCA and assess their stage. This popular staining results from the combination of two dyes: haematoxylin, that will stain the basophilic structures of the tissue (as nuclei) and eosin, that will bind to the acidophilic structures (as the cytoplasm).

To perform this staining, the frozen sections were taking out from the -80º freezer and left to warm up in room temperature for 10 minutes. Afterwards, the sections would be submerged into PBS for 5 minutes, followed by a quick wash in distilled water. The sections were stained then with haematoxylin Mayer's solution (Merck) for 5 minutes and washed with running tap water for 5 minutes. The eosin staining was performed afterwards, using 0.5% Eosin (Roth) for 1 minute. The last step was to dehydrate the slides submerging them in increasing concentrations of ethanol:

- 50% EtOH, dip 5 times
- 70% EtOH, dip 5 times
- 96% EtOH, 2 minutes
- 100% EtOH, 2 minutes

The last step before mounting the tissue was to give the sections two washes of xylene of 5 minutes each, in order to displace the ethanol. The sections were afterwards mounted with mounting medium (ProLong Gold Antifade Mountant, Thermo Fisher) and were left to dry overnight under the hood.

2.4.2 Collagen staining

To stain the collagen in the plaques, we used Sirius Red Staining. It was described in 1979 by Junqueira [182] and it allows the identification of total fibrillar collagen[183].

To perform this staining, the frozen sections were taken out from the -80º freezer and left to warm up in room temperature for 10 minutes. Afterwards, the sections were washed with PBS for 5 minutes. Then, the sections were stained for 1 hour with the Sirius Red solution 0.1% which was created with the following ingredients:

- 0.2 g Sirius Red (Waldeck)
- 200 ml picric acid (Sigma)

After 1 hour, the sections were washed for 2 minutes in 0.01% hydrochloric acid solution (created from stock of 37% HCl, Merck). The slides were dehydrate following these steps:

- 50% EtOH, dip 3 times
- 70% EtOH, dip 3 times
- 96% EtOH, dip 5 times
- 100% EtOH, dip 10 times
- 100% EtOH, dip 10 times

The last step before mounting the tissue was to give the sections two washes of xylene of 2 minutes each, in order to remove the ethanol.

The sections were afterwards mounted with mounting medium (ProLong Gold Antifade Mountant, Thermo Fisher) and were left to dry overnight under the hood.

2.5 Immunohistochemistry

To quantify the different cellular populations in the plaque, as well as specific proteins, we used antibodies conjugated with fluorophores.

The sections for immunohistochemistry were kept at -80°C after being cut in order to maintain the integrity of the proteins. To perform the staining, the frozen sections were taken out from the -80º freezer and left to warm up in room temperature for 30 minutes. Afterwards, the sections were fixed with acetone (Roth) for 10 minutes at room temperature. The acetone was washed with PBS and the area of the section that was going to be stained was circled with a

PAP-pen (Dako) to prevent the antibody staining solution to spread. Then, the slides were incubating for 1 hour at Room temperature with blocking solution. After the incubation, the remaining blocking solution was washed with a quick dip in PBS and the primary antibody solution was added then to the area circled by the PAP-pen. The antibodies used can be seen in **Table 5**.

Table 5. Antibodies used for immunohistochemistry

Primary antibody

Cell marker	Fluorophore	Clone	Company	Quantity
Ki67	-	SP6	Abcam	1/100

Secondary antibody

Reactivity	Fluorophore	Clone	Company	Concentration
Donkey anti Rabbit	AF594	Polyclonal	Thermo Fisher Scientific	1/500

The primary antibodies were left overnight in order to increase the binding efficiency at 4°C. The primary antibodies were removed with 3 rounds of a combination of washes in PBS-Tween (a solution of PBS with 0.02% Tween) and PBS. The primary antibodies without a direct fluorophore conjugation were stained with secondary antibodies, that were left to bind for 1 hour at room temperature in a 1/500 dilution in a wet chamber in order to prevent the dry of the slides. The secondary antibodies were removed with 3 rounds of a combination of washes in PBS-Tween and PBS. The nuclei of the cells were stained with DAPI (4',6'-Diamidino-2-phenylindol, ThermoFisher Scientific) at 1/10000 dilution for 15 minutes at room temperature. The last wash to remove the unbonded DAPI was one time PBS-Tween and one time PBS. The sections were afterwards mounted with mounting medium (ProLong Gold Antifade Mountant, Thermo Fisher) and were left to dry overnight under the hood.

2.5.1 ApopTag staining

ApopTag staining it's an immunohistochemistry procedure in order to detect the cells that are going through an apoptotic process in tissues.

The base of this kit is to identify the DNA fragments, which is associated with apoptotic cells. It is described that large DNA fragments are produced in the early stages of apoptosis. These fragments have a free 3´-OH end, that can be detected enzymatically using this kit (**Figure 7**). This kit is able to differentiate apoptosis from necrosis due to the fact that in necrosis there´s not a higher amount of DNA cleavage. The same principle is used to detect apoptosis from normal cells, in which the amount of free 3´-OH is too low to appear as stained in a section.

The kit is commercially available (ApopTag Red in Situ Apoptosis Detection Kit from Merck) and the procedure was done following the instruction of the manufacturer. First, the slides were fixed in 1% PFA for 10 minutes at room temperature. Afterwards, the slides were washed twice in PBS for 5 minutes each. The permeabilization of the tissue was performed by submerging the slides in Ethanol-Acetic Acid (1:1) in for 10 minutes at room temperature and the Ethanol-Acetic Acid was then removed with 2 washes of PBS of 5 minutes each. The areas of the tissue that were going to be stained were circled using a PAP-Pen (Dako). To avoid unspecific attachment of the ApopTag staining, blocking solution (5% Horse Serum in PBS) was added to the tissue for 30 minutes at room temperature.

The samples were treated with 30µL Equilibration Buffer and was incubated for at least 10 seconds at Room temperature. The Equilibration Buffer was removed by shaking the slides and the Working Strength TdT Enzyme (30% Enzyme with 70% Buffer) was applied. The TdT Enzyme solution was incubated for 1 hour at 37 degrees. Afterwards, the reaction was stopped with the Working Strength Stop Wash Buffer (6 ml Stop/Wash Buffer in 204ml dH2O), that was incubated for 10 minutes at room temperature.

The slides were washed 3 times in PBS and the excess of liquid was removed by shaking. 30 µL for Working Strength Conjugate (53% Blocking solution and 47% anti-digoxigenin Conjugate) was applied and incubated in a humid chamber for 30 minutes at room temperature. Then, the
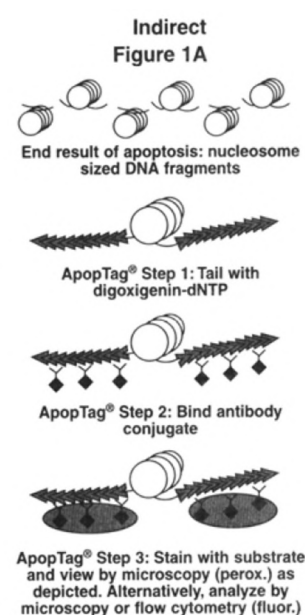
Figure 7. ApopTag® technology. Mechanism to detect cells undergoing early stages of apoptosis. Adapted from Merck Millipore©.

slides were washed in PBS four times and the sections were mounted using ProLong Gold Antifade Mountant (Invitrogen). The sections were left to dry overnight under the hood.

2.6 RNA-Seq Analysis

2.6.1 Sample preparation of BCA samples and other organs

The isolation of the RNA from the BCA for RNA-Seq procedures was performed using the RNeasy Mini Kit form Qiagen.

During the harvest, the organs were quickly put in 1mL Trizol in order to avoid the degradation of the RNA and they were homogenized as explained in **Section 2.1.2.1**. After the homogenization of the organs in Trizol, 0.2 mL of chloroform was added to every 1 mL of Trizol Reagent. The sample tubes were properly closed, and they were vortexed vigorously for 15 seconds. The samples were left at room temperature for 3 minutes and they were centrifuged at 4º and at a speed of 12.000 g for 15 minutes. After the centrifugation, the samples have separated in three phases: the lower one in a red colour (that contains all the proteins and membranes), a white interphase and an aqueous phase that contains the total RNA from the samples. This upper aqueous phase was transferred very carefully to a new tube and 1 volume of 70% ethanol (~600 µL) was added and mixed by pipetting. This mix was transferred to the columns of the RNeasy Mini Kit and the protocol from the manufacturer was followed. The column was placed in a 2ml collection tube and was centrifuged at >8000xg for 15 seconds. The flow-through that went from the column into the collection tube was discarded. If the volume of the mix of the upper phase and the ethanol was higher than 700 µL, the rest of the volume was added to the column and centrifuged afterwards.

Afterwards, 700 µL of Buffer RW1 was added to the column and centrifuged for 15s at >8000xg. The flow-through was discarded. 500 µL of Buffer RPE (with ethanol previously added) was added to the column and centrifuged for 15s at >8000xg. This step was repeated with another 500 µL of Buffer RPE and the sample was centrifuged for 2 minutes at >8000xg. The column was placed in a new 2ml collection tube and was centrifuged at maximum speed for 1 minute in order to dry the column and get rid of any possible leftover of the different Buffers. The column was then placed in a 1.5mL collection tube and 30 µL of RNAse-free water was added directly to the column. The column was centrifuged for 1 minute at >8000xg to

elute the RNA. Since we were expecting low amount of RNA, the elution was added again to the column and centrifuged for an additional minute at >8000xg.

The libraries were prepared in collaboration with Susanne Blachut from the Hübner Laboratory in the Max-Delbrück-Centrum für Molekulare Medizin in der Helmholtz-Gemeinschaft Center in Berlin. The strategy for the sequencing of the samples was to use TruSeq Stranded mRNA kit from Illumina, which created paired-reads of 75 base-pairs. The depth was stablished at 40 million reads per sample, for a total of 34 samples of BCAs harvested at 6 different timepoints of the day.

The isolation of the RNA of the rest of the organs that were analysed (Spleen, liver, kidney, colon, ileum, heart, lung, adrenal gland and white adipose tissue) was performed by PhD Katja Chernogubova, Research Coordinator at the Group of Molecular Vascular Medicine from the Karolinska University Hospital in Sweden following the protocol explained above. All the RNA isolated from the different organs from *Apoe*$^{-/-}$ and C57BL/6J mice were sent to an external provider (Novogene), who performed the library preparation and sequencing of the samples.

2.6.2 Sample preparation of Human samples

Human carotids from scheduled atherectomies were collected after surgery at different times of the day, from 8am until 18:30pm. The samples were prepared by the Department of Vascular Surgery from the Klinikum rechts der Isar (Technische Universität München) in collaboration with the research group of Lars Maegdefessel. The method used for the isolation of the RNA was trizol-based protocol, as explained in **Section 2.6.1**, but without the column purification; the upper phase created by the centrifugation after adding chloroform was mixed with isopropyl alcohol in order to precipitate the RNA, which was washed afterwards with ethanol and resuspended in RNAse free water.

The RNA was sent to an external provided (Novogene) in order to sequence the transcriptome.

2.6.3 Bioinformatics analysis

2.6.3.1 Quality control
The fastq files received from the external provider after the sequencing went first through a quality control check, in order to make sure that each sample has the same amount of reads

and that most of these reads had the desired length. Also, the possibility of contaminants was also checked.

For the quality control, we used the free-available program FastQC[184]. The different fastq files were visually checked in order to remove samples that had a very different library.

2.6.3.2 Mapping protocol

In order to associate every read to a mouse gene, we used STAR as aligner[185]. STAR is very well-known mapper created in 2013 that combines efficiency and accuracy when mapping well annotated genomes, as the mouse genome. STAR has been designated as the fastest mapper in several reviews comparing different mappers[186] and furthermore, combines a very low rate of false positives, with an adequate memory consumption[187].

The last version of STAR (STAR 2.7.9a) was downloaded from github (https://github.com/alexdobin/STAR) and was compiled under Linux, as indicated by the STAR developer.

The reference genome for human and mouse was downloaded from the ENSEMBL database, using the last version available in the moment of the sequencing:

- Mus_musculus.GRCm38.dna_rm.primary_assembly.fa.gz for mouse
- Homo_sapiens.GRCm38.dna_rm.primary_assembly.fa.gz for human

The first step to map the samples to the reference genome was to create the genome index. In this previous step, STAR creates an index of the reference genome to set up an order within the genome as an effort to reduce the computing time when mapping the samples (it´s basically like creating an index of a book). It very recommendable to set up an index before running the mapping when using extremely big genomes, as human or mouse genomes. To perform the genome index, a file with the complete genome in fasta is needed, besides a gene transfer format (GTF) file, which is a file that contains the annotation of the genome. The GTF file will have for each known gene information about the chromosome in which it´s located, the name of the gene, the start and end position within the chromosome, the strand…. among other data. The parameter "sjdbOverhang" is defined as "the length of the donor/acceptor sequence on each side of the junctions", which implies the maximum possible overhang for on read with the next aligned read (Information extracted from STAR manual version 2.7.10a).

This parameter is recommended to be set to the maximum read length-1 (sum of forward and reverse reads in the case of pair reads), so in our case is set up to 149.

When the mapping was done, several files were obtained. The file with the mapping result is the Sequence Alignment Map (SAM), which is a TAB-delimited file that has the information of where each read has been mapped, as well as the quality and accuracy with which it was mapped. The SAM file was used for the following steps in the pipeline.

The rest of the files created as output have information about the mapping process and the status of the mapping and were used to assess the quality of the process. As control check to detect libraries not correctly created, sequencing errors or mapping problems, these mapped results were checked, especially the following parameters:

- Uniquely mapped reads %
- % of reads mapped to multiple loci
- % of reads mapped to too many loci
- % of reads unmapped. Too many mismatches
- % of reads unmapped: too short
- % of reads unmapped: other

2.6.3.3 SAM and BAM files

With the SAM file created by STAR, the pipeline was continued. Besides the mapping information, the SAM file has also information considering the quality of the mapping, and they were also checked in order to detect abnormalities.

The SAM file has two different parts:

- The header
- The alignment section, with different fields with information about the position of the read, the quality of the mapping, the number of matches and mismatches within the read…. Among others.

For a quality checked, we focused on the FLAG and MAPQ columns

- The MAPQ (Mapping Quality) gives information about the probability that the mapping position is wrong.
- The FLAG informs about the presence of mistakes, mismatches, or other problems in the mapping[188].

Once the information about the mapping quality had been checked, the SAM files were transformed into BAM files, which is the binary form of SAM files. This transformation needs to be done in order to save storage but also because the BAM files are easier to manage and to manipulate.

To make the conversion, samtools was used. Samtools is a group of programs that analyse and process sequencing data[188]. The last version available (samtools-1-13) of the set of packages was downloaded from the official website (http://www.htslib.org/download/) and was installed following the instructions available on the website. To transform all the sam files into bam files, the command *view* was used.

Lastly, the BAM files were sorted, which facilitates the posterior creation of the summary table with the counts of each gene in each sample. The command *sort* from the package samtools was used to sort the samples.

2.6.3.4 Creation of the count matrix

Once all the BAM files had been sorted, it was time to create the final count matrix, that will contain the counts of every detected gene in each of the samples.

There are many programs that are able to perform this step, but one of the fastest and most user-friendly is the R-package Rsubread[189]. And afterwards the following command was launched in R Studio.

counts = featureCounts(files, annot.ext = "Mus_musculus.GRCm38.101.chr.gtf" , isGTFAnnotationFile = TRUE, GTF.featureType = "exon", GTF.attrType = "gene_id", GTF.attrType.extra = NULL, chrAliases = NULL, useMetaFeatures = TRUE, allowMultiOverlap = FALSE, isPairedEnd = TRUE, nthreads = 30, verbose=TRUE)

The command indicates the lists of bam files and the annotation of the genome, which is kept in a gtf file. Furthermore, the features that will be displayed in the final count matrix can be selected. Since the focus of the project is the study of the regulation of different genes at different times of the day, the chosen attribute was the gene, as it is indicated in the parameter "GTF: attrType".

2.6.3.5 DESeq2

DESeq2 is a broadly used R package designed to analyse Bulk RNA-Seq data using a negative binomial distribution. DESeq2 is designed as a method to study differential expression analysis among groups. Furthermore, for other types of analysis in which the different expression among groups is not performed (as it can be the assessment of the oscillation of genes across 24h) the normalization process implemented in the package, allows for a fine control of outliers and dispersion control. DESeq2 was also used to perform Heatmaps.

The counts obtained in the Package Rsubread (explained in the **Section 2.6.3.4**) were loaded into DESeq2 and a first filter to differentiate which genes were considered as expressed was performed. The threshold used was a minimum average of 10 reads per gene to consider a gene as expressed. Afterwards, a normalization was performed to scale the raw counts considering the library size.

The heatmap graphs are created using the package *pheatmap*, in which the object created in DESeq2 is directly loaded. The clustering method is calculated using Euclidean distances for rows and for columns.

Furthermore, DESeq2 was also used for the analysis of differential expressed (DE) genes between timepoints. For this, a Wald test comparison was applied followed by Bonferroni post-hoc correction using a threshold of q-value<0.1.

2.6.3.6 Outlier detection

After the normalization of the libraries, a test to detect the outliers per organ was performed. The samples were filtered according to Pearson correlation coefficient (test provided by DiscoRhythm package, explained in **Section 2.6.3.7.2**). The samples were filtered according to a two-step filtering:

- The correlation all each sample when considering all the timepoints from a genotype shouldn´t be smaller than 0.75 or 3σ (applying the most restrictive parameter)
- When comparing the two genotypes, the difference of the average correlation within all the samples shouldn´t be bigger than 0.1.

The correlation among all the samples in $Apoe^{-/-}$ and C57BL/6J is detailed in **Table 6**. The final number of samples per organ and per genotype is described in **Table 7**.

Table 6. Average correlation of all the sequenced samples in *Apoe*^{-/-} and C57BL/6J

	Average correlation Apoe^{-/-}	Average correlation C57BL/6J
Adrenal gland	0.9833	0.9823
Aorta	0.9735	0.9703
BCA	0.9000	0.9563
Colon	0.9029	0.9579
Heart	0.9969	0.9971
Illeum	0.9001	0.9316
Kidney	0.9959	0.9958
Liver	0.9855	0.9920
Lung	0.9865	0.9884
Muscle	0.9933	0.9885
Spleen	0.9076	0.8994
W.A.T.	0.9842	0.9488

Table 7. Total number of samples per genotype and per timepoint considered in the analysis.

	Outliers *Apoe*^{-/-}	Final N *Apoe*^{-/-}	Samples per timepoint	Outliers C57BL/6J	Final N C57BL/6J	Samples per timepoint
Adrenal gland	1	41	6-7	1	39	5-7
Aorta	1	37	5-7	1	34	5-7
BCA	1	27	4-5	2	21	2-5
Colon	3	38	5-7	2	38	4-7
Heart	1	41	6-7	1	37	5-7
Ileum	3	39	5-7	1	37	5-7

Kidney	2	39	6-7	2	38	6-7
Liver	5	36	5-7	1	36	6-7
Lung	5	35	4-7	1	36	4-7
Muscle	1	38	5-7	1	39	5-7
Spleen	0	42	7	1	39	6-7
W.A.T.	1	34	5-7	3	39	4-7

2.6.3.7 Oscillation pattern detection

The gene counts were analysed in order to detect the genes that show oscillatory patterns across 24h. For this purpose, we used two different R packages: Metacycle[190] and DiscoRhythm[191].

2.6.3.7.1 Metacycle

MetaCycle[190] is a publicly available R package that combines the analysis of different algorithms in order to detect oscillatory patterns among the transcriptome.

The combination of these several algorithms allows for a more robust result, in which the false positives are reduced. The algorithms that MetaCycle uses are ARSER[192], JTK_CYCLE[193] and Lomb-Scargle (LS)[194]. All the three algorithms have pros and cons that have been reviewed by the authors of MetaCycle using user´s experiences and several papers. This revision is available in the CRAN vignette from MetaCycle (https://cran.r-project.org/web/packages/MetaCycle/vignettes/implementation.html).

Briefly, ARSER is less influenced by noise and has a uniform P-value distribution, but it has a decreased value when analysing only one cycle of samples. JTK_CYCLE is very efficient and more robust to outliers but is biased by the Cosine curve and shows an abundant number of false negatives. LS classifies correctly signal and noise but has a high false negative rate in low sampling data. MetaCycle is presented as a solution to improve the accuracy in phase prediction and has a con the use of independently calculated p-values that have to be integrated by a post-hoc correction, as Fisher or Bonferroni and that can increase the false negatives.

The function *meta2d* from the MetaCycle package was used in order to detect the oscillatory genes from the transcriptome. Since the dataset contained replicates and the sampling was evenly done and without missing values, the algorithm ARSER was not included in the analysis, as it is recommended in the MetaCycle manual and vignette.

As post-hoc correction method, Fisher´s method, implemented also by MetaCycle, was performed.

We considered as part of the transcriptome the genes whose expression was higher than 10 normalized counts in average when considering all the samples.

2.6.3.7.2 DiscoRhythm

To complement the analysis realized by Metacycle and increase the robustness of the results that we obtained with Metacycle, DiscoRhythm was used to detect the oscillatory genes in the Bulk-RNA samples.

DiscoRhythm[191] is a R package which estimates different parameters (phase and amplitude) of the transcriptome using different algorithms (Cosinor, JTK Cycle, ARSER and Lomb-Scargle). The novelty of this package respect to Metacycle is the use of Cosinor, which was originally designed for data that was collected in non-equidistant periods[195], but with the extended method is used in combination with the other algorithms to calculate the period of the oscillation[191].

2.6.3.7.3 Cosinor regression

For the graphs in which the pattern of expression of different proteins, genes and pathways were represented, the cosinor adjustment of the data was calculated using Nonlinear regression model in GraphPad Prism 9 (GraphPad Software Inc). The equation used was the following:

$$Y = Baseline + Amplitude * cos(Frecuency * X + PhaseShift)$$

Using as initial values:

- Baseline=1
- Amplitude=0.5
- Frequency=0.2618
- PhaseShift=1

3.6.4.8 Enrichment analysis

In order to run an enrichment analysis with all the oscillating genes, a Java-based tool called Phase set enrichment analysis (PSEA)[196] was used.

This tool creates an analysis that can be divided in three steps:

- First step is the identification of genes that belong to the same biological group and that are transcribed with the same or similar phases. This identification of groups that are biologically related and that are expressed in a similar manner is done by using the Kuiper test. The Kuiper test compares the similarity of acrophases of the genes that belong to a specific group with the similarity of a randomly selected group of genes from the background. The background can be the total amount of genes provided or a uniform background distribution.

- Once a set is classified as "non-random" distributed phases or is classified as having a different behaviour from the genes in the background, the circular mean phase is calculated. This step calculates the "average" phase of the group of genes. The Circular mean is composed by two magnitudes: the phase and the magnitude
  - The phase measures the timing of the group of genes
  - The magnitude indicates how variable the acrophase inside the group of genes is (for example, a group of genes in which the genes have very similar acrophases would have a big magnitude)

- The last step quantifies the weight of each gene to the uniformity of the group. It is a useful step to identify "outlier genes" or genes that don't follow the pattern of the rest of the group. The authors of the technique implemented a "leave-one-out" approach, in which each gene is removed individually of the group and the Kuiper test is re-calculated with the remaining group of genes.

For this analysis, a file with the information about the interesting groups of genes or pathways needs to be provide for the user. We used the curated gene set from Reactome provided in the GSEA website (version 7.5.1, url: https://www.gsea-msigdb.org/gsea/msigdb/human/collections.jsp). The selected parameters for the PSEA analysis were a maximum simulations per test of 100000 with a q-value maximum of 0.1

Besides PSEA, in the cases in which the number of oscillating genes was not big enough to consider an acrophase-dependent enrichment analysis, a broad picture of the pathways that appear as enriched was provided by Enrichr[197], a web-based tool for gene-set analysis. The

selection of this tool was made based on its user-friendly interphase and its ability to provide fast and accurate information about the over-representation of pathways. In our case, we used the information provided by Enrichr using as background the database Reactome. Enrichr uses three approaches to calculate the enrichment in the dataset: the Fisher exact test (which assumes a binomial distribution and independence of each gene), a z-score that assess the deviation from the expected rank and a combination score of both[198].

2.7 Protein isolation for Proteome

The preparation of the samples for Proteomics analysis was performed according to the protocol published by Sean J. Humphrey in Nature protocols[199] and the isolation and analysis was performed in collaboration with Shibojyoti Lahiri from the group of Prof. Dr. Axel Imhof from the Biomedical Center Munich (LMU).

The arches from *Apoe$^{-/-}$* mice were used to extract proteins and perform the proteome measurement. Briefly, the protocol consisted in the preparation of a lysate of the tissues using chemical compounds (lysis buffer) and mechanical compounds (sonicator) in order to disrupt the tissue. Afterwards, a BCA (Bicinchoninic acid assay) assay was performed to quantify the proteins and create the dilutions of the samples in order to have them at the same concentration. The next step was the reduction and alkylation of the disulfide bonds to break the bonds that keep the quaternary structure of the proteins. The proteins were there digested using trypsin to create peptides. The samples for whole proteome were measured with LC-MS/Ms (Liquid chromatography-mass spectrometry). The measurements were taken by Ignasi Forné from the group of Prof. Dr. Axel Imhof.

2.7.1 Bioinformatics analysis

The package Differential Enrichment analysis for Proteomics data (DEP)[200] was used in order to detect differences in the expression of proteins between timepoints.

As first step, the amount of proteins detected in each sample was compared in order to eliminate samples with low detection, as shown in **Figure 8**.
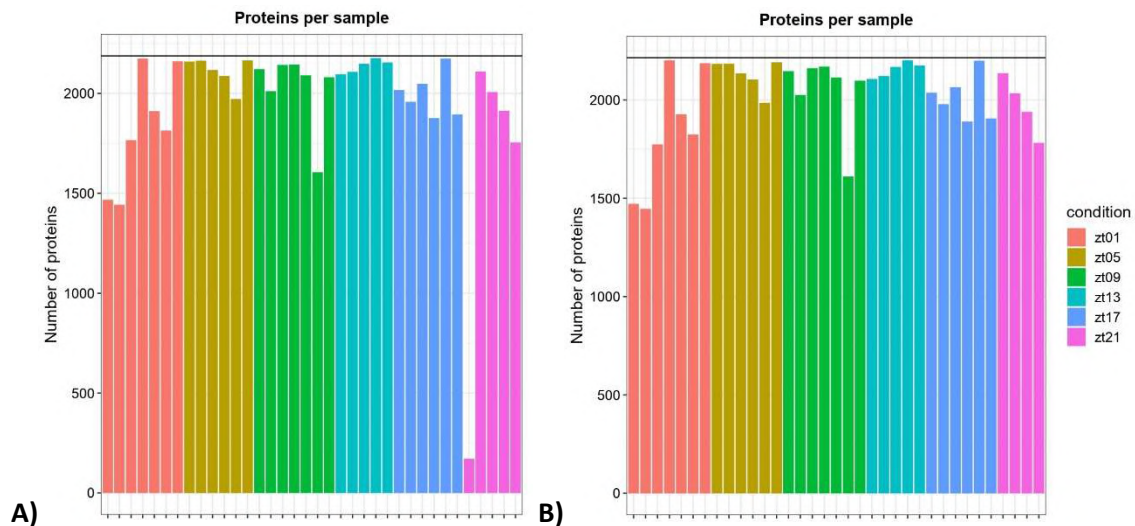
Figure 8. Representation of the number of proteins detected per sample. **A)** Quantification of the total amount of proteins detected per sample. The first sample belonging to the ZT21 group had a very inferior amount of proteins detected and was therefore eliminated. **B)** Final group of samples that were used for proteomics analysis.

With the non-eliminated samples, a differential expression analysis was performed without any imputation method for the missing values. With the proteins that were differentially expressed (considering an adjusted P-value ≤ 0.001 and a Log2 fold change ≥ 0.2) between any comparison among timepoints, an enrichment analysis using Reactome database implemented in EnrichR was performed (explained in **Section 3.6.4.8**).

2.8 Single Cell Sequencing

A single cell sequencing analysis from the BCA of *Apoe^-/-* mice was performed at two different timepoints (ZT1 and ZT13) to study the oscillations in the different populations of the atherosclerotic plaque.

2.8.1 Cell isolation for Single Cell Sequencing

The BCA and the blood of mice were harvested in order to perform bulk RNA-sequencing at the single cell level. We were interested in the study of the expression of genes in specific populations inside the plaque and how these specific genes would oscillate in a circadian

fashion. Furthermore, the analysis of the oscillation of the cell populations in the blood would give a broad image of the changes in the whole organism.

The BCA were extracted from mice at ZT1 and at ZT13. The BCA were cut into small pieces that were digested in Digestion Medium (RTI supplemented with 10% FCS) with liberase at a final concentration of 1.25 mg/ml (Roche). The BCA stayed in the digestion Medium for 55 minutes at 37°C. The digestion was stopped by adding 5 ml Hanks and it was filtered using a 100 µm strain. It was centrifuged to allow the pass of the cells through the strain at 300xg for 5 minutes. From all the processed BCAs, 10 BCAs (5 per timepoint) with best cellular populations (enough cell composition, representation of most of the cellular populations and best cellular viability) were chosen for further processing.

Since the different cell populations that were interesting for the project are presented in the plaque with very different proportions, two different approaches were followed. First, to get a general overview of the plaque, the digested BCA from 5 different animals per timepoint were labelled individually and pulled together. Secondly, in order to be able to detect populations that are not so abundant in the plaque, such as neutrophils or endothelial cells, the digested BCA was sorted to manipulate the proportions of each population, to increase the representation of these low-abundant populations and having an equilibrated representation of every population. The antibodies used for sorting the populations are listed in **Table 8**. The sorter used was a BC FACSAria III Cell Sorter (BD Bioscience).

Table 8. Antibodies used for sorting BCA samples prior to single-cell sequencing

Flurorophore	Antibody	Clone	Company	Targeted population
APCy7	CD45	30-F11	BioLegend	Leukocytes
PeCy7	B220	RA-3-6B2	BioLegend	B-cell
	Ly6G	1A8	BD Biosciences	Neutrophils
	CD31	MEC13.3	BioLegend	Endothelial cells
PerCP	CD3	17A2	BioLegend	T-cell
APC	F480	BM8	BioLegend	Macrophages and Microglia
	CD11b	M1/70	BD Biosciences	Macrophages

The blood was collected as explained in the **Section 2.1.2.1**. The different BCAs and the different samples of blood were stained with specific Hashtags that would allow to associate each BCA and blood sample to a specific mouse after demultiplexing.

The Hashtags (commercially known as TotalSeq-A and available at BioLegend) are antibodies conjugated to a unique oligonucleotide that contains an antibody Barcode. The cell suspension of each BCA or blood sample is incubated with a specific and different TotalSeq-A antibody that will attach to the surface of every cell in the sample. When the droplet separation happens and the posterior rupture of the cell takes place, the different copies of the antibody that were attach to the membrane of the cell will be in direct c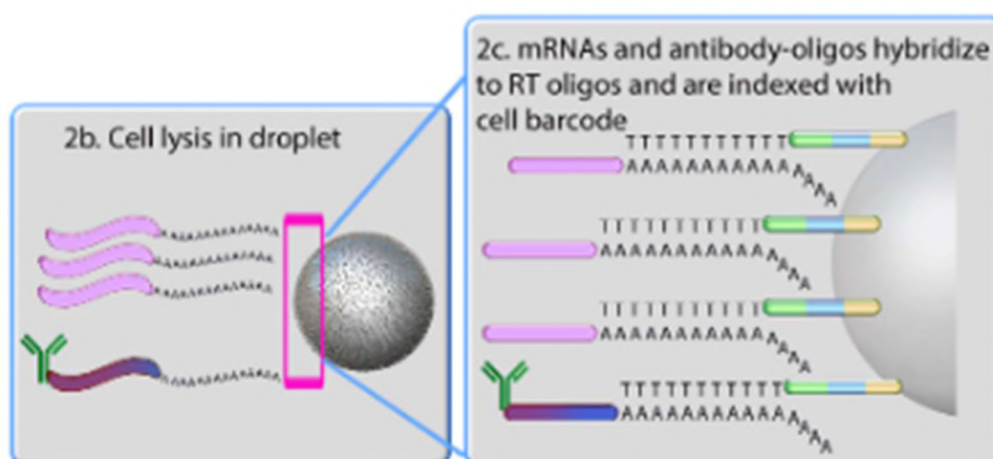ontact with the mRNA molecules that were carried by the cell. A posterior PCR will allow to integrate the Hashtag into the mRNA of every cell in each BCA or blood sample, creating the antibody-derived tags (ADTs), that would be separated from the mRNA-derived cDNA[201]. This process is explained in **Figure 9**.

A)
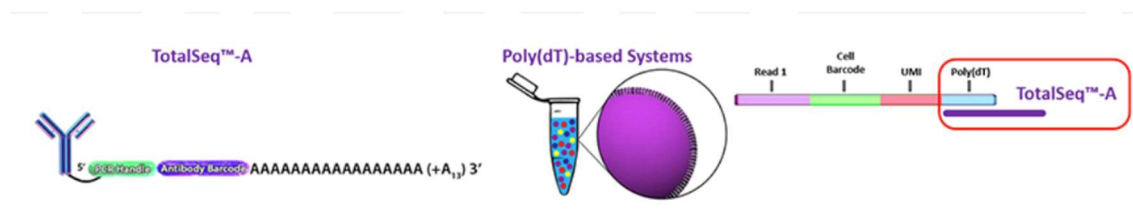
B)

Figure 9. Cell hashing with TotalSeq^{TM}. A) Schematic representation of an antibody-oligonucleotide conjugate. Adapted from BioSite (https://nordicbiosite.com/news/totalseq-

antibody-oligonucleotide-conjugates-reagents). **B)** Representation of the antibody-oligonucleotide conjugate and the oligos inside a droplet. The RT oligos without the antibody will be used for mRNA-derived cDNA library, while the antibody-oligonucleotide conjugate will create the antibody-derived tags (ADTs) library. Adapted from BioLegend (https://www.biolegend.com/en-us/totalseq-ebook).

2.8.2 Library protocol

After putting the right concentrations of each cell population, the 10x Chromium Next GEM Single Cell 3´ Regents Kits Protocol v3.1 (CG000206, 10xgenomics) was performed in order to be able to sequence the cell suspension and correctly associate every mRNA molecule to a specific individual cell and specific mouse.

The protocol starts with loading a Chromium Net GEM Chip G with the cell suspension. In this commercially available Chip, partitioning oil, gel beads and necessary reagents (template Oligos, Enzyme and buffer) perform a first PCR will be loaded. In this first step, the cell suspension would be conducted through microscopic capillaries to create a single cell row. This would allow each gel bead to surround one single cell and part of the components of the master mix, which is known as GEM (Gel Beads in Emulsion).

In the next steps, the cell would break, setting free all the mRNA molecules. The necessary reagents for the PCR, that were included in the master mix, would allow a first PCR step that would add to each molecule of mRNA a specific tag, used to associate each cell to a specific mouse. After this first PCR, several clean up steps would follow and the cDNA will be produced from the original mRNA. The cDNA will be amplified to increase the amount.

The final step would be to create the library, in which specific adapters would be attach to the cDNA. These adapters are necessary for the following RNA sequencing. The libraries were sent to an external provider (Novogene) to be sequenced.

2.8.3 Bioinformatics analysis

3.8.3.1 Mapping protocol
The mapping protocol was performed with the software "Cell Ranger" (version 6.1.2), provided by 10X Genomics.

Each lane was mapped using the function *count* and the mouse reference genome used was mm10 from 2020, available also from 10X Genomics.

For the lanes that needed to be compared, a further aggregation using the function *aggr* was performed. The option normalization was selected to scale the number of cells among the different lanes that were going to be compared.

3.8.3.2 Analysis

The analysis in order to create the single cell object was performed with the Bioconductor package *SingleCellExperiment*. Furthermore, the demultiplexing of the cells into different samples that allowed us to compare different timepoints was performed with the package DigestiFlow Demux.

In order to have a group of cells whose sequencing had been successful, the cells with less than 50 hashtags were eliminated. Furthermore, the cells expressing less than 500 genes were also removed, to make sure that most of the analysed population was in good quality in the moment of loading. Data was normalized using the scran pagkage[202], in order to avoid differences in capture efficiency and sequencing depth.

Lastly, the single cell object was separated in order to compare the expression of different genes between leukocytes ($CD45^+$ cells) and stromal cells ($CD45^-$ cells) at the two different timepoints.

3. Results

3.1 There are circadian changes in the plaque that affect many biological functions

In order to study the circadian changes in the advanced atherosclerotic lesion, *Apoe*^{-/-} mice that were fed with HFD for 16 weeks and sacrificed in intervals of 4 hours. In these mice, the atherosclerotic BCA was harvested, total RNA was extracted and mRNA was sequenced to study the daily oscillations of the transcriptome in the advanced atherosclerotic lesion.

3.1.1 An important percentage of the transcriptome of the atherosclerotic plaque changes during the day

Using mRNA isolated from the atherosclerotic plaques, we performed Poly A+ bulk-RNA sequencing (as explained in **Section 2.6.1**) with an average of 55.4 million 125-base pair reads per sample. The quality of the libraries was similar in all the samples, with a high ratio of uniquely mapped reads (average of 44.2 million reads). We successfully mapped an average of 80% reads (43.6 million reads) per sample (**Figure 10**).

The comparison among the different timepoints shows that a high proportion of genes have differences in their expression values through the day. Up to 14622 genes (72.28% of the total transcriptome) are differentially expressed (DE) when comparing any of the 6 different timepoints (**Figure 10.B**). There are differences in terms of the number of genes differentially expressed at different timepoints: ZT5 appears to be the most different timepoint with 12652 DE genes, followed by ZT17 and ZT9. On the other side, ZT21 exhibit the least differences when compared with the rest of the timepoints, having only 6687 genes DE.

Furthermore, when comparing pairs of timepoints with DESeq2 as explained in **Section 2.6.3.5**, we could also see an important variability among the number of genes that are DE, being ZT5 vs ZT17 the most different groups with 8786 genes DE and ZT9 vs ZT13 the most similar timepoints, with only 552 genes DE (**Figure 10.C**).
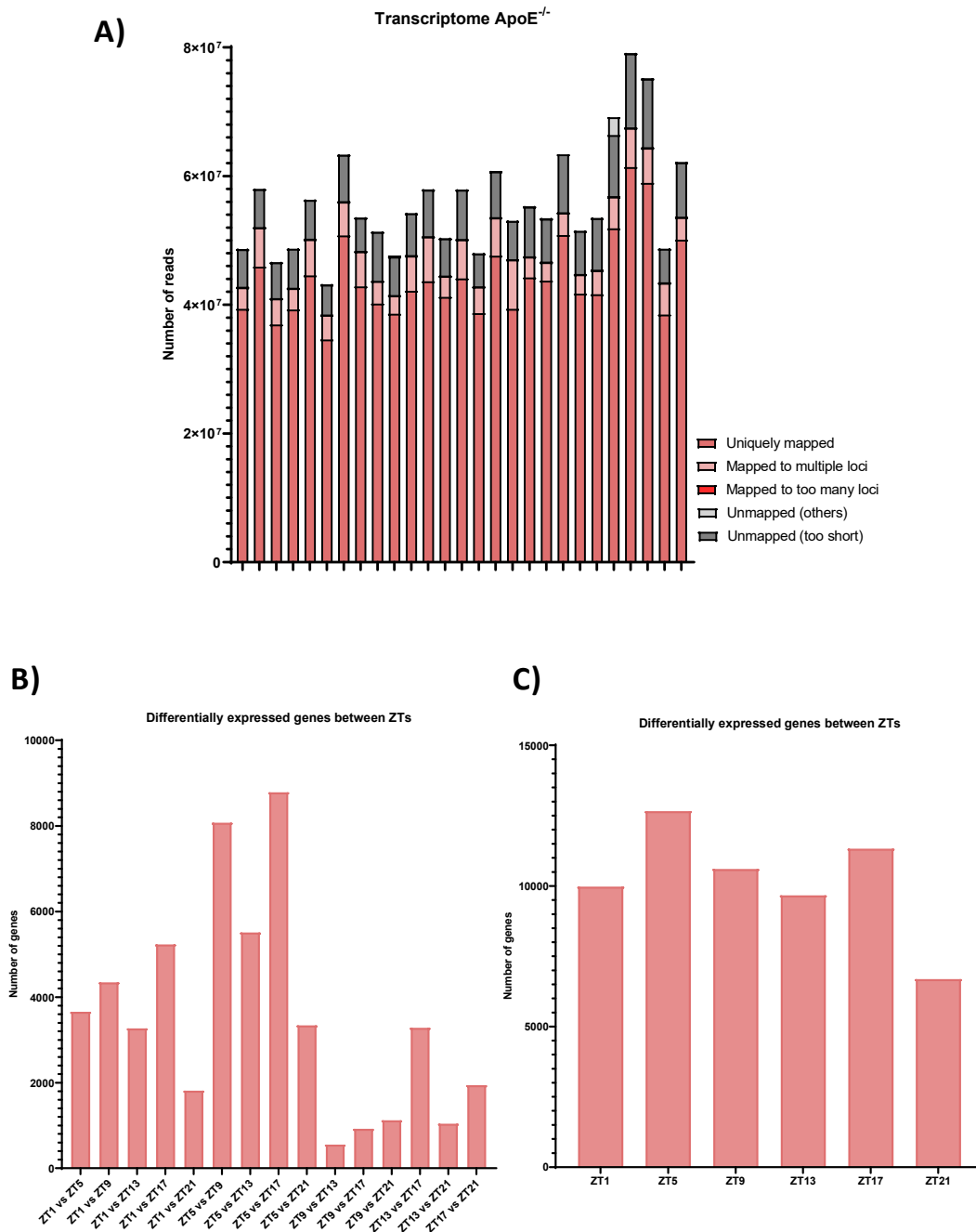
Figure 10. Library composition and transcriptomic differences between timepoints. A) Composition of libraries for each sample. Uniquely mapped reads and reads mapped to multiple loci when the number was lower than 10 loci were considered for subsequent analysis. **B)** Pairwise comparison between pairs of timepoints **C)** Pairwise comparison of the different timepoints, comparing one timepoint against all the rest. DE genes calculated using Wald test comparison and Bonferroni post-hoc correction (q-value<0.1).

Comparing in a pairwise manner the different timepoints helped us to get an idea about the differences in term of expression when comparing different timepoints of the day, but to detect 24h oscillation rhythms, we applied a high-throughput methodology that would comprise the whole transcriptome and all the timepoints available. To detect the genes that showed oscillation during the day, we used the R packages Metacycle[190] and DiscoRhythm[191]. The combination of the outcome of the two packages was done by combining all the genes that had a FDR<0.1 and an adjusted p-value<0.05 in any of the methods used by Metacycle and DiscoRhythm that would fit the composition of our dataset (**Figure 11.A**). The implementation of two algorithms allowed us to detect genes that had different patterns of oscillation, as can be seen in **Figure 11.B-G**. Metacycle was capable of detecting genes that had a peak or valley of expression in one or two times of the day (**Figure 11.E and 10.F**) while these genes were not detected by Cosinor algorithm.

We observed that there is an important percentage of the transcriptome (5534 genes out of 20229 genes, or 27.35%) that shows circadian oscillation at the gene expression level. When considering only the protein coding genes (PCG), 4162 PCG (26.60%) showed oscillation in the complete protein-coding transcriptome, composed by 15647 elements (**Figure 12.A**).

The changes of expression among genes were very variable, showing log2FC from 0.1 until almost 12 and with an average of 0.89, when comparing the highest and the lowest value of each gene across all timepoints (**Figure 12.C**). This variability indicates different sensitivity for each gene to the circadian changes together with the idea that there is aver complex downstream regulation from the core clock genes into more specific pathways and individual genes, in order to achieve a fine regulation of the expression in each gene.
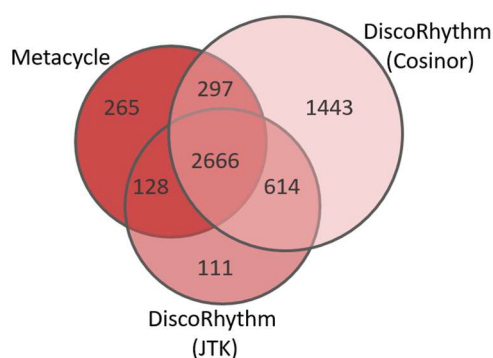
A)   **B)**
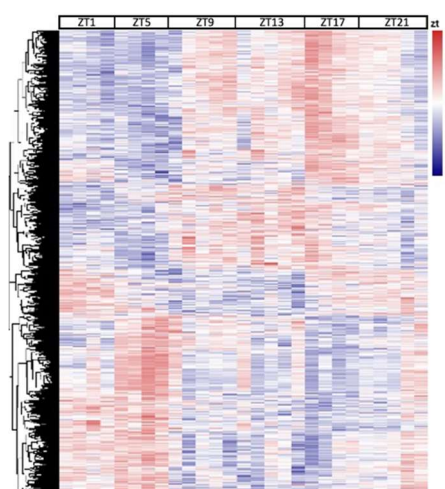
C)
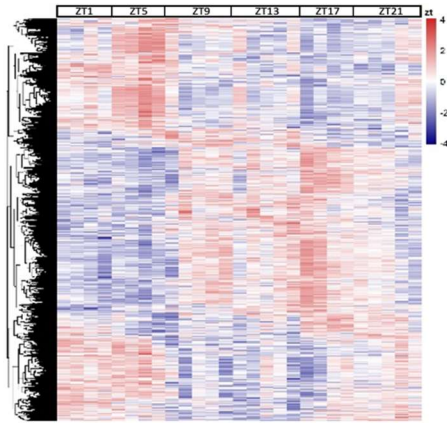
D)
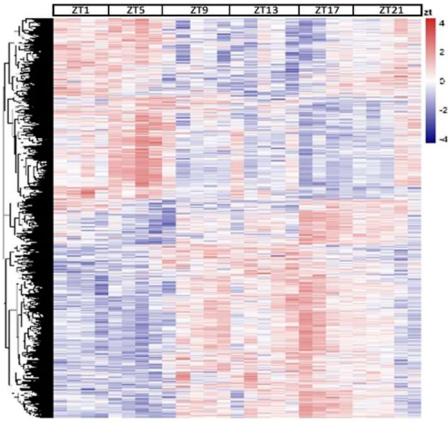
E)
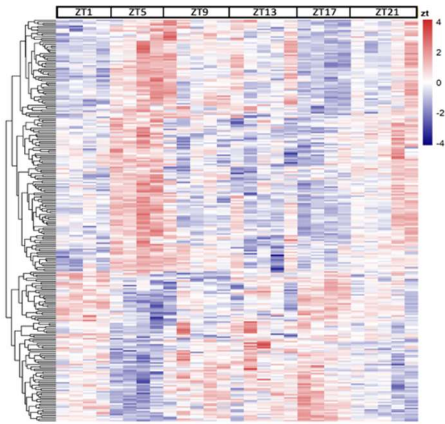
F)
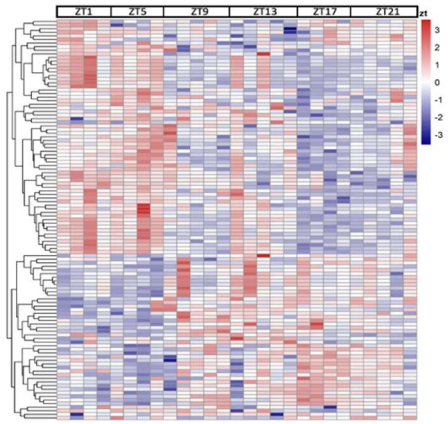
G)
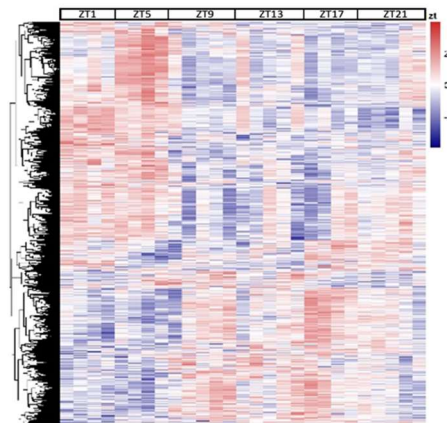
Figure 11. Oscillating genes in the BCA from *Apoe*-/- using different algorithms. A) Scheme of the origin of all the genes detected as oscillating. **B)** Heatmap showing genes detected as oscillating in Metacycle package (3356 genes). **C)** Heatmap showing genes detected as oscillating in Cosinor from Discorhythm package (5020 genes). **D)** heatmap showing genes detected as oscillating in JTK from Discorhythm package (3519 genes). **E)** Heatmap showing

genes only detected as oscillating in Metacycle package (265 genes). **F)** Heatmap showing genes only detected as oscillating in JTK from Discorhythm package (111 genes). **G)** Heatmap showing genes only detected as oscillating in Cosinor from Discorhythm package (1443 genes).

Transcriptome BCA - Apoe$^{-/-}$

PCG BCA - Apoe$^{-/-}$

A)

B)

C)
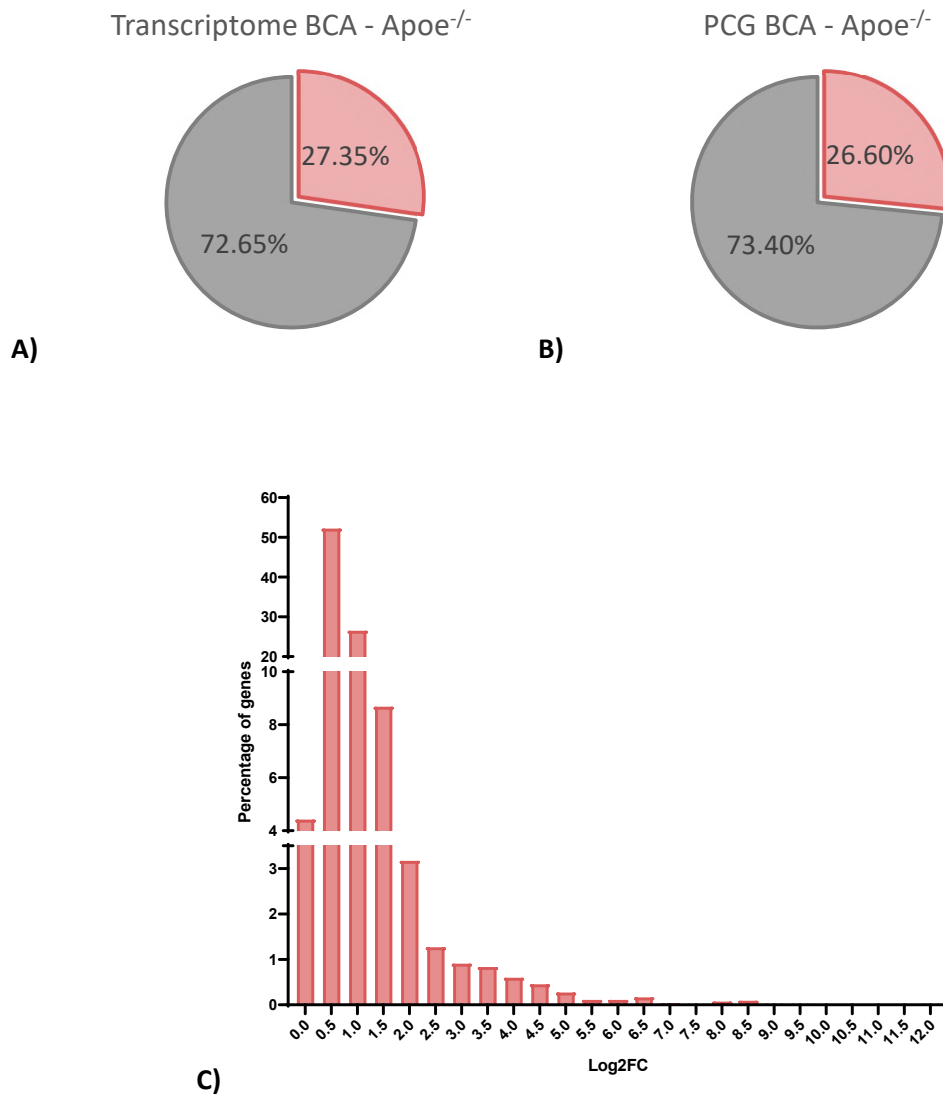
Figure 12. Percentage of oscillating genes in the transcriptome and distribution of its amplitude. A) and **B)** Percentage of oscillating genes **(A)** or oscillating PCG **(B)** from the total transcriptome. **C)** Histogram of amplitudes across all the oscillating PCG, having a maximum amplitude of 11.94.

3.1.2 The circadian oscillation of genes creates a temporal separation of biological functions

The total amount of oscillating genes can be divided into two big groups: one showing highest values at ZT1, ZT5 and other group showing highest values between ZT9, ZT13 and ZT21, as can be seen in **Figure 13**.
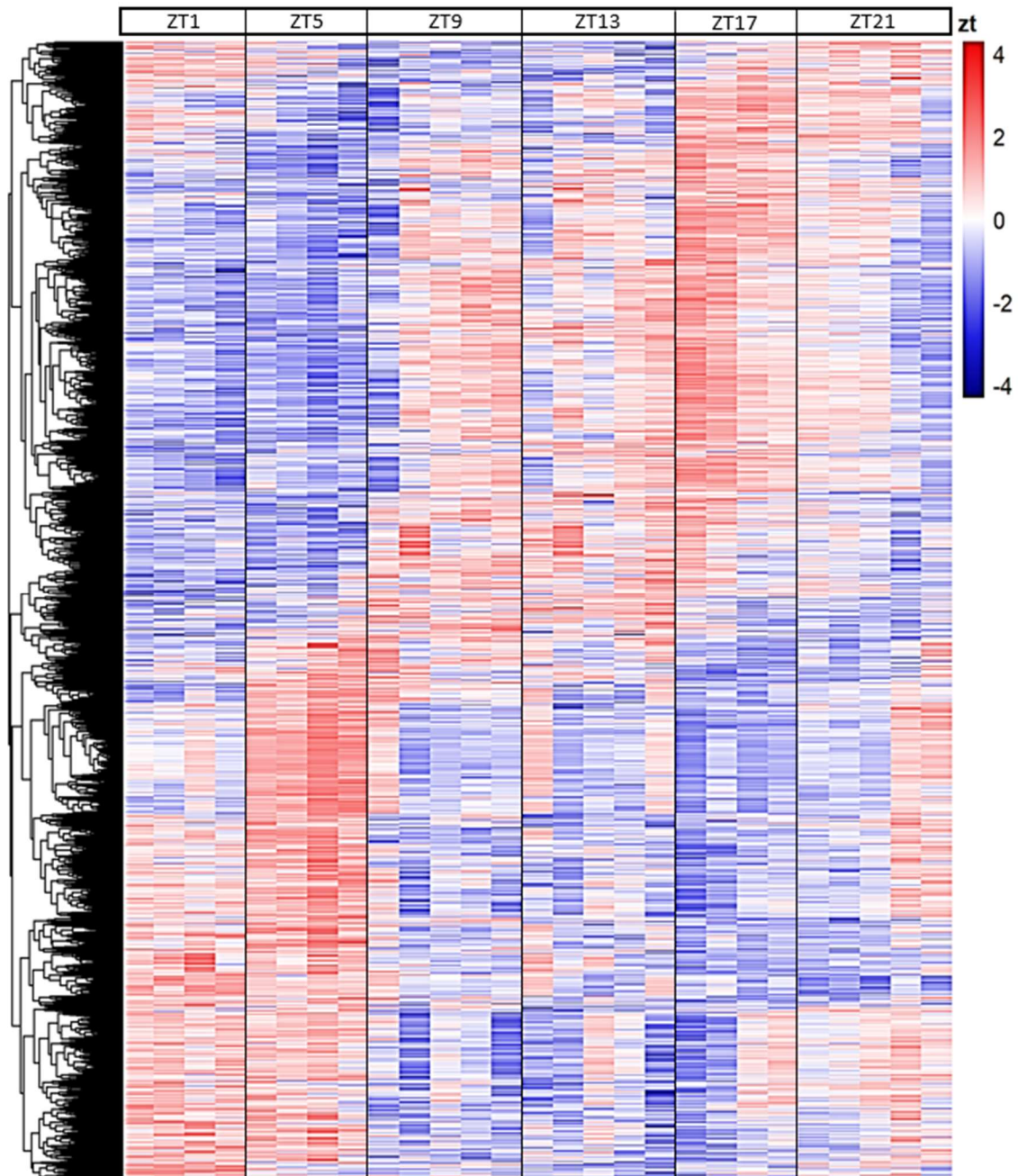
Figure 13. Heatmap of oscillating PCG in the BCA of *Apoe*-/-. Each column represents a different BCA from a *Apoe*-/- mouse.

To know which are the biological processes showing circadian oscillation, we used PSEA to get a broader picture of the biological processes and their oscillatory patterns over the course of 24h. PSEA is a tool to analyse the enrichment of different pathways and groups of genes, as explained in the methods section (**Section 3.6.4.8**). Reactome Database was used to create a background with all the information about biological pathways in PSEA.

473 pathways from the Reactome Database (considering all the hierarchical degrees of the database) showed an enrichment on oscillating genes when comparing the list of oscillating genes versus an uniform background or the rest of the oscillating genes (p.adj value < 0.05 and coverage of the pathway > 15%). To further study the functions with an oscillating pattern, the pathways were divided in different groups, taking as starting point the organization made by Reactome: metabolism, signal transduction, cell cycle, program cell death, transcription pathways, immune system, nervous system, cellular responses to stress, vesicle-mediated transport, cell-cell communication, haemostasis, organelle biogenesis, chromatin organization, circadian clock, muscle contraction and ECM organization. The complete list of pathways is displayed in the **Annex 2**.

Some groups of pathways showed a strong dependence from the time of the day, and the genes associated to them are jointly overexpressed at a specific timepoint. Next, we will detail the process showing circadian oscillation in the plaque.

3.1.2.1 Genes related to the metabolism of carbohydrates show circadian oscillation

The metabolism of carbohydrates, either glycogen or glycosaminoglycans, showed a strong circadian component, having a peak in the evening hours (between ZT13 and ZT17, as can be seen in **Figure 14.A**), when the mice are active and eating. Also, some protein-related pathways share this peak of activity, like the secretion of insulin induced by the peptide hormone glucose-dependent insulinotropic polypeptide (GIP) represented in **Figure 14.B**. There are many research papers that try to elucidate whether the control of the translation of these pathways related to metabolism are done by the circadian clock, the food intake or a combination of several stimuli[203,204].
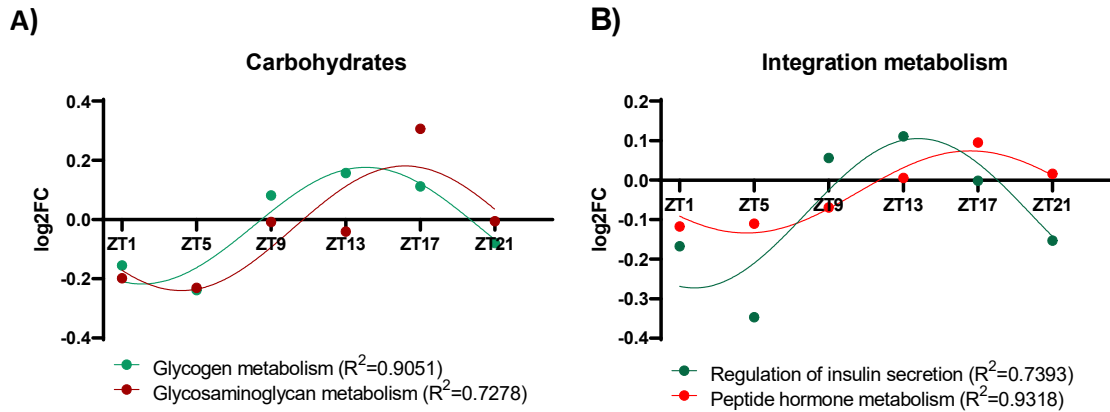
Figure 14. **Representation of the expression of PCGs related to carbohydrate metabolism and other metabolism processes in the plaque.**

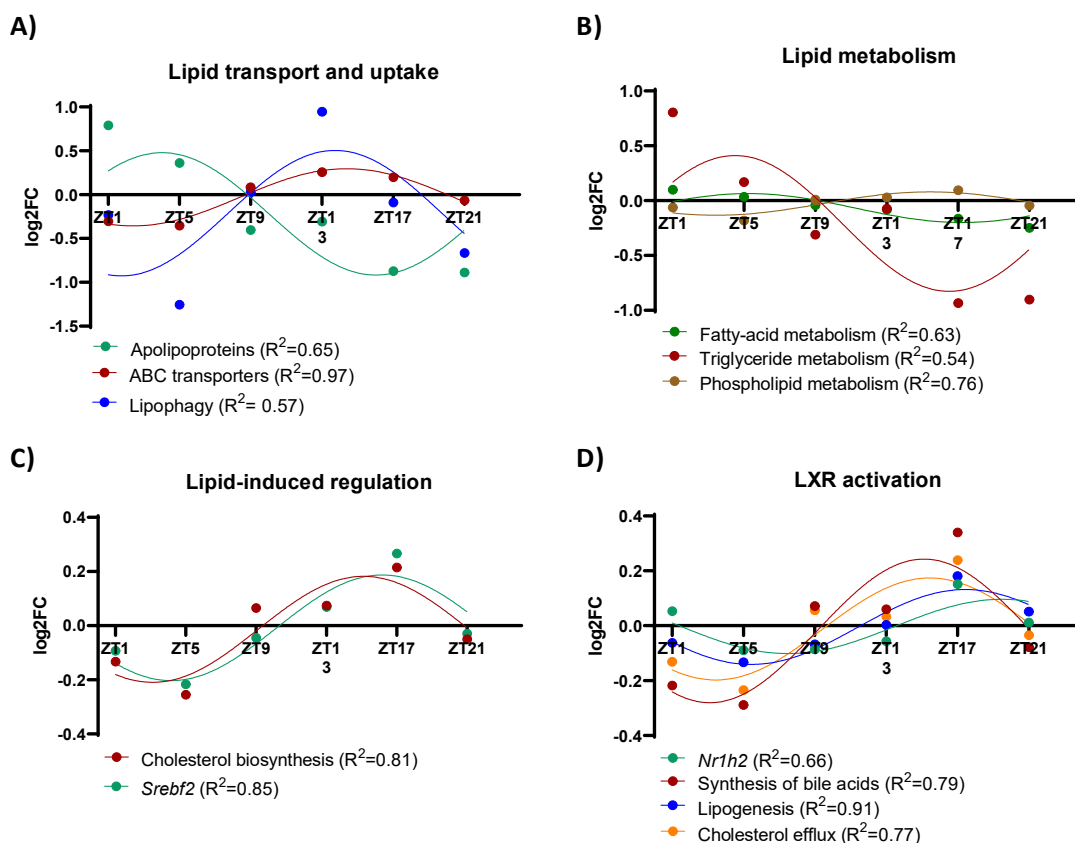3.1.2.2 Genes related to the metabolism of lipids show circadian oscillation

As can be seen in **Figure 15**, several pathways related to the metabolism of lipids oscillate throughout the day.

The expression of different genes that code for apolipoproteins, that either form HDL particles (as *Apoa1*, *Apoc4* and *Apol7*)[205] or form VLDL, chylomicrons and LDL (*Apoc4*)[206] or are necessary for the expression of apolipoproteins (*Apobec1* and *Apobec3*)[207] show higher abundance in the morning times (**Figure 15.A**).

On the other side, the genes that encode for ABC transporters (ATP-binding cassette transporter) and that regulate the import and export of several molecules[208], as cholesterol and lipids (*Abca6*, *Abca2*, *Abca3*, *Abca8*, *Abca9*), proteins and bile acids (*Abca9*), ions and receptors (*Abcc1*), steroids and bile acids (*Abcg2*) and fatty acids into the peroxisome (*Abcd4*) show a higher expression in the evening hours. The circadian oscillation of the ABC-transporter genes is similar to the genes involved in lipophagy (**Figure 15.A**).

The increase of lipids in the cell activates different pathways that control the expression of important genes for the metabolism of lipids[209]. SREBPs are transcription factors that control the expression of genes necessary for the lipid and cholesterol production[210], and their expression is negatively regulated by the presence of sterols[209]. The synthesis of cholesterol is higher at the end of the active phase when the income of cholesterol from the diet is not that high anymore (**Figure 15.C**). Furthermore, different pathways related to the liver X receptors (*Nr1h2*, also known as *Lxrb*) show the same pattern (**Figure 15.D**).

The metabolism of lipids occurs in different timepoints in the atherosclerotic plaque. The metabolism of phospholipids shows a higher expression in the evening hours (**Figure 15.B**). On the contrary, the genes that control the fatty-acid metabolism show a slight increase in the morning hours, while the genes that control triglyceride metabolism have a huge difference during the day, being also more expressed in the morning hours (**Figure 15.B**).

A)

Lipid transport and uptake

Apolipoproteins (R^2=0.65)
ABC transporters (R^2=0.97)
Lipophagy (R^2= 0.57)

B)

Lipid metabolism

Fatty-acid metabolism (R^2=0.63)
Triglyceride metabolism (R^2=0.54)
Phospholipid metabolism (R^2=0.76)

C)

Lipid-induced regulation

Cholesterol biosynthesis (R^2=0.81)
Srebf2 (R^2=0.85)

D)

LXR activation

Nr1h2 (R^2=0.66)
Synthesis of bile acids (R^2=0.79)
Lipogenesis (R^2=0.91)
Cholesterol efflux (R^2=0.77)

Figure 15. Representation of the expression of PCGs related to lipid metabolism in the plaque.

The oscillation of the different PCGs related to lipid metabolism are complementary to our results on plasma abundance of cholesterol and triglycerides. As observed in **Figure 16.A**, the abundance of cholesterol in plasma is quite stable between ZT1 and ZT13, coinciding with the resting phase and the beginning of the active phase for mice. After this time, the abundance of cholesterol drops to its minimum at ZT17, which coincides with the highest expression of ABC transporters and genes related to lipophagy and the highest expression of genes related to the cholesterol biosynthesis. After this period, the abundance of cholesterol in blood is re-established due to the diet supply.

The amount of triglyceride in plasma doesn't oscillate as much as cholesterol (**Figure 16.B**), and the levels are quite stable except in the end of the resting time, around ZT9, in which the reserves in plasma are at their lowest level. The expression of genes related to the metabolism of triglycerides is also quite stable, with a peak at ZT1 in the plaque.

A)

Cholesterol abundance

$R^2 = 0.8131$

B)

TG abundance

$R^2 = 0.3321$
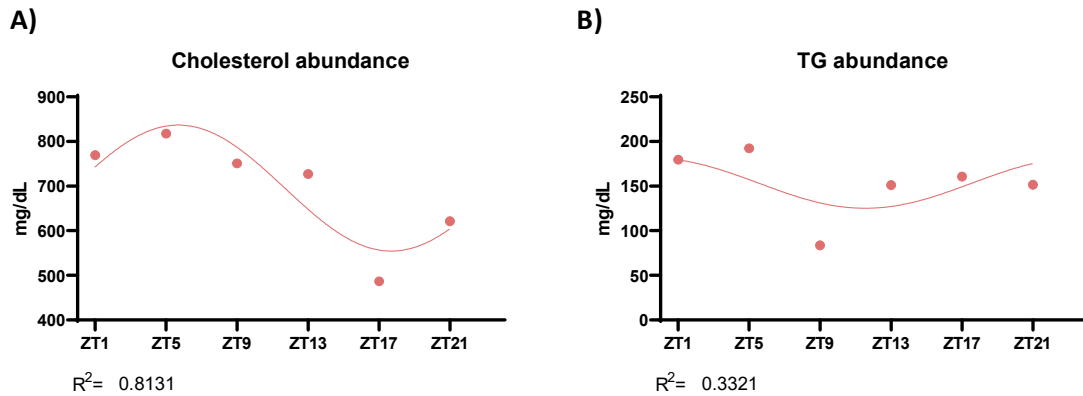
Figure 16. Oscillation of the abundance of cholesterol and triglycerides in the plasma from *Apoe* mice fed with HFD for 16W.

3.1.2.3 Genes related to the transcription and translation show circadian oscillation

Transcription are translation are described as processes highly dependent of the circadian clock[142,211-213]. The sets of genes controlling the mRNA stability, rRNA processing and the capping of introns and mRNA have a higher transcription rate during the morning time, having a steep peak at ZT5 as can be seen in **Figure 17.A** and **17.B**. These activities shared the peak with translation and protein folding activities, indicating a simultaneous control of these two activities. In the other side, post-translation modifications, which include ubiquitination, neddylation, deubiquitination, glycosylation and sumoylation, happen mostly in the evening times.
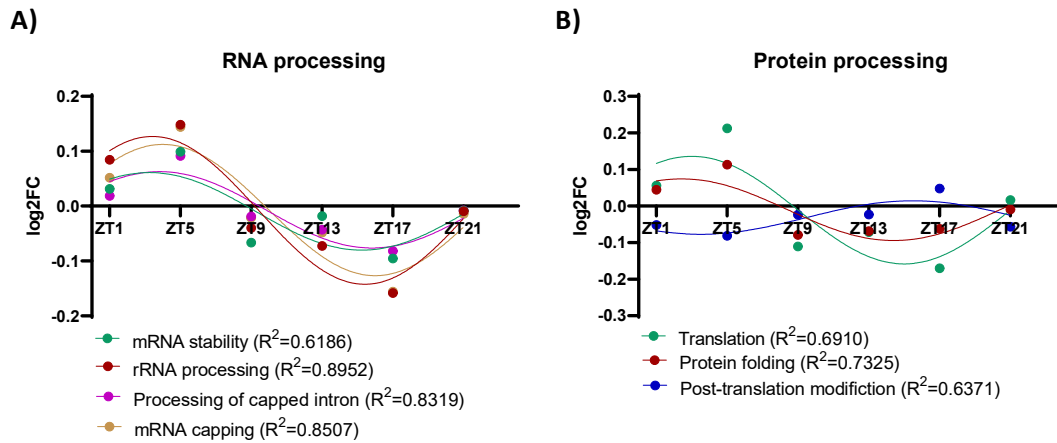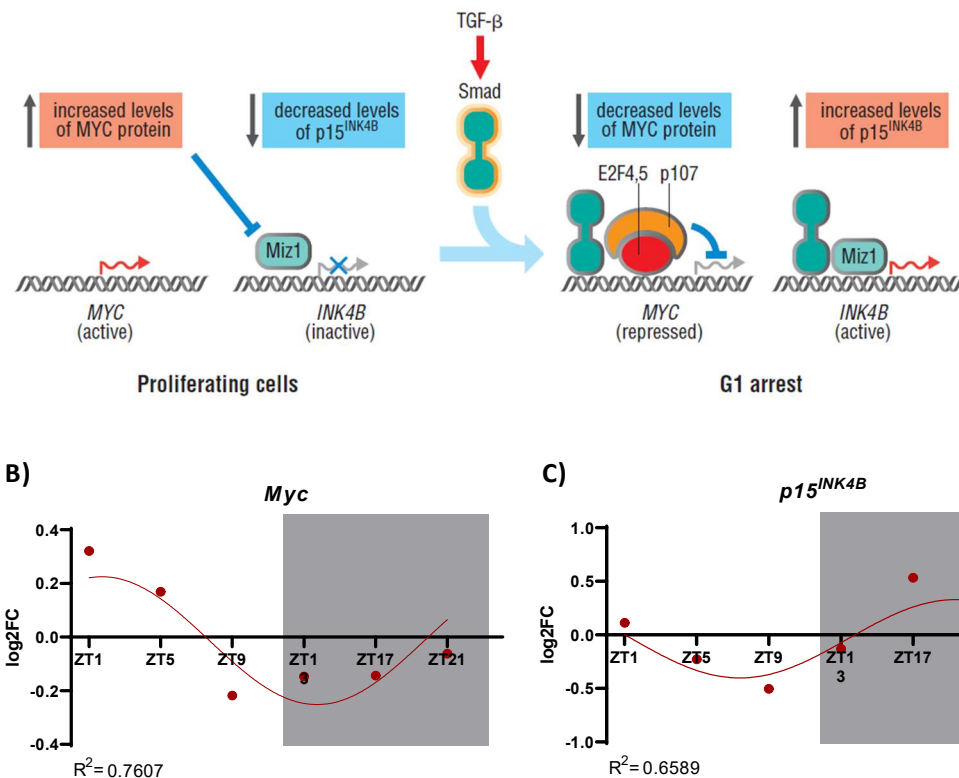
Figure 17. Representation of the expression of PCGs related to RNA processing and gene translation and protein post-translation modification.

The circadian control of the translation and the post-translation modification, which is necessary for the correct functioning of the proteins, could extend the circadian influence to genes and proteins that don't show oscillatory control of transcription or translation, -i.e., those genes whose expression is controlled by proteins that do oscillate-, increasing the percentage of PCGs and biological functions influenced by circadian rhythms.

3.1.2.4 Genes related to the cell cycle and cell survival show circadian oscillation

Cell cycle and cell survival show an important percentage of oscillating genes. In the case of cell cycle, different processes during the mitosis, as well as the genes that code for proteins in charge of mitotic checkpoints are expressed in a circadian fashion.

In proliferating cells, the transcription of several genes is tightly controlled by the cell cycle, to keep a regulation of the cycle. After a mitogenic stimulation, the levels of *Myc* increase, while the levels of *p15*[INK4B] decrease[214]. On the other side, when a cell cycle inhibitor is present, as TGF-β, the transcription of *Myc* ends, and the levels of *p15*[INK4B] increase, as can be seen in **Figure 18**.

Figure 18. Regulation of the cell cycle in the atherosclerotic plaque. **A)** Schematic representation of the transcription of *MYC* and represesion of the transcription of *INK4B* in proliferating cells and shift to the stop of transcription of *Myc* and increase of *p15^INK4B* after anti-proliferating sign (represented in this case by TGF-β) that puts the cell into G1 arrest. Image adapted from *The Cell Cycle: Principles of Control[215]*. **B)** Oscillation of the expression of *Myc* and *p15^INK4B* in the mouse plaque.

The start of the replication of the DNA during the G1-S transition is regulated by the complex Cyclin A/Cdk2, E2F and SCF and the three of them are regulated in a circadian manner, with a peak of expression at ZT5. The expression of the genes controlling the synthesis of DNA during phase S follow a very similar pattern as compared to the genes involved in the transition between phase G1 and S.

On the other hand, the transition between G2 and M phase is delayed in time, with a peak in ZT17, as can be seen in the graph representing the oscillation of several pathways involved in Mitosis in **Figure 19.B**. During this transition, several processes occur, as the maturation of centrosomes, there is a downregulation of TP53 by GTSE1 to allow the progression of the cell
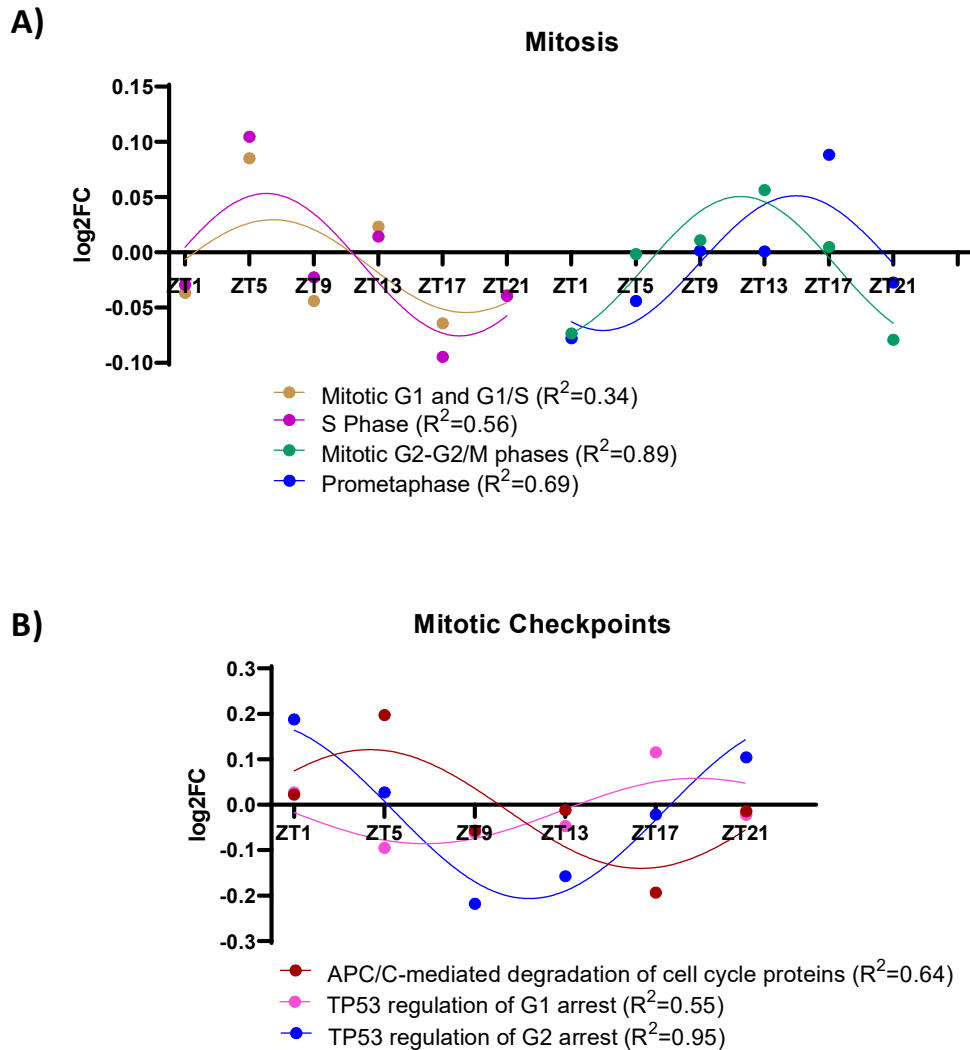
cycle[216], regulation of PLK1 (required for cell cycle progression and activation of cellular proteins during phase M)[217] and the activation of cyclins A/B1/B2.

The M phase also follows a circadian regulation in very specific processes, as the recruitment of NUMA, which is a critical protein to maintain the spindle poles that separate sister chromatids in the prometaphase[218,219]. The expression of the genes involved in the first phase of the mitosis (Prometaphase) had the highest expression in ZT17, at the same time than the transition between G2 and M.

The cell cycle has many checkpoints in order to regulate the proliferation of the cells. The Anaphase Promoting Complex or Cyclosome (APC/C) becomes activated by CDC20 during the M phase. PCGs that code for proteins controlling the phosphorylation of APC/C (like *Plk1*) show a peak of expression at ZT5 and the inhibition of APC/C at the end of the anaphase is also circadianly regulated (**Figure 19.B**).

TP53 also controls the correct progression of the cycle at different points. It regulates the oscillatory transcription of genes involved in G1 arrest and also in G2 arrest. The peaks of expression of these two groups of genes are opposite and coincide with the peak of expression of genes that are involved in G1 and G2, correspondingly (**Figure 19.B**).

Overall, we see a temporal compartmentalization of the transcription of pathways related to cell cycle, with the early stages (G1 and S) having a peak in the morning times, around ZT5 and the later phases (G2 and M) showing a later peak, around ZT17.

A)

Mitosis

Legend:
- Mitotic G1 and G1/S (R^2=0.34)
- S Phase (R^2=0.56)
- Mitotic G2-G2/M phases (R^2=0.89)
- Prometaphase (R^2=0.69)

B)

Mitotic Checkpoints

Legend:
- APC/C-mediated degradation of cell cycle proteins (R^2=0.64)
- TP53 regulation of G1 arrest (R^2=0.55)
- TP53 regulation of G2 arrest (R^2=0.95)

Figure 19. Representation of the expression of PCGs related to cell cycle. For representation reasons, the different phases of the mitosis have been displayed in a 48h graph.

Cell survival and signals to downregulate pro-apoptotic signals are also related to activation of cell cycle. Several groups of pathways, commonly known as "Signal transduction" pathways in Reactome, are activated as response to second messenger activation or by different agonists interacting with receptor tyrosine kinases, non-receptor tyrosine kinases, MAPK or MTOR.

The activation of the pro-survival pathway initiated by AKT oscillated over the day. AKT will be activated by PIP3 in a circadian fashion. Furthermore, the regulation of PTEN, which suppresses this activation, is also controlled circadianly (**Figure 20.A**).

Different activators orchestrate the activation of AKT by PIP3. These activators are normally classified in receptor tyrosine kinases (RTK) and non-tyrosine kinase receptors (no-RTKs).

Among the RTKs that oscillate in the plaque, we can find MET, IGFR1, PDGF, FGFR, ERBB4, VEGF and NTRKs (**Figure 20.B**). The no-RTKs are less abundant, but important pathways related to PTK6, RAS and mTOR show oscillation (**Figure 20.C**).
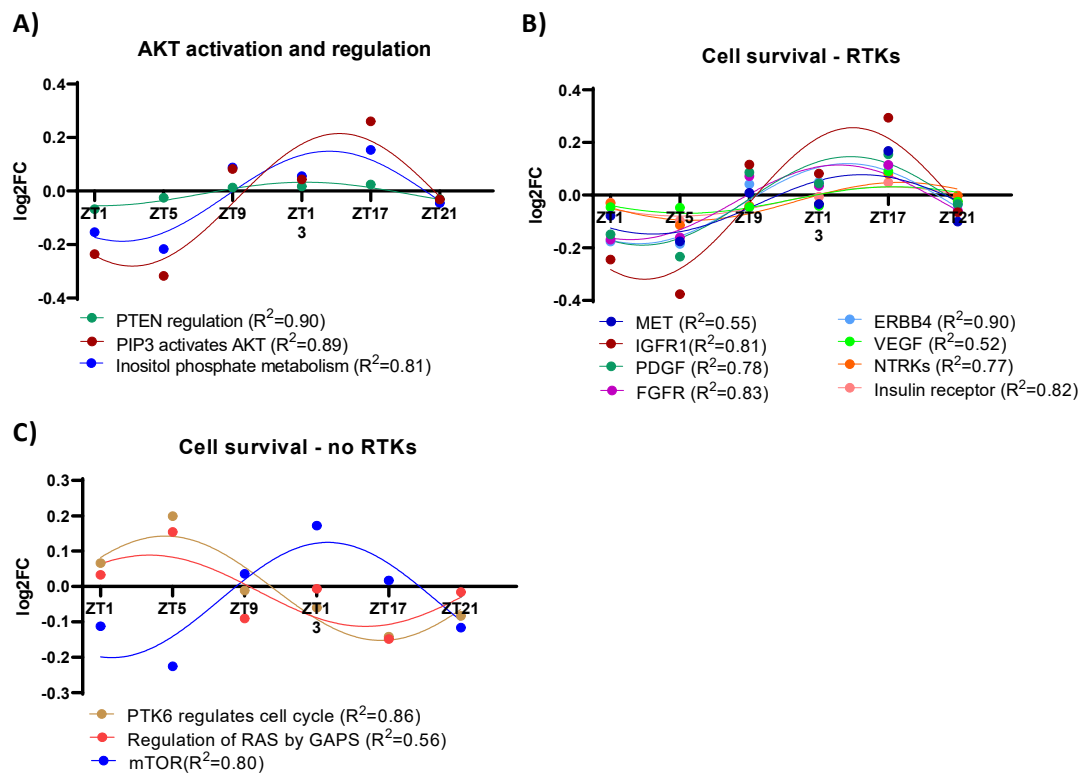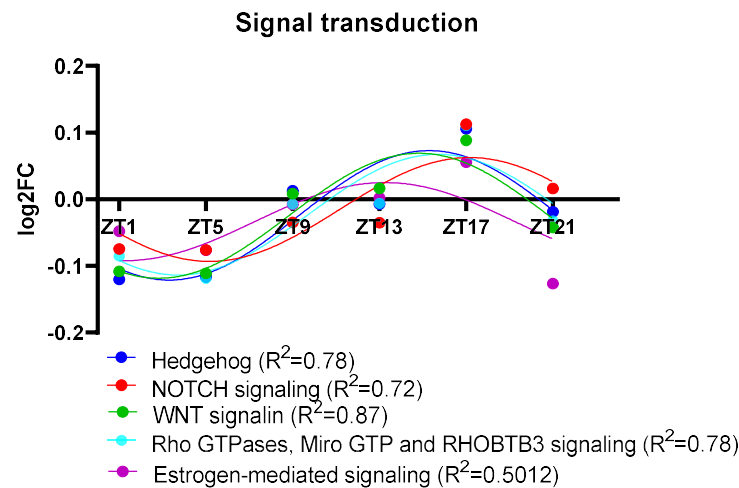

Figure 20. Representation of the expression of PCGs related to cell survival, cell growth and cell cycle pathways. It is important to notice that in **B)** and **C)** the oscillation of the expression of PCG belonging to the pathways activated by each receptor are displayed (f.e, MET in B) referst to the oscillation of the PCG that belong to the Pathway "Signaling by MET") and not to the expression of the PCG that codes for the different receptors.

3.1.2.5 Genes related to different signalling processes show an oscillatory pattern

Other signalling processes show an oscillatory pattern, as can be seen in **Figure 21**. These pathways are central pathways of the cell function and there will are briefly described hereinafter. This is the case of Rho GTPases, WNT signaling pathway, Notch signaling pathway and Hedgehog.

It is well known that oestrogens and other hormones interact with the circadian system to regulate the timing in which different biological processes occour[220]. The signalling pathways

activated by oestrogen receptors show oscillation in our dataset, specifically the extra-cellular signalling, which leads to the activation of many signalling pathways, as RAF/MAP kinase, PI3K/AKT, apoptosis, proliferation.

Figure 21. Representation of the expression of PCGs related to signalling transduction pathways.

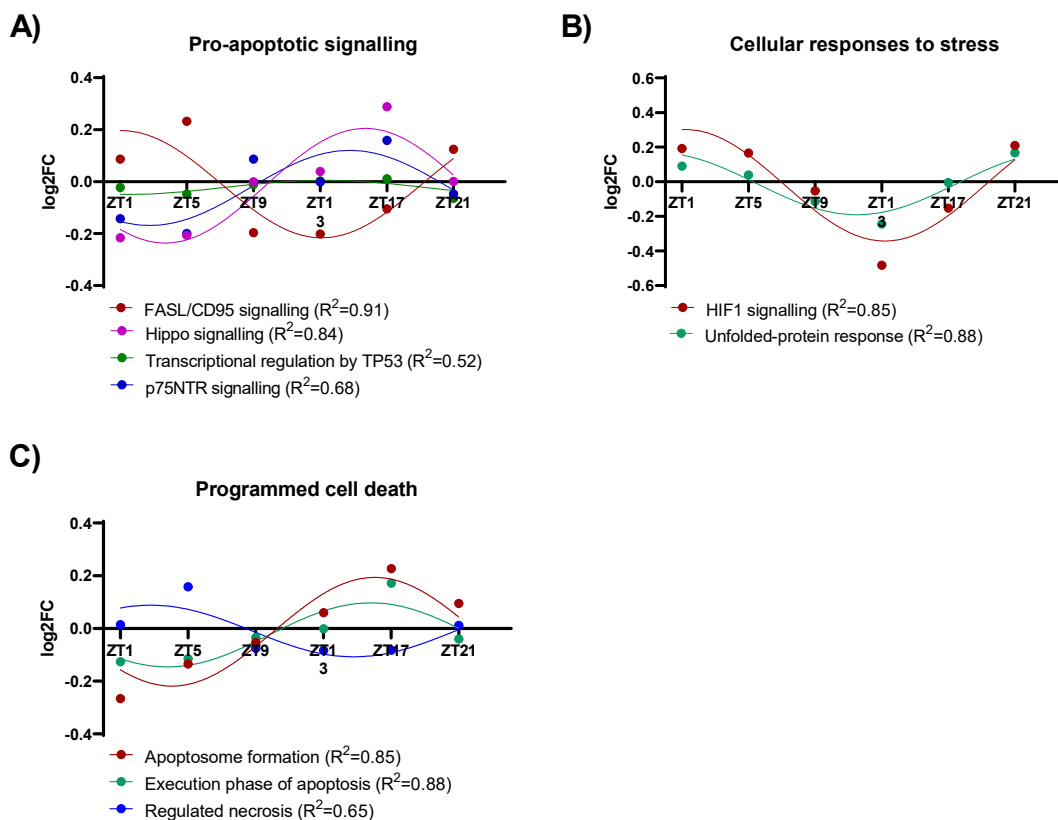### 3.1.2.6 Genes related to cell death show circadian oscillation

In parallel to these signals, that control the survival and differentiation mainly, we can also find **pro-apoptotic signals**, as the Hippo pathway or the FASL/CD95L pathway.

Hippo is another cell proliferation/apoptosis regulator, promoting apoptosis[221]. This pathway ends up with the activation of pro-apoptotic genes. The FASL/CD95L signalling pathway, which activates apoptotic pathway, is under circadian regulation, with an important percentage of the pathway (40%) showing oscillating patterns. Besides FASL/CD95L, p75NTR signalling pathway also oscillates. In our dataset, this pathway shows oscillation concerning the negative control of the cell cycle by the regulation of cyclin E (**Figure 22.A**). TP53 also has a close relationship with the initiation of the cell death process. As consequence of cellular stress or damage, TP53 accumulates in the cell, which leads to the transcriptional activation of pro-apoptotic effectors[222].

The presence of some molecules produced by immune cells, as TNF can activate pathways that lead to apoptosis[223]. Furthermore, stress processes sensed by the can also activate cell death[224]. HIF1, which regulates cell response to hypoxia, is highly expressed in the plaque and its signalling pathway oscillates with a maximum in the morning hours (**Figure 22.B**).

There's oscillation of pathways that protect the cell from unfolded and/or misfolded proteins, with higher expression in the morning times (between ZT21 and ZT5), as it is displayed in **Figure 22.B**. These pathways activate the ERAD (Endoplasmic-reticulum-associated protein degradation) pathway. If the ERAD pathway is not successful or the cause of unfolded proteins continues, this leads to an apoptotic process.

As well as the pro-apoptotic signalling, the **programmed cell death** is circadian regulated, especially apoptosis. The intrinsic apoptosis pathway, in response to stress, DNA damage, ER stress or death receptor signalling ends with the formation of the apoptosome, that will activate the caspase-9, which will cleave different cellular proteins[94]. The formation of the apoptosome has an important percentage of oscillating genes and a well-defined peak at ZT17 (**Figure 22.C**). The posterior cleave of cellular proteins is also circadian regulated. Regulated necroptosis has also a circadian control, even though the percentage of oscillating genes is lower than in apoptosis.

Figure 22. Representation of the expression of PCGs related to cell death and activation of different pathways that lead to apoptosis.

3.1.2.7 Genes related to the immune system show circadian oscillation

One of the big groups of genes that show a strong temporal compartmentalization is the **immune system** regulation. Both the innate and the adaptive immune system show a significant degree of oscillation in their pathways, with the highest expression in the morning times (ZT1-ZT5).

In the case of **innate immune system**, the pathways related to different pathogen-associated molecular patterns (PAMPs) or damage associated molecular pattern molecules (DAMPs) show oscillation in the plaque (**Figure 23**).

Nod1 and *Nod2*, two different types of NOD-like receptors (NLRs), show circadian oscillation in their expression. Furthermore, their activated pathway also oscillates in a circadian fashion (**Figure 23.A**). Similarly, toll-like receptor 3 (*Tlr3*) and *Tlr4* exhibit oscillation and also the downstream pathways controlled by them, as the production of Type-I INFs and TRIF-dependent programmed cell death and RIP3-dependent necroptosis (**Figure 23.B**). In the case of C-type lectin receptors (CLR), several of them as CLEC7A and CLEC6A activate signalling pathways that are dependent on cytokines whose production is controlled by CLR, as IL-1, IL-10 and IL-12[225,226], follow the same oscillatory pattern as CLEC7A and CLEC6A (**Figure 23.C**). All the pathways related to PAMPs and DAMPs that show oscillation have a similar profile of expression, with a high value around ZT5.

Lastly, the activation of NF-kB directly by PAMPs without the mediation of any receptor and through the activation of alpha-protein kinase 1 (ALPK1) peaks also in the morning hours (**Figure 23.D**).
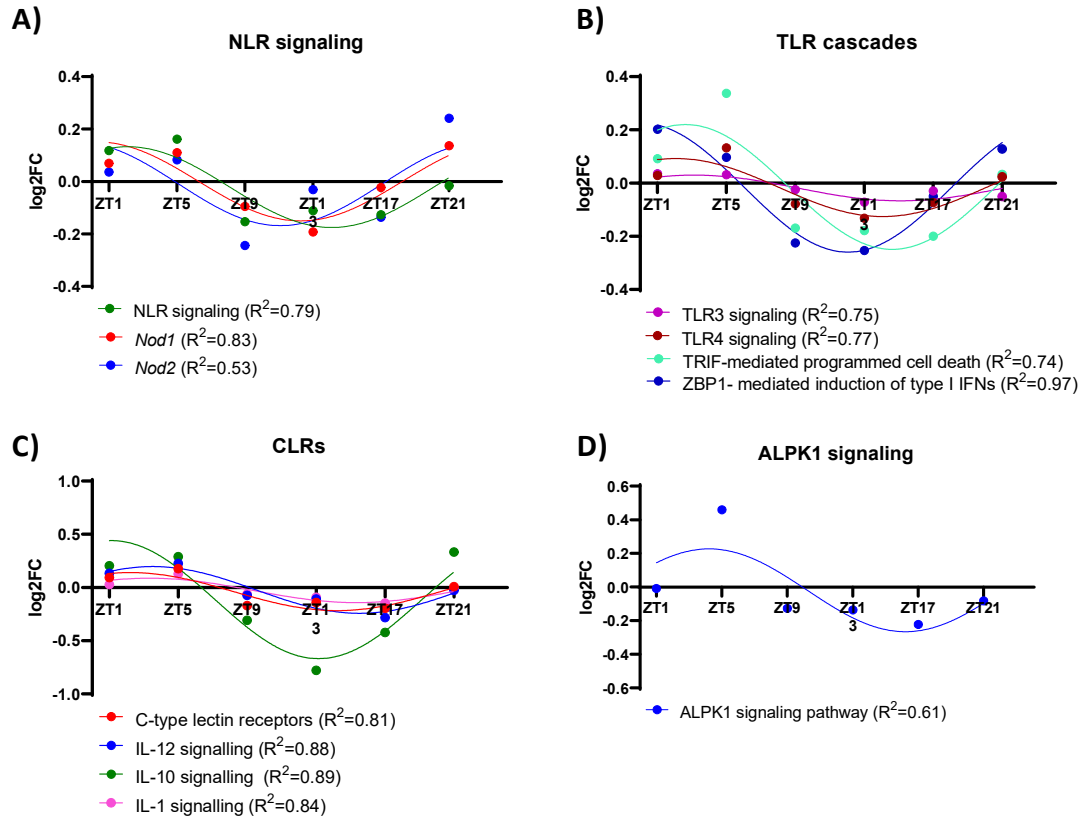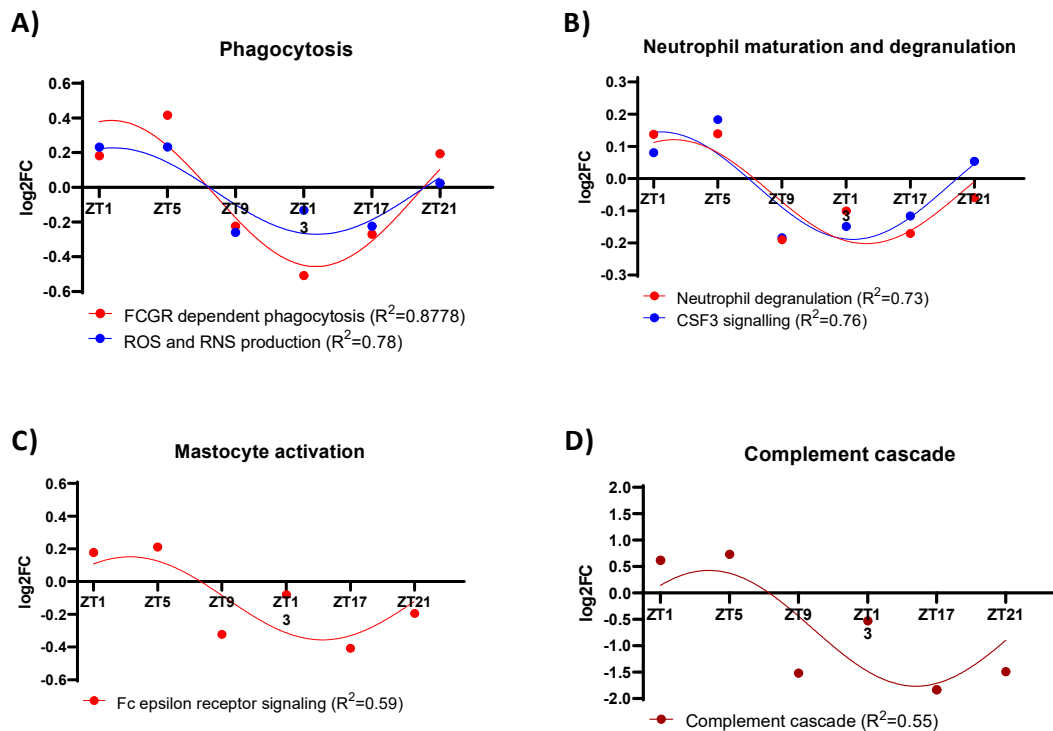
Figure 23. Representation of the expression of PCGs related to the activation of different pathogen or pattern-recognition receptors.

After the "threaten" has been sensed by NLRs, CLRs or TLRs, the innate immune system responds to minimize and neutralize the danger through different mechanisms. Several phases of the phagocytosis process, as the recognition of the particle by Fc gamma receptors (FCGRs) and the production of reactive oxygen and nitrogen species (ROS and RNS) to neutralize the particle share similar gene expression patterns with a maximum peak at ZT5 (**Figure 24.A**).

Other processes associated to neutrophil function, such as the exocytosis of the granules of neutrophils have a strong circadian component. Furthermore, the signalling by CSF3, which regulates the maturation of neutrophils and granulocytes[227], also oscillates in a circadian manner (**Figure 24.B**).

In the same manner as phagocytosis, the activation of mast cells through FCERI-bound antigen-specific IgE shows variation along the day with a peak at ZT5 (**Figure 24.C**). But the immune cells are not the only components in the innate immune system that oscillate. The terminal

pathway of the complement, when C5b, C6, C7, C8 and C9 create the membrane attack complex (MAC)[228] that will form a pore in a cell, oscillates circadianly (**Figure 24.D**).

Figure 24. Representation of the expression of PCGs related to several first-defense activites carried by the innate immune system.

The **adaptive immune system** also shows several patterns under circadian oscillation.

As observed for pathways of the innate immune system, we found that genes associated with antigen presentation namely the two MHC class molecules show oscillatory activities. In the antigen-presenting cell, both the fragmentation of peptides and the posterior presentation to T-cells by MHC class I and II are upregulated in the morning hours (**Figure 25.A**). Similar expression patterns were found in genes associated with the activation of T-cells, the PI3K/Akt activation and the signalling pathways regulated by IL-3, IL/4 and IL/21, which are often expressed in type/2 T helper cells and the TNFR2 activation of NF-kB in highly activated T cells, which can result in cell proliferation (**Figure 25.B**). Besides T cells, B cell activation is also increase in the morning hours, having the regulation by CD22 a peak at ZT1 (**Figure 25.C**).
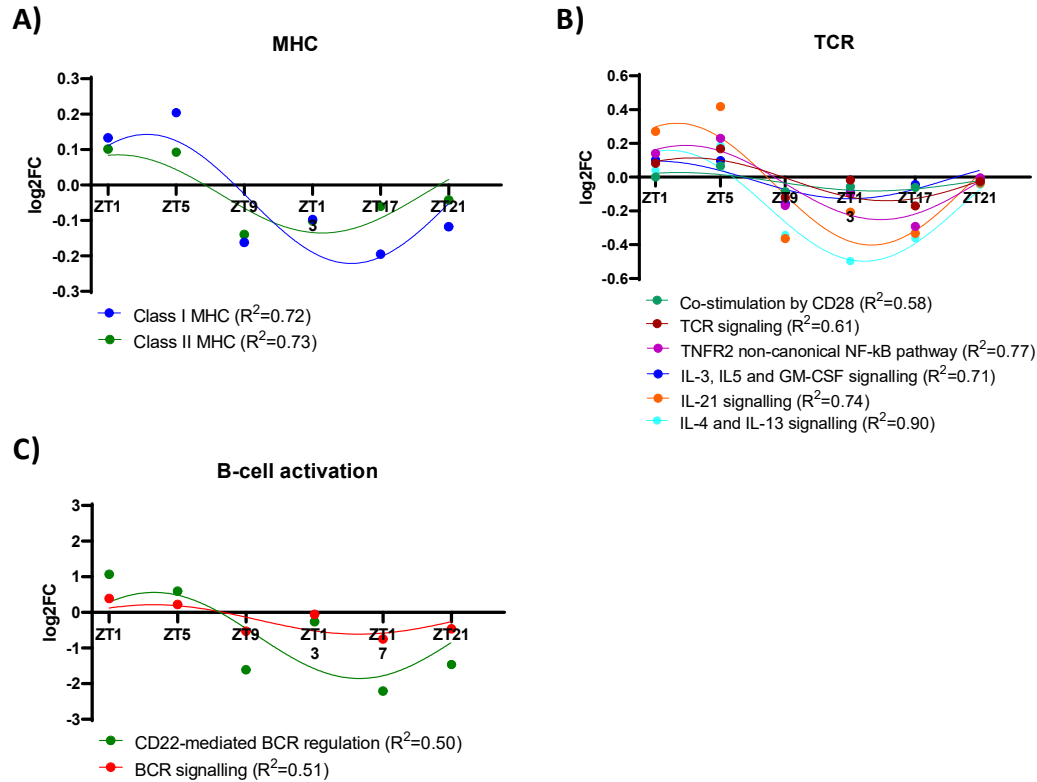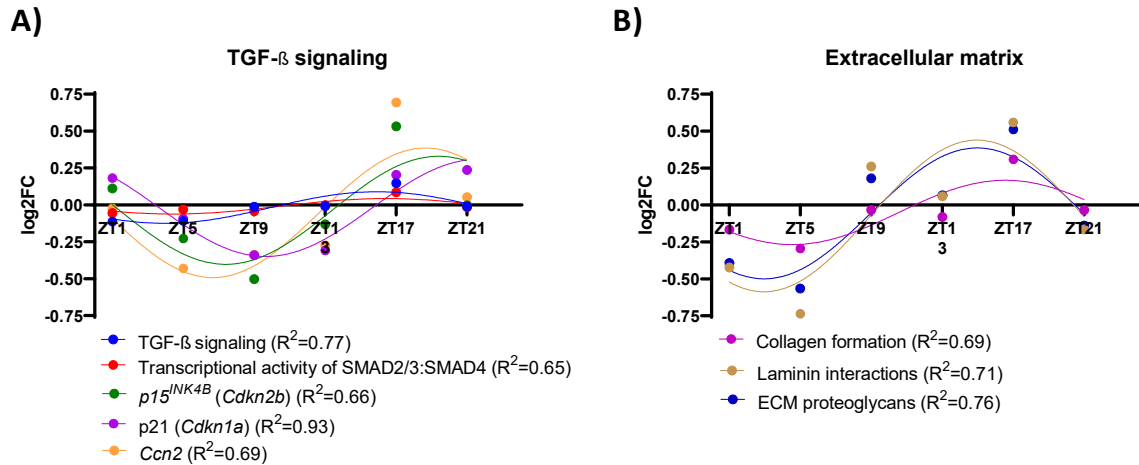
Figure 25. Representation of the expression of PCGs related to activation of different cells form the adaptive immune system.

3.1.2.8 Genes related to TGF- β and to extracellular matrix organization show circadian oscillation

TGF-β (Transforming growth factor-beta) family has a high percentage of oscillating genes (40%) which cover the receptor complexes but also downstream processes, as BMP or the SMAD2/3:SMAD4 complex, that control the expression of inhibitors of the cell cycle, as the CDKIs *p15^INK4B* and p21 (also known as *Cdkn2b* and *Cdkn1a*)[229].

The control of the TGF-β of the extracellular matrix production is done via the activation of intermediates, as *Ccn2* (connective tissue growth factor)[230], which shows an increased expression at ZT17 (**Figure 26.A**). As it is displayed, several pathways related to the extracellular matrix formation, as collagen, laminin and proteoglycans, show also a higher expression in the evening hours (**Figure 26.B**).
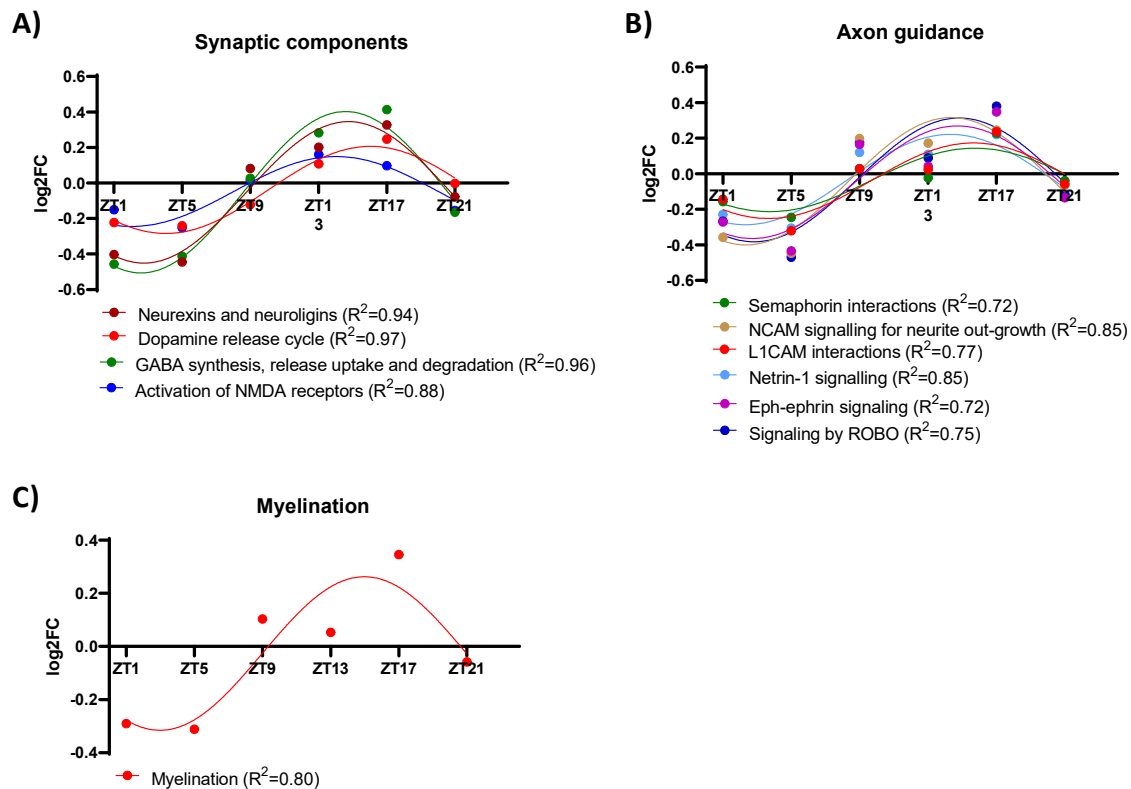
Figure 26. Representation of the expression of PCGs related to TGF signalling and the extracellular matrix remodelling.

3.1.2.9 Genes related to the neuronal system show circadian oscillation

In the same way that the immune system, the **neuronal system and the nervous system development** also show high temporal compartmentalization of its pathways, with a higher expression in the evening hours.

Several components of the synaptic process are under circadian oscillations, as the synthesis and release of the neurotransmitters Dopamine and GABA and the activation of GABA and NMDA receptors (**Figure 27.A**).

Axon guidance also oscillates circadianly, with a peak around ZT17. Several of the pathways activated by molecules that control axon and neurite growth (as semaphorins, NCAM, L1CAM, Netrin-1, EPH-ephrin and ROBO) are circadian regulated (**Figure 27.B**). Besides axon guidance, the posterior myelinization of the axon by Schwann cells has different expression during the day, having its maximum levels at ZT17 (**Figure 27.C**).

Figure 27. Representation of the expression of PCGs related to neuronal development.

3.1.4 The oscillations in the transcriptome are also detected at the protein level

In order to study whether the oscillation at the gene level was also detected in the protein level, the aortic arches of *Apoe*^{-/-} mice that had been on HFD for 16W were processed for proteomic analysis. Due to the different nature of the proteome analysis, the pipeline used with the transcriptome to detect circadian oscillations couldn´t be applied for the proteome. In order to detect changes in the expression of proteins, a different approach using the R package DEP (Differential Enrichment analysis of Proteomics data[200]) was used as explained in **Section 2.7.1**.

3.1.4.1 An important percentage of proteins show differential expression across timepoints
An average of 2120 proteins were detected in the analysed samples, with a minimum of 1402 and a maximum of 2456 proteins detected (**Figure 8.B**).

In the arch of *Apoe*^{-/-} mice, 36.4% of the proteins analysed (807 proteins out of 2215) showed differences in expression between at least two timepoints (adj. P value≤0.01 and Log2 fold change≥0.2).

The enrichment analysis of these proteins showed very similar pathways to the ones detected in the analysis of the oscillating PCGs, in which pathways related to lipid metabolism, cell cycle, cell death, immune system and development of neuronal system were overrepresented, as can be seen in **Figure 28**.
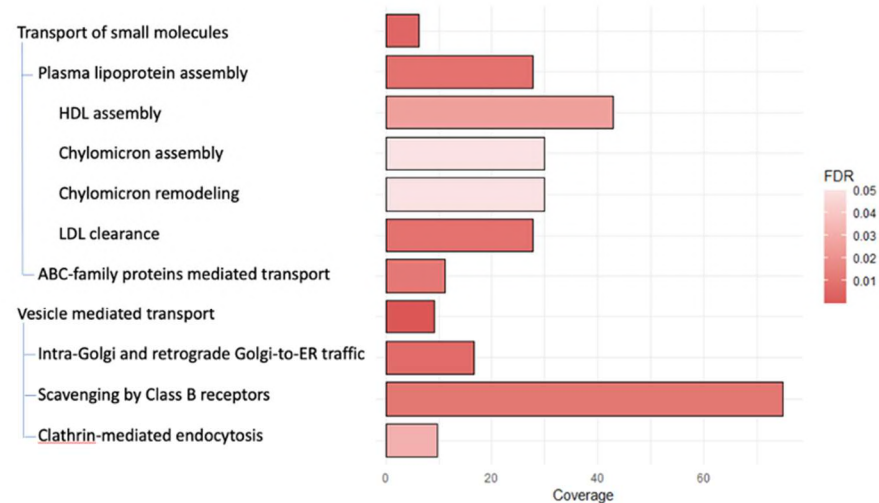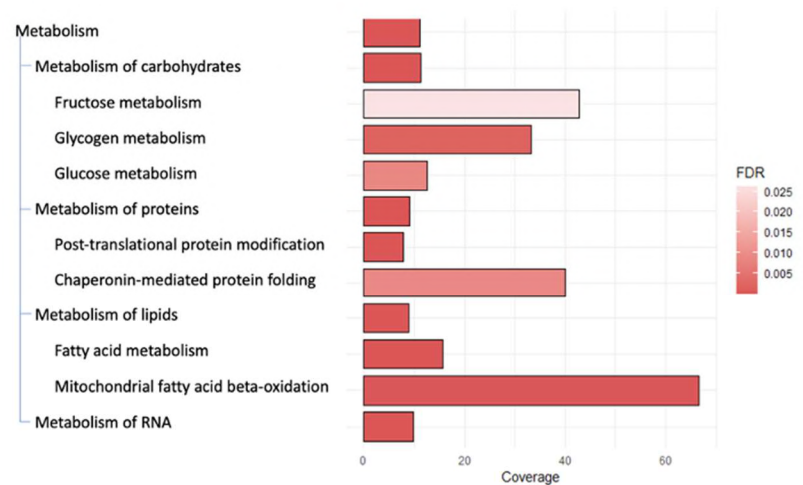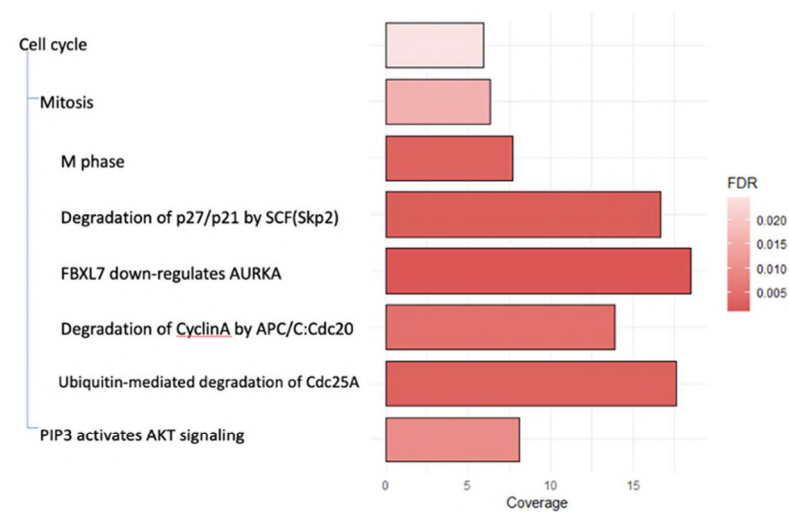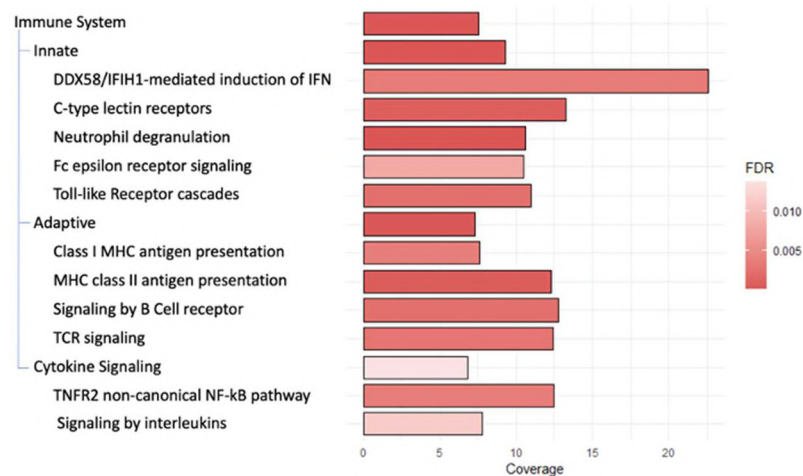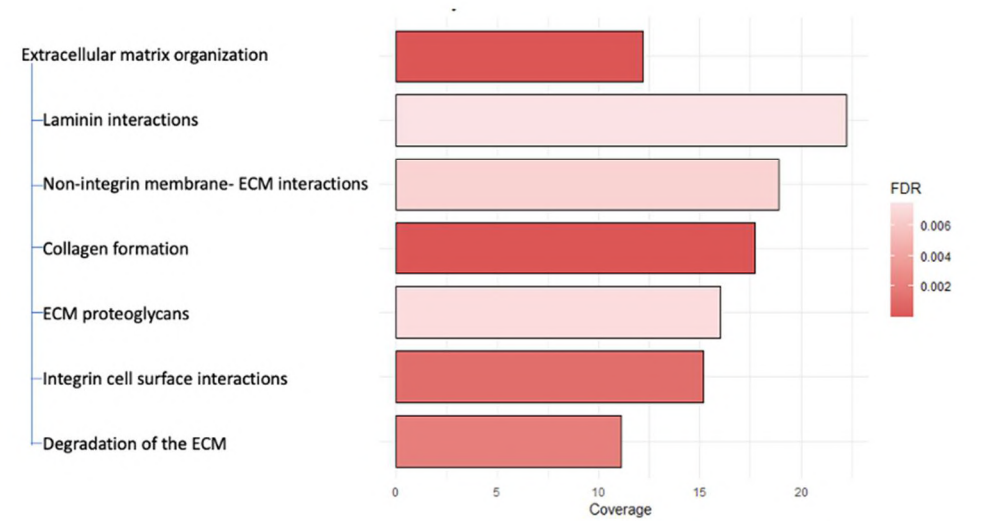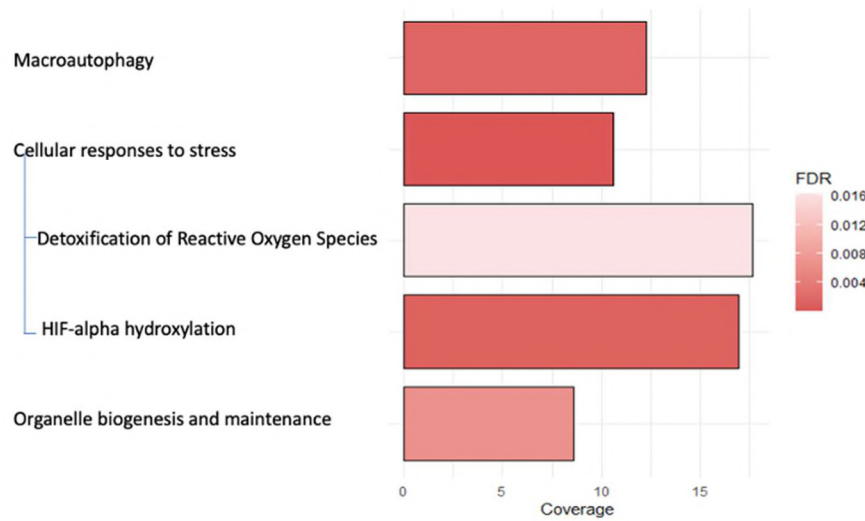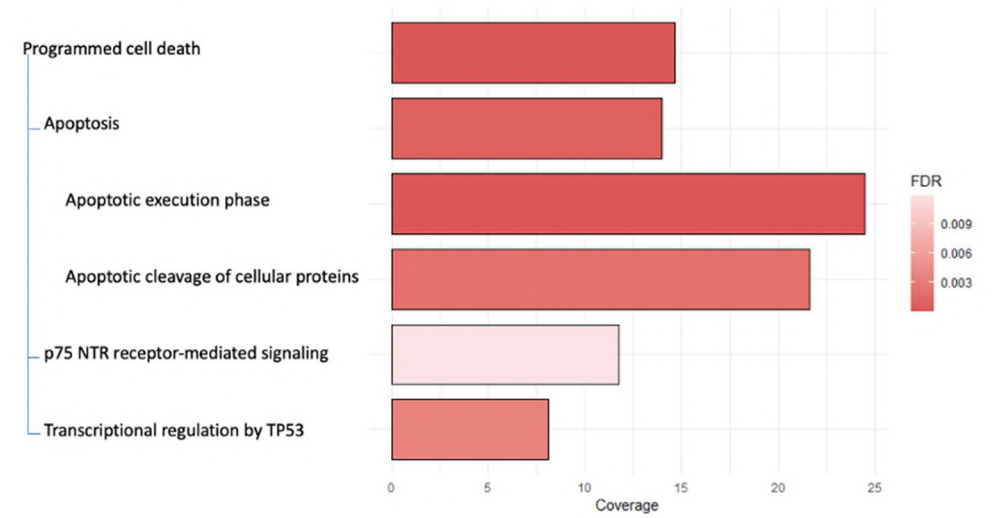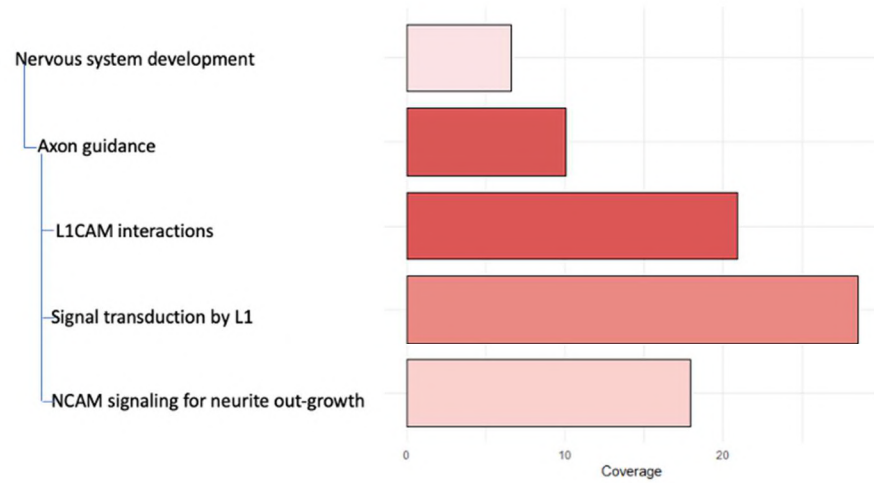
Figure 28. Enriched pathways from the group of oscillating proteins. The different tables show pathways from several biological functions that appear overrepresented in an enrichment analysis done with Enrichr using Reactome database, as explained in **Section 2.6.4.8**. The threshold used to select the enriched pathways was p.adj-value<0.05. Coverage (represented in the X axis) represents the percentage of proteins from the pathway that oscillate circadianly.

3.1.4.2 Proteins related to the immune system show changes in abundance across timepoints

As can be seen in **Figure 28**, several processes related to innate and adaptive immune system show differences between timepoints. The migration of leukocytes to the plaque is circadianly controlled and the adhesion molecules that facilitate the extravasation, as PECA1, exhibit circadian oscillation too. Furthermore, the expression of proteins related to functions associated with macrophages and phagocytosis, as MRC1, VA0D2, LAMP1[231-233], show oscillations with highest abundance at morning times (ZT1 and ZT5) as can be seen in **Figure 29**. This oscillation coincides with our transcriptomic data (**Figure 24**). The activity of proteins related to antigen presentation throughout the major histocompatibility complexes, as CATS and ERAP1[234,235], also share this pattern, as well as proteins that regulate the function of lymphocytes, as IRF3 and ILF2[236,237] (**Figure 29**).
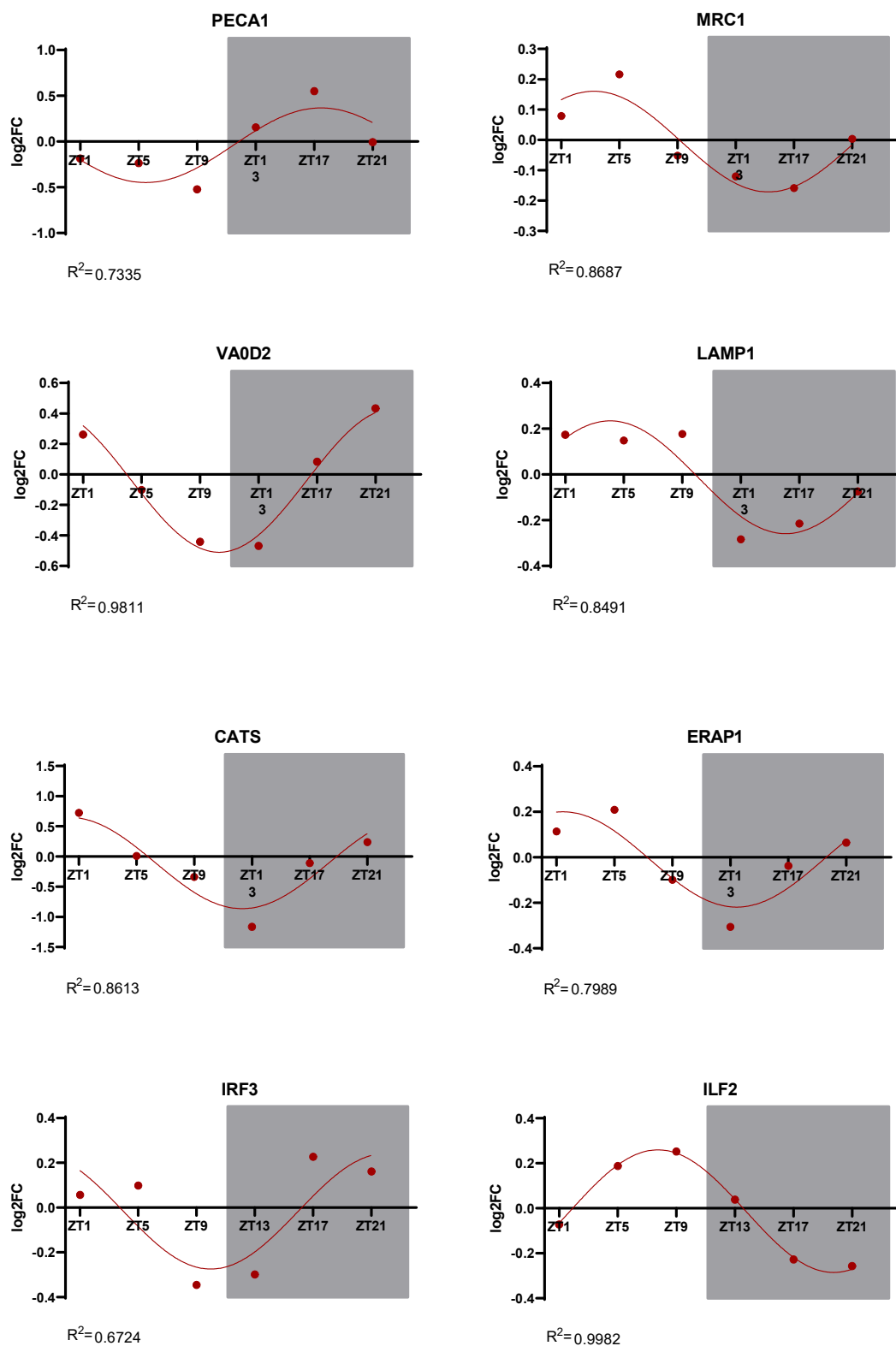
Figure 29. Changes in protein abundance over 24h in proteins related to leukocyte transmigration, phagocytosis, antigen presentation and lymphocyte activation.

3.1.4.3 Cell proliferation shows oscillation at the protein level

Different proteins from several stages of the cell cycle change their abundance across the day. In this group of proteins, we can find several proteins in charge of the cytoskeleton organization during the cell division, as TBB6, TBG1, CLAP1, BUB3 and NUMA1[238-241]. Besides, proteins related to the ubiquitination of different elements of the cell cycle during the G1-S phase transition as SKP1[242] and CCNE1 and CCNE2[243] also oscillate (**Figure 30**).
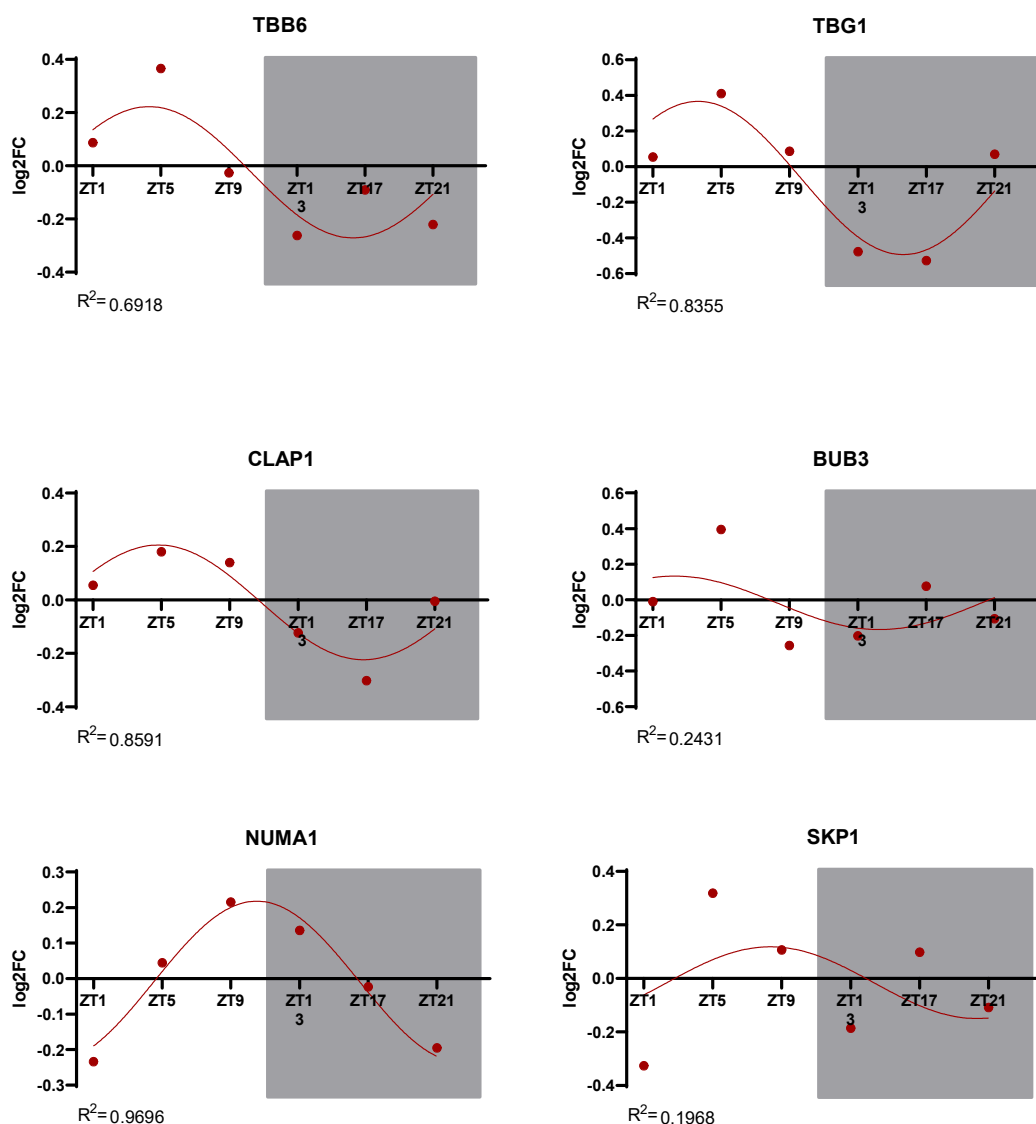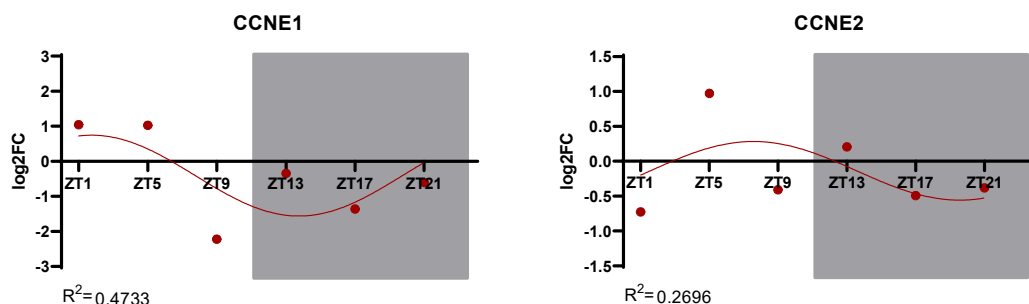
Figure 30. Changes in protein abundance over 24h in proteins related to different processes during the cell cycle. The pathways to which these proteins belong are microtubule cytoskeleton organization, chromatin sister separation, kinetochore establishment and transcription of several cell-cycle components.

Other phases later in the cell cycle, as G2, also have specific gene signatures, as it is the expression of GTSE1 (G2 and S-phase expressed 1 gene)[216] in **Figure 31**. The difference in the expression of the previous proteins, necessary for the beginning of the cell cycle and whose peaks are in the morning hours between ZT1 and ZT5 and GTSE1, which has a peak at ZT17 and whose expression is limited to S and G2 phases, coincides with the expression of different genes from the cell cycle throughout the day.
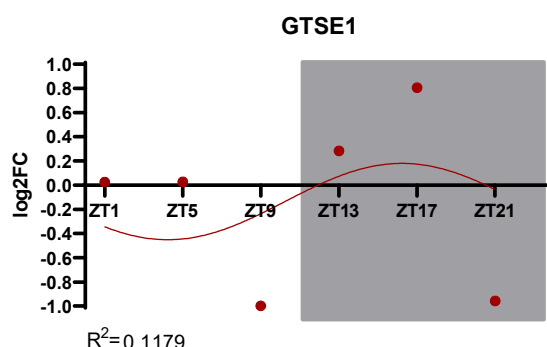

Figure 31. Changes in abundance of the protein GTSE1 over 24h

The results obtained from the transcriptomic analysis and the proteome analysis are concordant with the detection of BrdU⁺ cells in the plaque at two different timepoints by flow cytometry.

In the experiment, BrdU was injected in *Apoe*^-/- mice on HFD for 16 weeks 2h before killing them at ZT1 and ZT13 as explained in **Section 2.1.1.2**. The BCA and the arch were digested together and stained with different fluorescent markers, among which are markers for cellular proliferation and cell death as BrdU, Ki67 and Annexin V (see **Section 2.3.1**)

There´s an increase of BrdU⁺ cells in the BCA and Arch of *Apoe*^-/- mice in the morning time (ZT1) when compared with the evening time (ZT13), as can be seen in **Figure 32.A** and **32.B**. The results obtained with BrdU staining are quite similar to the ones obtained with the immunohistochemistry analysis of atherosclerotic plaque sections from the BCA staining the marker Ki67. In the case of proliferating cells, the highest value at ZT1 when compared to ZT13 is also detectable.
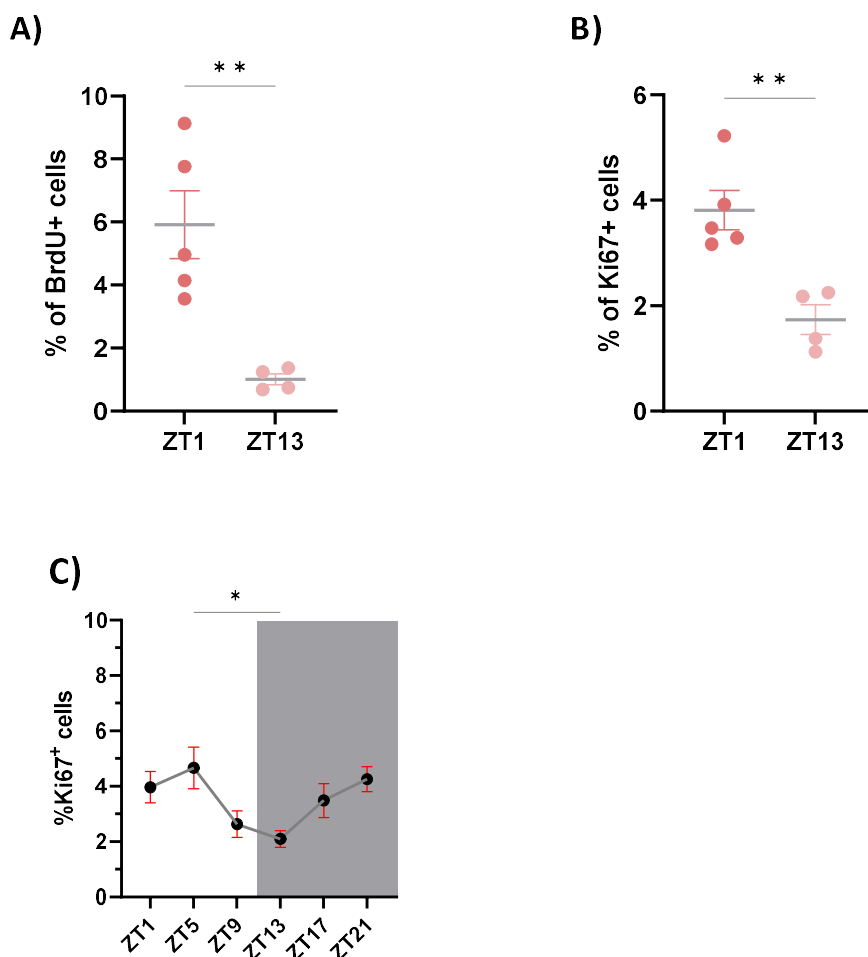
Figure 32. Quantification of proliferating cells at different times of the day. Percentage of positive cells for BrdU **(A)** or Ki67 **(B)** detected through flow cytometry analysis. The total amount of positive cells for the markers was divided by the total amount of living cells (Dapi⁻

cells). **C)** Percentage of positive cells for Ki67 detected through immunostaining. The percentage of positive cells was calculated taking into consideration the total amount of cells positive for DAPI inside the intima area. Statistical analysis made using one-way ANOVA ($^*p<0.05$, $^{**}p<0.01$). Data represented as mean±SEM.

As Ki67 and BrdU are intercalated in the diving cells in troughout the S phase, when the strands of the DNA separate, the proteomics data, together with the data obtained through flow cytometry and immunohistological stainining suggest that the S phase starts in the late evening, later than ZT13 and that the cells constantly accumulate more Ki67 or BrdU gradually, until early morning, when the cell cycle would start again.

3.1.4.4 Cell death shows oscillation at the protein level

In the same way as proliferation, programmed cell death is also enriched among the proteins that show changes in abundance and the changes in protein abundance of specific proteins related to cell death are represented in **Figure 33**.

BAP31 is involved in the recognition of abnormally folded proteins and it collaborates in its transport to the ER, where they will be eliminated[244]. As we could see in the transcriptome analysis, the chemical stress due to the presence of unfolded or abnormally folded proteins is an enriched pathway when considering the oscillating genes in the plaque (**Figure 22.B**). If the amount of unfolded proteins is above the limits or the ER fails to eliminate them, a ER stress-associated programmed cell death would develop[245]. The trigger for cell death can come from other molecular processes, as TNF-α. DNM1L participates in de TNF-α-induced mitochondrial signalling and stabilization of P53 in conditions of oxidative stress[246]. Besides DNM1L, other proteins are crucial for the expression and stability of P53, as RPS27a[247].

Different cellular triggers will activate caspases, which will induce apoptotic chromatin condensation, one of the most used criteria to detect apoptotic cells[248]. The protein ACINU induces chromatin condensation after having been activate by caspase 3[249].

DAPK3 also mediates in mitochondrial-dependent apoptotic cell death, while RIPK1 contributes to the rupture of the membrane during necrosis[250]expose content from the cytoplasm and enhance the proinflammatory function, promoting the recruitment of leukocytes[251].
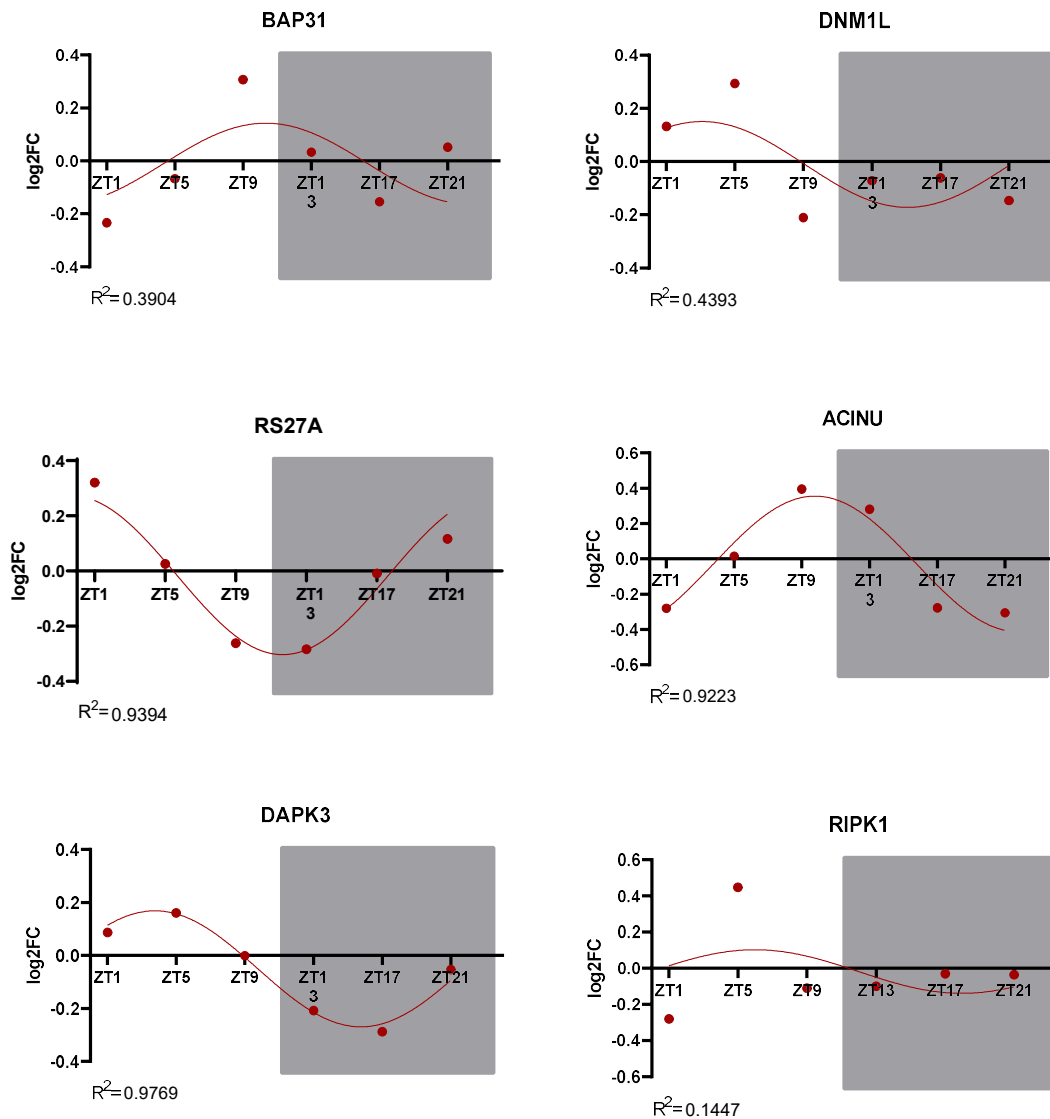
Figure 33. Changes in protein abundance over 24h in proteins related to different processes during cell death and apoptosis, as different signalling and effectors.

In case of cells going though apoptosis (AnnexinV$^+$ cells), the outcome is similar, as can be seen in **Figure 34**. There is a four-fold increase of dying cells in the morning timepoint versus the evening timepoint in **Figure 34.A**. On the other hand, the tissue sections stained using Tunel staining didn´t show differences between ZT1 and ZT13 (**Figure 34.B**), but the number of apoptotic cells in the morning timepoints (ZT1, ZT5 and ZT9) is significantly higher than the number of dying cells in the evening timepoints (ZT13, ZT17, ZT21).
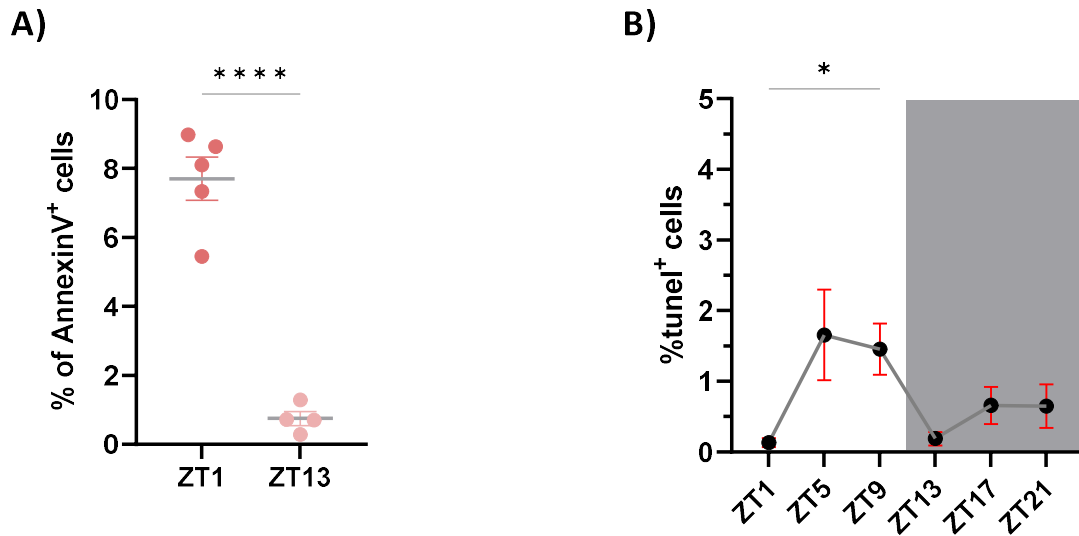
**Figure 34. Quantification of cell death at different times of the day.** Percentage of positive cells for AnnexinV **(A)** detected through flow cytometry analysis. The total amount of positive cells for the markers was divided by the total amount of living cells. **B)** Percentage of positive cells for Tunnel detected through immunostaining. The percentage of positive cells was calculated taking into consideration the total amount of cells positive for DAPI inside the intima area. Statistical analysis made using one-way ANOVA ($^*p<0.05$, $^{****}p<0.0001$). Data represented as mean±SEM.

3.1.4.5 Proteins from the extracellular matrix exhibit changes in their abundance across the day

The abundance of proteins from the extracellular matrix shows changes of concentration during the day. These proteins are of extreme importance for the stability of the atherosclerotic plaque and it´s abundance is going to be decisive in the prevention of a rupture[252].

Several components of the extracellular matrix, as laminin (LAMB1) or collagen (CO1A1), show a decrease of their abundance in the evening times, being the lowest value detected at ZT17. On the contrary, the abundance of metalloproteinases is opposite, with highest peaks at ZT17.
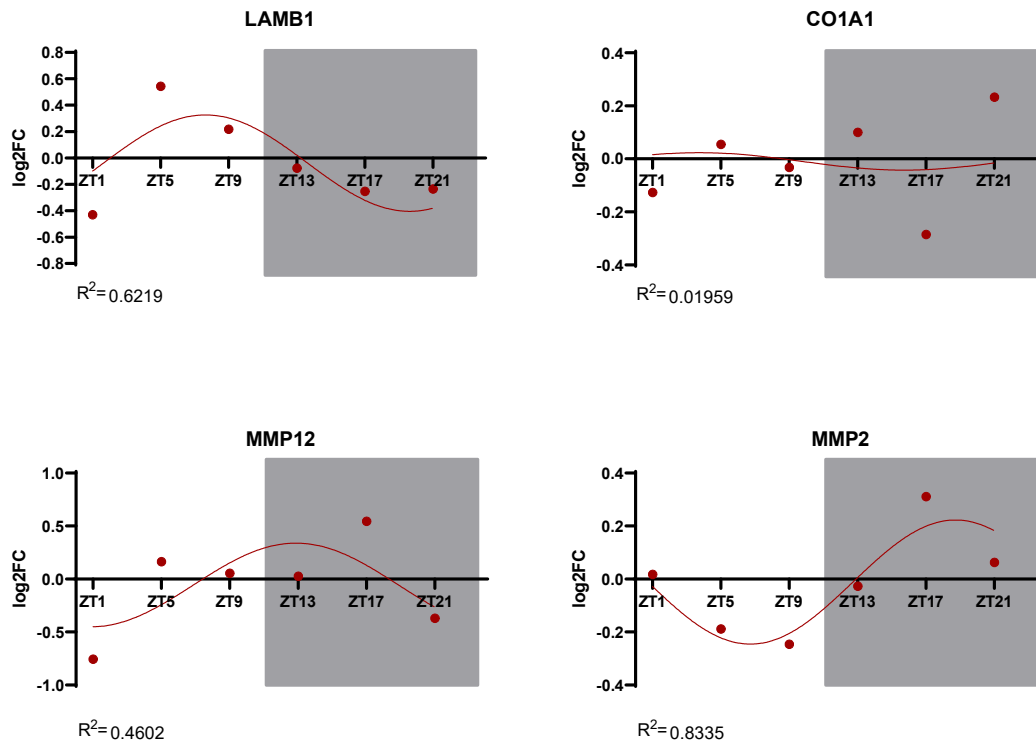
Figure 35. Changes in protein abundance over 24h in proteins forming the ECM and metalloproinases.

The lower amount of CO1A1 detected in the proteome is comparable to the results obtained with the Sirius red staining, in which different types of collagen are detected (**Figure 36.A**). Together with the diminishment of collagen, the thickness of the fibrous cap, measured as fibrous cap index and minimum fibrous cap thickness, also have the minimum amounts between ZT13 and ZT17, indicating a probable timepoint prone to plaque rupture (**Figure 36.B** and **36.C**). The highest areas of necrotic core are also found between ZT17 and ZT21 (**Figure 36.D**).
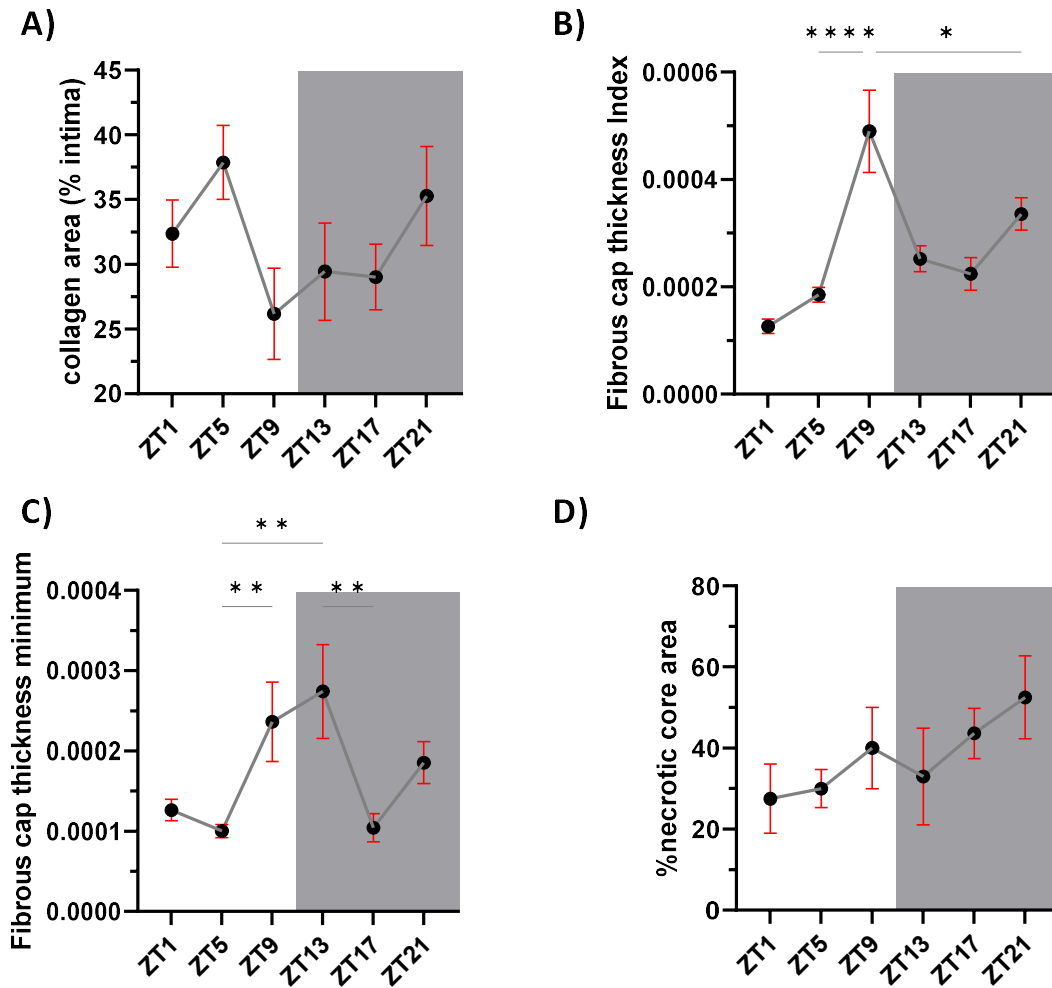
Figure 36. Plaque stability and fibrous cap composition. A) Percentage of collagen in the plaque over 24h. **B)** and **C)** Measurements of fibrous cap thickness, represented as fibrous cap thickness index **(B)** and the minimum thickness **(C)**. **D)** Percentage of total area covered by necrotic core. Statistical analysis made using one-way ANOVA ($^*p<0.05$, $^{**}p<0.01$, $^{****}p<0.0001$). Data represented as mean±SEM.

3.1.4.6 Proteins related to plasma lipoprotein assembly change their abundance during the day

In the context of atherosclerosis and plaque development, the lipid handling is extremely important since lipid extravasation and accumulation is the starting point of the atherosclerotic plaque and the subsequent accumulation and incapacity of efficient elimination of these lipids is a main feature of the advanced atherosclerotic lesion[253]. In the

proteome analysis, we detect oscillation in several proteins that have several functions related to lipid import and export and lipid metabolism, as can be seen in **Figure 37**.

The increase in abundance of CD36, together with the increase in APOA and APOB at the end of the resting phase (from ZT9) indicate that this is the maximum point of lipid extravasation to the plaque[254,255]. Together with these proteins, other enzymes that are involved in the esterification of cholesterol in macrophages and the hydrolysis of cholesterol esters, as NCEH1 and SOAT1[256,257], show an increase of abundance that follows a delayed pattern when compared with CD36, APOA and APOB. The entrance of lipids activates several pathways related to lipid metabolism in an effort to reduce the amount of lipids in the cytosol, such as CPT1B and CPT2B[258,259].
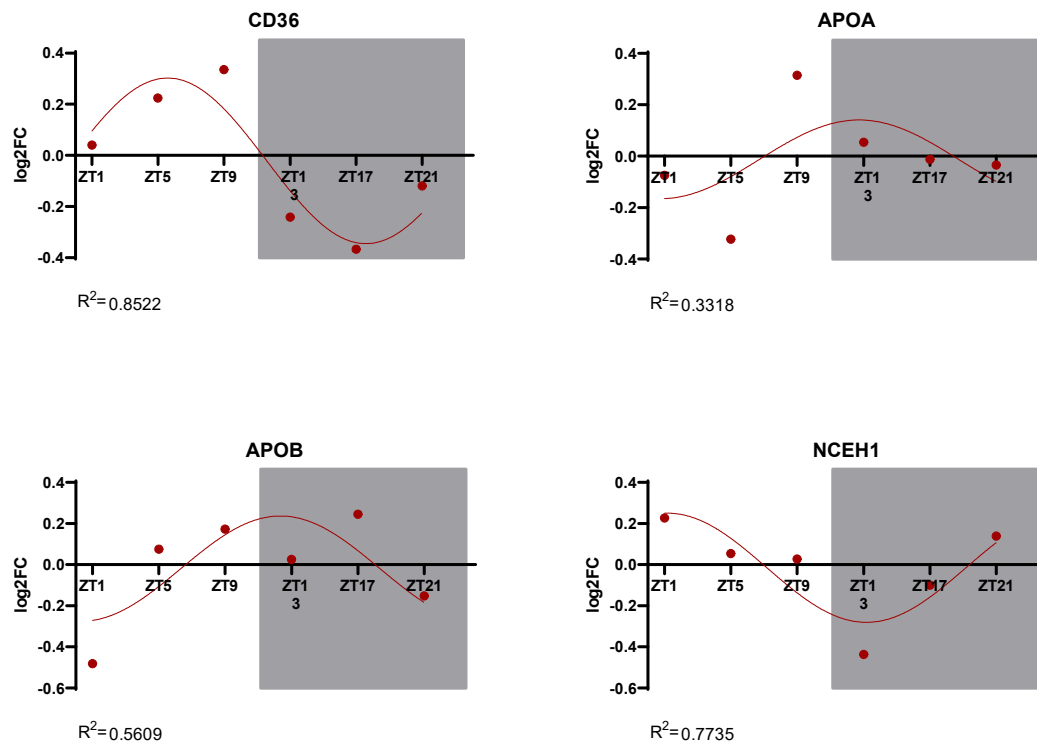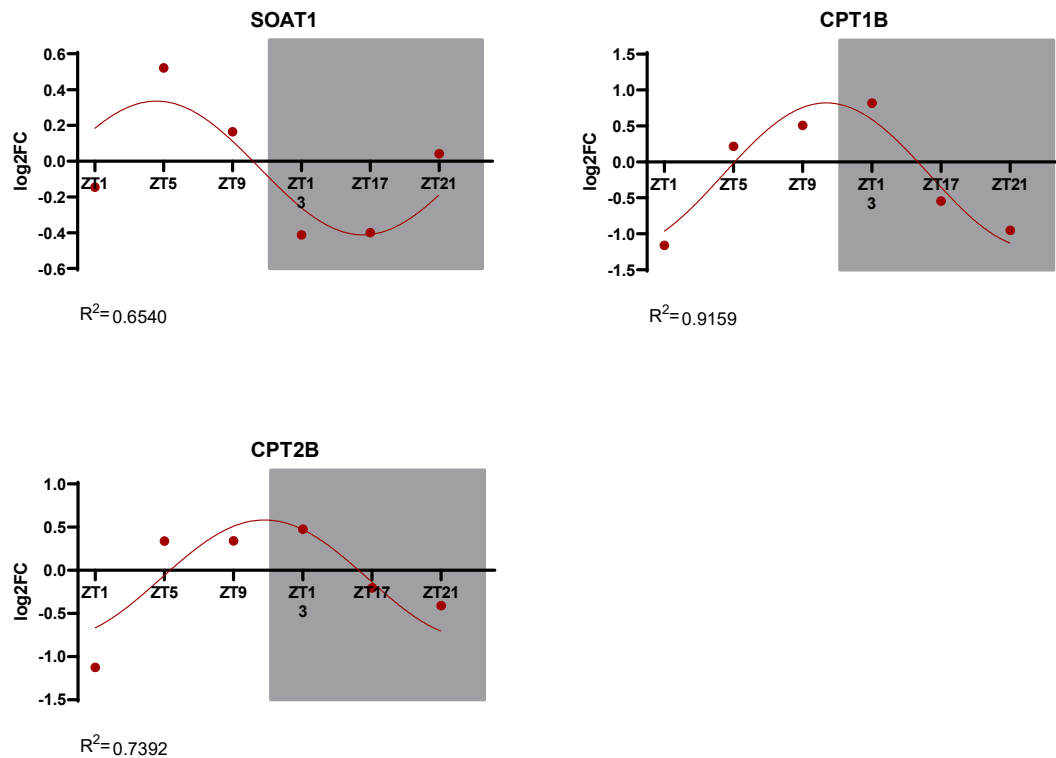
Figure 37. Changes in protein abundance over 24h in proteins related to lipid extravasation, lipid transformation and lipid metabolism.

3.1.5 Are the oscillations due to the number of cells or to the activity of the cells?

The changes in the counts per gene or in protein abundance can be due to an increase of the gene expression or the increase of the number of cells that are present in the plaque. The cellularity of the plaque and the plaque area remain constant during the day, as can be seen in **Figure 38** but there are changes in the abundance of each cellular population, giving as result changes in the plaque composition during the day.

A)

Cellularity

B)
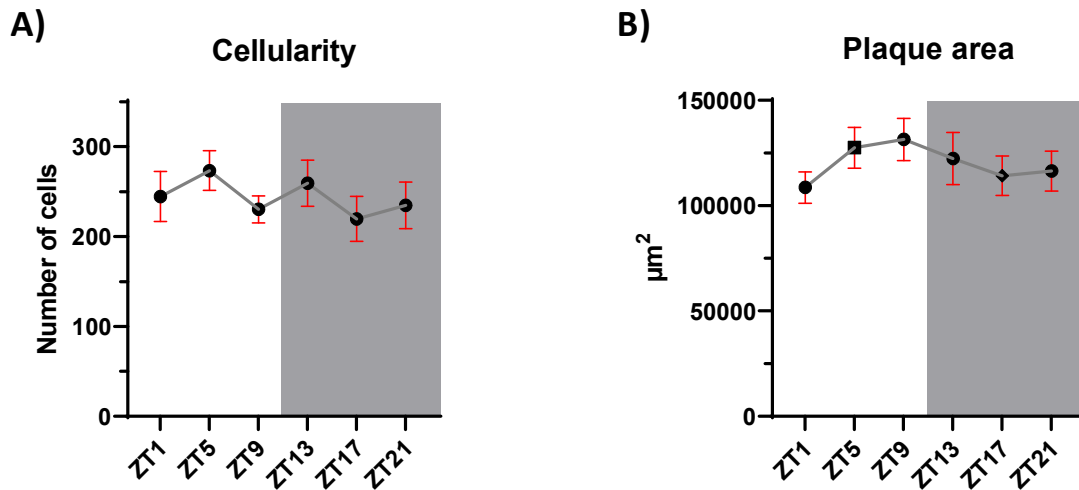
Plaque area

Figure 38. Changes in cellularity and plaque size over time. A) Cellularity based on DAPI staining of the atherosclerotic plaques over 24h. **B)** Plaque area measurement over 24h. No differences were found after using one-way ANOVA. Data represented as mean±SEM.

Despite having a constant number of cells in the plaque, the composition of the plaque in teams of stromal cells and immune cells changes over the day, as **Figure 39A** shows. This pattern is also observed with other populations of leukocytes, as can be seen in **Figure 39.B, 39.C** and **39.D** in which a higher amount of CD68$^+$, T cells and B cells are detected after ZT9.

A)

B)

C)

D)
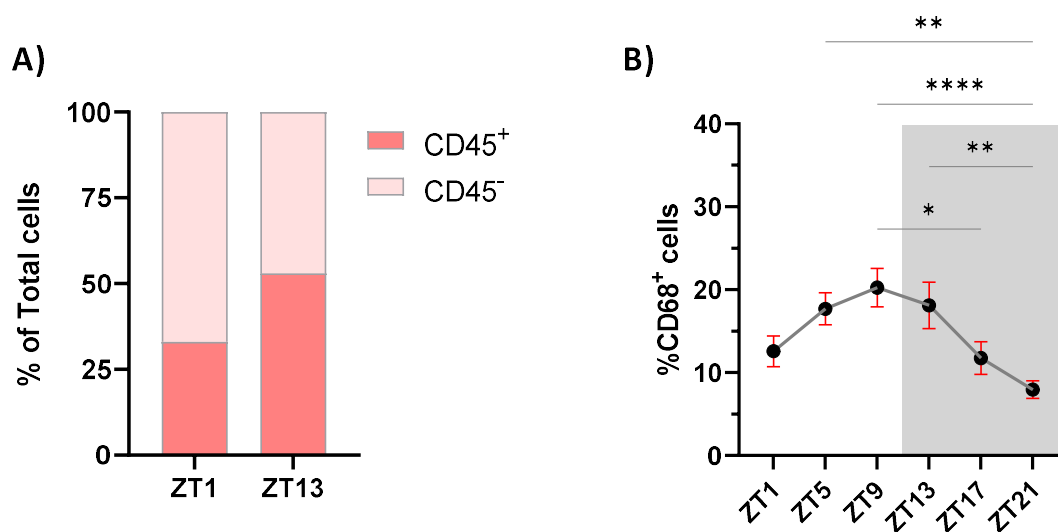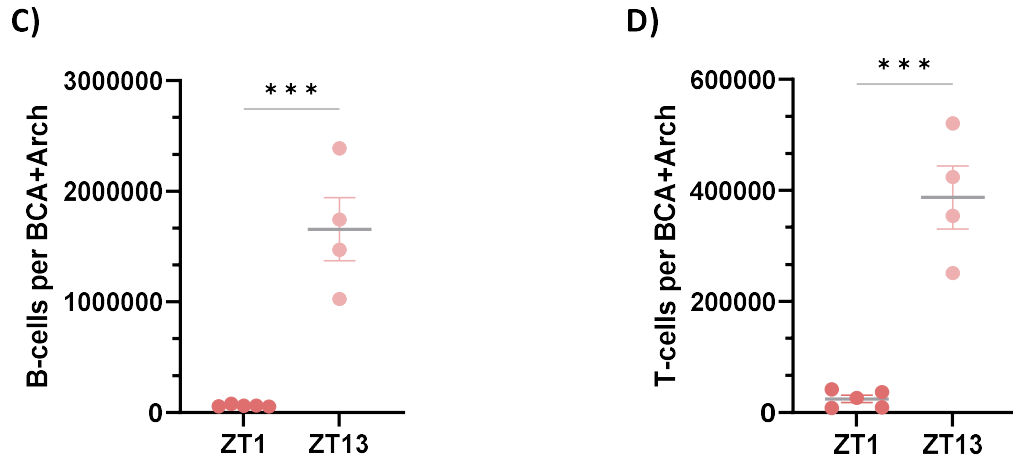
Figure 39. The abundance of different cellular populations in the plaque shows changes over the day. A) Percentage of CD45$^+$ and CD45$^-$ cells detected by flow cytometry of the BCA and the upper part of the aortic arch. **B)** Percentage of CD68$^+$ cells detected by immunohistochemistry of the BCA. **C)** Abundance of B-cells detected through flow cytometry of the BCA and the upper part of the aortic arch. **D)** Abundance of T-cells detected through flow cytometry of the BCA and the upper part of the aortic arch. Statistical analysis made using one-way ANOVA (*p<0.05, **p<0.01, ***p<0.001, ****p<0.0001). Data represented as mean±SEM.

The fraction of CD45$^-$ cells also show oscillation in terms of abundance (**Figure 39.A**), as it´s the case of SMA$^+$ and CD31$^+$ cells inside the plaque. The oscillation in their abundance is noticeable with immunohistochemistry techniques (**Figure 40**).

A)

B)
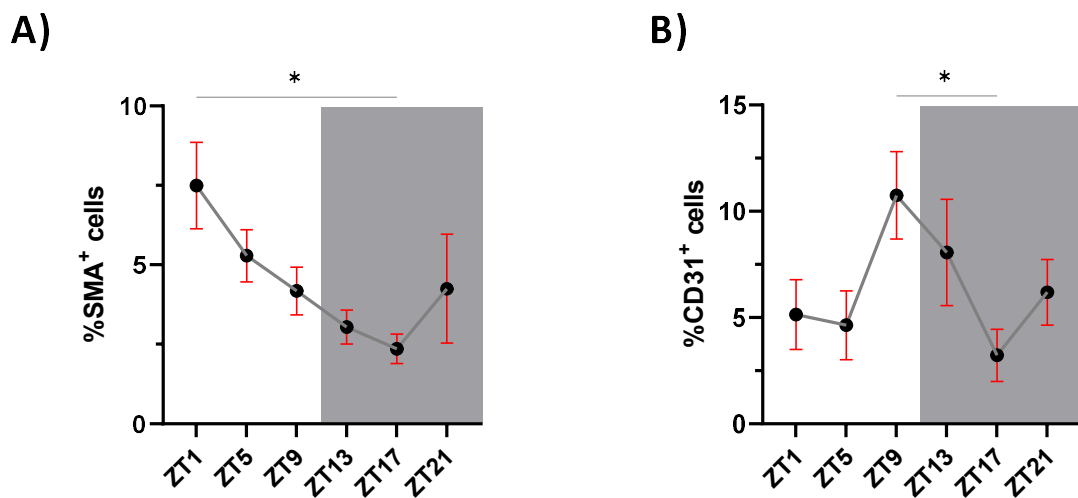
Figure 40. Changes in the CD45⁻ fraction of the plaque over the day. A) Percentage of SMA⁺ cells detected by immunohistochemistry of the BCA. **B)** Percentage of CD31⁺ cells detected by immunohistochemistry of the BCA. Statistical analysis made using one-way ANOVA (*p<0.05). Data represented as mean±SEM.

The abundance of cytokines that are used to recruit the different cellular types to the plaque and to allow their survivance and activation oscillate in plasma across the day, as can be seen in the **Figure 41**, in which the abundance of several molecules is measured in a Legendplex assay, as explained in **Section 2.2.2**. The low abundance of BAFF, CCL5, CXCL9 and CXCL10 between ZT13 and ZT17 can indicate a reduction of the number of leukocytes migrating and extravasating towards the atherosclerotic plaque in the beginning of the active phase for the mice, while the highest values are detected at the beginning of the resting phase (ZT21 and ZT1).
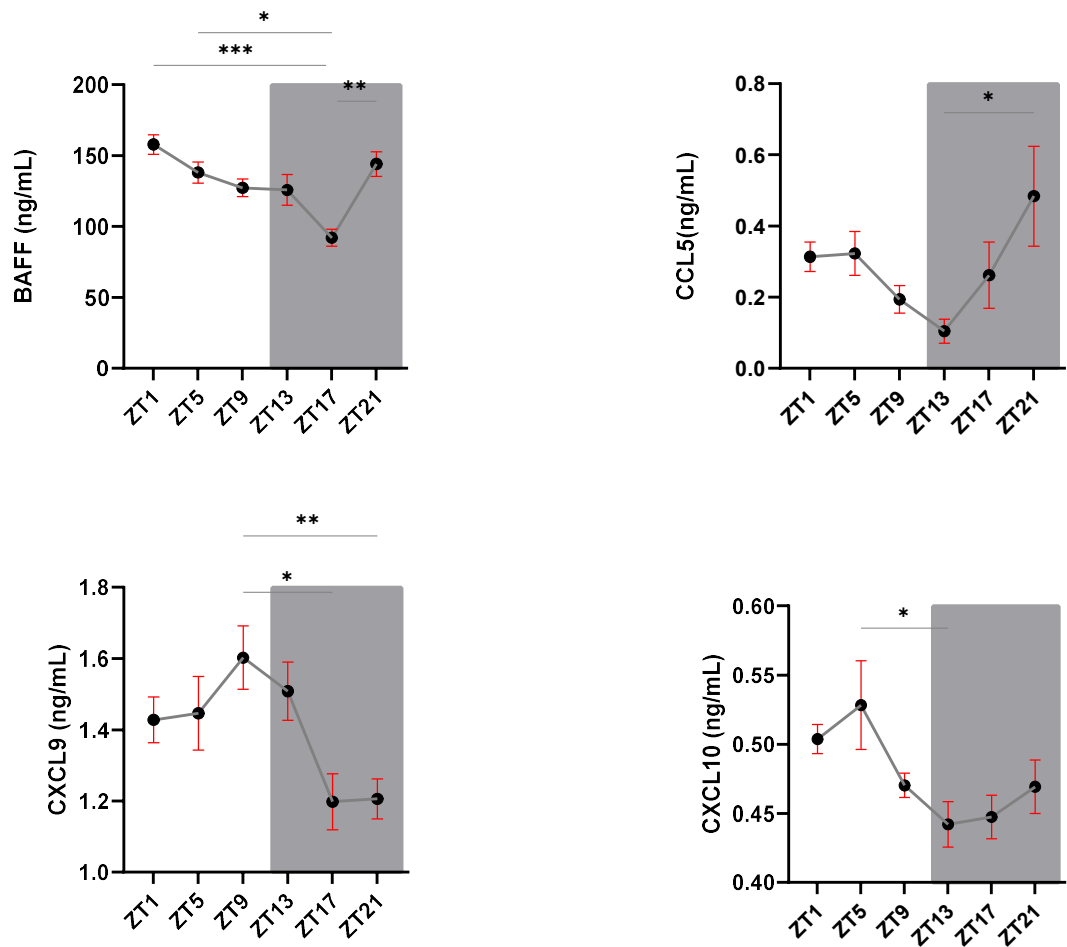
Figure 41. Abundance of different cytokines in the plasma of *Apoe*^{-/-} mice fed with HFD for 16 weeks. The abundance was detected using a LegendPlex panel, as explained in Section 2.2.2. Statistical analysis made using one-way ANOVA ($^*p<0.05$, $^{**}p<0.01$, $^{***}p<0.001$). Data represented as mean±SEM.

The low abundance of these cytokines in the beginning of the dark period matches the lowest abundance of the main groups of leukocytes in blood, as can be seen in **Figure 42**, in which the peak of abundance of all the populations of leukocytes considered is in the morning times around ZT5.
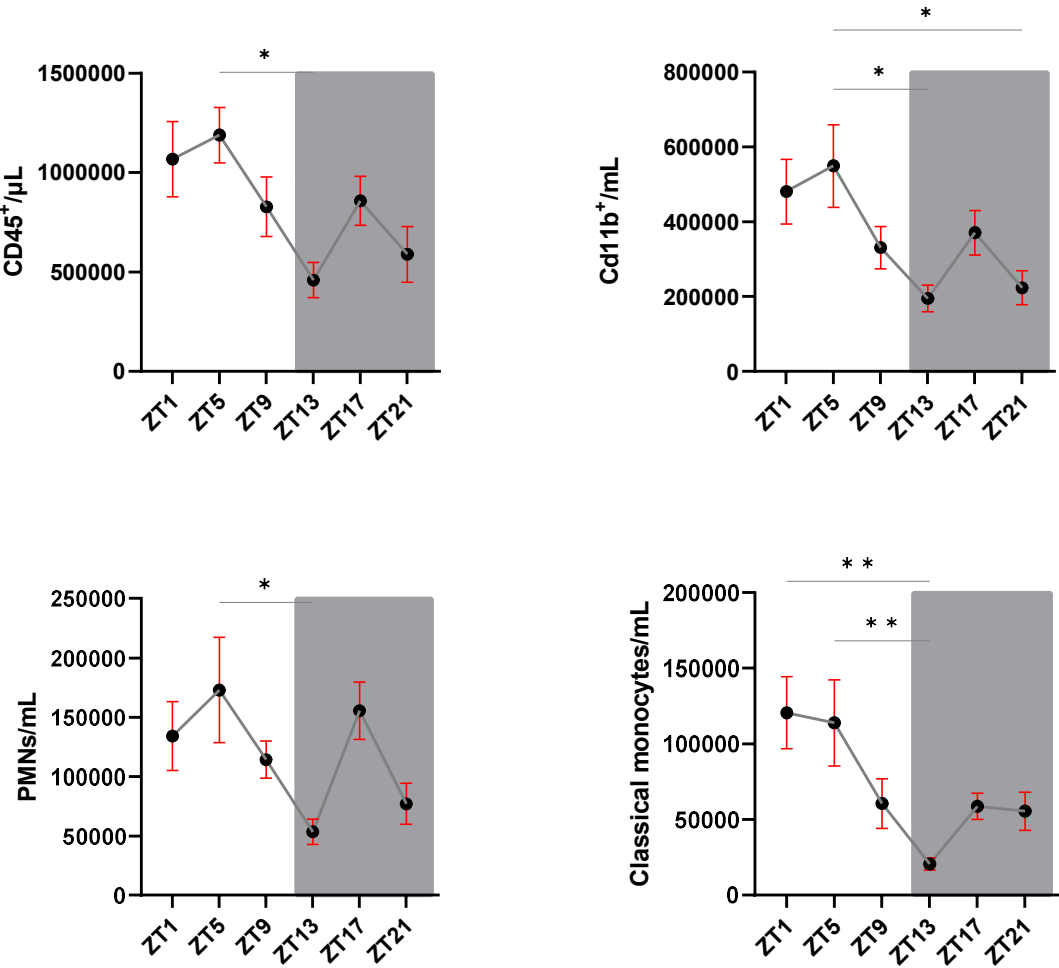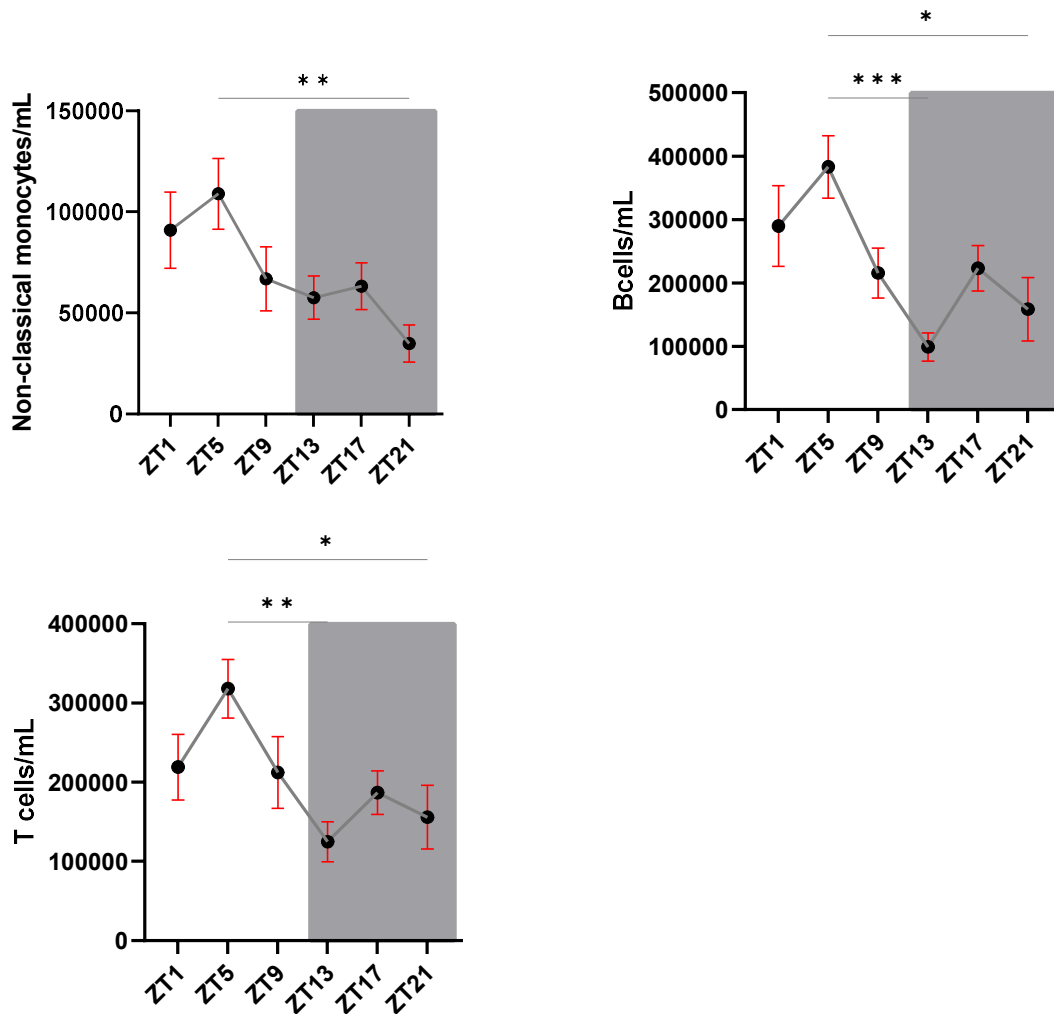
Figure 42. Abundance of different leukocytes in the blood of _Apoe_[-/-] mice fed with HFD for 16W. The populations were detected using flow cytometry as explained in Section 2.3. Statistical analysis made using one-way ANOVA ($^*p<0.05$, $^{**}p<0.01$, $^{***}p<0.001$). Data represented as mean±SEM.

3.1.6 Different cell types have their own rhythms

In the previous analysis (proteome and transcriptome), the behaviour of specific cell populations couldn't be assessed due to the homogenization of the samples and the inability to detect whether the oscillation of the proteins and genes was general or attributed to a specific cell population. To study the behaviour of specific populations inside the plaque, techniques as flow cytometry and single-cell transcriptomics were applied.

One striking example is the composition of the oscillating genes in the morning and in the evening timepoints in the plaque. As we could see in **Figure 32**, the percentage of BrdU$^+$ cells at ZT1 is higher than at ZT13, but the composition of the dividing group is not equal. As we can see in **Figure 43.A** less than 50% of the proliferating cells in the morning times are leukocytes, this percentage increases to almost ¾ at ZT13. Furthermore, the majority of the dying cells are CD45$^+$ leukocytes, accounting for 66% and 93% of all the apoptotic cells at ZT1 and ZT13, respectively. These trends follow the composition of the plaque from **Figure 39**, in which it was stated that the composition of the plaque is also different at ZT1 and ZT13, being CD45$^+$ more abundant at ZT13.
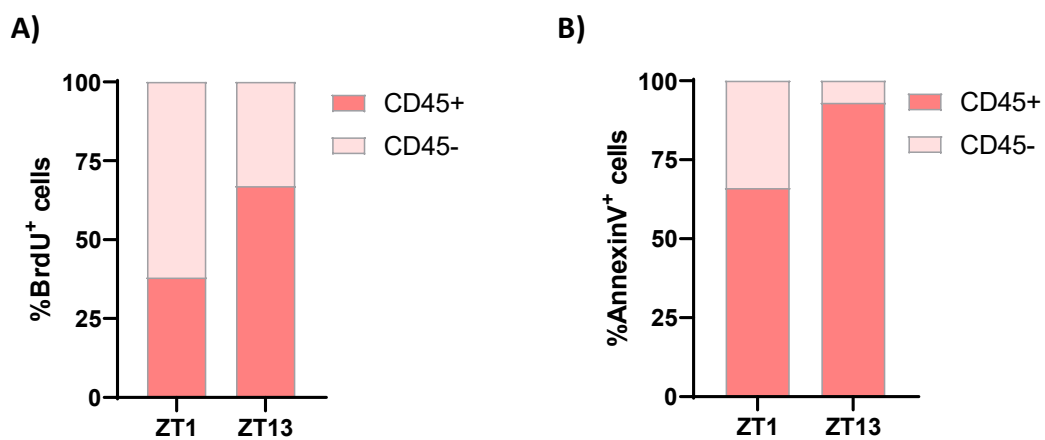
Figure 43. Contribution of different populations to cell death and cell proliferation. Immune and non-immune cell composition of the group of proliferating cells **(A)** and cell undergoing apoptosis **(B)** in the BCA at ZT1 and ZT13.

This different behaviour is also observable in the transcriptome of different cell populations through single cell. As can be seen in **Figure 44.A**, the percentage of cells expressing *Myc* in the plaque is very different when CD45$^+$ and CD45$^-$ populations are compared using Single Cell Sequencing (as explained in **Section 2.8**). In concordance with the BrdU results, the percentage of CD45$^+$ cells expressing *Myc* is higher at ZT13, while the population of CD45$^-$ cells follows a completely different approach, with very little difference among timepoints. The tendency of CD45$^+$ in the plaque follows the same trend than the leukocytes in the blood, that also show higher number of cells expressing *Myc* at ZT13. Despite this tendency, the percentage of leukocytes in blood that express *Myc* is much lower than in the plaque. This tendency is also followed by other biological processes, as the expression of genes related to cell death, like Caspase 3 (*Casp3*).

A)

Myc-expression in the plaque
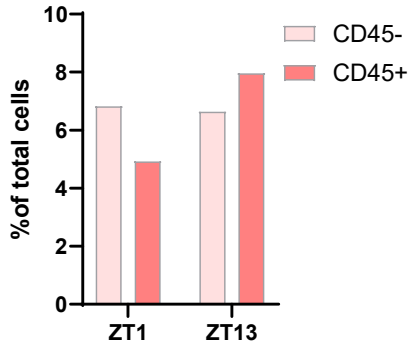
B)

Myc-expression in the blood
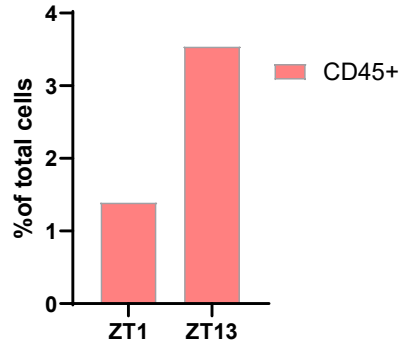
C)

Cells expressing Casp3
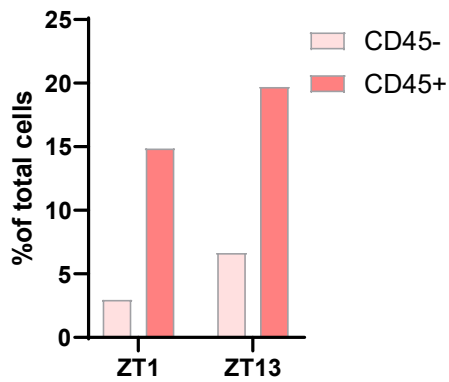
Figure 44. Expression of proliferation and apoptosis markers in different cellular populations. Percentage of cells expressing Myc in the atherosclerotic plaque **(A)** or in the blood **(B)**. **C)** Percentage of cells expressing Casp3 in the atherosclerotic plaque. The percentages are calculated as the percentage of cells expressing *Myc* or *Casp3* in the plaque using single-cell RNA-Seq without considering the abundance of the transcript.

3.2 There are important differences among the oscillating genes in *Apoe^-/-* mice and the C57BL/6J mice

3.2.1 Wild mice (C57BL/6J) have less oscillating genes in the BCA

To study the oscillatory patterns in the transcriptome of the plaque in *Apoe^-/-* mice, we compared the oscillating transcriptome of BCA from *Apoe^-/-* mice that had been on HFD for 16W versus C57BL/6J mice on chow diet for 16W. The tissue preparation, mRNA isolation, libraries and sequencing were performed together for the two groups, in an effort to avoid batch effect. The average number of reads per sample was 53.6 million reads, and the different types of reads can be observed in **Figure 45.A**.

We detected a very similar composition in the transcriptome of C57BL/6J mice, in which we could detect a total of 19449 genes (expressed with more than 10 reads on average after normalization). Most of these genes (96.51% or 18772 genes) are shared in both transcriptomes (**Figure 45.D and 45.E**). From now on, only the PCGs expressed in both the BCA from *Apoe^-/-* and C57BL/6J will be used for the analysis.

Despite these similarities in the transcriptome composition, the number of oscillating genes in the BCA from C57BL/6J is significantly lower than in *Apoe^-/-*. In C57BL/6J we find a total of 1617 oscillating genes (p-value<0.05 and FDR<0.1), which represents 8.31% of the total transcriptome. If only PCG are considered, 1305 PCG (8.34%) are oscillating in the PCG transcriptome of C57BL/6J mice (**Figure 45.B** and **45.C**).

A)

Transcriptome C57BL/6J

Number of reads

- Uniquely mapped
- Mapped to multiple loci
- Mapped to too many loci
- Unmapped (others)
- Unmapped (too short)
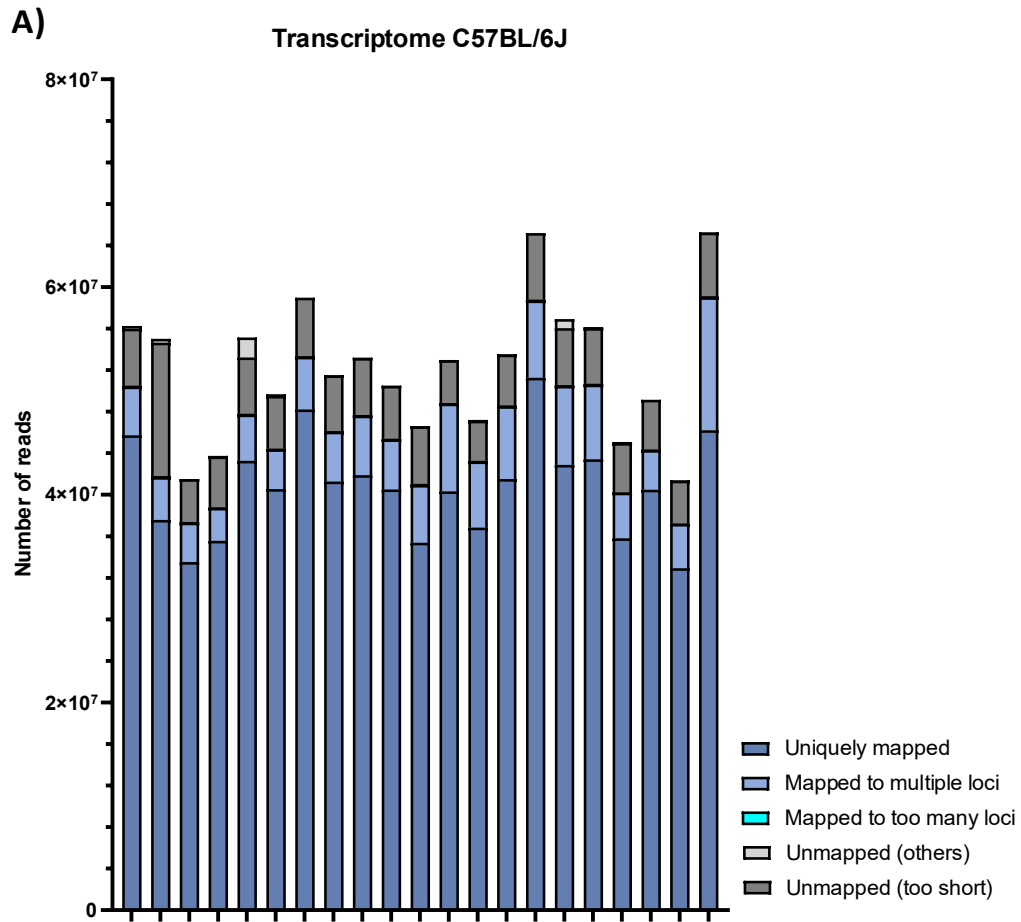
B)

Transcriptome BCA - C57BL/6J

7,99%

92,01%

C)

PCG BCA - C57BL/6J

8,34%

91,66%
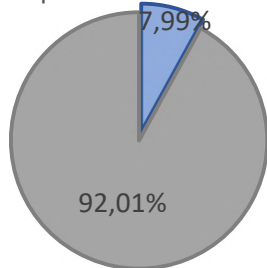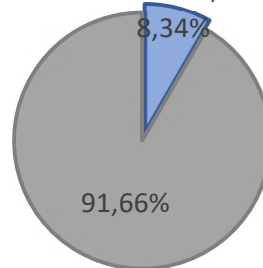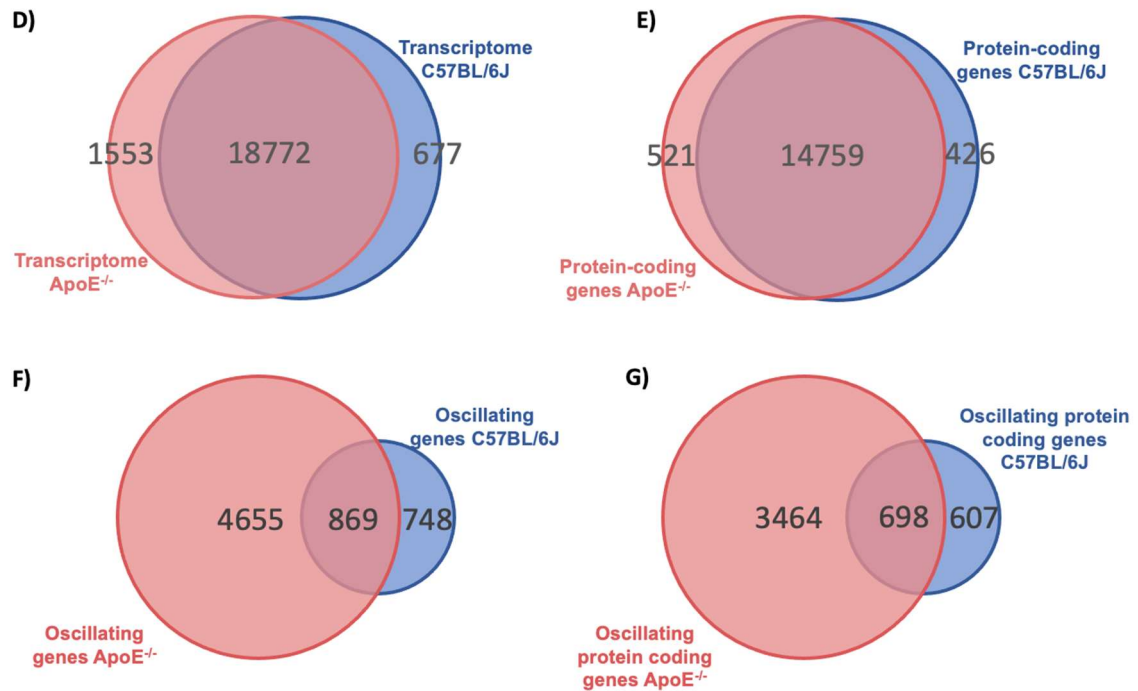
Figure 45. Library composition and oscillating transcriptome of BCA from C57BL/6J. A) Library composition for each sample. **B)** Percentage of oscillating genes in the BCA of C57BL/6. **C)** Percentage of the oscillating PCG in the BCA of C57BL/6. **D)** Venn diagram of total genes expressed in the transcriptome of *Apoe*^{-/-} (red) and C57BL/6J (blue). **E)** Venn diagram of oscillating PCG in *Apoe*^{-/-} and C57BL/6J. **F)** Venn diagram showing shared oscillating genes between *Apoe*^{-/-} and C57BL/6J. **G)** Venn diagram showing shared PCG between *Apoe*^{-/-} and C57BL/6J.

3.2.2 Genes oscillating in the BCA of C57BL/6J and *Apoe*^{-/-} show different pattern of expression

The differences between *Apoe*^{-/-} and C57BL/6J are not only in the number of genes that show oscillation, but also in the pattern of the genes that oscillate in both genotypes. From the 698 PCG that are oscillating in *Apoe*^{-/-} and C57BL/6J (**Figure 45.F**), we saw differences in the oscillating patterns, with differences in the peaks, lowest points and changes of expression throughout the day. Most of the genes that oscillate in C57BL/6J and *Apoe*^{-/-} belong to basic pathways to keep cellular functions, as post-translational protein modification, translation, signalling by GTP-ases, splicing… But there are also important genes related to pathways that have an extreme importance in atherosclerotic development and plaque stability, as cell cycle, innate and adaptive immune system and lipid metabolism (**Figure 46**).
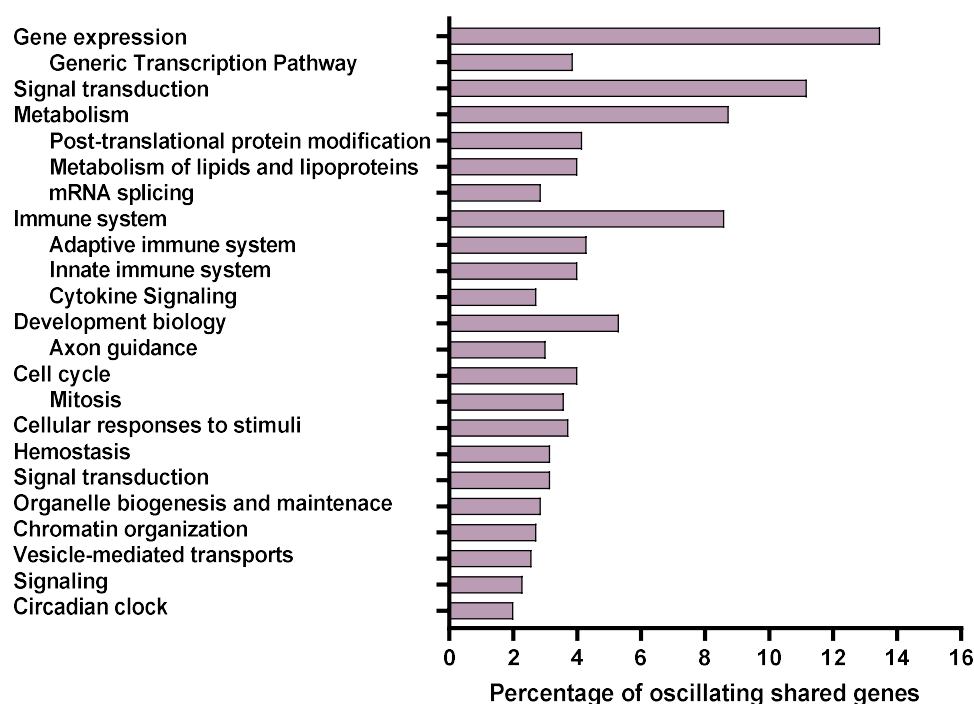
Figure 46. Enriched pathways in the group of PCG that show oscillatory patterns both in *Apoe*$^{-/-}$ and C57BL/6J. The enrichment analysis was done with Enrichr using the Reactome database as explained in **Section 3.6.4.8**

In this group of PCG, we can also find the core clock genes (*Bmal1*, *Clock*, *Cry1*, *Cry2*, *Per1*, *Per2* and *Per3*), that show differences in the pattern of expression (**Figure 47**). *Bmal1*, *Clock* and *Cry1* have a significant reduction of the amplitude during the day in *Apoe*$^{-/-}$ when compared to C57BL/6J (log2FC max/min in *Bmal1-Apoe*$^{-/-}$ 2.73 and 4.26 in *Bmal1*-C57BL/6J, log2FC max/min in *Clock-Apoe*$^{-/-}$ 0.59 and 1.28 in *Clock*-C57BL/6J and log2FC max/min in *Cry1*-Apoe$^{-/-}$ 1.63 and *Cry1*-C57BL/6J 2.51). In the rest of the genes, the differences of amplitude are blunted and the pattern of expression is more similar, except for the expression of *Per1*, in which the peak of expression is situated at ZT9 in *Apoe*$^{-/-}$ mice and at ZT13 in C57BL/6J mice.

114

A) *Bmal*

B) *Clock*

C) *Cry1*

D) *Cry2*

E) *Per1*

F) Per2

G) *Per3*

H) Core clock genes amplitude
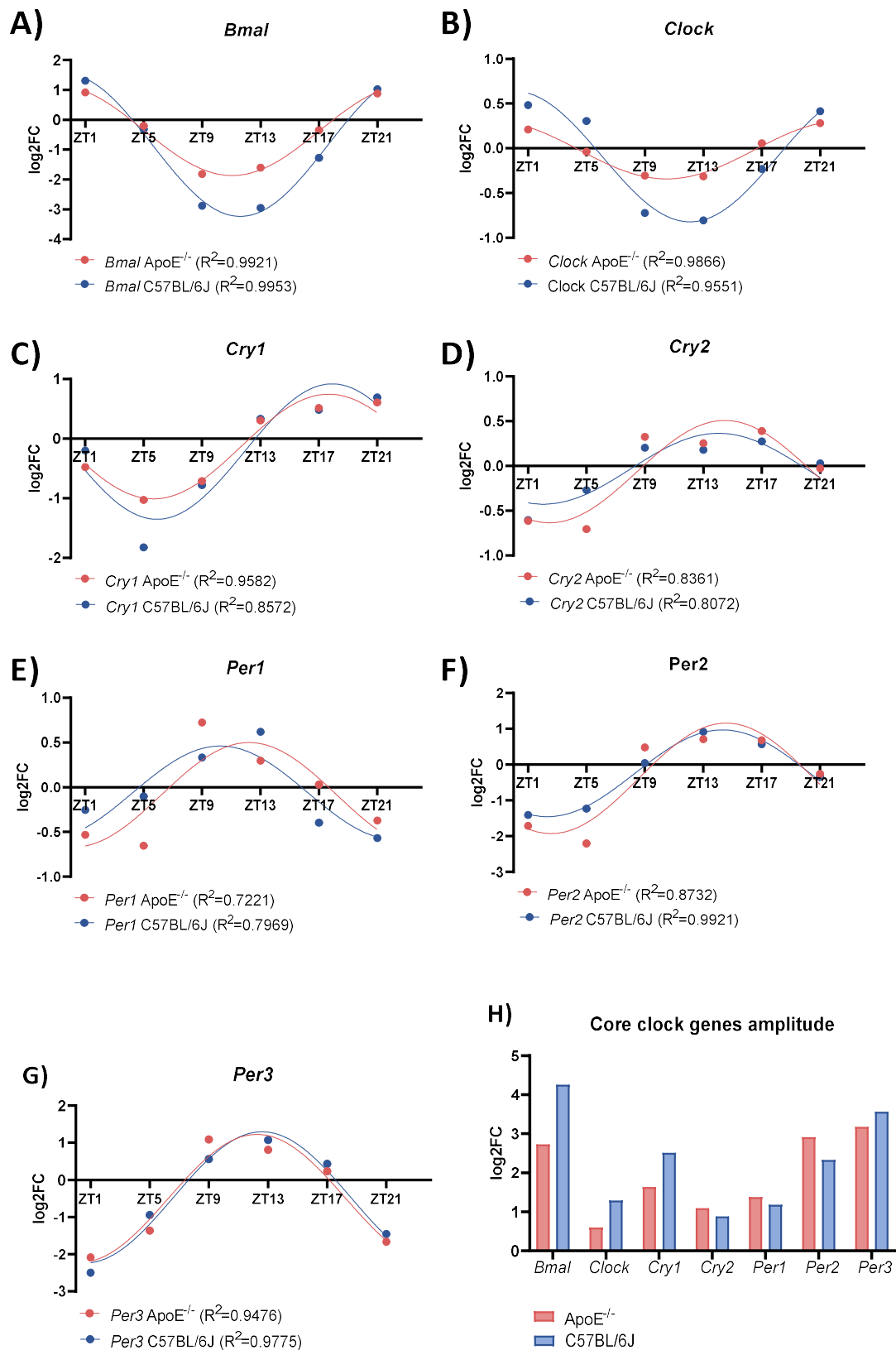
Figure 47. Comparison of the expression of core clock genes in *Apoe*^{-/-} and C57BL/6J. A-G.Comparison of oscillating patterns in *Apoe*^{-/-} and C57BL/6J for the different core clock genes. **H)** Amplitude of each core clock genes in *Apoe*^{-/-} and C57BL/6J.

Changes in the amplitude of the oscillation of the PCG can be also observed in other PCG, as for example *Hilpda* (**Figure 48**), a gene involved in intracellular lipid accumulation and the expression of cytokines, also shows changes in the pattern[260]. The expression profiles between *Apoe*^{-/-} and C57BL/6J don't differ enormously, but the amplitude is double in *Apoe*^{-/-} versus C57BL/6J.

Hilpda

ApoE^{-/-} (R^2=0.8948)
C57BL/6J (R^2=0.9083)
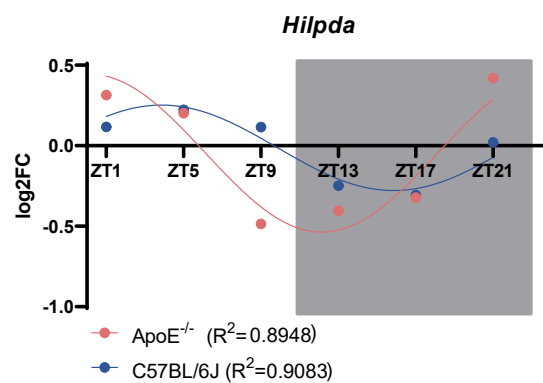
Figure 48. Differences in the pattern of expression of *Hilpda*. *Hilpda* is classified as oscillating gene in both *Apoe*^{-/-} and C57BL/6J.

From the total amount of PCGs that show oscillation in the two genotypes, only 18.05% (126 PCG) of the PCG genes have their lowest values and the highest values in the same ZTs in *Apoe*^{-/-} and C57BL/6J (**Figure 49**). Furthermore, from the PCG that have a different highest and/or lowest value, 11.21% (64 genes out of 572 genes with same highest/lowest or different highest and lowest) have a considerable shift in the pattern of expression, being the difference between peaks and lowest values higher than 4 hours when comparing *Apoe*^{-/-} and C57BL/6J.
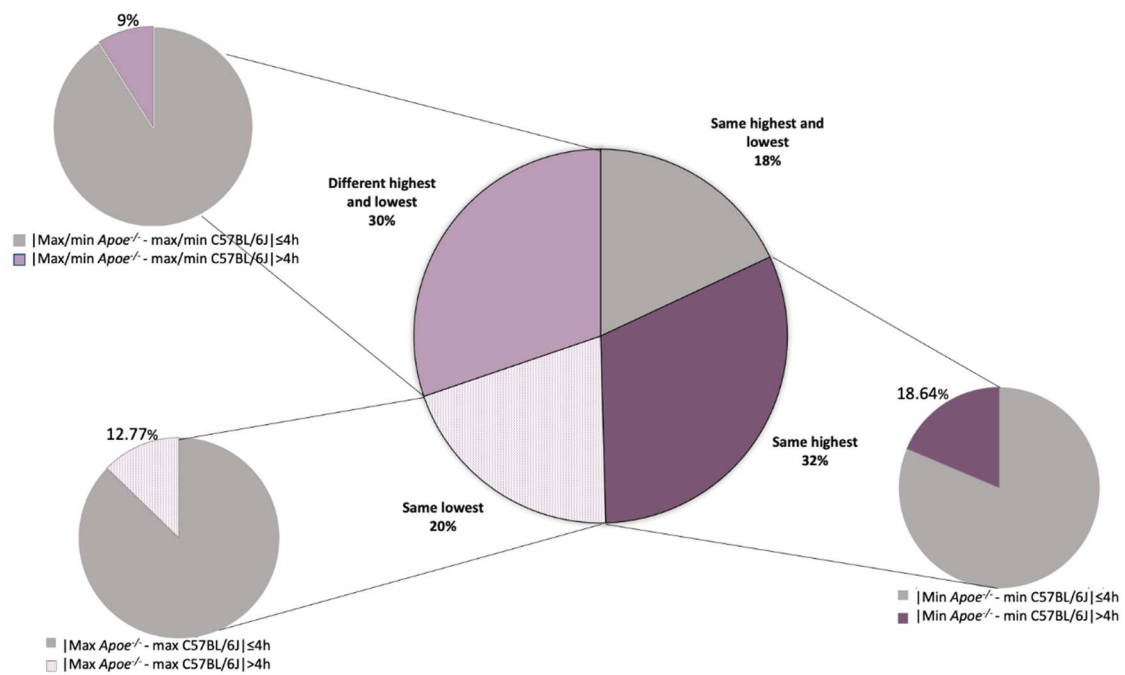
Figure 49. Representation of the different groups of PCG that oscillate in _Apoe_^{-/-} and C57BL/6J.

Some genes related to cell cycle and apoptosis show an antiphase expression in _Apoe_^{-/-} and C57BL/6J (**Figure 50**). This is the case of _Myc_, which shows a peak of expression in morning hours (between ZT1 and ZT5), while in the case of C57BL/6J the peak happens between ZT9 and ZT13. Other genes related to cell division and cell growth, as _Mtor_, show differences in the pattern of expression. In the case of _Apoe_^{-/-}, _Mtor_ has a peak of expression that last between ZT9 and ZT17, while in C57BL/6J there's a clear peak at ZT17 only. This could indicate the _Mtor_ is activated for a longer period in the BCA from _Apoe_^{-/-}. In the opposite way to _Mtor_, _Cdkn2b_, which is a tumour suppressor gene, has in C57BL/6J an increased period during which the maximum expression is achieved (from ZT17 until ZT1), while the maximum expression in _Apoe_^{-/-} is reduced to a peak at ZT17. _Rasa3_, which is a negative regulator of Ras pathway, shows a complete opposite pattern of expression in _Apoe_^{-/-} and C57BL/6J.
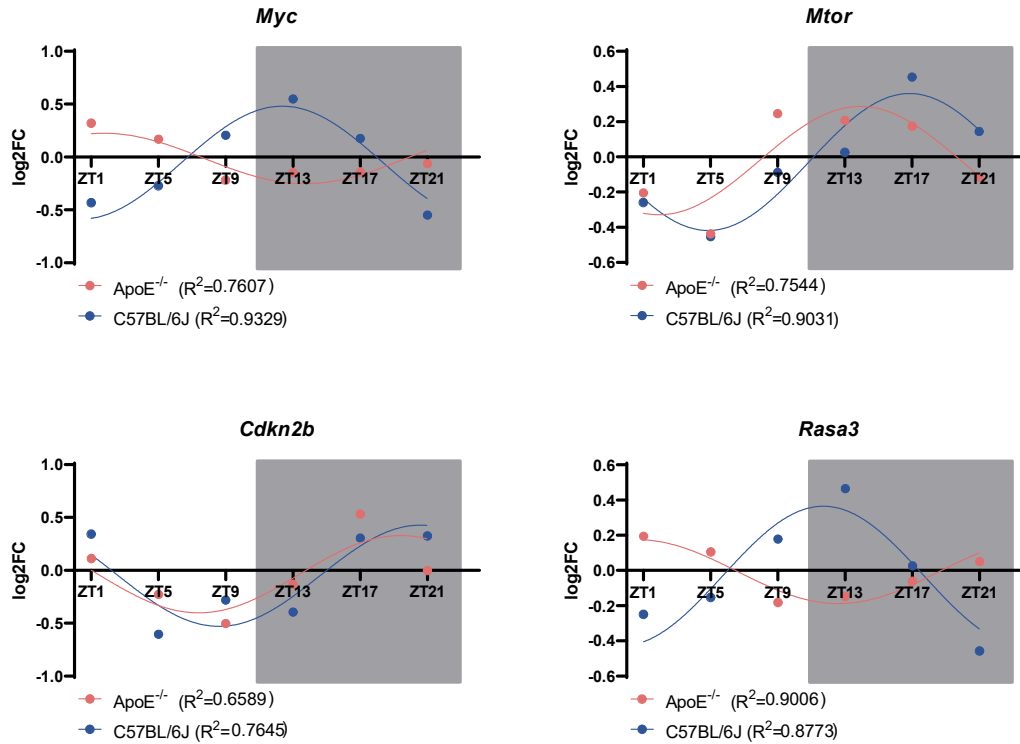
Figure 50. PCGs related to proliferation with a very different pattern of expression between _Apoe_^{-/-} and C57BL/6J.

When considered the pathways that are enriched in C57BL/6J and _Apoe_^{-/-}, we can see the differences in terms of oscillation. While in the **Figure 19** we could observe that different pathways in the cell cycle were being expressed gradually in the plaque, in C57BL/6J we can see that all the PCGs related to cell proliferation that oscillate have a peak between ZT9 and ZT13 (**Figure 51**). Besides, some mitotic checkpoints, as the APC/C degradation of cell cycle proteins, presents a peak in C57BL/6J later that it was in _Apoe_^{-/-}.
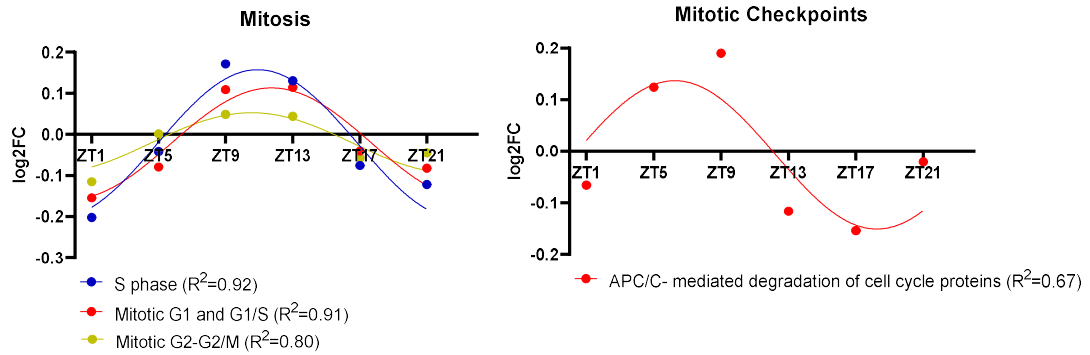
Figure 51. Representation of gene expression in different pathways from the cell cycle in C57BL/6J.

3.2.3 A percentage of genes lose oscillation in BCA in *Apoe*^{-/-}...

Despite the fact that we find more oscillating genes in *Apoe*$^{-/-}$ than in C57BL/6J, there's an important percentage of genes that show oscillation in C57BL/6J but not in *Apoe*$^{-/-}$. These 607 genes (46.44% of the oscillating genes in C57BL/6J) have functions related to very different cellular processes.

Some of the genes that lose oscillation in *Apoe*$^{-/-}$ are related to lipid accumulation in macrophages (*Sqstm1*, *Eva1a*)[261,262], cell survival and proliferation (*Pim3*, *Pcna*)[263,264], expression of inflammatory genes (*Irak1*)[265], cell death (*Bik*, *Dido1*, *Dedd2*)[266-268]. The comparison on the different patterns of these genes in *Apoe*$^{-/-}$ and C57BL/6J is shown in **Figure 52**.
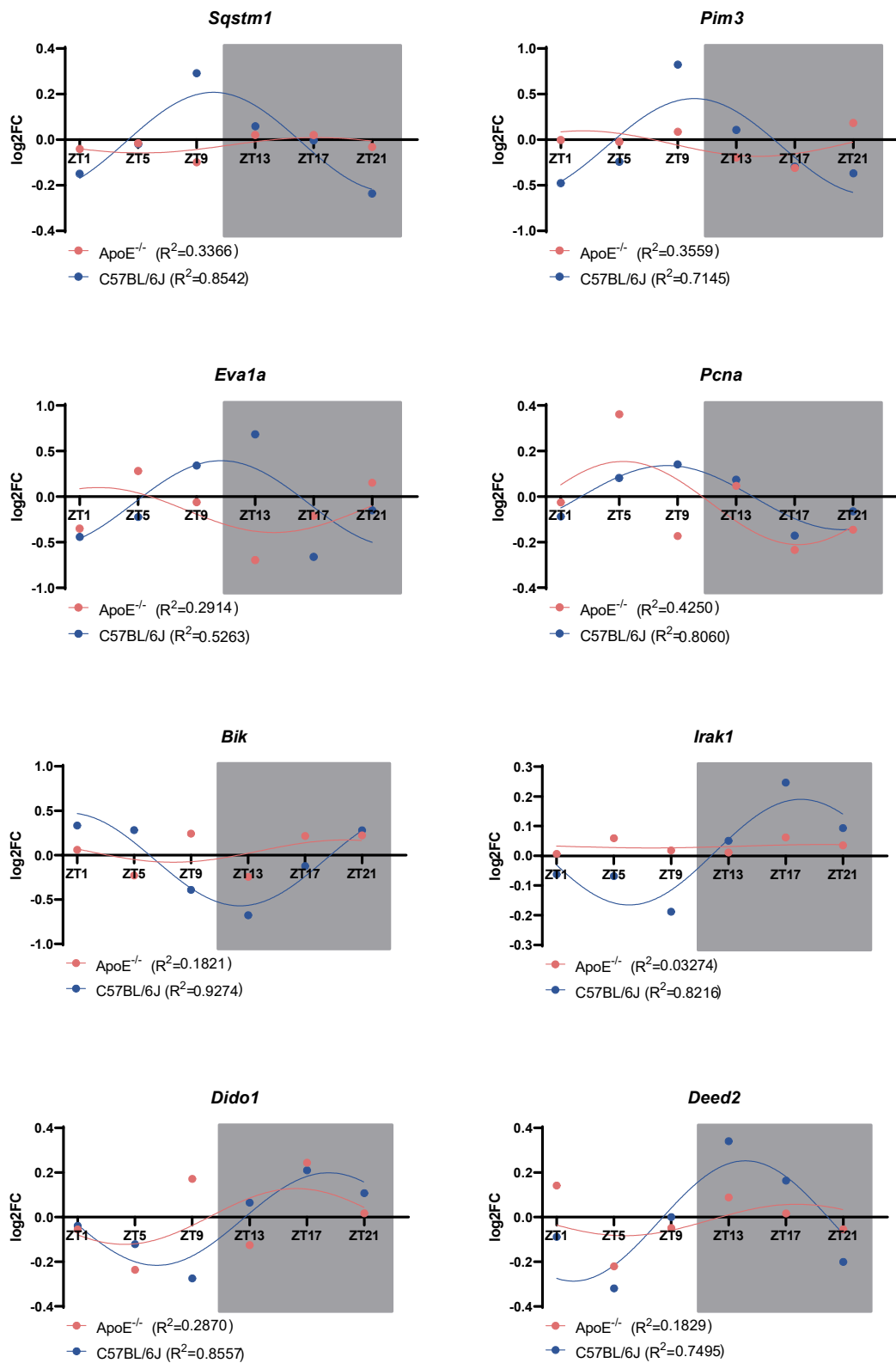
Figure 52. Representation of several PCGs that oscillate in C57BL/6J but have lost oscillation in *Apoe*^{-/-}.

Figure 52. Representation of several PCGs that oscillate in C57BL/6J but have lost oscillation in *Apoe*-/-.

3.2.4 …And a percentage of genes acquire oscillation in BCA in *Apoe*^{-/-}

Most of the genes (3464 or 83.23%) that oscillate in *Apoe*^{-/-} are not classified as oscillatory genes in the BCA of C57BL/6J.

An important percentage of these genes are related to cell death. These genes are expressed also in the BCA from C57BL/6J mice, but in these mice they don´t show an oscillatory pattern. Among the genes that oscillate only in *Apoe*^{-/-} we can find genes related to the cell death regulation, as *Bid* and *Bax*, but also effector genes, as several Caspases (**Figure 53**).
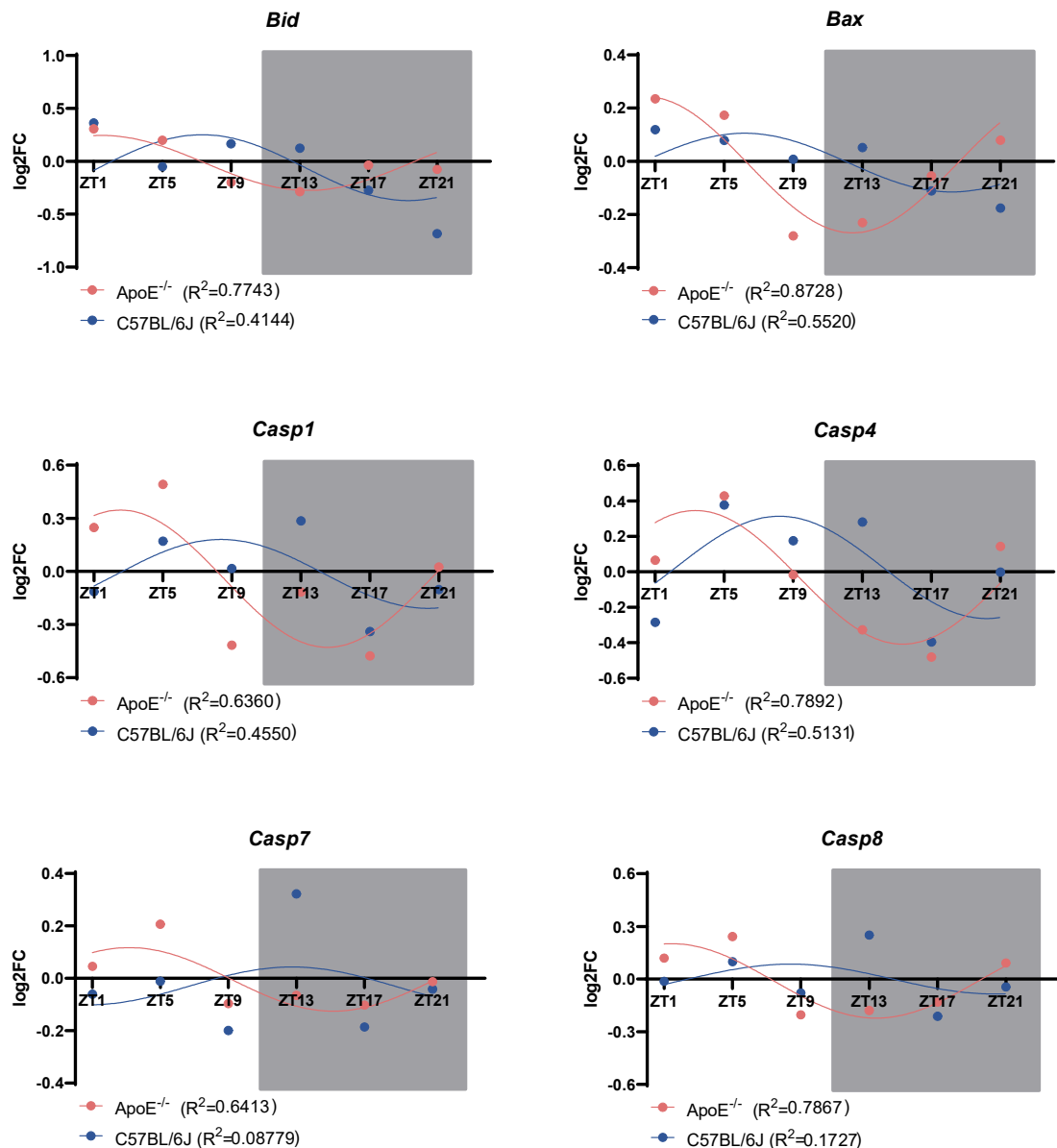
Figure 53. Representation of several PCGs from different pathways related to cell death that oscillate in *Apoe*^{-/-} but have lost oscillation in C57BL/6J.

The differences in the pattern expression across the day in *Apoe*^{−/−} and C57BL/6J are very noticeable when considering all the genes (detected as oscillating or not) related to the Programmed Cell Death signature from Reactome (R-MMU-5357801), which consists of 212 genes . Although most of the genes are expressed in both genotypes (198 or 93.34% in *Apoe*^{−/−} and 197 or 92.93% in C57BL/6J), a general oscillation across the day can be observed in the signature as a whole, while this effect is much more diluted in C57BL/6J (**Figure 54**).
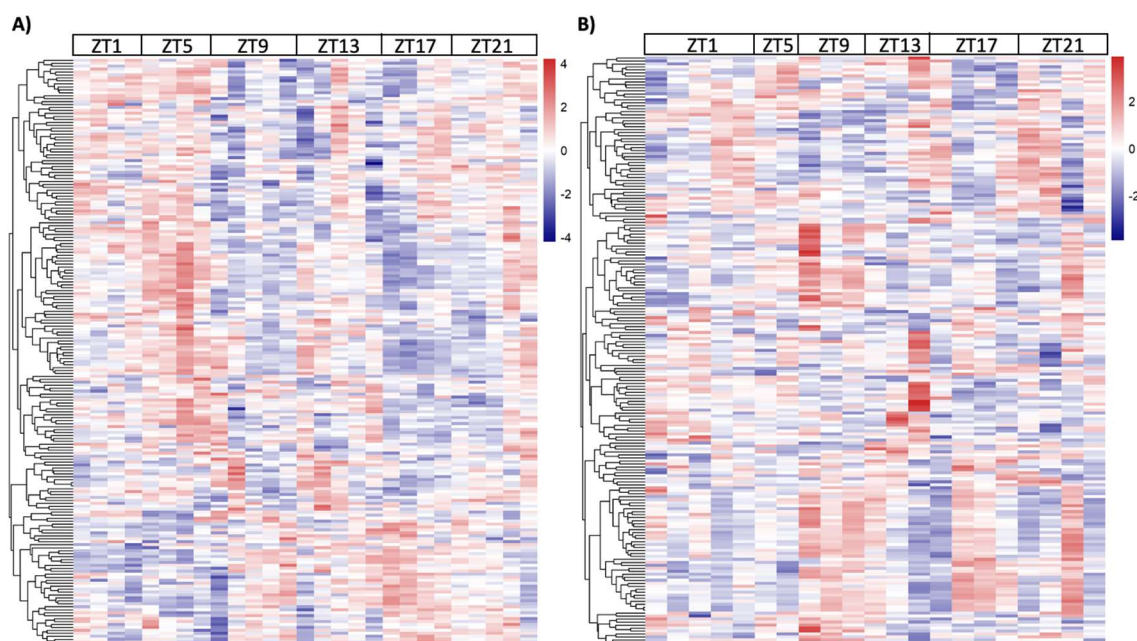
Figure 54. Heatmap of genes from the Programmed Cell Death from Reactome (R-MMU-5357801) expressed in the BCA from *Apoe*[−/−](A) and C57BL/6J (B).

In a comparable way to cell death, many genes related to cell cycle show an oscillatory pattern in *Apoe*^{−/−} but not in C57BL/6J (**Figure 55**). Most of them are cell cycle regulators that control the different checkpoints during mitosis and stop the proliferating process in case of DNA damage or cellular stress due to radiation, ROS or hyperosmotic conditions. Protein-coding genes involved in the transcription of different genes involved in the cell cycle (*Tfdp1*)[269], the G1 to S transition (*Anapc15*)[270] and the G2/M transition (*Plk3*, *Cdc14a*)[271,272] are found in this group. Furthermore, we can also find PCG that code for proteins that carry out indispensable functions during Mitosis, as Cyclins (*Ccnd2*)[273], cyclin-dependent kinases (*Cdk2*)[274] or proteins involved in the chromosome stability during mitosis (*Smc3*)[275].

Tfdp1

Anapc15

Plk3

Cdc14a

Ccnd2

Cdk2

Smc3

123
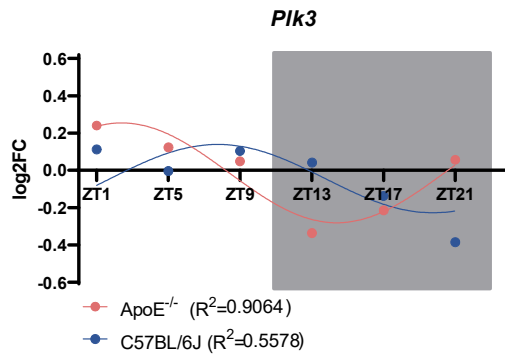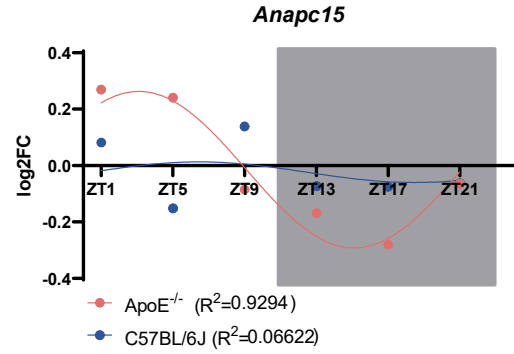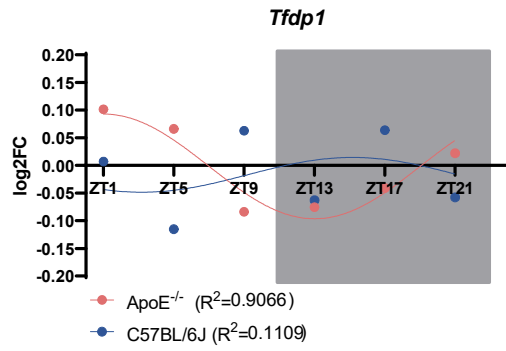
Figure 55. Representation of several PCGs from different pathways related to cell cycle and proliferation that oscillate in *Apoe*^{-/-} but have lost oscillation in C57BL/6J

In the same way, the heatmap of the Cell Cycle pathway in Reactome (R-MMU-1640170) shows a different level of circadian compartmentalization in *Apoe*^{-/-} and in C57BL/6J. In this case 97.76% of the genes from the pathway (656 genes out of 671 genes) were detected in *Apoe*^{-/-} and (658 genes out of 671 genes) were detected in C57BL/6J (**Figure 56**).
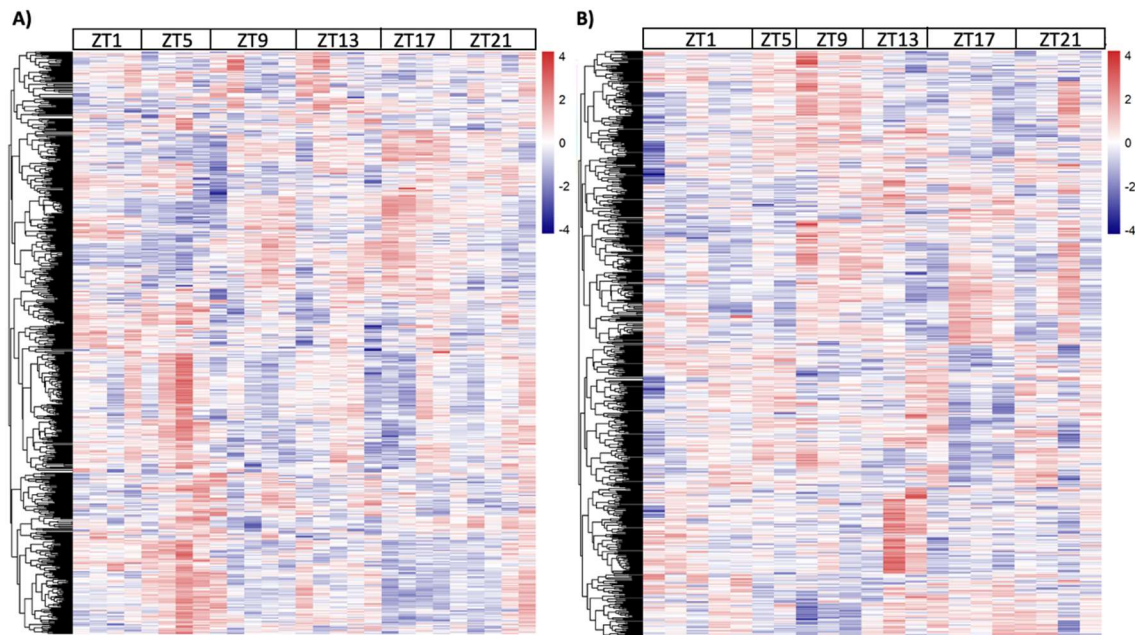
Figure 56. Heatmap of genes from the Cell Cycle Pathway from Reactome (R-MMU-1640170) expressed in the BCA from *Apoe*[-/-](A) and C57BL/6J (B).

The immune system follows the trend of Cell Cycle and Programmed Cell Death Pathways (**Figure 57**). Genes related to tumor necrosis factor family (*Tnfrsf13bB*, *TANK*, *Tnfrsf4*, *CD40*, *Lta*, *Ltb*)[276-278], interferons (*Irf3*, *Jak1*)[279], TLR pathway (*Myd88*)[280], NF-Kb modulators (*Ikbkb*)[281] and B-cell development (*Btk*)[282].

125
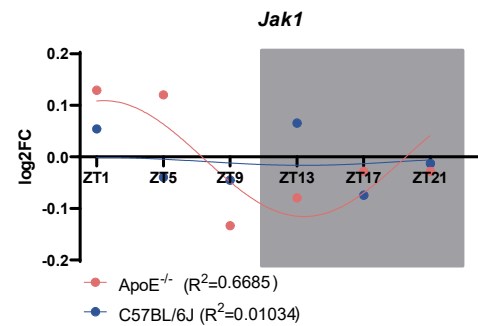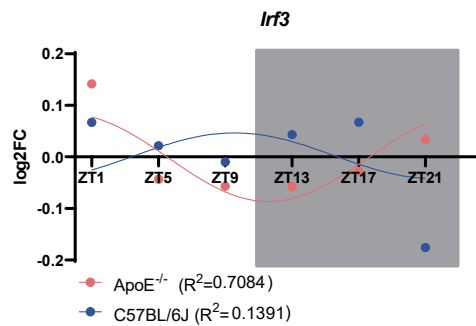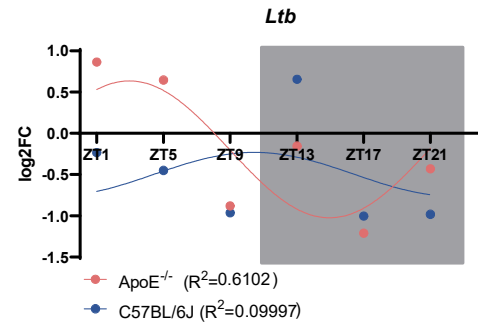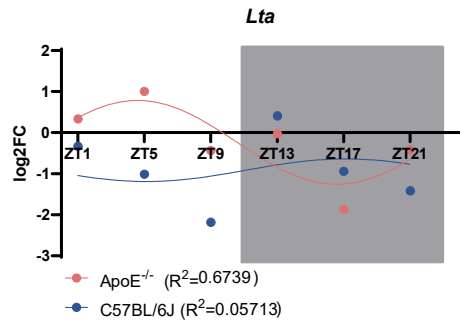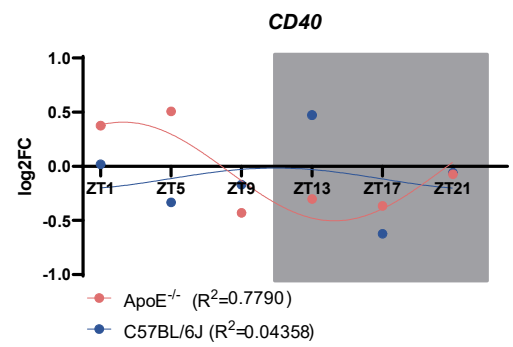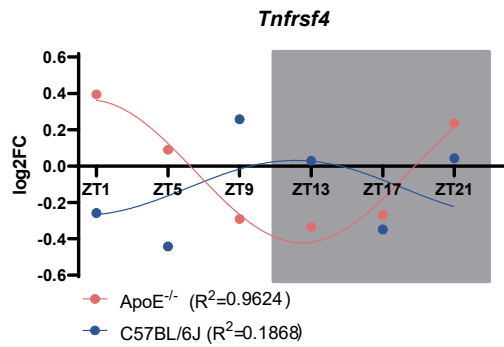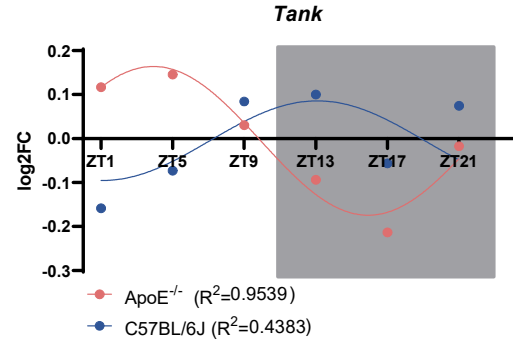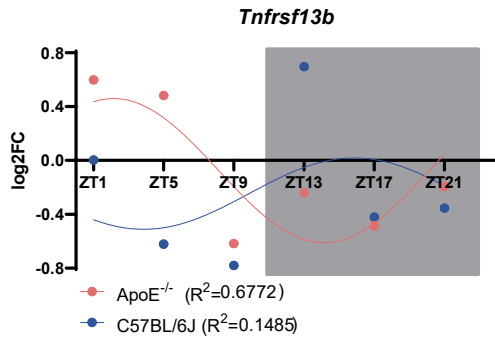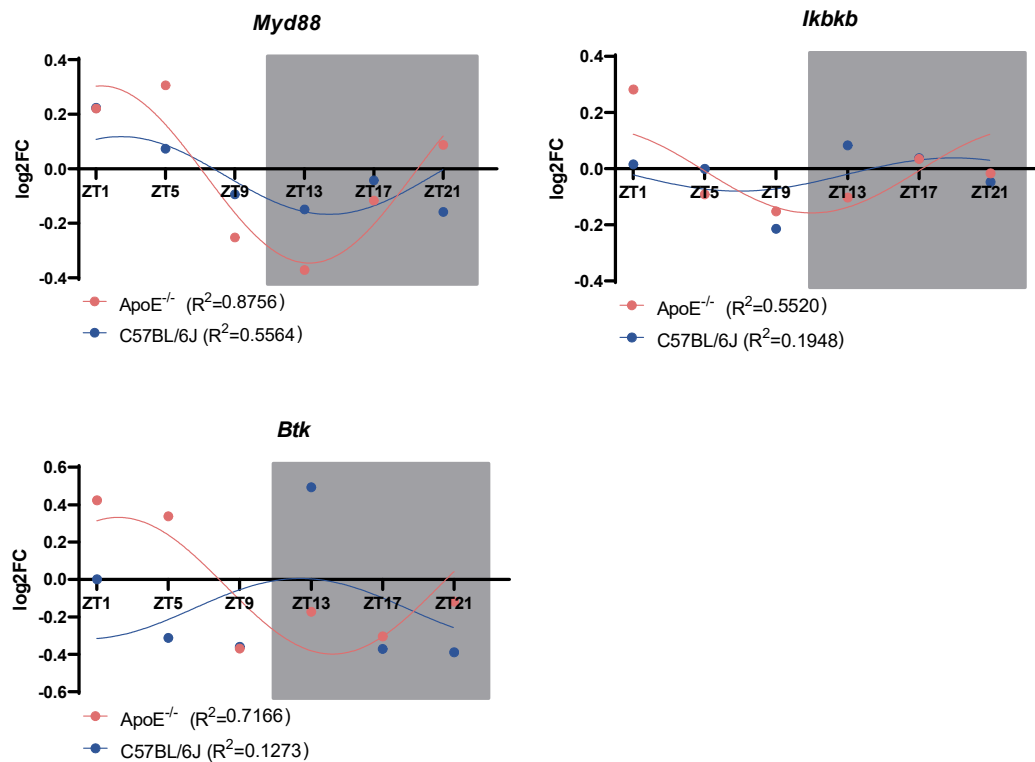
Figure 57. Representation of several PCGs from different pathways related to immune system that oscillate in *Apoe*^{-/-} but have lost oscillation in C57BL/6J.
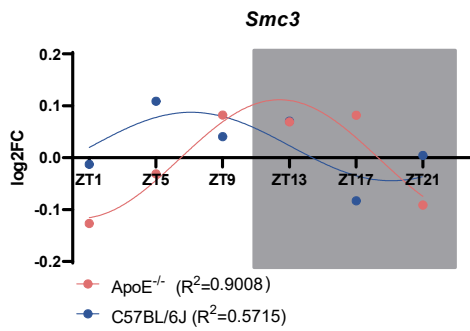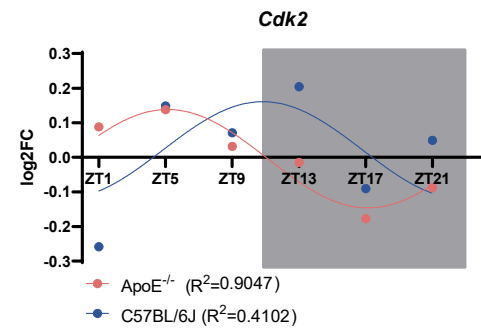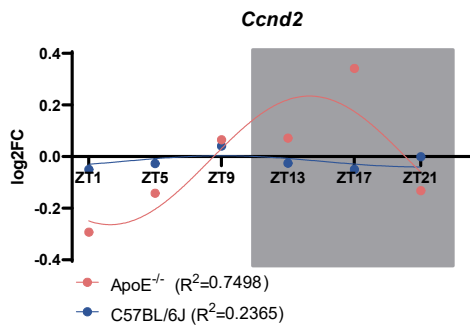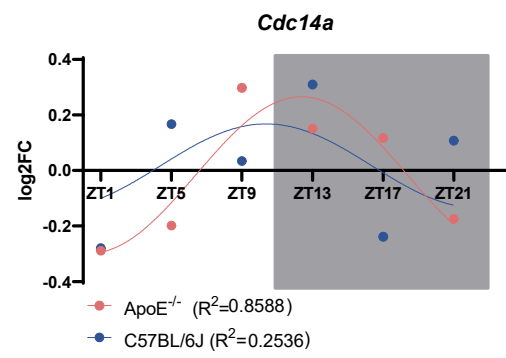
The heatmap of the Immune System pathway in Reactome (R-MMU-168256) shows a different level of circadian compartmentalization in *Apoe*^{-/-} and in C57BL/6J (**Figure 58**). In this case 92.97% of the genes from the pathway (1323 genes out of 1423 genes) were detected in *Apoe*^{-/-} and 93.11% (1325 genes out of 1423 genes) were detected in C57BL/6J.
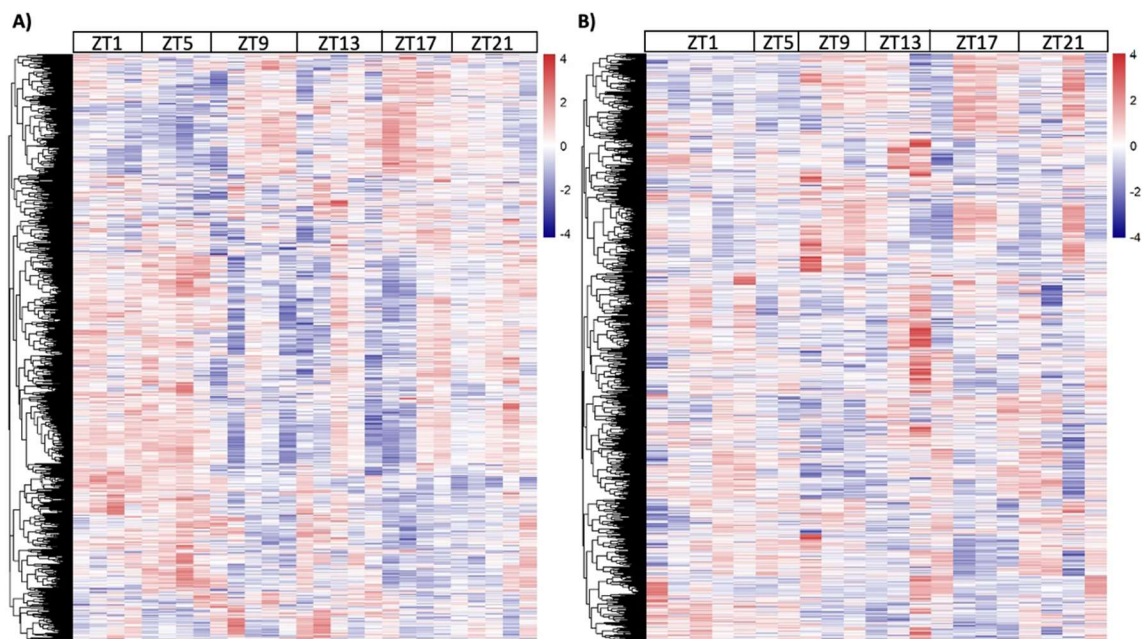
Figure 58. Heatmap of genes from the Immune system Pathway from Reactome (R-MMU-168256) expressed in the BCA from *Apoe*^{-/-} (A) and C57BL/6J (B).

These three groups of pathways (cell death, proliferation and immune system) are predominantly in an atherosclerotic plaque and their oscillation could be linked to the more presence of immune cells that can undergo through proliferating or death processes. Nevertheless, other groups of pathways that belong to neuronal system also follow this behaviour (**Figure 59**). Genes related to axon guidance (*Evl*, *Unc5c*, *Unc5a*, *Unc5d*)[283], neuron growth and differentiation (*Nrg2*)[284], and GABA pathway (*Gabrq*, *Gabrr2*)[285] oscillate circadianly only in Apoe^{-/-}.
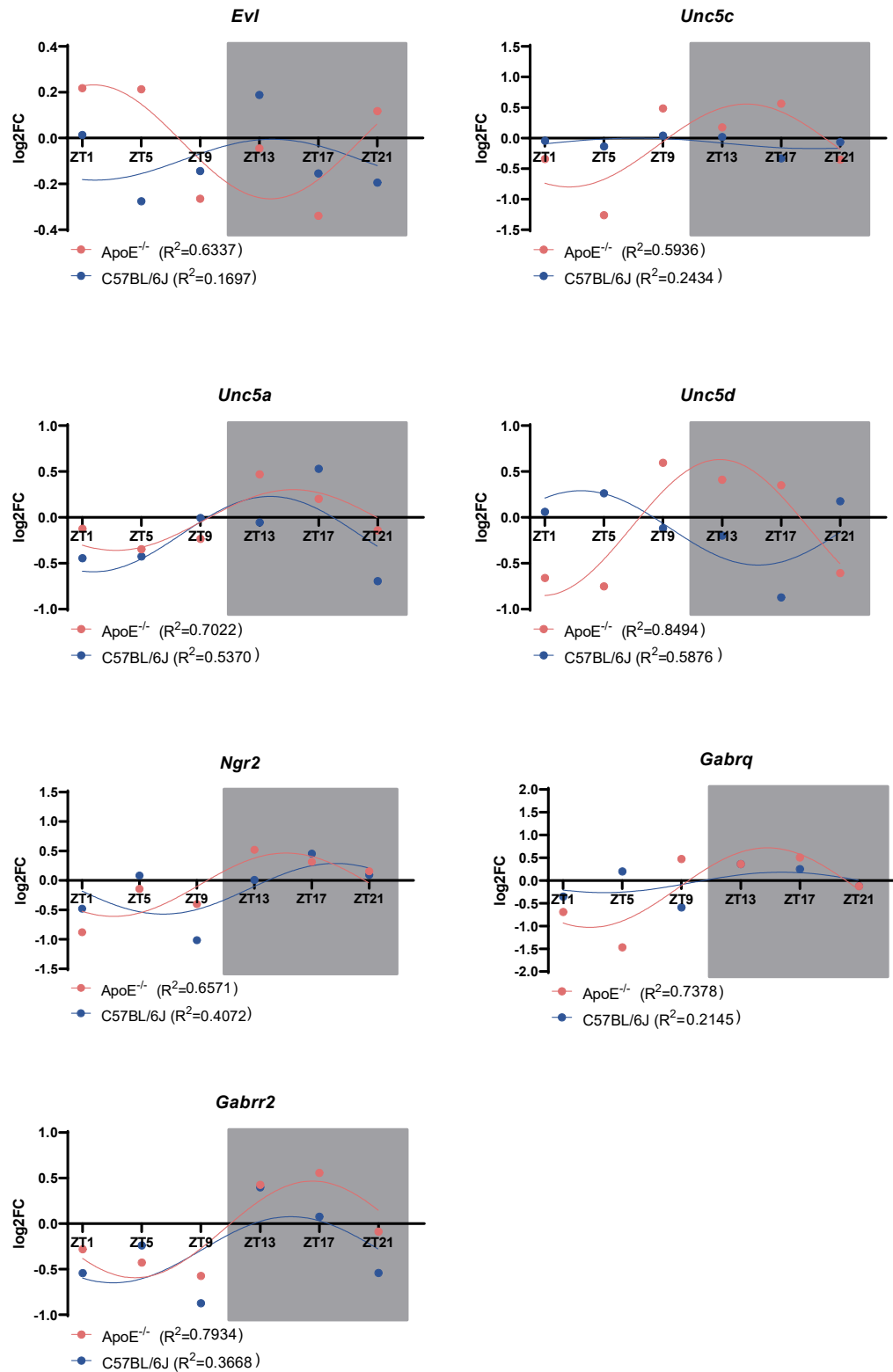
Figure 59. Representation of several PCGs from different pathways related to neuronal system that oscillate in *Apoe*^{-/-} but have lost oscillation in C57BL/6J

The heatmaps of the Neuronal System from Reactome (R-MMU-8849932) and Nervous System Development Pathway from Reactome (R-MMU-9675108) have also different pattern across the day when comparing the two genotypes (**Figure 60**), despite the fact of being most of the genes detected in both genotypes (298 out of 402 or 74.12% and 538 out of 572 or 94.05% in *Apoe*-/- and 311 out of 402 or 77.36% and 537 out of 572 or 93.88% in C57BL/6J).
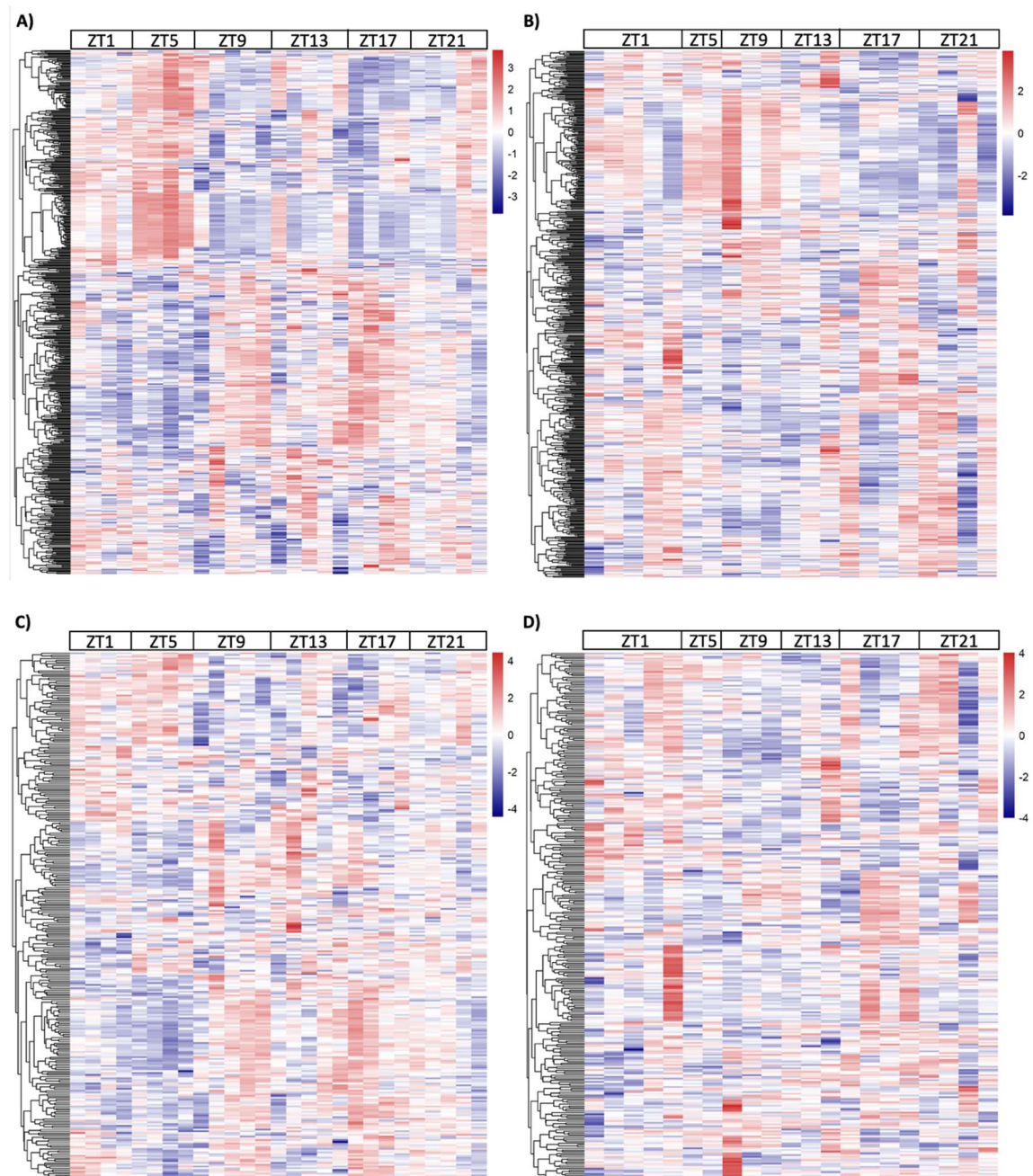
Figure 60. Heatmap of genes from the Neuronal System from Reactome (R-MMU-8849932) expressed in the BCA from *Apoe*-/-(A) and C57BL/6J (B). Heatmap of genes from Nervous

System Development Pathway from Reactome (R-MMU-9675108) expressed in the BCA from *Apoe^{-/-}*(C) and C57BL/6J (D).

3.3 The changes in circadian oscillation due to HFD are not limited to the atherosclerotic plaque

A diet in high fat and high cholesterol content does not only affect the rhythmicity in the BCA or the aorta, but also in different organs of the organism. In order to study the changes in oscillation in different organs as a result of a hypercholesteraemic diet, 11 organs (adrenal gland, aorta, colon, heart, ileum, kidney, liver, lung, muscle, spleen and white adipose tissue) were sequenced from mice killed at 4h intervals during 24h. The sequencing procedure was the same as for the BCA and the samples were filtered to include the ones with the highest number of uniquely mapped reads (see Annex 3).

3.3.1 The analysed organs share a big proportion of PCG in their transcriptome

The number of detected PCG per organ oscillates between the almost 15000 PCG in BCA to the 12815 in Muscle. Combining all the genes from all the organs, we detect a total of 17844 PCG. From those, all the organs share a group of 11573 (64.85%) PCG. Very few PCG (1090 or 6.11%) are organ-specific and the amount of signature PCGs per organ is very variable (**Figure 61**).
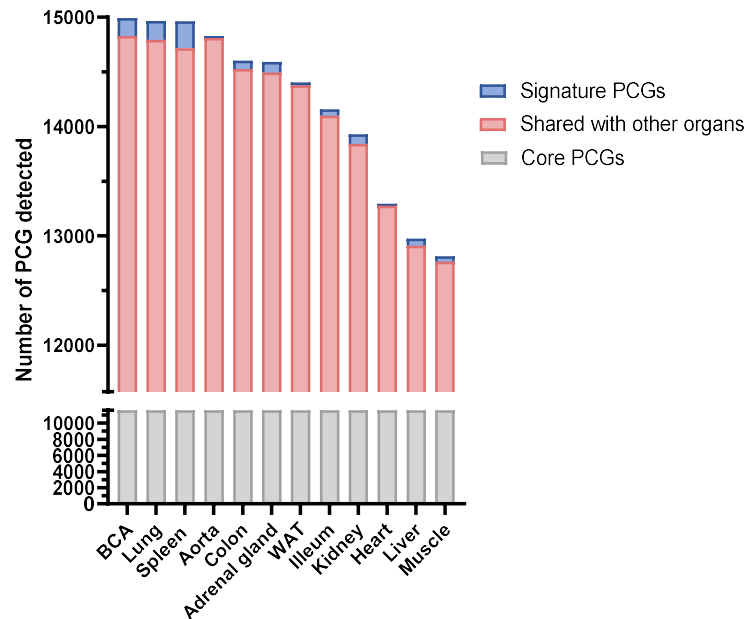
Figure 61. Quantity of oscillating genes per organ. Distribution of the PCGs detected in each organ into core PCGs (PCGs detected in all the organs), PCGs shared with other organs and Signature PCGs (expressed only by one organ).

3.3.2 A very variable proportion of PCG oscillate in each organ and a hypercholesterolemic diet affects the number, identity and amplitude of the oscillating PCG

The percentage of oscillating genes in each organ varies significantly, being the liver the organ with the most oscillating genes in both genotypes (71.60% in $Apoe^{-/-}$ and 77.42% in C57BL/6J), followed by kidney and lung. The organs with the least percentage of oscillating genes are spleen, BCA and aorta (**Figure 62, Figure 63.A** and **63.B**).

Not all the organs are affected by the hyperlipidaemia and hypercholesterolemia to the same extent. In case of the percentage of genes that oscillate in either $Apoe^{-/-}$ or C57BL/6J, the most striking change appears in the BCA, where we detect a more than 3-fold increase in $Apoe^{-/-}$ when compared to C57BL/6J, while the organs with the most similar percentages are colon, liver and ileum (**Figure 63.C**). In most of the organs (8 out the 12 analysed), we detect an increase in the number of genes that oscillate, except for the liver, colon, muscle and WAT, in which the number of oscillating genes in C57BL/6J is higher than in $Apoe^{-/-}$. The identity of oscillating genes in each genotype also experiences changes. The percentage of similarity between the genes that oscillate in both genotypes also varies from more than 80% in liver to less than 20% in spleen and BCA (**Figure 63.D**).

131

Furthermore, the amplitude of the oscillating PCGs is also altered in the organs when comparing the genotypes (**Figure 64**). It is extremely noticeable in colon and ileum, where the amplitude of the oscillating PCGs is very high in C57BL/6J (an average of 3.5 and 3.8 log2fold increase in maximum value vs minimum value per gene) and it drops dramatically in *Apoe*^{-/-}, in which the average amplitude of the oscillating PCGs doesn't reach the value of 1 in any of the two organs.

	ApoE−/−	C57BL/6J	Oscillating PCGs
Kidney	59.97%	56.77%	2208 — 6145 — 1762
Liver	71.60%	77.42%	690 — 8600 — 1444
Lung	54.30%	46.35%	3145 — 4982 — 1955
Muscle	24.42%	29.97%	1201 — 1929 — 1911
Spleen	11.40%	8.39%	1286 — 420 — 836
WAT	26.50%	34.36%	1448 — 2369 — 2580
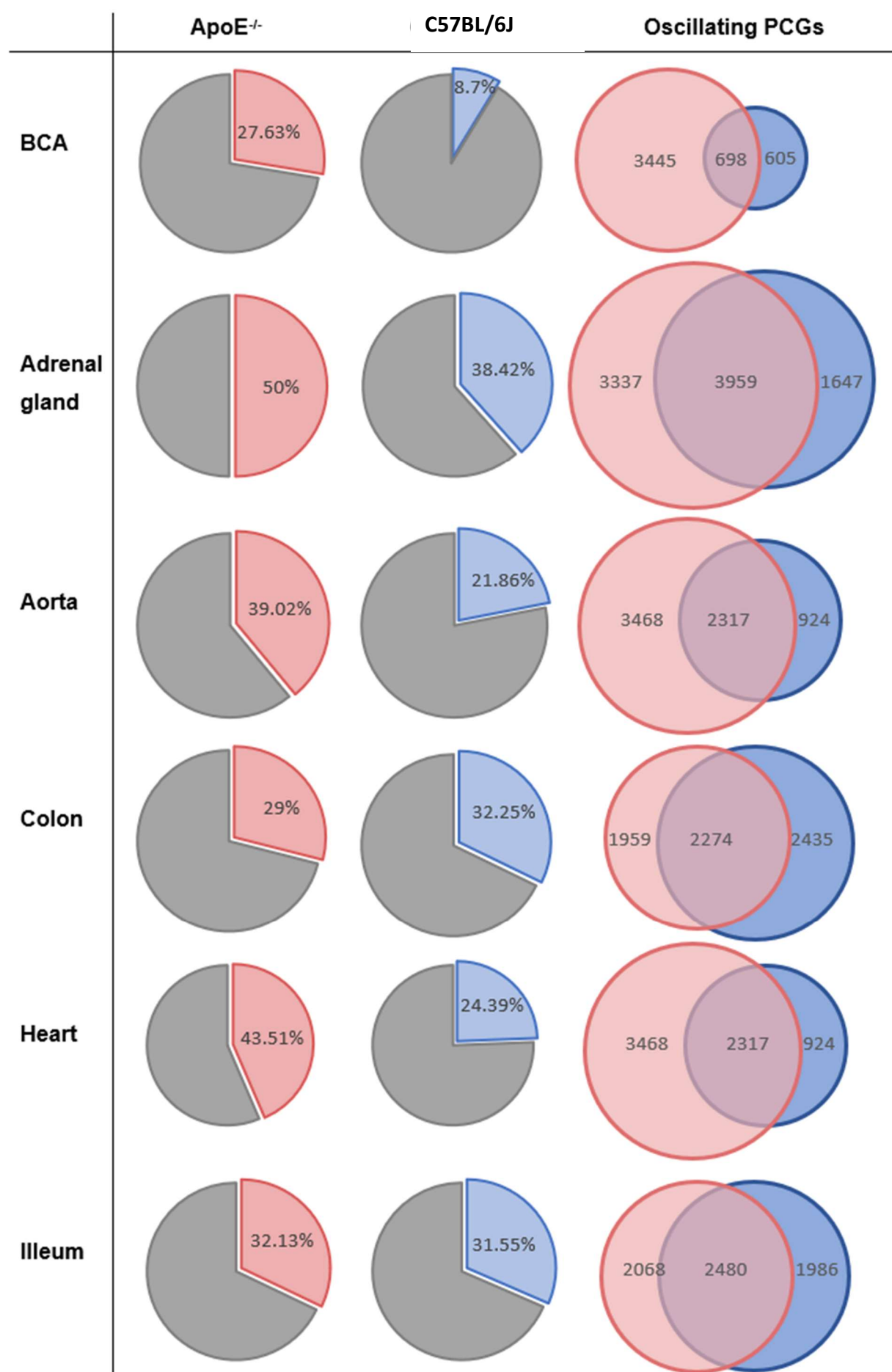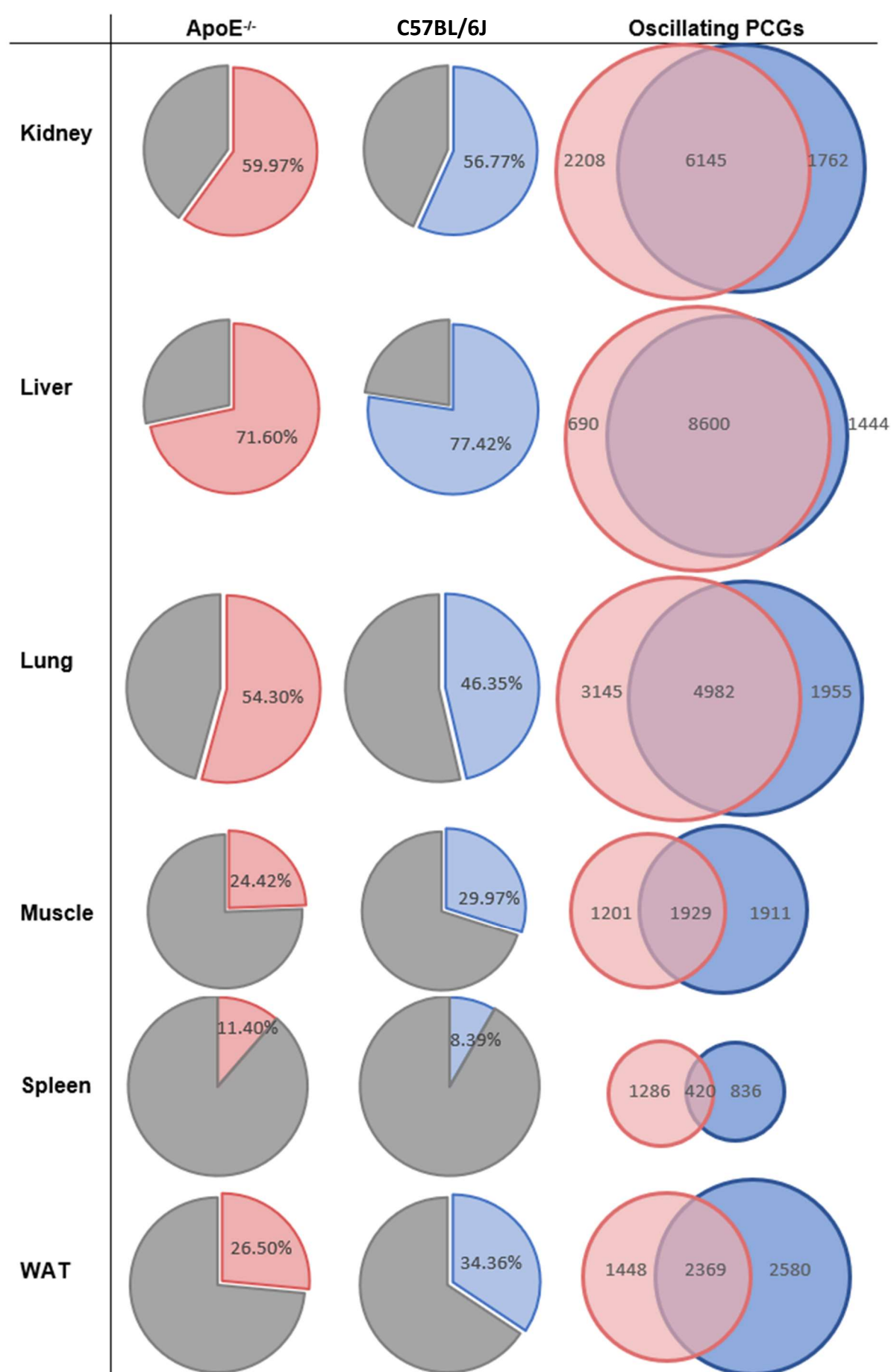
Figure 62. Oscillating genes in *Apoe*^{-/-} and C57BL/6J. Representation of the percentage of oscillating PCGs in each genotype (*Apoe*^{-/-} and C57BL/6J). Representation of the number of oscillating PCGs that are shared between the two genotypes.
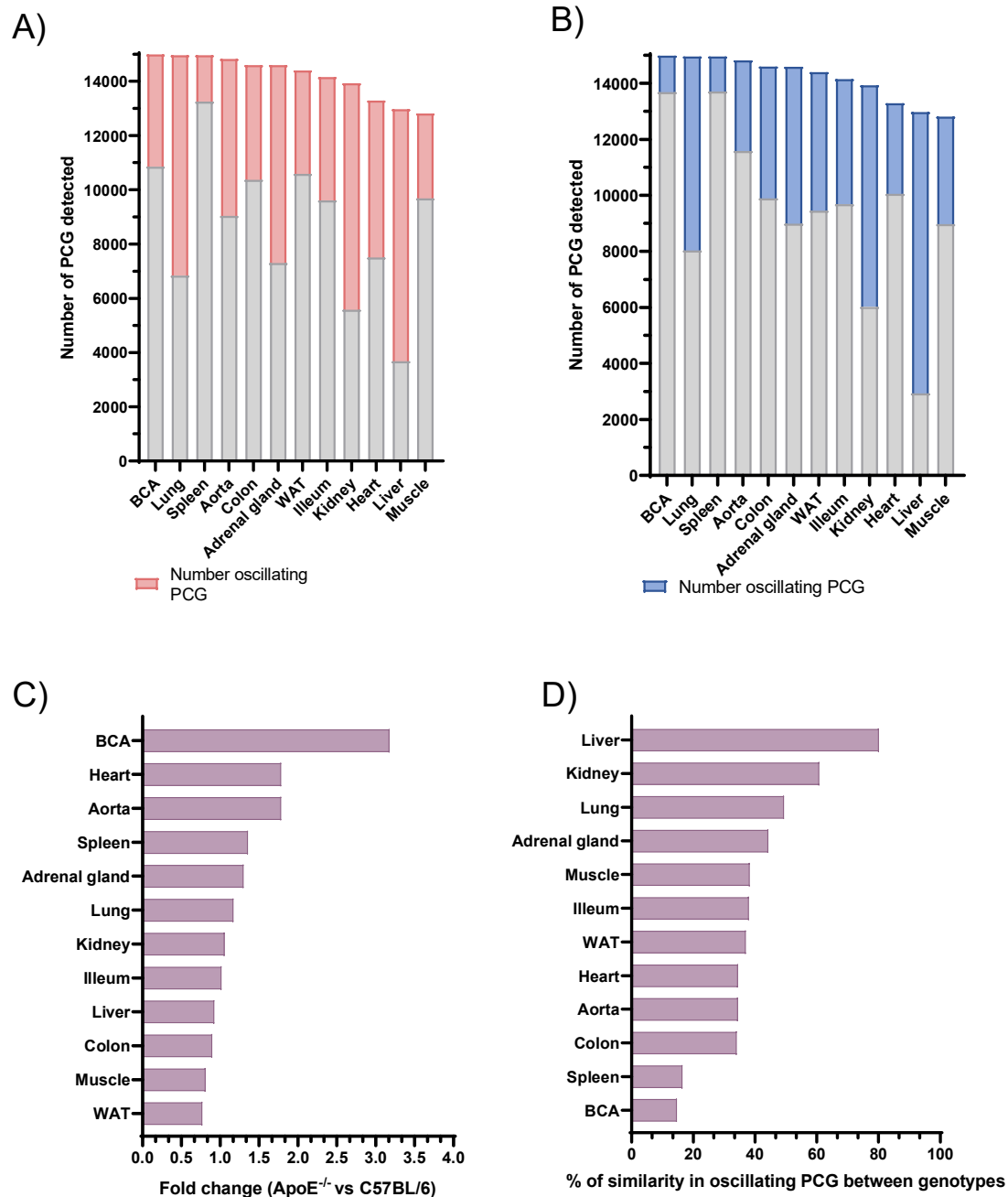
Figure 63. HFD has an impact in the percentage of genes that oscillate in *Apoe* vs C57BL/6J, as well as in the identity of the genes that oscillate. A) Number of oscillating PCG and total PCG detected in each organ in *Apoe*^{-/-}. B) Number of oscillating PCG and total PCG detected in

each organ in C57BL/6J. C) Comparison (log2FC) of the amount of oscillating PCGs detected in *Apoe*^{-/-} and C57BL/6J. D) Percentage of similarity in the group of oscillating PCG in *Apoe*^{-/-} and C57BL/6J.
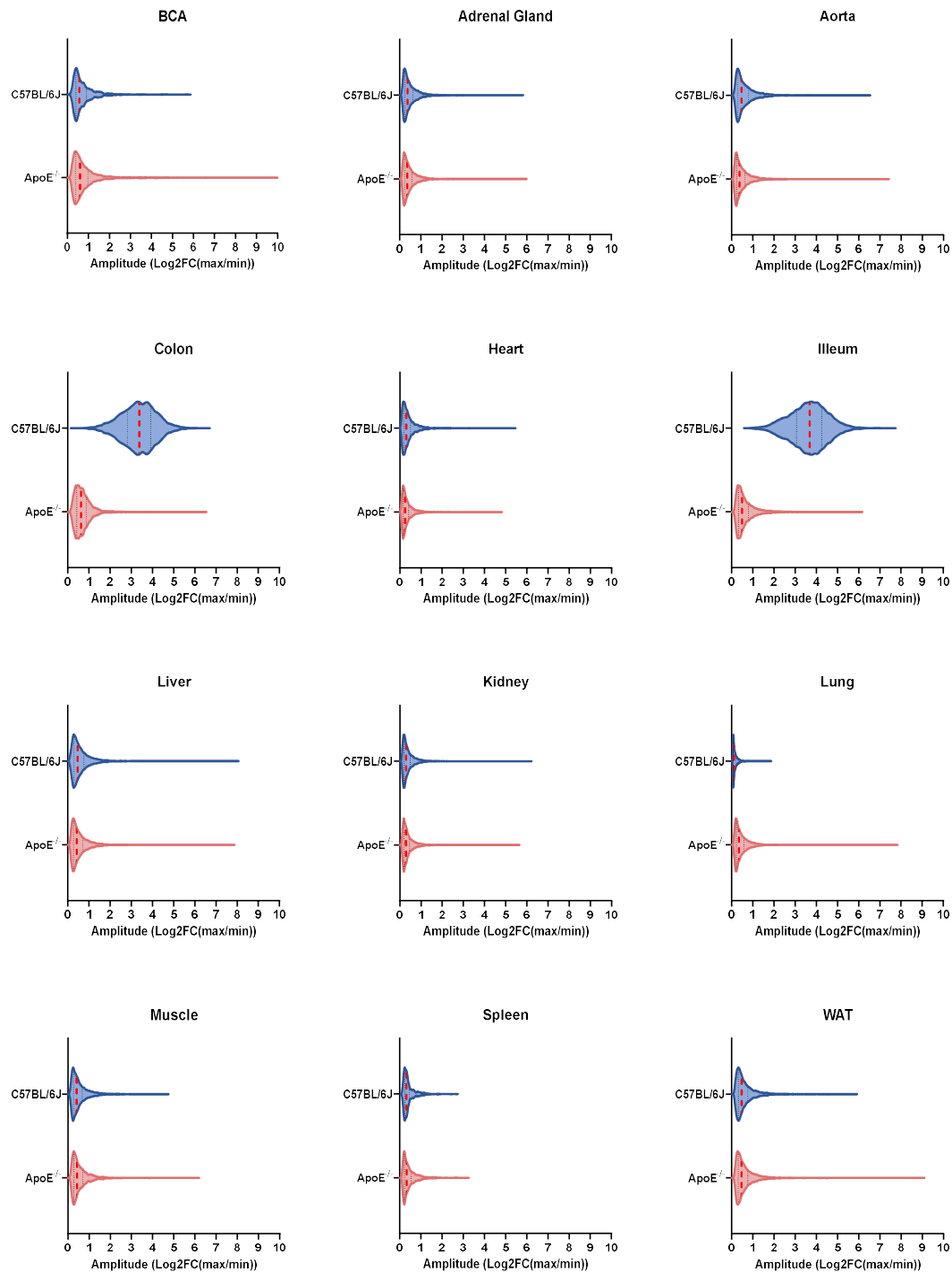
Figure 64. Distribution of amplitude in oscillating PCGs in the organs from the two genotypes.

3.3.3 Almost 87% of all the PCG show oscillation

From all the PCGs detected, 86.69% (15469 PCGs out of 17844) oscillate in at least one tissue in *Apoe*$^{-/-}$, although the core of oscillating PCGs in all the organs sequenced is composed by only 56 PCGs. In the case of C57BL/6J, the percentage PCGs that oscillate in at least one tissue is very similar (84.66%) and the core of oscillating PCGs is composed by 40 PCGs. The total amount of PCGs detected to oscillate are very similar between *Apoe*$^{-/-}$ and C57BL/6J (**Figure 65.B**) while the shared PCGs from the core group of oscillating genes is lower (**Figure 65.B**). The group of genes that oscillates in all the organs in both genotypes comprehends the core clock genes (*Bmal1*, *Cry1*, *Cry2*, *Per1*, *Per2*, *Per3*, *Nr1d1*, *Nr1d2*, *Npas2*, *Dbp*, *Ciart*).
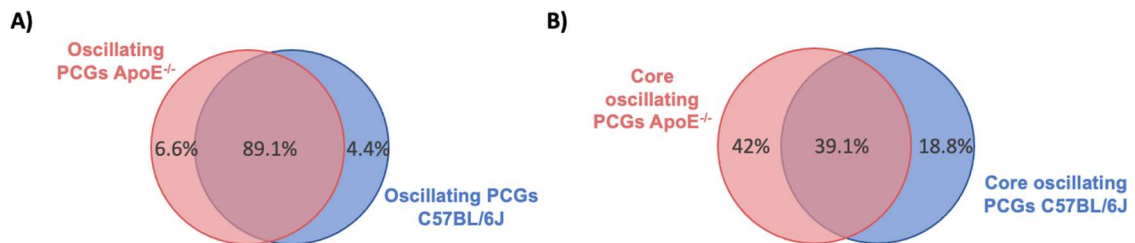
Figure 65. Total oscillating PCG and PCGs oscillating in every organ. A) Representation of PCGs oscillating in at least one organ in *Apoe*$^{-/-}$ and C57BL/6J. B) Core of oscillating PCGs in *Apoe*$^{-/-}$ and C57BL/6J.

3.3.4 The similarities among oscillating PCGs between organs are independent of their transcriptome

Besides the core of oscillating PCGs, several organs share an important percentage of the oscillating PCGs, which is independent of the similarity of their transcriptome. As can be seen in **Figure 66**, the percentage of shared detected PCGs is completely independent of the percentage of shared oscillating PCGs. The most extreme case can be seen in heart and aorta, in which the percentage of similarity among their transcriptomes is not striking when comparing with the similarities that the rest of organs have (86.90%), but their share all the oscillating genes in both genotypes.
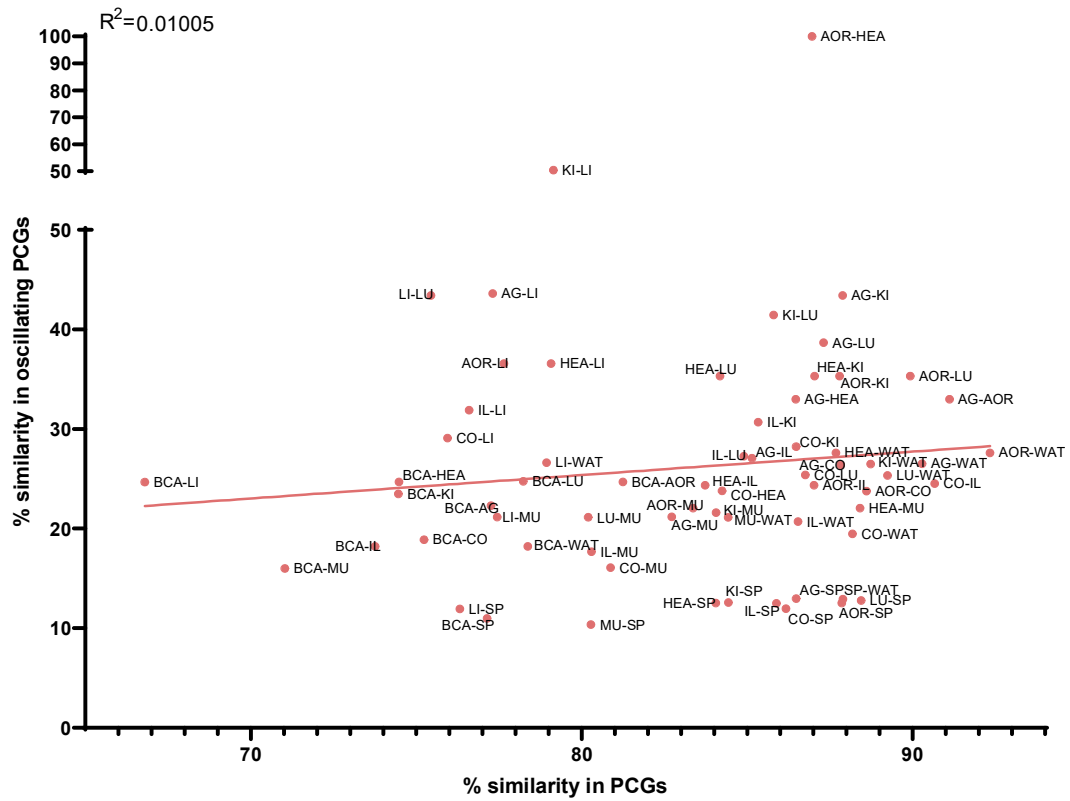
A)

B)
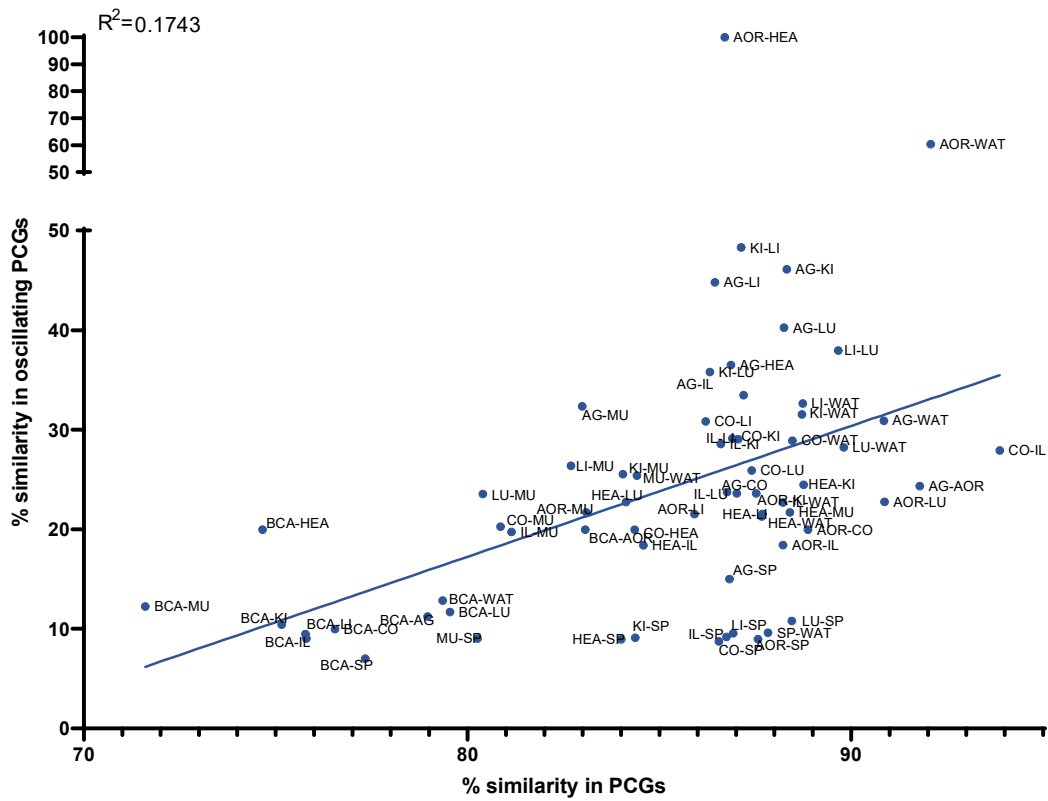
3.3.5 Changes in core clock genes in each organ

When comparing in **Figure 67** the oscillation of the core clock genes (*Bmal1*, *Clock*, *Cry1*, *Cry2*, *Per1*, *Per2*, *Npas2*, *Nr1d1*, *Nr1d2*, *Rorc* and *Dbp*), we can observe striking differences between the genotypes. The most notorious difference is the reduction of the amplitude of Cry2 to almost disappear in all the organs in *Apoe*$^{-/-}$, while in wild mice with a chow diet, Cry2 show a slight oscillation. The rest of the core clock genes don´t show noticeable differences in their oscillation among genotypes.
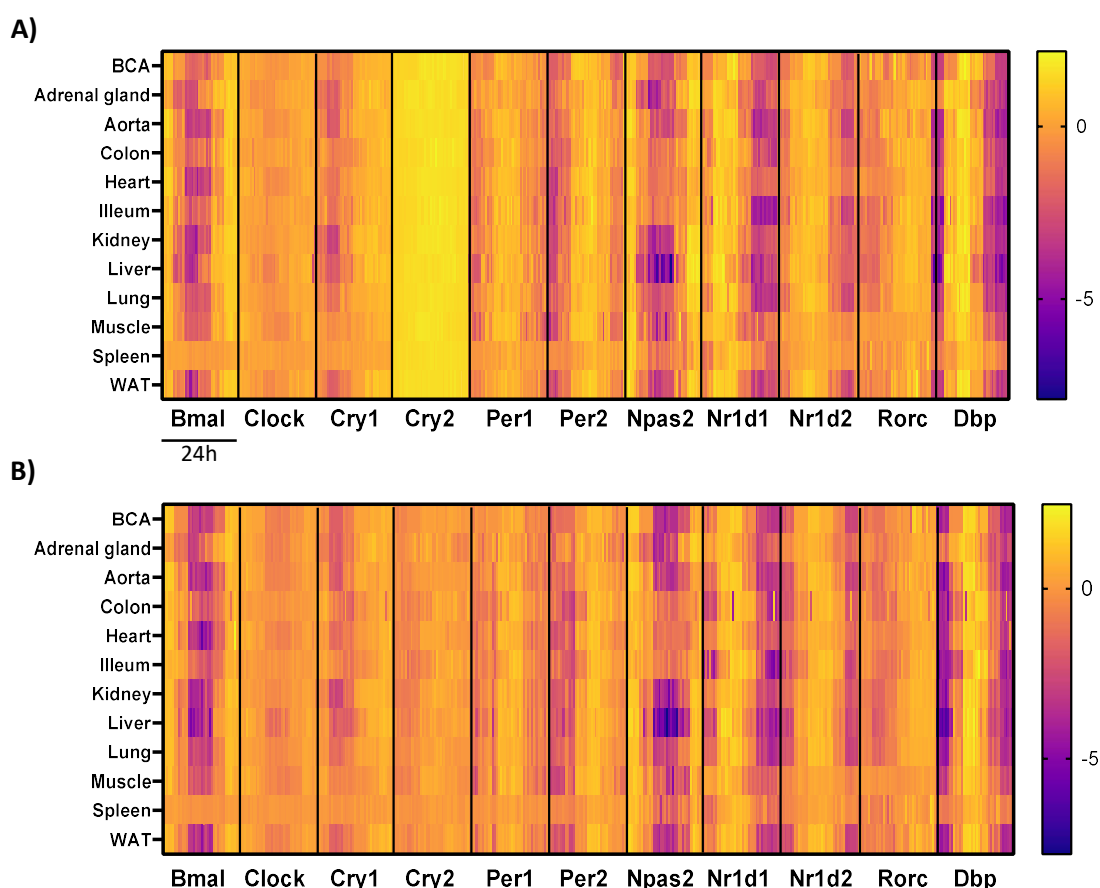
Figure 67. Heatmap of the expression of different core clock genes in all the timepoints per organ in *Apoe*$^{-/-}$ (A) and C57BL/6J (B).

Among different organs, the spleen is the organ with smallest amplitude in the core clock genes, with very little oscillation throughout the day. In other organs, like colon, ileum, lung and muscle, there is also very little oscillation, especially in the early genes of the clock system (*Bmal1* and *Clock*). On the other hand, organs like the heart, kidney, liver, lung and WAT have a more noticeable oscillation. These differences can be more clearly observed in **Figure 68**, where the amplitude of each core clock gene is displayed in every organ.
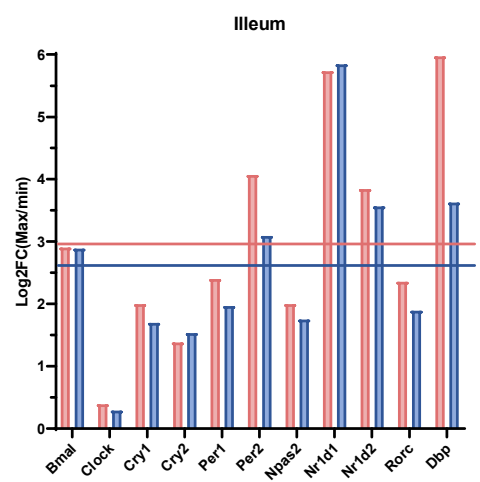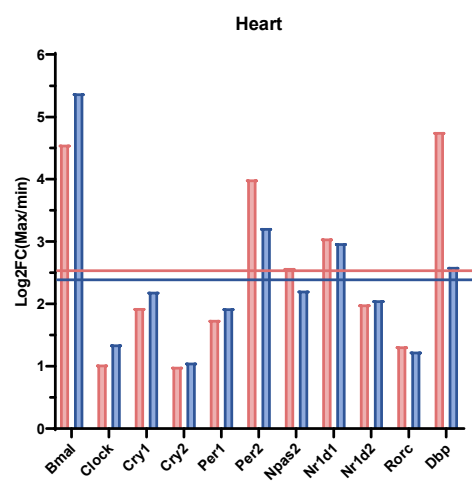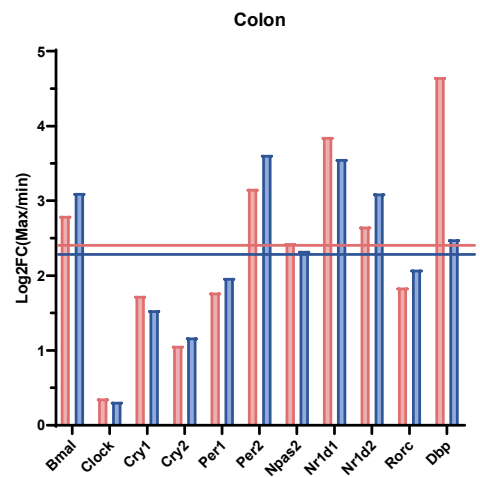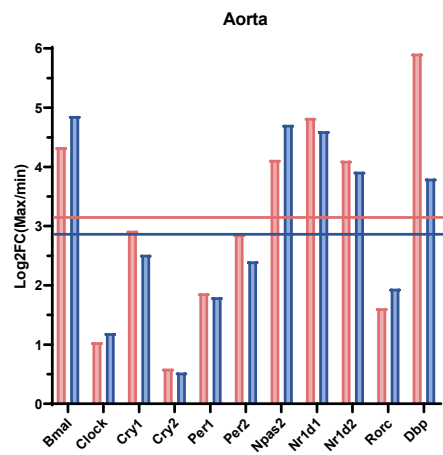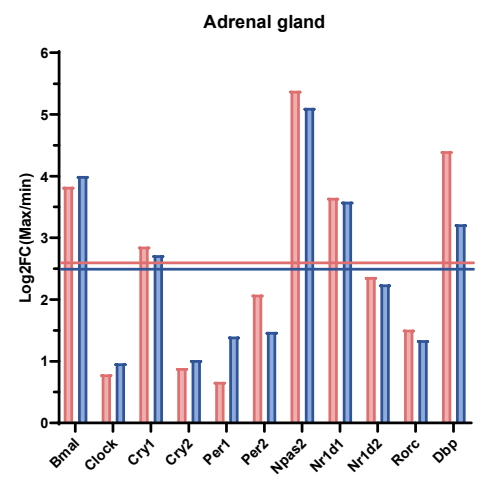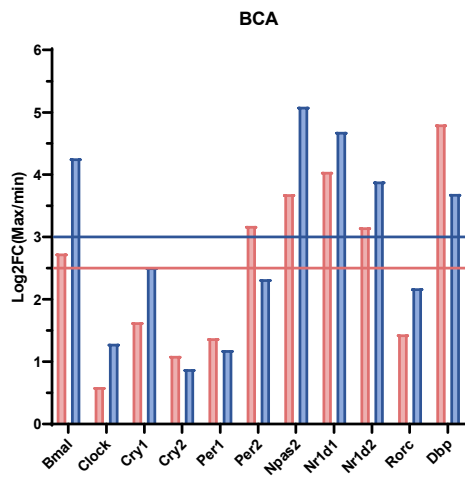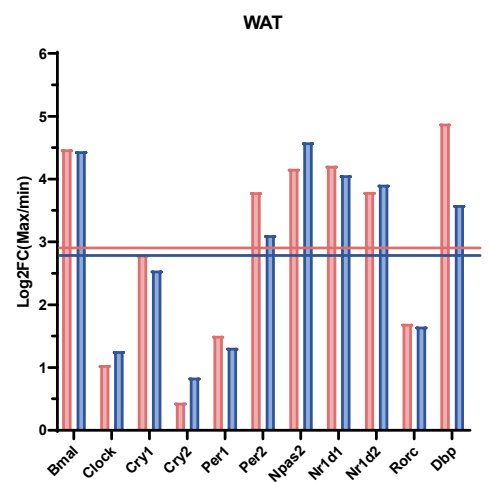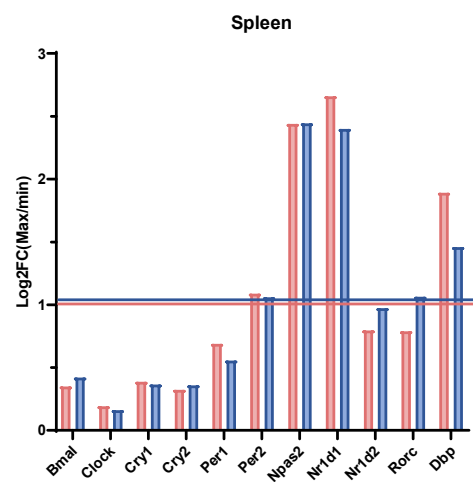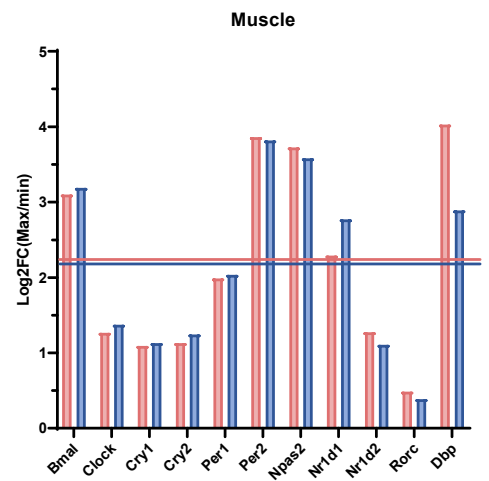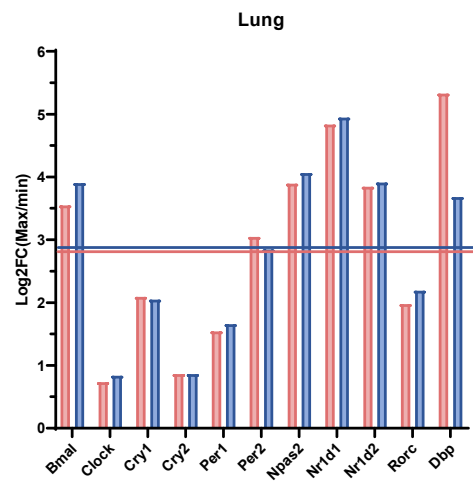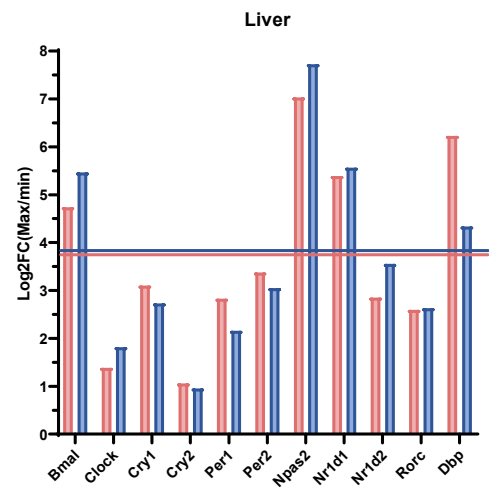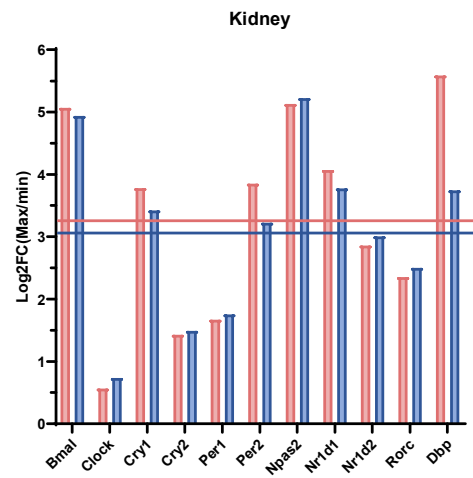
Figure 68. Amplitude of the different core clock genes in all the analysed organs in *Apoe*$^{-/-}$ and C57BL/6J.

The fact that spleen and muscle are the organs that exhibit a lowest difference between the maximum and minimum value and organs like liver and kidney show the highest, while being respectively the organs with fewest and highest number of oscillating genes make us consider the correlation between the amplitude of the core clock genes and the percentage of oscillatory genes in each organ. As can be seen in **Figure 69**, there´s a correlation in the percentage of genes that show oscillation and the amplitude of the core clock genes, considering both genotypes.
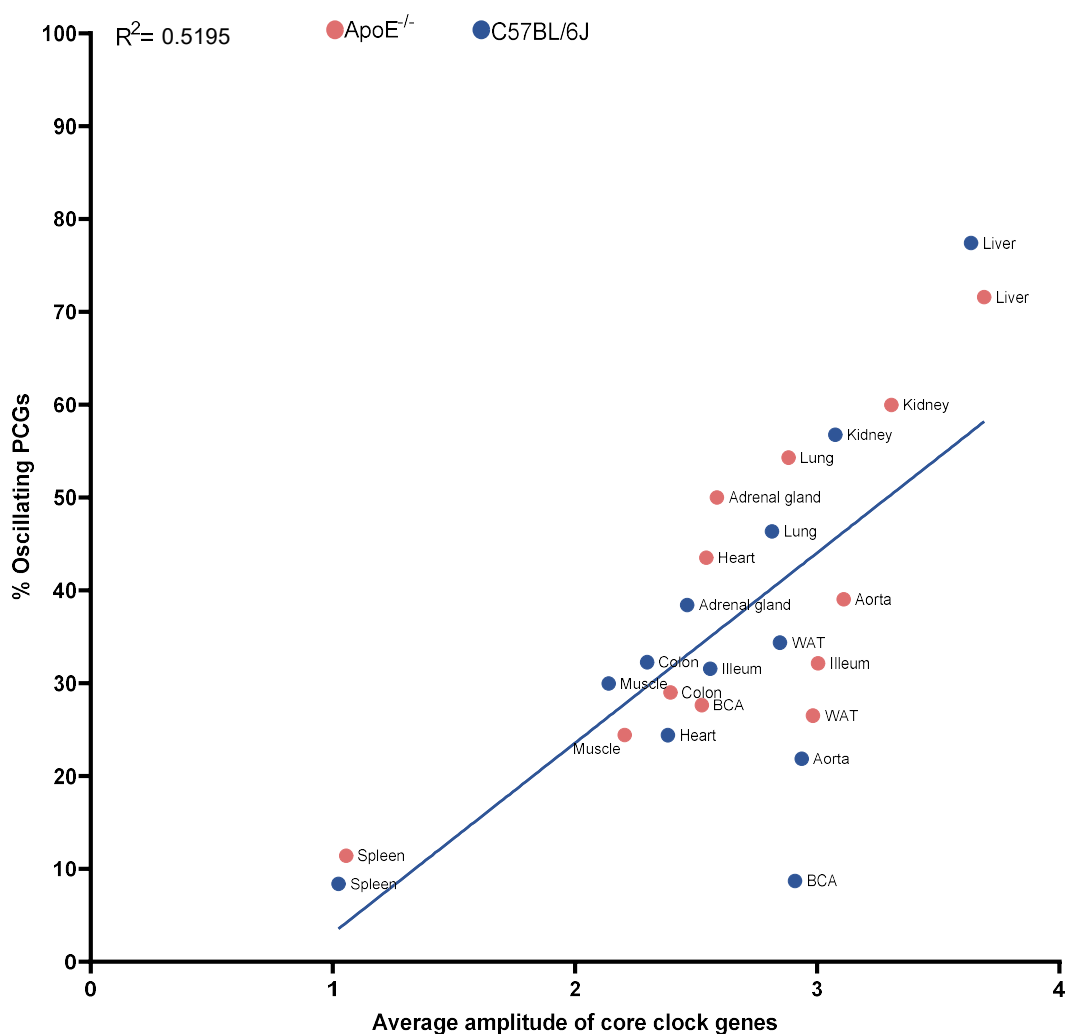
Figure 69. Linear correlation between the amplitude of core clock genes and the percentage of oscillating genes in each organ.

3.3.6 Important signatures in the development of the atherosclerotic plaque exhibit different patterns of oscillation across organs

The percentage of oscillating PCG of several pathways that are very closely related to atherosclerosis (cell cycle, programmed cell death, nervous system development, immune system) shows important differences when considering the oscillating genes in the analysed organs, as can be observed in **Figure 70**.
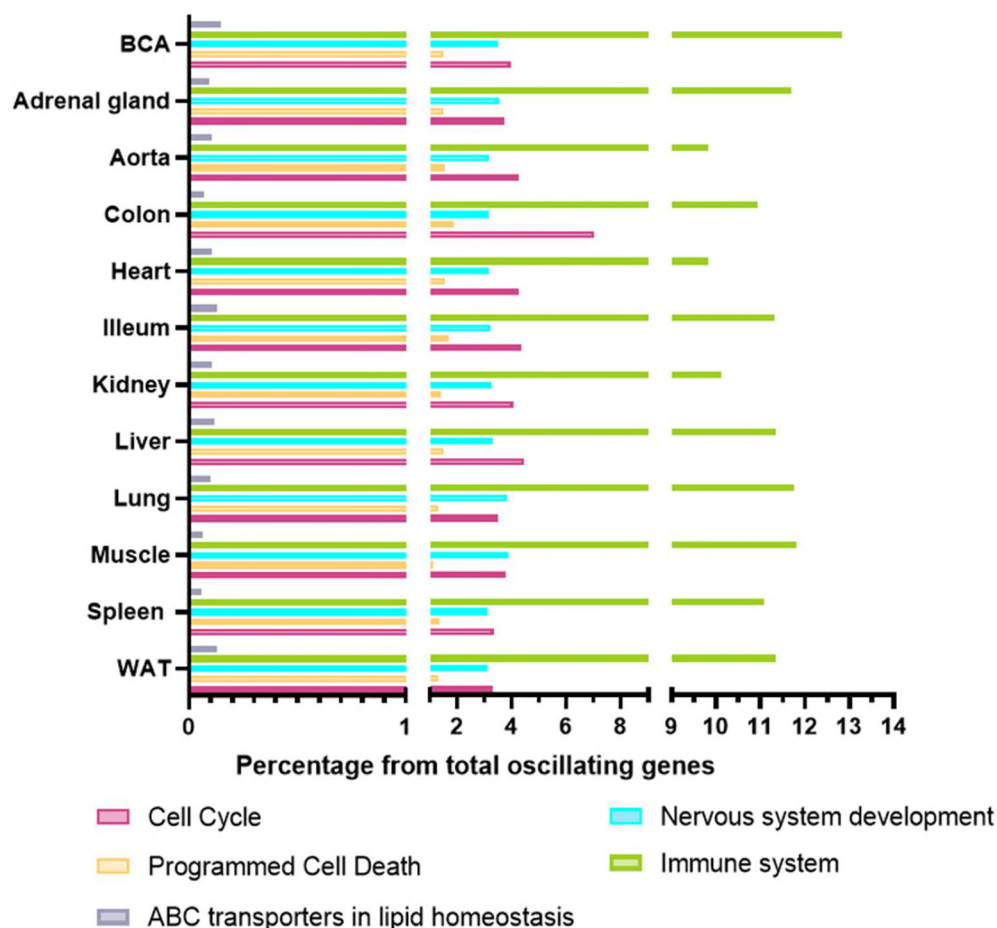
Figure 70. Composition of oscillating PCGs based on the main pathways related to atherosclerosis in the different organs considered in *Apoe*^{-/-}.

Besides the changes in the percentage of oscillatory PCGs that belong to each signature, we can also observe changes in the distribution of peaks and troughs of these signatures in each organ (**Figure 71**). In the case of cell cycle, none of the studied organs, except of BCA, have a strong peak at ZT5. The few different organs that have also high values of expression at ZT5 (adrenal gland, kidney and muscle) don't have the peak of expression of cell cycle PCGs at ZT5.

A similar situation also happens when considering the signature of Programmed cell death PCGs. In this case, the BCA shows a distribution with two peaks, being the one at ZT5 bigger.

This peak is also shared with the aorta and the liver, that have a peak of expression of these PCGs from ZT1 to ZT9 and from ZT5 to ZT9, respectively.

In the case of PCGs related to nervous system development, the pattern showed by BCA is not so unique, due to the fact that the peak that this organ shows at ZT17 is also present in kidney and liver and other organs, as the adrenal gland and the colon show high levels of expression at ZT17.

The pattern of expression of PCGs related to the immune system is very variable across the different organs. BCA shares its pattern, with a peak of expression between ZT1 and ZT5 with aorta, liver and lung and other organs, as the muscle and WAT also show a high expression at ZT5. When considering the expression of the lipid transporters, BCA and lung show an increase expression at ZT1, while ileum and muscle also have high values at this timepoint.

Leaving aside the comparison of the BCA with the rest of the organs, it is noticeable the fact that, even when sharing totally the identity of the oscillating PCGs, as it happens in the case of heart and aorta, the patterns of oscillation of the different signatures are not shared in these two organs and some of these signatures, as cell cycle, programmed cell death and ABC transporters show striking different distributions of the maximum and the minimum values of expression.

	Heart	Illeum	Kidney	Liver
Cell cycle				
Programmed cell death				
Nervous system development				

147

	Adrenal gland	Aorta	BCA	Colon

Immune System

ABC transporters in lipid homeostasis

	Heart	Illeum	Kidney	Liver
Immune System				
ABC transporters in lipid homeostasis				
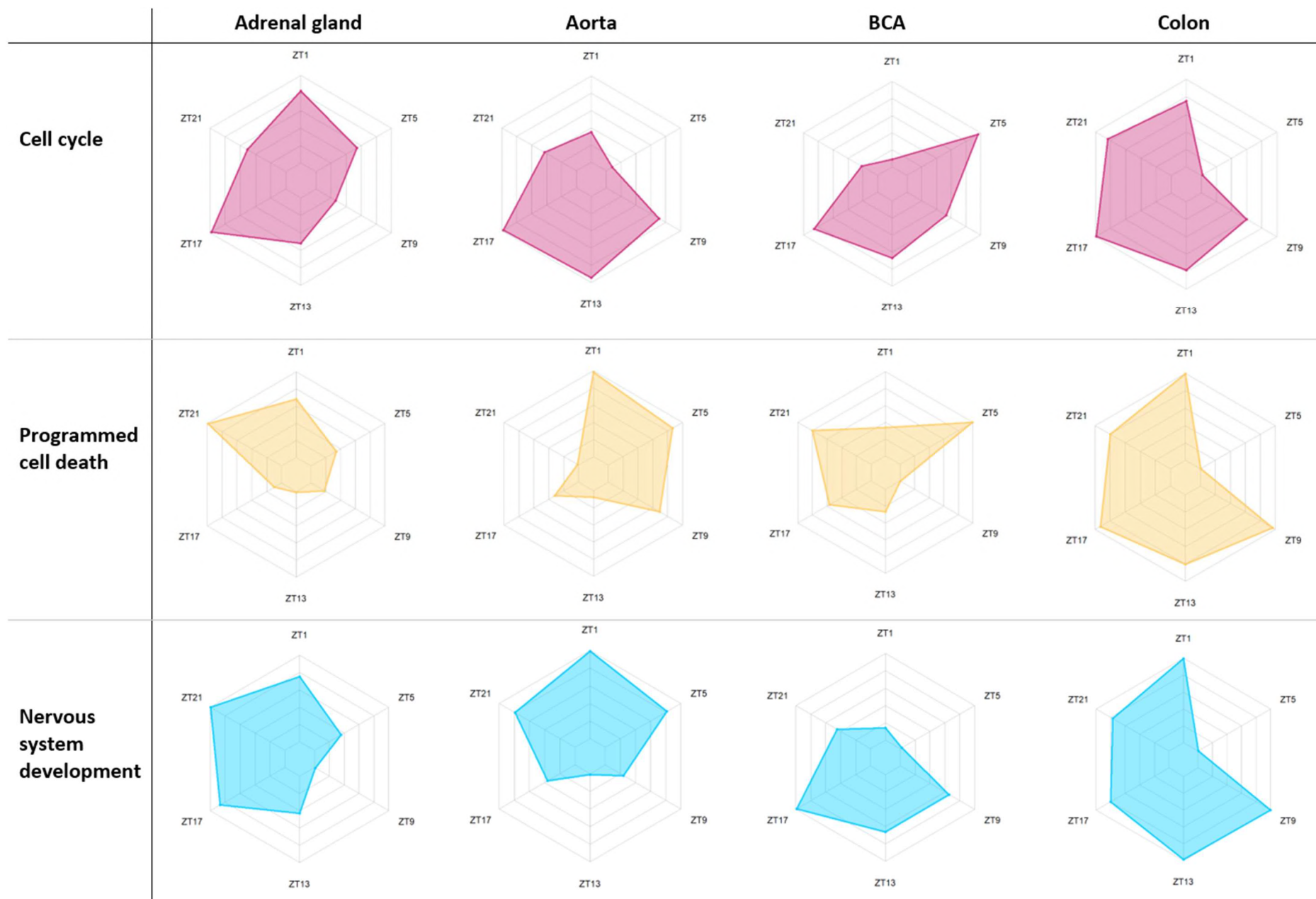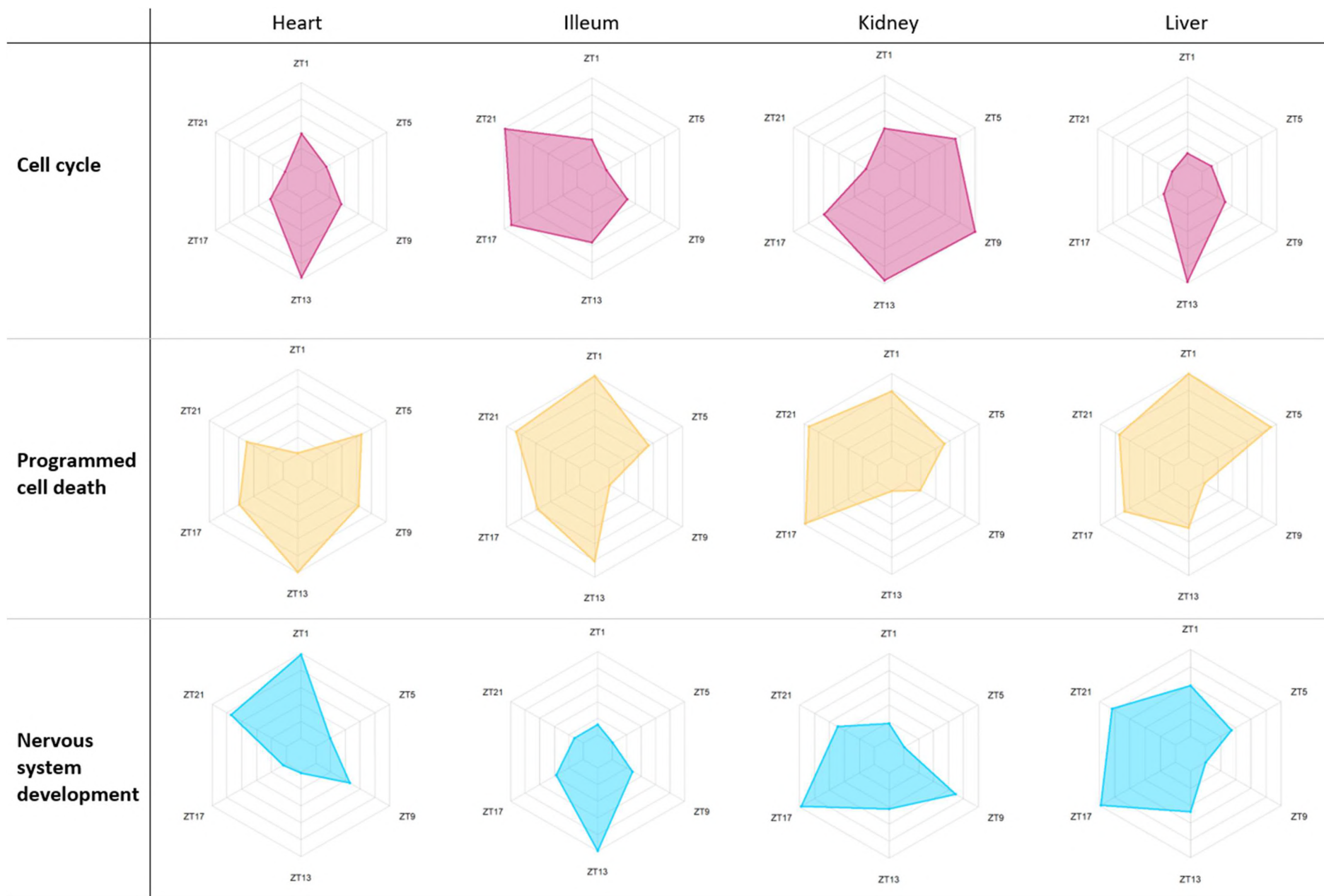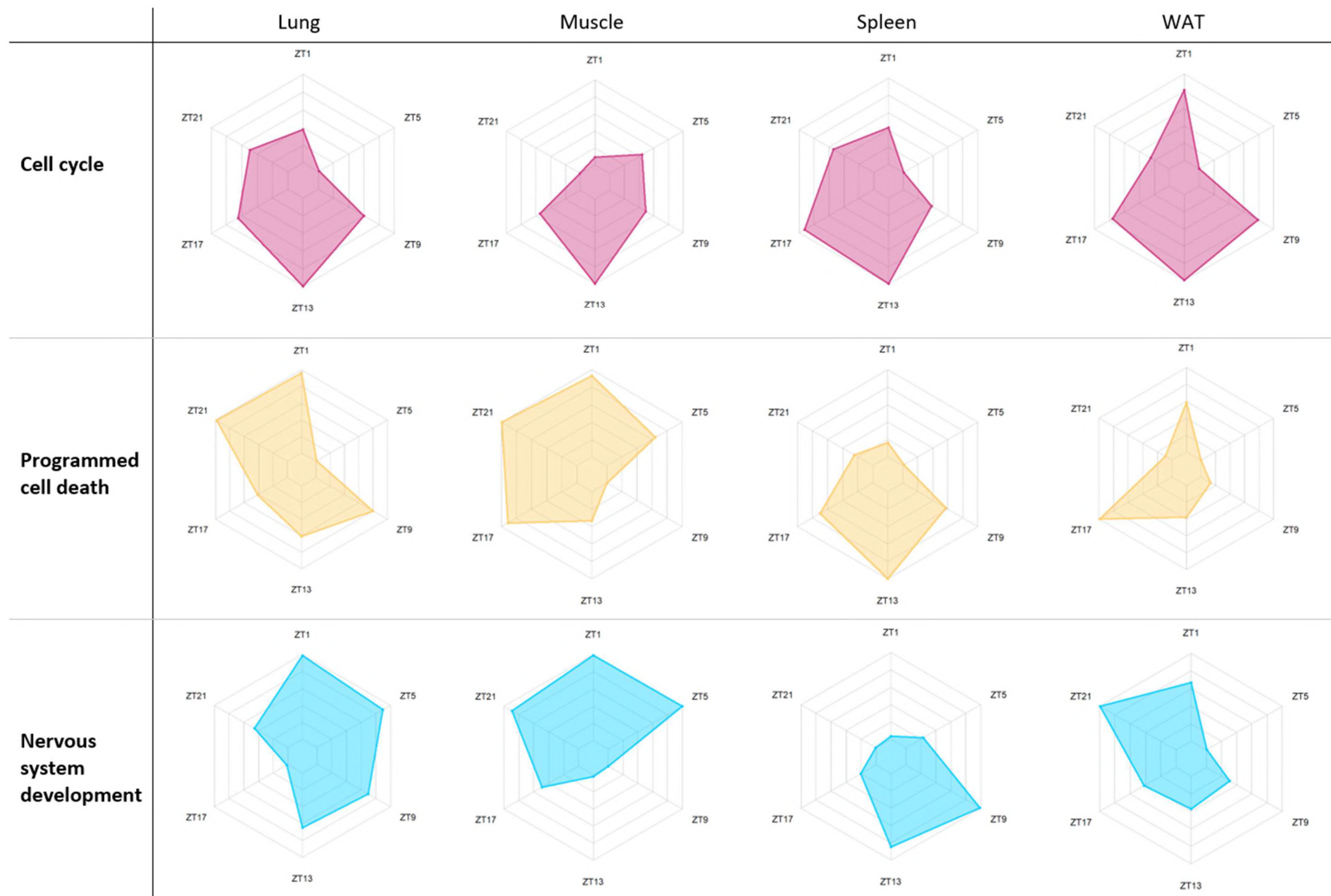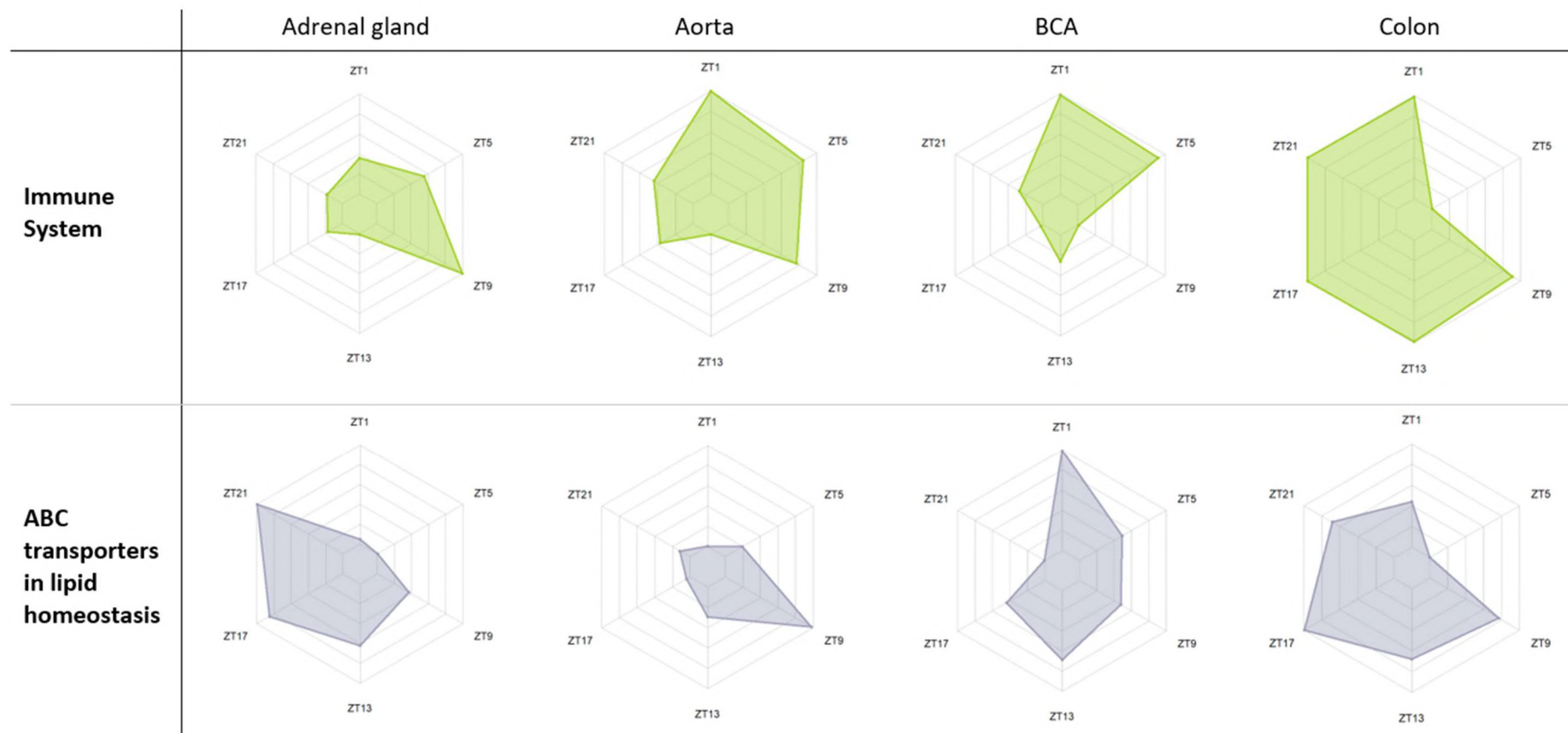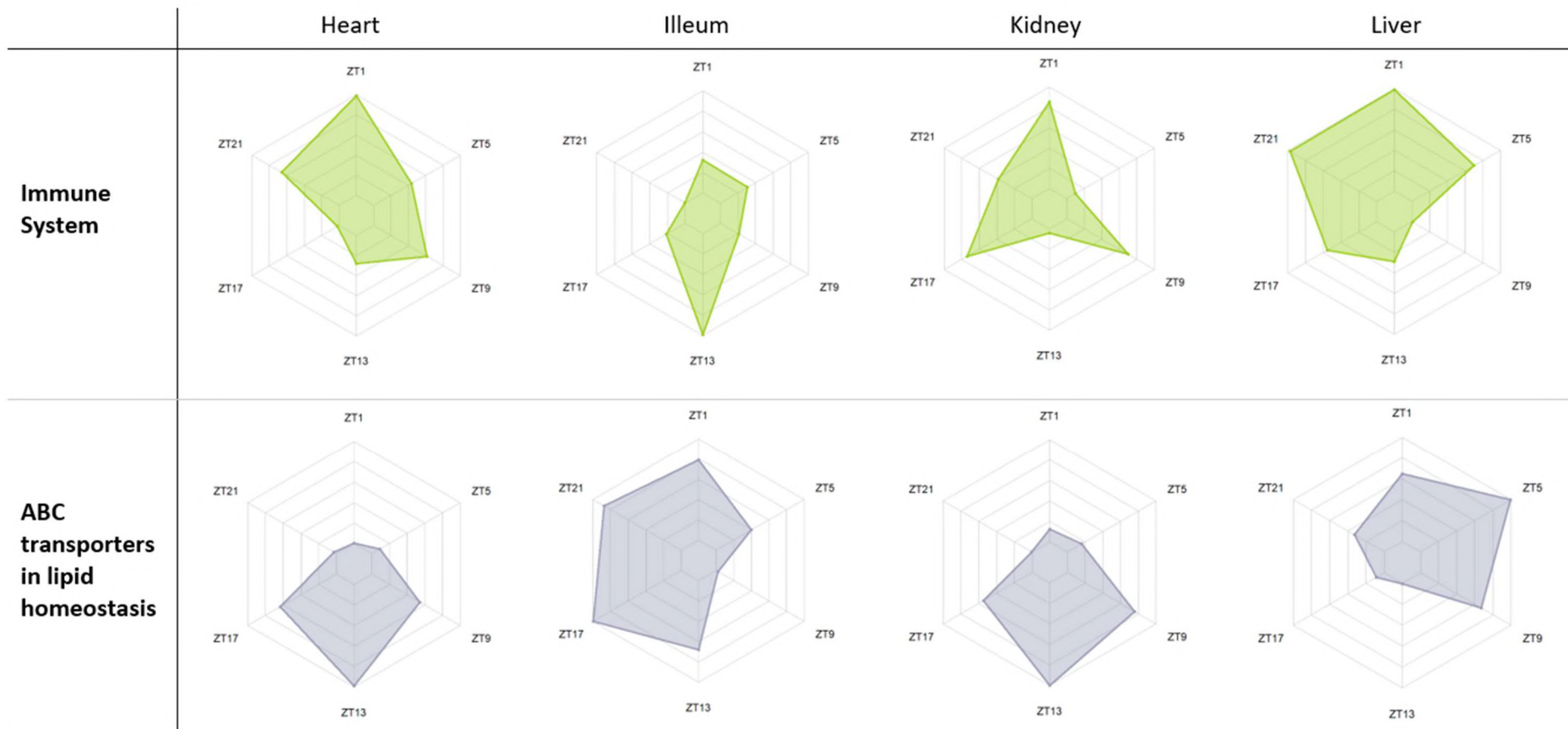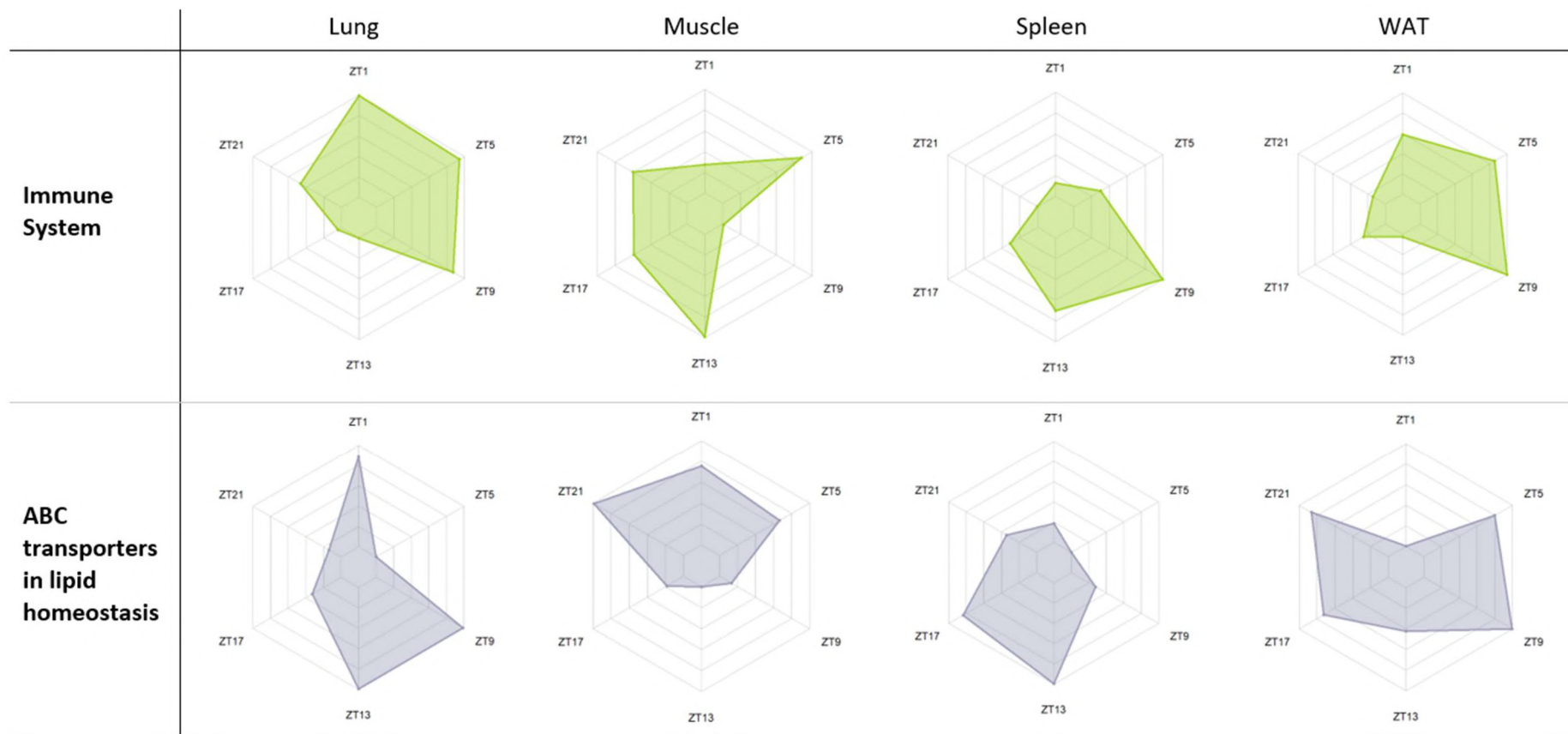
Figure 71. Representation of the expression of the fraction of oscillating genes from different signatures in the studied organs.
The axis have been individually created for each signature and each organ, according to the amplitude of the specific signature.
Therefore, comparisons among organs and/or signatures should be avoided.

When we compare the percentage of cells that are either in the process of division or cell death, we can detect some of the differences exposed above. As we can see in **Figure 72**, the percentage of BrdU$^+$ cells or Ki67$^+$ cells at ZT1 is significantly higher than at ZT13 in the BCA, tendency that is only shared by kidney, although the differences in the last case are not significative. In the case of cell death, the fact that the percentage of AnnexinV$^+$ cells is higher at ZT1 than at ZT13 is again shared between BCA and kidney. Nevertheless, the percentage of cells going either cell death or dividing are much higher in the BCA than in the rest of the considered organs.
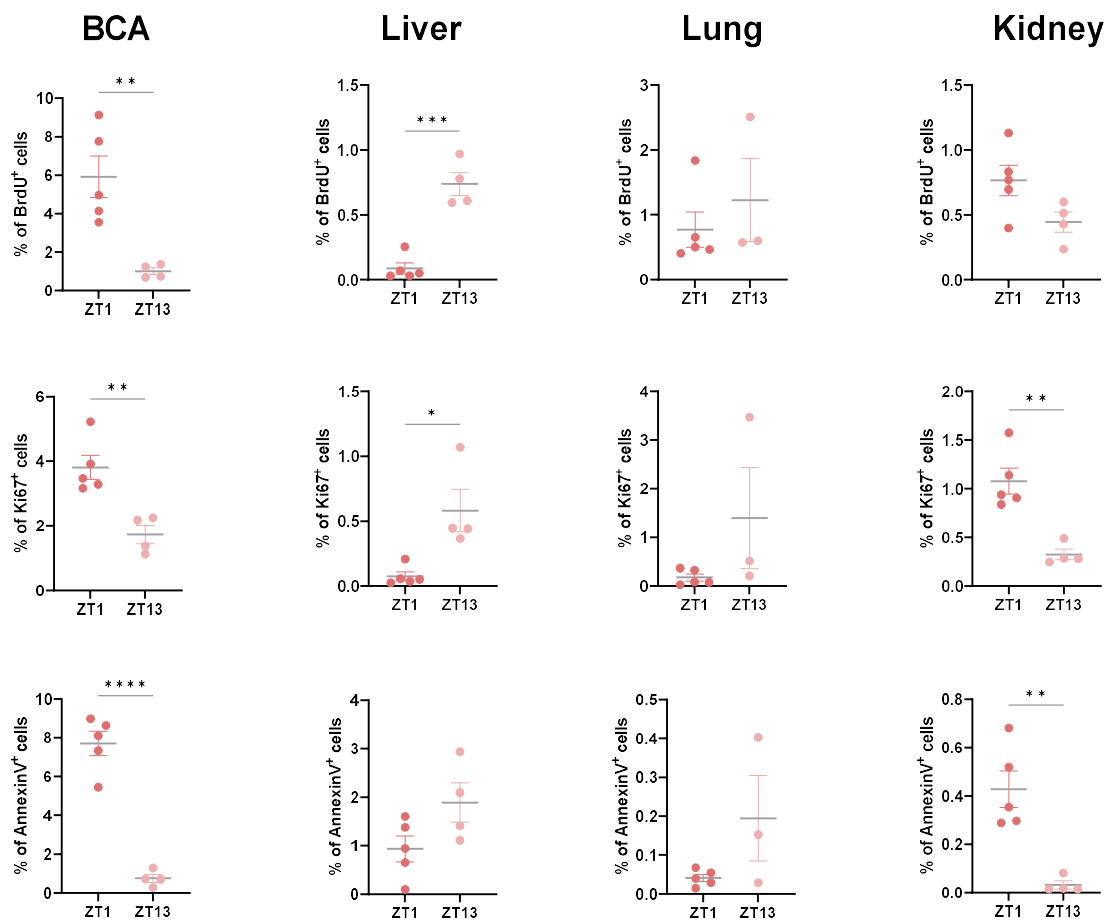
Figure 72. Quantification of positive cells for BrdU, Ki67 or AnnexinV in the BCA, liver, lung and kidney at ZT1 and ZT13 using flow cytometry. Statistical analysis made using one-way ANOVA (*p<0.05, **p<0.01, ***p<0.001, ****p<0.0001). Data represented as mean±SEM.

3.4 Human plaques exhibit oscillatory rhythms that affect several biological functions

Human plaques from the carotids of patients undergoing preventive atherectomy were sent for bulk RNA sequencing. The surgeries of the patients were scheduled in a span of 9.5 hours (from 9 am until 18:30 pm), as it is represented in **Figure 73.A**. The samples were harvested and the sequencing was done quickly after the surgery in order to avoid the degradation of the genetic material. The samples were quite homogeneous considering the library composition, as can be seen in the **Figure 73.A**.

A)

B)
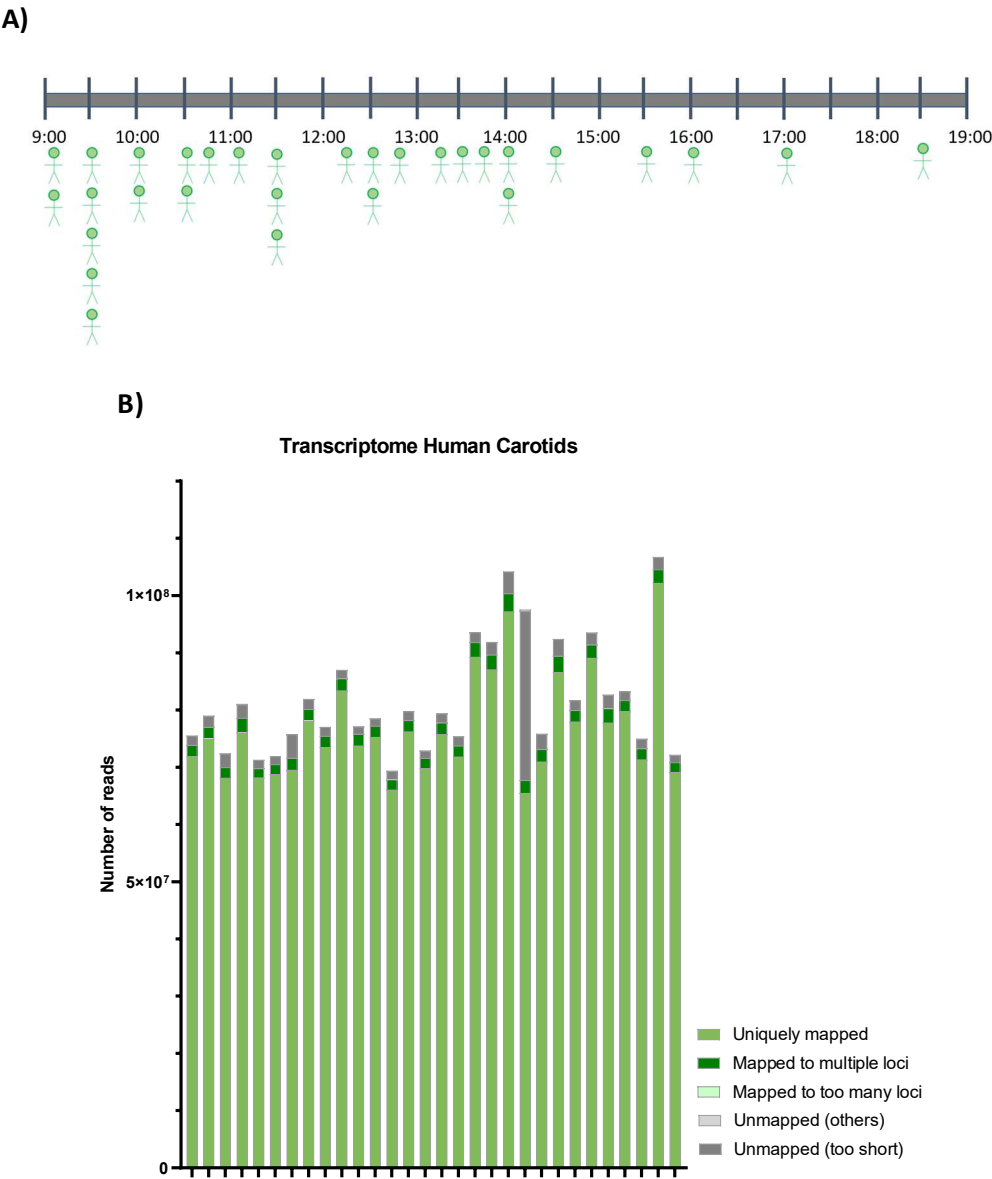
Figure 73. Human sampling collection and library quality. A) temporal distribution across 9:30 hours of human samples. **B)** Composition of the libraries from the human samples.

Due to the special features of the human data (uneven sampling, higher variability among the samples, less than 24h covered…) the techniques used in the organs of *Apoe*^{−/−} and C57BL/6J to detect circadian oscillation at the transcriptional level couldn't be applied.

After using DESeq2 to normalize all the libraries, detecting genes expressed (average expression higher than 10 reads) and filtering for protein coding genes (PCGs), we ended up with 17.979 PCGs expressed in the human carotids. To filter for genes that show rhythmic oscillation, instead of using JTK or LS, the only option to detect oscillation among the genes was to adjust each gene expression to a Cosinor curve. To do this adjustment, the Cosinor algorithm provided by the R Package DiscoRhythm was used, as explained in the **Section 2.6.3.7.2**. Furthermore, the R Package Metacycle was used in order to calculate the normalized amplitude (rAmp) of each gene. The detection of rhythmic oscillation was done using previous published analysis in a cohort similar to the one that we have[286] and the parameters for the identification of rhythmically oscillating genes were a false discovery rate < 0.05, amplitude higher ≥0.1 and a coefficient of determination (R^2) ≥ 0.1. As result, 1285 PCGs (7.1% of the detected PCGs) were considered rhythmic genes in the atherosclerotic plaque from human carotids.

Despite the fact that this number might seem quite inferior to the percentage of detected PCG in the BCA from *Apoe*^{−/−}, which was 27.23%, we have to bear in mind the fact that we are comparing a very genetically homogeneous group of mice that were cohoused in very similar conditions (food supply, presence of external stimuli as light, humidity, noise) with a very heterogenous group of humans with different stages of plaque and daily habits. Furthermore, the sampling collection in the case of the human group was incomplete, covering only 9 and half hours of the day and without samples in the evening and night times. As can be seen in **Figure 75**, even the core clock genes exhibit low oscillation, which can be a clear indication that the number of oscillating PCGs is an underestimation due to the sampling methodology.

After searching for the orthologs in mouse from these 1285, we obtained 1267 PCGs results in mouse, that were compared with the oscillating PCGs in BCA from *Apoe*^{−/−}. The human carotids and the BCA from *Apoe*^{−/−} mice share 315 PCGs (6.2% of the PCGs considered), as can be seen in **Figure 74.B**.

The pathways that appear significantly overrepresented after an enrichment analysis using the Reactome database provided by the online tool Enrich are very similar to the results obtained after the enrichment analysis of the oscillating genes in the BCA from *Apoe*^{-/-}. Some pathways related to the antigen presentation through Class I MHC or the regulation of Tp53 are some of the most covered pathways that we can find in the enrichment analysis (**Figure 74.C).**
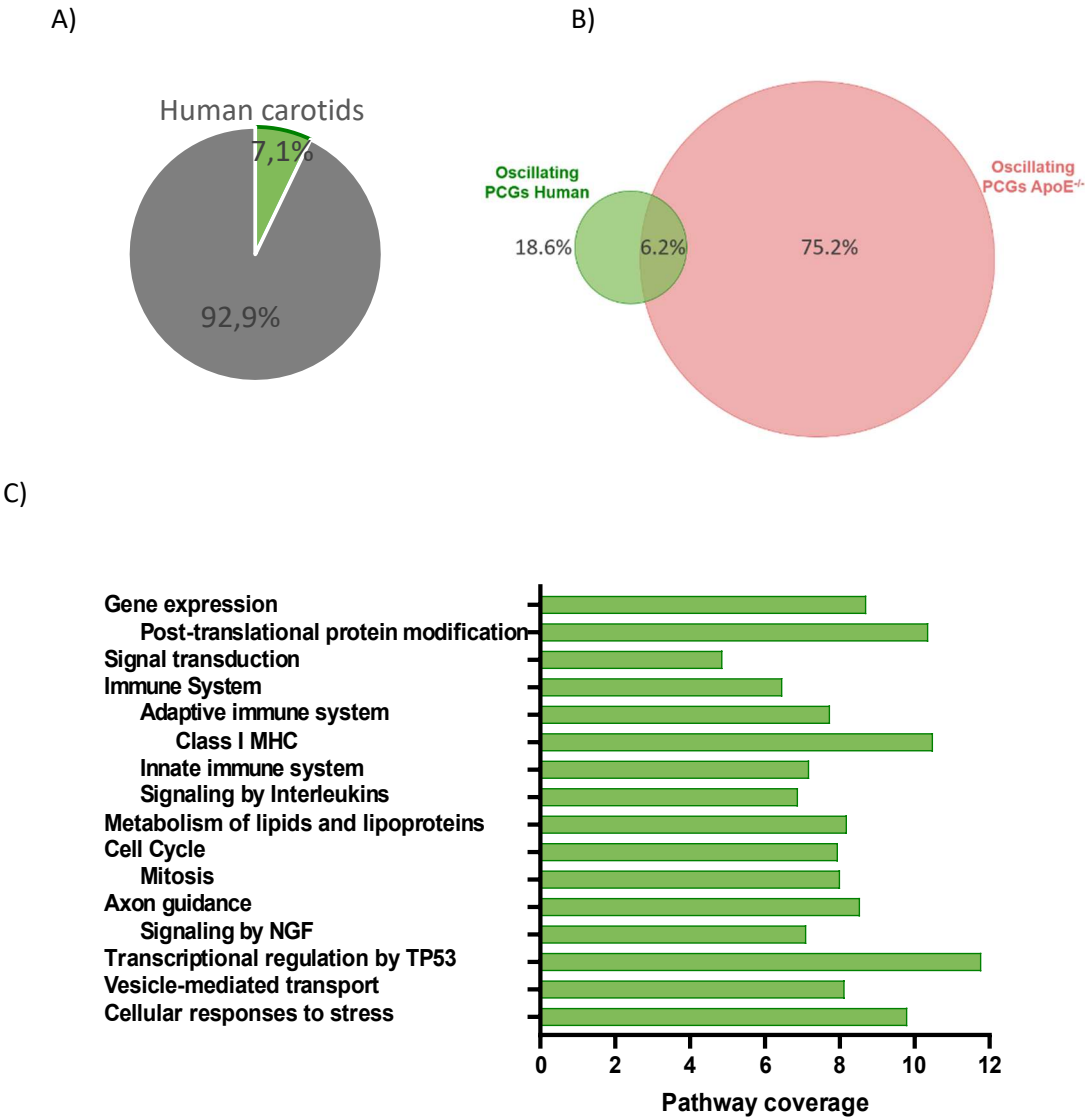
Figure 74. Oscillating transcriptome in human carotids. A) Percentage of oscillating PCG in the human carotids. **B)** Comparison of PCGs oscillating in *Apoe*^{-/-} and in human carotids. **C)** Enrichment analysis of pathways in the group of oscillating PCG in humans.
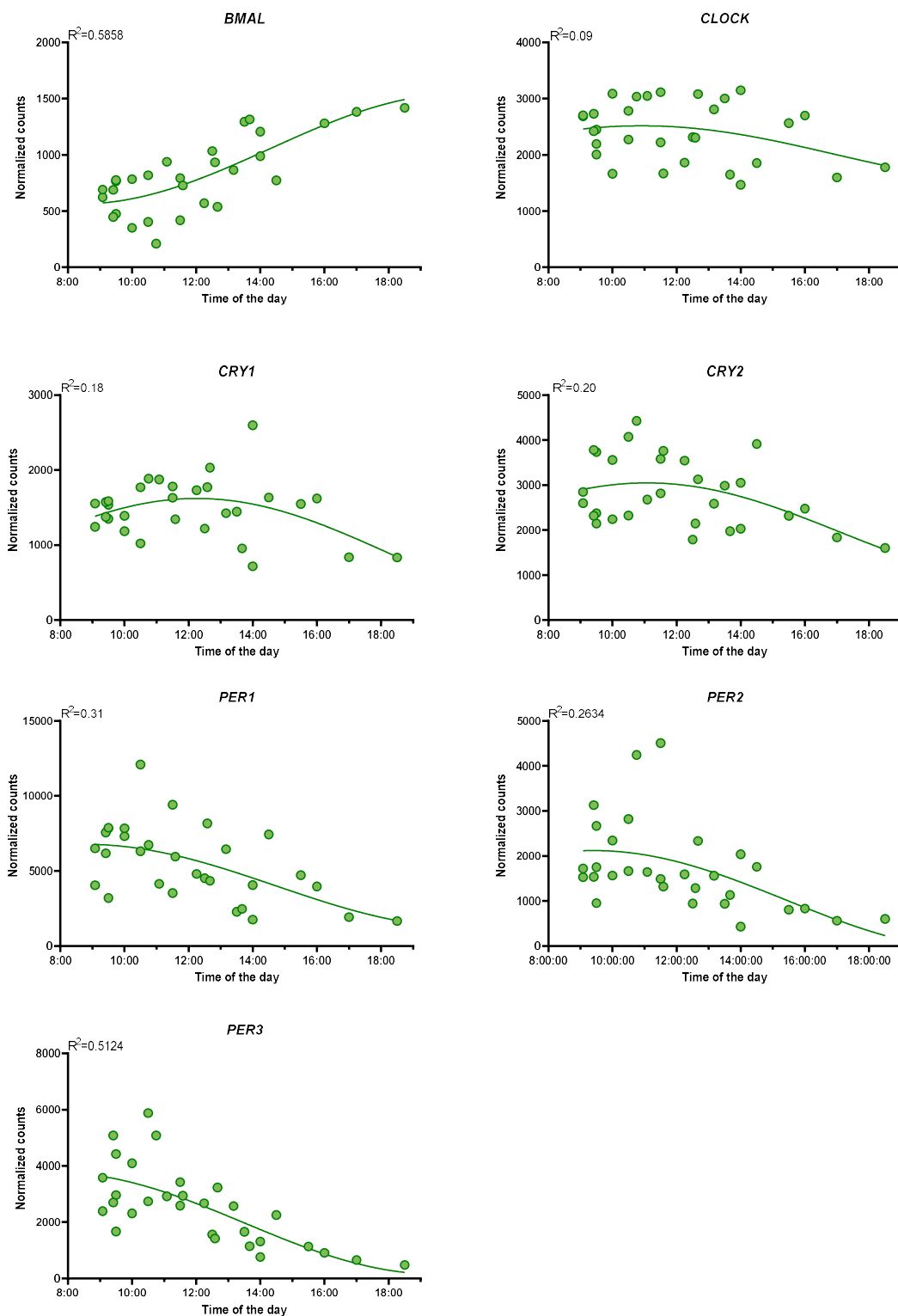
Figure 75. Representation of the oscillation of the main core clock genes in the human carotids.

From the group of 315 PCGs that oscillate in human carotids and BCA from *Apoe*^{-/-} mice, interesting proteins in charge of biological processes that can have an impact in plaque stability and/or plaque development can be considered. This is the case of PCGs related to cell death (such as *GSDMD*, *DAXX*, *BAX* and *RASSF1*)[285,287,288], to innate immune system (*IRF3* and *CACTIN*)[289], to the adaptive immune system (*TCIRG1*, *CD40* and *ITGAX*)[290,291] and to cell cycle (*CINP*, *E2F4*, E4F1)[292-294]. Other PCG related to oxidative stress, like *APEX1*[295] and *HSF1*[296] also show oscillation (**Figure 76**).

While the PCGs related to these pathways exhibited a higher expression in the earliest timepoints of the day in the BCA of *Apoe*^{-/-} mice, this pattern changes in the human carotids, in which all these PCGs show a higher expression in the evening times.

Even thought the signalling by TGFß was present in the group of oscillating PCG in the BCA from *Apoe-* mice, the main component (*Tgfb1*) didn't show pass the threshold of oscillation. The situation is diferent in the human carotids, in which *TGBF1* shows oscillation and so does *NFKB2*. The signalling pathway activated by TGFB1 is a key player in the regulation of many biological functions related to cell proliferation, cell deth, matrix remodelation, inflammation and cell migration, which are key developmental processes in the atherosclerotic plaque that have been shown to oscillate in the animal model and in the human plaque.
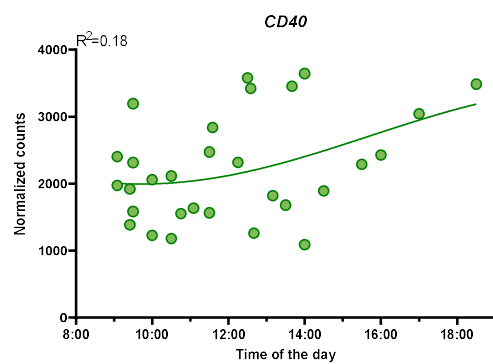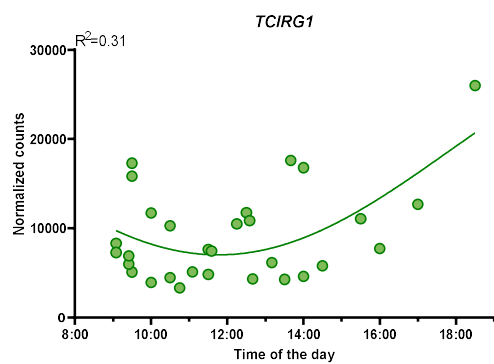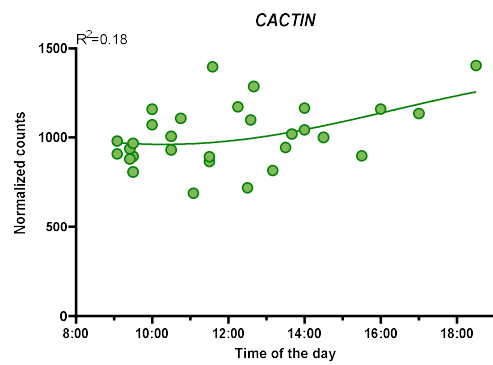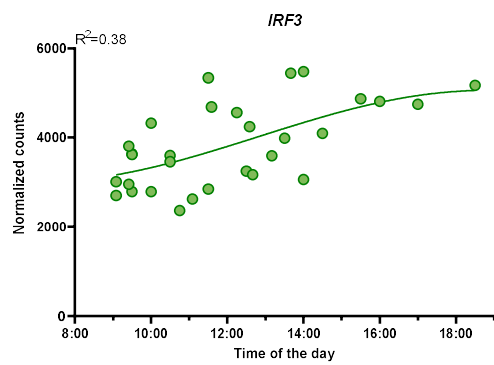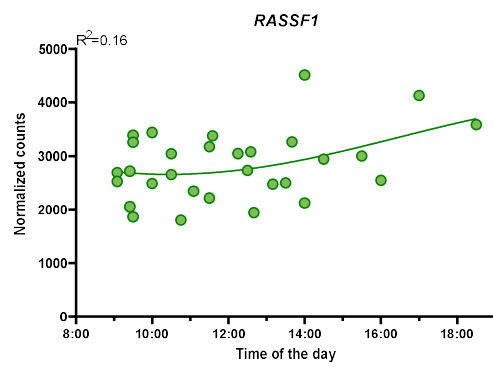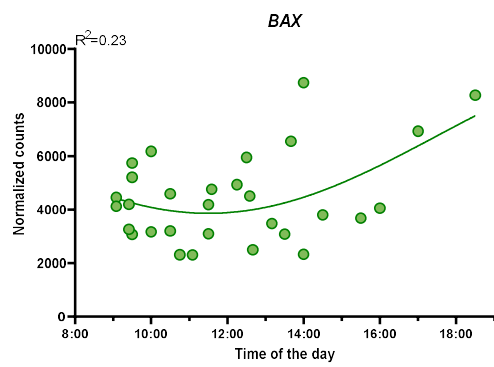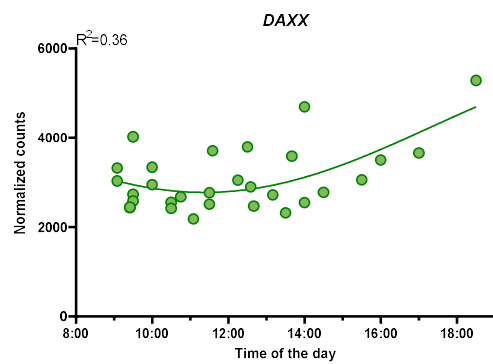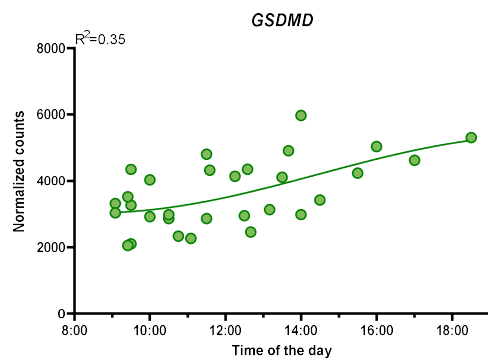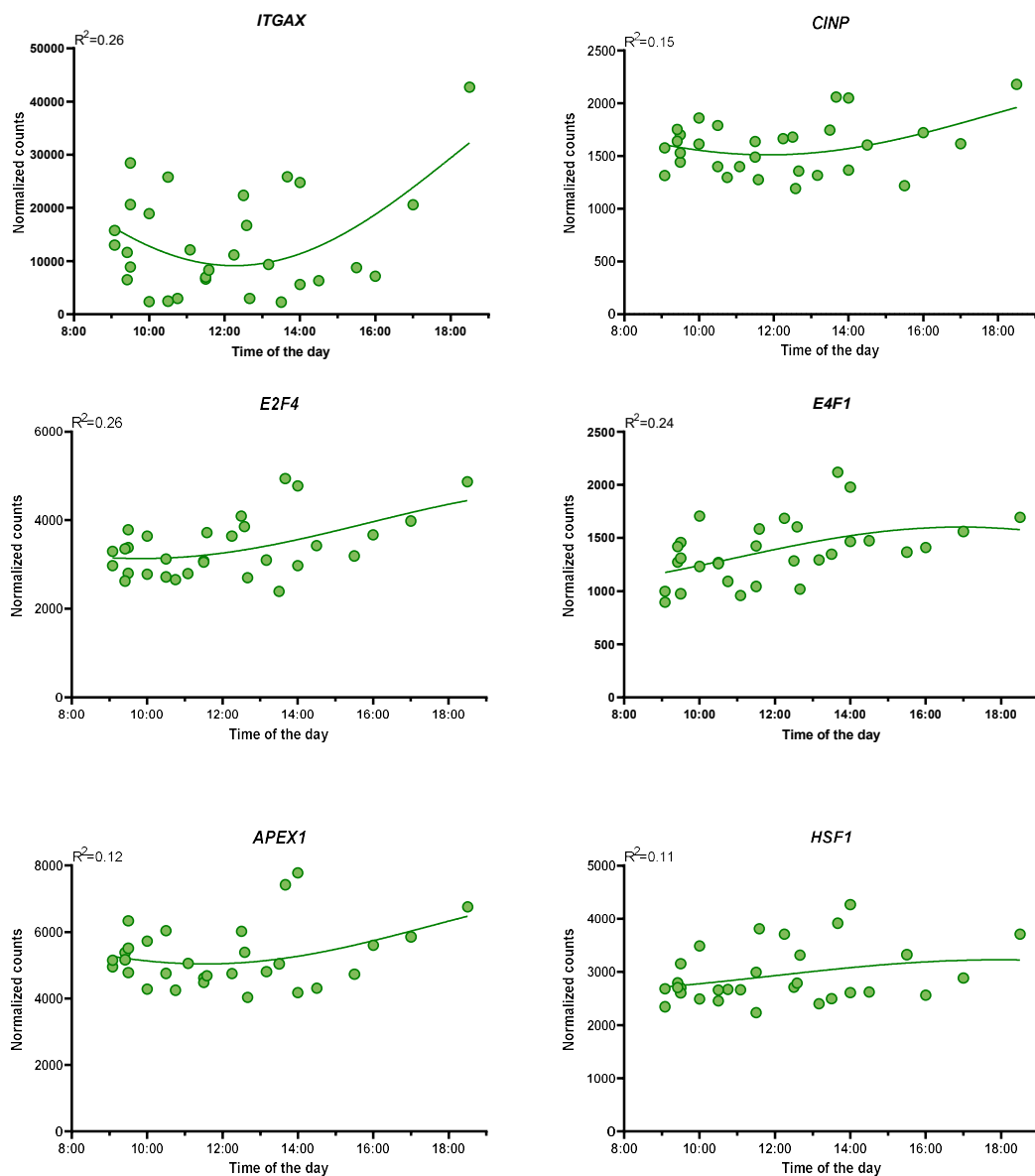
Figure 76. Representation of key PCG in atherosclerosis that oscillate in human carotids.

3.4.1 Oscillating genes in BCA from *Apoe*^{-/-} mice and human carotids appear as druggable

Several PCGs that have oscillatory patterns in BCA and human carotids belong to the "druggable genome"; a set of genes that are direct or indirect targets of drugs that are licensed, drugs in late phase development, genes that code for proteins that have similar structure or function to the ones that are targeted by approved drugs[297].

When we compare the list of 315 PCG shown to be oscillating in BCA and human carotids with the human druggable genome, we get 49 targets of PCGs that code for proteins whose activity can be modulated through drug administration.

Among the oscillating drug targets, we find interesting results, as can be seen in **Figure 77**. This is the case of CD40, which has an important role in ERK pathway in macrophages and B cells[298], both key role players in atherosclerotic development.

The apoptotic process as consequence of endoplasmic stress has appeared several times during the project and some of the proteins related to this pathway are targets of approved drugs. This is the case of HSPA5, ERP29[299], EDEM2[300], MANF[301], SSR2[302], MAN1B1[303].

Another pathway that has been a constant is cell cycle and cell survivance. We can also find targets that either block the apoptotic signals or are positive regulators of the proliferation. AKT1S1, which is a subunit of mTORC1 that gets activated by TGF-ß[304] and regulates positively these two functions[305], appears as a druggable target.
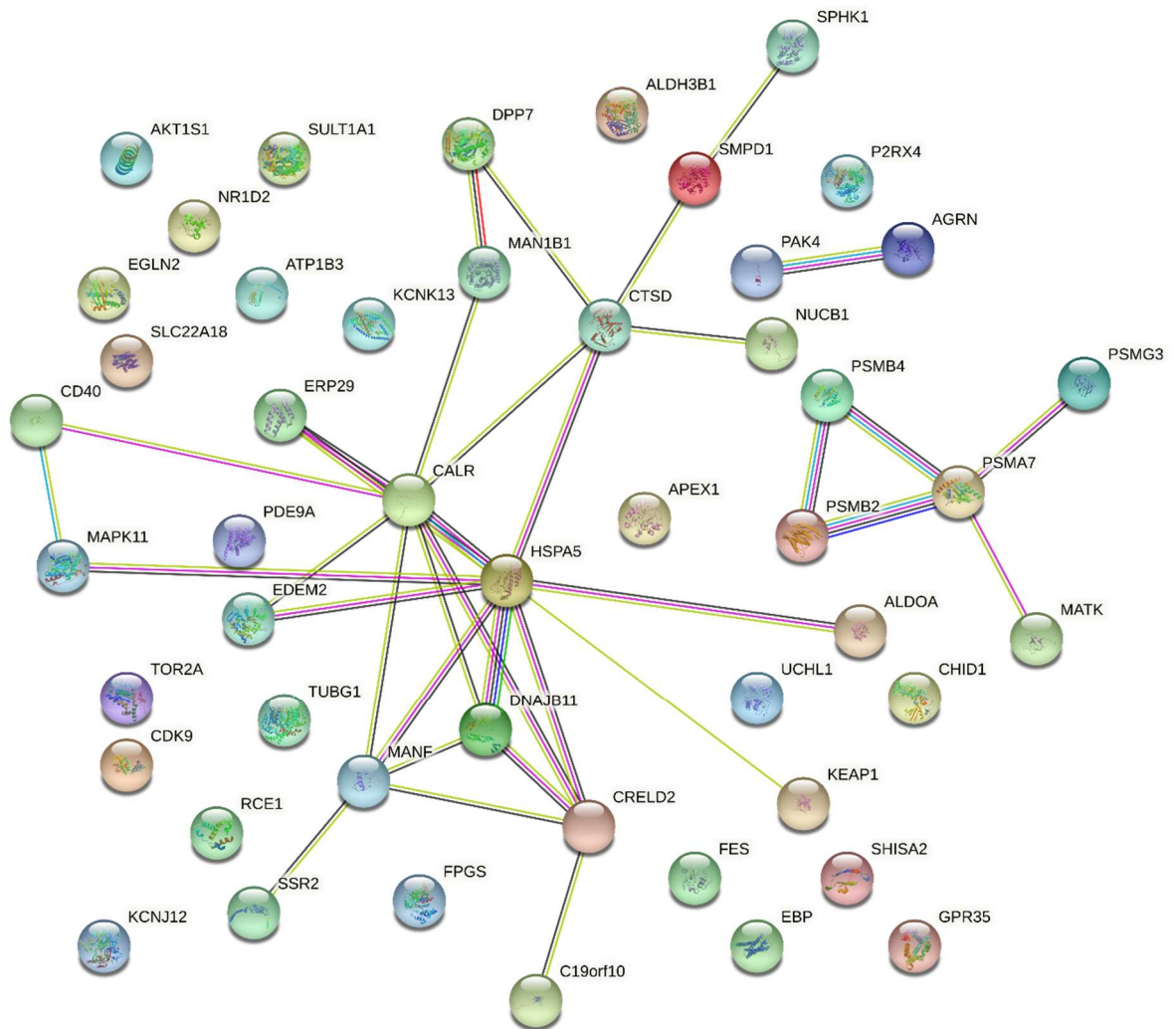
Figure 77. Interaction network among the oscillating PCGs in the BCA of *Apoe*^{-/-} and human carotids with atherosclerotic plaque. In the image, the proteins that are a product of the oscillating PCG shared between *Apoe*^{-/-} and human are displayed, so the interactions that are illustrated are described at the protein level. The colour of the nodes are randomly chosen, while the colour of the connections between proteins indicates: known interactions from curated databases(━), known interactions experimentally determined (━), predicted interactions based on gene co-occurrence (━),gene fusions (━), co-expression (━) or textmining (━). The interaction network was created using String-db version 11.5 (https://string-db.org/) using as minimum required interaction score of highest confidence (0.900).

4.Summary

4.1 The advanced atherosclerotic plaque in *Apoe*^{-/-} shows oscillation at the transcriptome level

With the analysis of the transcriptome of the brachiocephalic artery on Apoe$^{-/-}$ mice that had been fed 16 weeks on HFD, we have identified numerous pathways that oscillate in the transcriptome of the advanced atherosclerotic lesion. Furthermore, we have been able to detect the transmission of these oscillation also in the proteomic and by immunohistochemistry methods. Many of these pathways, such as proliferation, immune activation, cell death and extracellular matrix remodelling, have a close relationship with the development of the plaque and have a decisive impact in the swift from a stable plaque to an unstable plaque prone to rupture.

Lastly, we have been able to identify the oscillatory differences between different cellular populations in the plaque, such as leukocytes (CD45$^+$ cells) and stromal cells (CD45$^-$ cells).

4.2 The circadian oscillation of the BCA in *Apoe*^{-/-} shows important differences to the oscillation of the BCA in a wild-type model (C57BL/6J)

The percentage of PCG that show oscillation on the BCA in *Apo*$^{-/-}$ is surprisingly higher than the percentage of PCG that show oscillation on the BCA from wild type mice (C57BL/6J) of the same age that have been fed on chow diet. But the differences between the two genotypes go far beyond the amount of PCG. On the one hand, there are PCG oscillating in only one of the models, which means than the percentage of oscillating PCG in *Apoe*$^{-/-}$ is not just an extension of the oscillating PCG in C57BL/6J. On the other hand, we have described that PCG that oscillate in both genotypes might have a different pattern of expression, being in some cases even antiphase when comparing the two genotypes.

4.3 A western diet has systemic effects and these effects are very variable among organs

In this study, we have analysed the transcriptome of a total of 12 different organs (BCA, lung, liver, spleen, colon, ileum, WAT, adrenal gland, heart, aorta, kidney and muscle) and compare their transcriptomes in *Apoe*$^{-/-}$ after 16W of HFD with a wild type model (C57BL/6J). All the analysed organs show changes in the percentage and identity of the PCG that show oscillation,

being these changes of different magnitude between the organs. Furthermore, we have described changes in the oscillation of the core clock genes in these two conditions.

Focusing on *Apoe*$^{-/-}$, we have compared the oscillation of the main pathways that have an impact in the stability of the plaque between all the organs, with the aim to describe groups of pathways that have a different pattern of expression in BCA versus the rest of the organs, and that would be interesting therapeutic approaches to be targeted with chronopharmacology.

4.4 A percentage of the PCG oscillating in the BCA of *Apoe*$^{-/-}$ shows also oscillation in human carotids with advanced atherosclerotic plaque

We have been described the oscillation in human samples of some of the oscillating PCG in the advanced lesion from *Apoe*$^{-/-}$. Furthermore, we have been able to sort oscillating PCG shared between our murine model and the human samples that can be targeted by already approved drugs, drugs under the last stages of development or that have a similar structure to other targets.

In summary, in this study we have characterized the oscillating pathways in the advanced atherosclerotic lesion for the first time using high-throughput techniques. Besides, we have extrapolated our results to human samples and we have described the changes that a western diet has in terms of oscillatory patterns. We have created robust and consistent data that comprehends gene regulation, protein regulation and pathway regulation that we hope that contributes in the development of therapeutic approaches that would reduce the high mortality of cardiovascular diseases.

5.Discussion

5.1 The need of new therapeutic targets in Atherosclerosis

Cardiovascular diseases (CVD) are the most common cause for death in the whole world, representing 32% of all the deaths in 2019. From all the deaths caused by CVD, 85% had their cause in heart attack and stroke, which are commonly caused by complications associated with advanced atherosclerosis disease[306]. The extensive period of time during which the plaque starts and develops, can last for several decades, in some cases it can even begin early in childhood[307], which makes atherosclerosis a chronic disease that needs constant monitoring and long-time medication. Furthermore, the cost of cardiovascular care comprehends a significant portion of the total health care in many different countries and this cost increases exponentially, rising from 212 billion dollars in 1996 in the USA to 320 billion dollars in 2016[308]. Despite having lived with this disease for millenniums (there is evidence of ancient Egyptian mummies with atherosclerotic plaques[309]) the only treatments available at the moment for the atherosclerosis treatment aim at systemic approaches in order to reduce the circulating cholesterol, reduce the blood pressure and preventing blood clots, besides raising awareness of the population to adhere to healthy habits. At the moment, there is no treatment available that aims at the elimination or even reduction of the atherosclerotic plaque or its stabilization and the existing treatments are not effective for all patients or have serious side effects[310]. In the last years, there has been a shift in the design of new therapeutic approaches, going from drugs that focus in lipoprotein metabolism and cholesterol blood management to immunotherapeutic approaches, focusing on the modulation of immune responses and aiming to treat atherosclerosis under the prism of a chronic inflammation disease[310-312].

In the process of drug design, it has been known for long that the time of the day when the drug is given has a strong influence on its outcome and the efficiency. This time dependence influence has been proven in different diseases, as multiple sclerosis, vaccination against influenza, asthma, chemotherapy, arthritis and bone marrow transplant, among others[178]. Even cholesterol-limiting statin simvastatin was the first official implementation of chronopharmacology after being prescribed to be taken once a day in the evening[181]. Despite the fact that the influence of time dosage has been proved in several clinical studies since the 1990's, as the impact of chronotherapy in chemotherapy toxicity and effectiveness in metastatic colorectal cancer[313], very few drugs have a time-of-dosing recommendation and very few clinical trials consider time dosage in their protocols and results, being most of the ones that do consider it small clinical trials with less than 500 patients[181]. Moreover, the

impact of the dosing time in the outcome of a specific disease is still not clear, with different studies suggesting opposite outcomes and exposing the need for larger and long-term follow-up trials[314].

In the case of cardiovascular diseases, it is long known that there is a higher prevalence of infarctions in the early hours of the day[125,166,315]. This higher prevalence is associated with changes in the blood pressure, but also can be linked with different biological processes that have a direct impact in the plaque and that have been described here to be under the circadian clock, like the immune system activation, cell cycle and cell death. Besides, other biological processes related to the extracellular matrix organization and degradation, cholesterol uptake and neuronal development show also a strong oscillating pattern in *Apoe*.

This is the first study in which an atherosclerotic plaque is analysed using different high-throughput techniques in order to describe the circadian variations of different biological processes in the plaque. Furthermore, in the study we have included the analysis of 12 different organs with a very close relationship with atherosclerotic development and circadian control with the aim to describe the systemic changes that a diet rich in fat content has and point different potential therapeutic targets to be treated by making use of chronopharmacology.

5.2 Atherosclerosis: more than an accumulation of fat and debris

Far from being a structure created by random and passive accumulation of fat and cellular debris, the atherosclerotic plaque is an entity itself with different processes that affect its development and stability taking place. The accumulation of several types of cells from the immune system and the combination of anti and pro-inflammatory signals for an extended period of time create an independent organoid in which complex biological processes are happening. In my study, these different functions, among which we can find proliferation, cell death, ECM remodelling and neuronal development show different patterns of activity throughout the day. Several of these processes have a direct connection with plaque stability, which is defined as the probability of a plaque rupture followed by the release of high pro-thrombotic material, which can create a thrombus and block the efferent blood flow towards peripheral organs, causing ischemia and necrosis.

The connection between circadian oscillation of plaque stability and cardiovascular events whose cause is linked with atherosclerotic plaque rupture, as myocardial infarction, ictus or sudden cardiovascular health has been described for more than 35 years[166].The possibility to study the oscillation of the biological processes that have a direct correlation with changes in plaque stability in order to establish new targeted approaches opens a completely new dimension of drugs and treatments of the cardiovascular pandemic. However, this is the first study done applying different high-throughput techniques on a collection of atherosclerotic lesions in a 24-hour span.

In the advanced atherosclerotic plaque, several structures can be differentiated, as necrotic core, fibrous cap, endothelial layer or intima area. Several processes that are known to affect the stability of these structures have been detected as oscillatory. Some of the pathways that have shown a very striking difference between timepoints are related to the immune system. The oscillation of different pathways in the immune system, as release from bone marrow, abundance in circulation and recruitment, have been already described[135,158,316]. Besides corroborating that there's a different rate of extravasation of immune cells from the blood to the plaque, we have described that different processes involving the innate and the adaptive immune system, as can be antigen presentation, phagocytosis, cytokine signalling or the interaction between these two compartments of immunity oscillate. We have also demonstrated that the immune cells follow different oscillating patterns than stromal cells when comparing their activities inside the plaque in very critical aspects, as cell death and cell proliferation, suggesting a temporal compartmentalization of biological functions in different cell types.

Intimal cell proliferation is an important hallmark of atherosclerosis development and destabilization, specifically at late stages of the disease[17,123]. It has been published that the transcription of *Myc* is controlled by PER2[317] and that BMAL1 has an important role in SMC proliferation[318]. In the plaque, we have detected the oscillation of *Myc*, but furthermore, we have been capable of describing an opposite contribution from the group of stromal cells and from the group of leukocytes into the group of proliferating cells, initiating the idea of being able to target the proliferating profile of a specific population. The proliferation in the plaque is quite extended among the cells and in our experiments. Surprisingly, the rate of dividing cells in the plaque has exceeded the rate of division in other organs which are considered to have high rates of division, namely the liver. Despite the fact that the plaque is composed by mature and differentiated cell types, several cell groups proliferate (vascular smooth muscle cells, leukocytes and endothelial cells) at different rates[319]. The ability to proliferate of

macrophages is know from over half a century[320] and it is also long known that oxidized LDL together with the combination of hyperlipidaemia and hyperglycaemia positively regulates cell growth and cell proliferation[106,108], making macrophage proliferation the main source of this cellular type, over monocyte extravasation from circulation[17]. The proliferation of macrophages has been associated with an effort to reduce inflammation and deal with the accumulation of oxidized lipids[321]. On the other side, as the plaque grows, vascular smooth muscle cells migrate from the media to the intima and also proliferate, while endothelial cells don't seem to actively proliferate in the plaque due to the presence of oxidized lipids[108]. Despite creating the illusion that higher number of VSMC could increase the production of collagen and therefore the stability of the plaque, VSMC with higher proliferating rate are associated with a loss in contractility. The proliferative capabilities of VSMC and macrophages are considered to be key therapeutic strategies to target[17,322]. For example, attempting blocking cell proliferation in the morning time might reduce the proliferation of leukocytes (mainly macrophages) which is associated with plaque destabilization and plaque growth[323] while it wouldn't interfere with the proliferation of stromal cells, that proliferate more abundantly in the evening times and are associated with plaque stability due to their contribution to the thickening of the fibrous cap[324].

A similar phenomenon happens with cell death. The different types of cell death (apoptosis, necroptosis, pyroptosis…) have different degrees of importance throughout the development of the lesion. While at the beginning of the lesion, when the intima starts to expand, the number of dying cells is extremely low, it quickly increases with the accumulation of fat and leukocytes[325]. The death is caused by different stimuli, like oxidized-LDL, cholesterol overload, hyperglycaemia or by molecules produced by other cells, as TNF-α[326]. In our analysis, we have detected an important amount of PCGs and proteins that were oscillating and belong to the pathways related to endoplasmic-reticulum-associated protein degradation (ERAD) and endoplasmic reticulum stress. The accumulation of oxidated lipids, hyperlipidemia and a lack of control of calcium accumulation interfere in a negative way in the synthesis, folding, post-translational modification and transport of the proteins, causing an accumulation of misfolded and unfolded proteins. This accumulation causes ER stress, which is already activated by sheer stress[327]. ER stress will end up with the activation of several pro-inflammatory pathways and, if the ER stress is prolonged, pro-apoptotic pathways will be initiated through the activation of several caspases, as caspase 9 and caspase 3, which in our dataset oscillate in the same manner as proteins from the ERAD pathway[328]. The death of each cell type contributes to modify differently the stability of the plaque. In the case of endothelial cells, its death can lead

to plaque erosion besides contributing to thrombin formation and acquiring procoagulant features[329]. In the case of smooth muscle cells, their death contributes directly to the stability of the plaque, since these cells synthetize the collagen that stabilizes the fibrous cap[330]. In the case of leukocytes, the death is mostly caused by an overload of lipids in the cytoplasm. When talking about macrophages and other phagocytic cells, the higher accumulation of cholesterol in the endoplasmic reticulum exacerbates the endoplasmic stress[331] and their transformation into foam cells thanks to the accumulation of free cholesterol through phagocytosis and pinocytosis and the iron accumulation[332], processes that oscillate in a similar manner in the plaque. The death of these phagocytic cells contribute to the accumulation of apoptotic cells that are deficiently cleared in the plaque, due to a defective efferocytosis and the apoptosis of cells capable of clearing the apoptotic cells[333]. Furthermore, they contribute to the accumulation of modified lipids in several degrees of digestion.

Together with cell cycle, cell death and activation of immune system, one other pathway that has shown a strong circadian regulation is the nervous system development. Although the association between the neuronal system and atherosclerosis might look weak, recent studies describe a higher density of axons in the plaque when compared to healthy arteries, also mentioning a reduction of the atherosclerotic plaque in mice without innervation in the adventitia close to the area with plaque[334]. In our dataset, we have been able to find several pathways related to neuronal innervation and neuronal development that show oscillation with a peak around ZT17. These pathways comprehend different synaptic components (NMDA receptors, GABA synthesis and release, dopamine...) and the growth of new axons and their posterior myelination (semaphoring, L1CAM, NCAM, netrin…). The influence of some of these molecules in atherosclerotic development has been already addressed. For example, some semaphorins, as Sema3A, induce apoptosis of endothelial cells and macrophages and regulates leukocyte transmigration during atherogenesis[335]. Furthermore, the emergence during atherosclerosis progression of different structures that facilitate neuroimmune cardiovascular interfaces (NICIs)[336] would explain the intense signalling in the plaque concerning different pathways related to axon growth and nerve development.

5.3 Hypercholesterolemia exerts systemic alterations of the host

This study has also allowed the comparison of a wide range of tissues in healthy state and under hypercholesterolemia. A diet rich in fats and cholesterol exacerbates the development of the disease, together with different other factors, such as smoking, high blood pressure and

sedentarism. Under hypercholesterolemia, the high levels of cholesterol in the blood affected all the organs studied at a different extent. In our study, the number and identity of the protein coding genes that oscillate in each of the studied organs has experienced changes when comparing wild mice versus a genetically modified murine model for atherosclerosis fed with HFD.

These changes that we see when comparing the changes in oscillation as a consequence of HFD feeding are in agreement with previous studies describing changes in the expression of circadian clock genes in mice being fed with HFD or obese patients versus mice on normal diet and lean patients[337-340] and the outcome is in all the cases a striking alteration of the circadian rhythms in the different analysed tissues. Some of these studies correlate a high-fat diet with a dampening of the circadian rhythms, loss of rhythmicity and a reduction of the circadian oscillation[338,339,341,342]. Similarly, in our dataset, we can detect differences in the amplitude of different core clock genes when comparing *Apoe*^{-/-} and C57BL/6J, but despite the fact that we see a correlation between the average amplitude of the main core clock genes and the percentage of oscillating PCG in each organ (**Figure 69**), the tendency is not completely clear. Interestingly, such alterations are not affecting each organ in a similar fashion, suggesting organ-dependent effects, with organs showing an increase in the percentage of oscillating genes (i.e. BCA, adrenal gland, heart, spleen), decreased (i.e. WAT, muscle) or very similar (ileum, kidney, liver). For example, in one of the first and most known publications about the changes in the oscillation of core clock genes caused by a high-fat diet[338], the authors described changes in the amplitude of some core clock genes (*Per2*, *Bmal1*, *Rev-erbα* and *Dbp*) in the liver when comparing ad libitum HFD versus ad libitum normal diet. In contrast, when we compared the amplitude in the liver from *Apoe*^{-/-} mice fed with HFD versus wild mice fed with normal diet, we registered very minimal differences in the liver, with some of the core clock genes having a larger amplitude in *Apoe*^{-/-} and some others exhibiting a dampening of the amplitude, but in all cases, being the differences smaller than 1 unit (**Figure 68**). Furthermore, the average amplitude of all the oscillating genes in wild mice and *Apoe*^{-/-} mice in the liver were very similar, with an average of 0.517 in *Apoe*^{-/-} and 0.619 in C57BL/6J.

This situation changes when comparing other organs between the two genotypes. For instance, we detect an extreme difference in the average amplitude of the oscillating genes in both of the intestinal tissues analysed (colon and ileum, **Figure 64**). In these organs, the average amplitude drops from 3.649 in ileum and 3.35 in colon to 0.653 in ileum and 0.713 in colon, when comparing C57BL/6J and Apoe. Furthermore, the organ with the biggest difference between *Apoe*^{-/-} and C57BL/6J when considering the average amplitude of the core

clock genes is the BCA, but in a contra intuitive way: the BCA with plaque from *Apoe*^{-/-} shows a higher amount of oscillating PCG than the healthy aorta from C57BL/6J.

Furthermore, the changes in the identity of the oscillating genes are also worth mentioning, since in some organs the changes in the PCG that oscillate in each genotype are very noticeable. This is the case of the BCA and the spleen, organs in which the similarity in oscillating genes between Apoe^{-/-} and C57BL/6J is less than 20%. In fact, in most of the organs, the similarity between oscillating PCG is less than 50%. These results can be linked with studies that claim that HFD induce a systemic chronic low-grade inflammation (studies reviewed in Duan et al.[343]) that could attribute the systemic changes of a HFD feeding to the changes of the immune system caused by the diet.

In our study, we described that high-fat diet feeding has a much deeper effect in the percentage of oscillating protein-coding genes in the transcriptome and also in the identity of these protein coding genes. Furthermore, in our comparison of the brachiocephalic artery in *Apoe*^{-/-} mice fed with HFD and wild type mice, we described changes in the oscillatory pattern of genes belonging to key pathways in atherosclerotic development, such as immune system, cell cycle or lipid metabolism when the two genotypes are compared. We also described the differences in the oscillatory pattern of protein coding genes that oscillate in both genotypes, adding several dimensions of complexity to the description of the impact of feeding in circadian oscillation, even when the protein-coding genes that were expressed only in one genotype weren't considered.

5.4 The importance of oscillation in the transcriptome

This study, in which an important variety of organs and tissues have been analysed, it has been described that the number of genes that have circadian oscillation represents an important percentage of the total transcriptome. This result is in agreement with other published studies in different species. In a study published in 2014 by Zhang et al.[147], the authors analysed 12 different organs (liver, kidney, lung, brown fat, heart, adrenal gland, aorta, white fat, skeletal muscle, cerebellum, brainstem and hypothalamus) in mouse fed with chow diet, detecting that at least 43% of the protein-coding genes oscillated (using JTK_CYCLE algorithm with a 5% FDR and a 24-h period) in at least one organ and they forecast that with the addition of more organs, up to a 55% of all PCG detected would oscillate in at least one organ. This result was strongly outnumbered by a more recent study made by Mure et al.[148] in which 64 different tissues from 22 different organs of baboons (eye, adrenal gland, pituitary, thyroid, bone marrow, spleen, liver, pancreas, testis, prostate, white fat, skin, bladder, kidney, brain, aorta, heart, colon, ileum, oesophagus, stomach, lymph node) were analysed and 80% of all the

protein codding genes exhibited a 24-h rhythm in at least one organ (using meta2d with a p-value<0.05). In our analysis, with 12 organs sequenced, we have detected almost 87% of all PCG oscillating in at least one organ in *Apoe*^{-/-} and almost 85% in C57BL/6J, which gives a more similar result to the second study. The differences in the results are most likely due to the differences in the techniques (a combination of RNA-Seq and DNA arrays in the first case versus a complete NGS pipeline in the case of the second study and our study). Despite the results of the comparisons of the total percentage of oscillating genes, the percentage of oscillating genes per organ is more similar to the study published by Zhang. In here, liver, kidney and lung are the three organs with a higher percentage of oscillating genes, results that are shared with our dataset when considering either *Apoe*^{-/-} or C57BL/6J. On the contrary, in baboon the organs with the higher percentage of oscillating genes are the thyroid, stomach fundus and the gastrocnemian muscle, leaving liver, kidney and lung in the bottom 67% of the organs. When considering only the shared organs between the baboon study and our dataset, heart, ileum and the adrenal gland are the three organs with most oscillating genes, which in our dataset are in the middle 25% of the organs by percentage of oscillating genes. These considerations could implicate a different regulation of the circadian pattern when considering different species, but additional experiments and a unification of techniques and pipelines should be performed to confirm these findings.

Furthermore, we have described a striking lack of similarity between the transcriptome and the group of oscillating PCG among organs. The most noticeable comparison is among the aorta and the heart, in which the percentage of similarity in the transcriptome of both organs is quite modest (close to 87%) and not very different to the rest of organs, but they share the totality of the oscillating genes. On the other side, the similarities when considering the similarities in PCG of some pairs of organs like the BCA and the liver or the BCA and the muscle, that share more than 65% of the transcriptome, are below 30%. Despite the fact that the pattern of expression of these PCG haven't been analysed and we don't possess information whether they oscillate in antiphase or in phase, the fact that they share the totality of the oscillating PCG suggests an interorgan regulation of oscillating biological processes, with a collaborative approach among organs.

5.5 A very good gene candidate or a very good pathway candidate to target

We have been describing the oscillatory patters of many genes and proteins related to different biological processes in the BCA of *Apoe$^{-/-}$* mice, but not all the processes are suitable drug targets. Finding pathways and biological activities that are temporarily separated in BCA and the rest of the organs would be a very interesting solution from a chronopharmacological point of view, since being able to target a process which has a peak in BCA at the same time that displays troughs in the rest of the organs would noticeably diminish the side effects of the therapeutic approach while increasing the efficacy.

In our study, we have shown that some biological pathways, as proliferation and cell death, have a strong oscillation in the plaque and furthermore, show an antiphase peak in most of the other considered organs. The proliferation and cell death are intimately associated with the immune system, either because leukocytes are the main cells proliferating and dying in the plaque or because of their production of different cytokines that positively activate pro-apoptotic pathways in other cell types. Furthermore, as we have already mentioned, a HFD produces low-levels of sustained systemic inflammation[343,344], that could be linked with the general differences in oscillation among all the considered organs. This theory, together with the increase of acceptance of seeing atherosclerosis as a chronic inflammatory disease, leads to the consideration of pharmacological approaches that would target these three biological pathways, in an effort to increase the plaque stability.

A very interesting pathway that interferes with proliferation, cell death, immunoregulation and extracellular matrix remodelling is the signalling activated by transforming growth factor- β (TGF- β)[230]. The TGF-β family is a promising therapeutic target for several diseases, such as cardiovascular diseases, cancer[345], diabetic kidney disease[346] and renal fibrosis[347], cerebrovascular diseases[348] or skeletal diseases[349]. For example, in the cancer field, the fact that this molecule exhibits a dual behaviour, inhibiting tumour progression in the early stages and enhancing it in the late stages, makes TGF-β an attractive target molecule. Nevertheless, the first clinical outcomes of assays that target TGF- β are not as positive as expected and the hypothesized reason behind it might be this dual nature of the molecule, together with the fact that its ability to stop tumour growth needs to be combined with another drug to actually kill cancer cells[350].

In the case of atherosclerosis, TGF- β has been considered as a therapeutic target since the early 1990s[351]. The source of TGF-β1 in the plaque is diverse, being produced by inflammatory, vascular cells and platelets[230]. Same that in cancer, the role of TGF- β signalling in atherosclerosis is dual, with some studies describing its anti-atherogenic role, mentioning that its inhibition causes different pro-atherogenic changes in the plaque, as reduction of SMC differentiation, increase inflammation, intraplaque haemorrhage and accelerated lesion formation, towards a configuration of a more unstable plaque. On the other side, TGF- β enhances the production of different components of the extracellular matrix, which can be seen as a way to stabilise the plaque, but it can enhance the accumulation of lipoproteins and enlarge the plaque. Furthermore, even though is seen as an anti-inflammatory cytokine, it stimulates leukocyte chemotaxis. All these studies describing the duality of TGF- β were reviewed by Nachtigal et al[352,353].

As we have already described, several components of the TGF-β pathway show oscillation in the atherosclerotic plaque (SMAD2/3, SMAD4, CTGF). This finding, together with the fact that most of the biological processes that are influenced by TGF-β action and the oscillation of TGFB1 in the atherosclerotic plaques from humans places this pathway in a privileged position to be considered as a potential drug target when developing a chronopharmacological targeted approach.

Besides TGF- β pathway, other drugs that are currently under development or even already being used in clinic practice for the treatment of atherosclerosis target pathways that we have described as oscillating and which efficiency could be improved when administered at a specific timepoint. This is the case of drugs targeting inflammation, such as anti-IL-6 (ziltivekimab)[354], anti-IL-1β (canakinumab)[355], IL-1 receptor (anakinra)[356] or TREM-1 (LR12 peptide)[357] that would target specific pro-inflammatory pathways, that we have seen with a very specific peak of expression between ZT1 and ZT5. Very closed related to inflammation we can find the inhibition of NLRP3 (MCC950)[358], which will reduce the pyroptosis in macrophages, which is a pro-inflammatory cell death that exacerbates leukocyte recruitment into the plaque[359].

5.6 Limitations of the study

5.6.1 Genes, proteins and pathways

In the study, different genes have been described as oscillatory genes and from their oscillation and the percentage of genes that interact together, the oscillation of different

pathways has been inferred. This can lead to a misleading representation of the actual oscillation of the pathway as a whole. In the analysis, nor the genes or the proteins have been weighted, implying that all the elements contribute equally to the pathway and that the oscillation of any gene would contribute equally to the total oscillation of the pattern. Furthermore, interactome of a gene haven't been assessed and we don't possess the information of the consequences in the pattern of a gene that doesn't show oscillation by itself, but that needs of the assistance of an oscillatory gene to carry its function.

Moreover, the part of the analysis that has created the leading description of the oscillation in the atherosclerotic plaque has been the bulk sequencing, due to its coverage and depth and the possibility to detect a wide range of results, which couldn't be equalled by proteome or single-cell analysis. The fact that most of the drugs interact with proteins would make the testing of oscillating patterns at the protein level using alternative techniques (ELISA, immunohistology staining) necessary to assess their real oscillation. Furthermore, it needs to be considered the possibility that there might be a phase-shift between transcription and translation.

5.6.2 Are mice a good model?

All the experiments described in this thesis were done with sacrifices of mice at different timepoints of the day. Despite the fact that the cholesterol levels in blood of all the mice were tested in order to include only the mice that had developed hypercholesterolemia, there is diversity in the stage of the plaque that have been considered, especially when using techniques in which no histological information could be gathered, as bulk-RNA Sequencing, single-cell sequencing and proteomics. Furthermore, the unavailability of proper imaging in-vivo techniques makes it impossible to assess changes in the atherosclerotic plaque in a longitudinal matter, measuring parameters in the same animal at different timepoints of the day. Lastly, another aspect to be considered is the fact that mice are nocturnal animals, while humans are diurnal primates. This important factor should be extensively considered when using animal models with the aim to translate the results into patients, since the difference between nocturnal and diurnal animals doesn't only consist in a 12-hours-shift in the pathways, but rather a combination of antiphase and phase pathways together with different effects of same factors, as melatonin or GABA[360].

5.6.3 The problem of humans

Our end goal is the description of changes in the atherosclerotic plaque that are translatable to human individuals and that can be used as drug targets. For this reason, we included in our study a collection of samples from 30 different patients whose atherosclerotic plaque from the carotid was surgically removed at different timepoints from 9 am until 18:30 pm. Due to the effort that it always means the collection and study of the scarce and valuable human samples, our study extrapolated the results from a coverage of less than twelve hours into the oscillation of the genes in a 24-hour setting, due to the unavailability of getting fresh samples in the evening and night times. The lack of coverage during more than half of the day reduced significantly the number of oscillating genes, as it is already explained in the **Section 3.4** from the Results. Nevertheless, our sample collection is a unique collection of deep, high-quality sequenced atherosclerotic human plaques at different timepoints of the day, which can complement other studies like a single cell composition of human plaques done by Fernandez et al.[361] or a creation of a circadian atlas for human tissues[286].

5.7 Outlook

Our strongest and most robust technique due to the number of samples and the depth and range of the measurements is bulk-RNA sequencing. We have applied other techniques to test whether the oscillation that we see in the transcriptome level is phenocopied at the proteome level and finally affect a biological process. Nevertheless, complementary techniques using proteome measurements, as western blot or immunohistochemistry assays, should be included.

Another question that comes to our mind when studying the changes caused by HFD is where the changes in the circadian oscillation occur, which could help in the design of treatments that aim to reduce the extend of the atherosclerotic plaque in early stages. We have seen strong changes in organs from the digestive tract, but these are also seen in organs like adrenal gland, in which the average amplitude doesn't show significant changes, but the percentage of oscillating genes increases notably in *Apoe*$^{-/-}$. The study of the oscillation in the suprachiasmatic nucleus would be an important target to address. Besides, many of the organs that show higher changes in the number of genes or in their amplitude are related to the immune system, like spleen, WAT, lung or the BCA itself. The bone marrow should be studied.

Lastly, there is the question about whether the differences of oscillation when comparing *Apoe*^{-/-} mice on HFD versus C57BL/6J mice appear gradually and if they are detectable short after the start of the HFD. There are publication about the fact that short time (4 weeks) HFD feeding doesn't have any effect on any circadian-clock genes in the liver, heart, skeletal muscle or adipose tissue in rats[362], while 8 weeks HFD feeding also didn't show significant differences in adipose tissue and liver[363]. In the same way, other studies describe several approaches to restored circadian rhythms in the periphery through the application of time-restricted feeding[338], a low-carbohydrate and high-protein diet[364] in order to restore the amplitude and rhythmicity of the core clock genes. Besides of modifications in the diet, there are targeted approaches that hypothesize the possibility to drug the clock using small molecules that will increase the amplitude of core clock genes, as Nobiletin[179] that targets RORs, several components that target REV-ERBs or CRYs (reviewed in Huang et al.[365] and in Scheiermann et al.[178]). Another possibility is to regulate the communication between the suprachiasmatic nucleus and the peripheral tissues using the potential as chronopharmacology drugs from glucocorticoids[366]. Nevertheless, besides the potential of these drugs to interfere in the circadian rhythm and ameliorate the consequences of a high fat diet, the impact that they can have in the development and stability of the atherosclerotic plaque needs to be assessed.

Bibliography

1.   Roth GA, Huffman MD, Moran AE, et al. Global and regional patterns in cardiovascular mortality from 1990 to 2013. Circulation 2015;132(17):1667-78, doi:10.1161/CIRCULATIONAHA.114.008720

2.   Herrington W, Lacey B, Sherliker P, et al. Epidemiology of Atherosclerosis and the Potential to Reduce the Global Burden of Atherothrombotic Disease. Circ Res 2016;118(4):535-46, doi:10.1161/CIRCRESAHA.115.307611

3.   Mackinnon ES, Goeree R, Goodman SG, et al. Increasing Prevalence and Incidence of Atherosclerotic Cardiovascular Disease in Adult Patients in Ontario, Canada From 2002 to 2018. CJC Open 2022;4(2):206-213, doi:10.1016/j.cjco.2021.10.003

4.   Kim H, Kim S, Han S, et al. Prevalence and incidence of atherosclerotic cardiovascular disease and its risk factors in Korea: a nationwide population-based study. BMC Public Health 2019;19(1):1112, doi:10.1186/s12889-019-7439-0

5.   Rafieian-Kopaei M, Setorki M, Doudi M, et al. Atherosclerosis: process, indicators, risk factors and new hopes. Int J Prev Med 2014;5(8):927-46

6.   Libby P, Ridker PM, Hansson GK. Progress and challenges in translating the biology of atherosclerosis. Nature 2011;473(7347):317-25, doi:10.1038/nature10146

7.   Gerhardt T, Ley K. Monocyte trafficking across the vessel wall. Cardiovasc Res 2015;107(3):321-30, doi:10.1093/cvr/cvv147

8.   Weber C, Zernecke A, Libby P. The multifaceted contributions of leukocyte subsets to atherosclerosis: lessons from mouse models. Nat Rev Immunol 2008;8(10):802-15, doi:10.1038/nri2415

9.   Tabas I, Williams KJ, Borén J. Subendothelial lipoprotein retention as the initiating process in atherosclerosis: update and therapeutic implications. Circulation 2007;116(16):1832-44, doi:10.1161/CIRCULATIONAHA.106.676890

10.   Tacke F, Alvarez D, Kaplan TJ, et al. Monocyte subsets differentially employ CCR2, CCR5, and CX3CR1 to accumulate within atherosclerotic plaques. J Clin Invest 2007;117(1):185-94, doi:10.1172/JCI28549

11.   Sumagin R, Prizant H, Lomakina E, et al. LFA-1 and Mac-1 define characteristically different intralumenal crawling and emigration patterns for monocytes and neutrophils in situ. J Immunol 2010;185(11):7057-66, doi:10.4049/jimmunol.1001638

12.   Gisterå A, Hansson GK. The immunology of atherosclerosis. Nat Rev Nephrol 2017;13(6):368-380, doi:10.1038/nrneph.2017.51

13.   Mills CD. M1 and M2 Macrophages: Oracles of Health and Disease. Crit Rev Immunol 2012;32(6):463-88, doi:10.1615/critrevimmunol.v32.i6.10

14.   Martinez FO, Gordon S. The M1 and M2 paradigm of macrophage activation: time for reassessment. F1000Prime Rep 2014;6(13, doi:10.12703/P6-13

15.   Lantz C, Radmanesh B, Liu E, et al. Single-cell RNA sequencing uncovers heterogenous transcriptional signatures in macrophages during efferocytosis. Sci Rep 2020;10(1):14333, doi:10.1038/s41598-020-70353-y

16. Willemsen L, de Winther MP. Macrophage subsets in atherosclerosis as defined by single-cell technologies. J Pathol 2020;250(5):705-714, doi:10.1002/path.5392

17. Robbins CS, Hilgendorf I, Weber GF, et al. Local proliferation dominates lesional macrophage accumulation in atherosclerosis. Nat Med 2013;19(9):1166-72, doi:10.1038/nm.3258

18. Patten DA, Shetty S. More Than Just a Removal Service: Scavenger Receptors in Leukocyte Trafficking. Front Immunol 2018;9(2904, doi:10.3389/fimmu.2018.02904

19. Alberts A, Klingberg A, Hoffmeister L, et al. Binding of Macrophage Receptor MARCO, LDL, and LDLR to Disease-Associated Crystalline Structures. Front Immunol 2020;11(596103, doi:10.3389/fimmu.2020.596103

20. Kruth HS. Fluid-phase pinocytosis of LDL by macrophages: a novel target to reduce macrophage cholesterol accumulation in atherosclerotic lesions. Curr Pharm Des 2013;19(33):5865-72, doi:10.2174/1381612811319330005

21. Park YM, Febbraio M, Silverstein RL. CD36 modulates migration of mouse and human macrophages in response to oxidized LDL and may contribute to macrophage trapping in the arterial intima. J Clin Invest 2009;119(1):136-45, doi:10.1172/JCI35535

22. Tabas I. Macrophage apoptosis in atherosclerosis: consequences on plaque progression and the role of endoplasmic reticulum stress. Antioxid Redox Signal 2009;11(9):2333-9, doi:10.1089/ars.2009.2469

23. Tabas I. The role of endoplasmic reticulum stress in the progression of atherosclerosis. Circ Res 2010;107(7):839-50, doi:10.1161/CIRCRESAHA.110.224766

24. Swirski FK. Monocyte recruitment and macrophage proliferation in atherosclerosis. Kardiol Pol 2014;72(4):311-4, doi:10.5603/KP.a2014.0021

25. Bi Y, Chen J, Hu F, et al. M2 Macrophages as a Potential Target for Antiatherosclerosis Treatment. Neural Plast 2019;2019(6724903, doi:10.1155/2019/6724903

26. Drechsler M, Megens RT, van Zandvoort M, et al. Hyperlipidemia-triggered neutrophilia promotes early atherosclerosis. Circulation 2010;122(18):1837-45, doi:10.1161/CIRCULATIONAHA.110.961714

27. Pérez-Olivares L, Soehnlein O. Contemporary Lifestyle and Neutrophil Extracellular Traps: An Emerging Link in Atherosclerosis Disease. Cells 2021;10(8), doi:10.3390/cells10081985

28. Soehnlein O. Multiple roles for neutrophils in atherosclerosis. Circ Res 2012;110(6):875-88, doi:10.1161/CIRCRESAHA.111.257535

29. Nowak WN, Deng J, Ruan XZ, et al. Reactive Oxygen Species Generation and Atherosclerosis. Arterioscler Thromb Vasc Biol 2017;37(5):e41-e52, doi:10.1161/ATVBAHA.117.309228

30. Chistiakov DA, Grechko AV, Myasoedova VA, et al. The role of monocytosis and neutrophilia in atherosclerosis. J Cell Mol Med 2018;22(3):1366-1382, doi:10.1111/jcmm.13462

31.   Garman SC, Wurzburg BA, Tarchevskaya SS, et al. Structure of the Fc fragment of human IgE bound to its high-affinity receptor Fc epsilonRI alpha. Nature 2000;406(6793):259-66, doi:10.1038/35018500

32.   Yamasaki S, Ishikawa E, Sakuma M, et al. LAT and NTAL mediate immunoglobulin E-induced sustained extracellular signal-regulated kinase activation critical for mast cell survival. Mol Cell Biol 2007;27(12):4406-15, doi:10.1128/MCB.02109-06

33.   Lagraauw HM, Wezel A, van der Velden D, et al. Stress-induced mast cell activation contributes to atherosclerotic plaque destabilization. Sci Rep 2019;9(1):2134, doi:10.1038/s41598-019-38679-4

34.   Sun J, Sukhova GK, Wolters PJ, et al. Mast cells promote atherosclerosis by releasing proinflammatory cytokines. Nat Med 2007;13(6):719-24, doi:10.1038/nm1601

35.   Bot I, de Jager SC, Zernecke A, et al. Perivascular mast cells promote atherogenesis and induce plaque destabilization in apolipoprotein E-deficient mice. Circulation 2007;115(19):2516-25, doi:10.1161/CIRCULATIONAHA.106.660472

36.   Amarante-Mendes GP, Adjemian S, Branco LM, et al. Pattern Recognition Receptors and the Host Cell Death Molecular Machinery. Front Immunol 2018;9(2379, doi:10.3389/fimmu.2018.02379

37.   Chen G, Shaw MH, Kim YG, et al. NOD-like receptors: role in innate immunity and inflammatory disease. Annu Rev Pathol 2009;4(365-98, doi:10.1146/annurev.pathol.4.110807.092239

38.   Lim KH, Staudt LM. Toll-like receptor signaling. Cold Spring Harb Perspect Biol 2013;5(1):a011247, doi:10.1101/cshperspect.a011247

39.   Falck-Hansen M, Kassiteridi C, Monaco C. Toll-like receptors in atherosclerosis. Int J Mol Sci 2013;14(7):14008-23, doi:10.3390/ijms140714008

40.   Nyati KK, Masuda K, Zaman MM, et al. TLR4-induced NF-κB and MAPK signaling regulate the IL-6 mRNA stabilizing protein Arid5a. Nucleic Acids Res 2017;45(5):2687-2703, doi:10.1093/nar/gkx064

41.   Kaiser WJ, Offermann MK. Apoptosis induced by the toll-like receptor adaptor TRIF is dependent on its receptor interacting protein homotypic interaction motif. J Immunol 2005;174(8):4942-52, doi:10.4049/jimmunol.174.8.4942

42.   Geijtenbeek TB, Gringhuis SI. Signalling through C-type lectin receptors: shaping immune responses. Nat Rev Immunol 2009;9(7):465-79, doi:10.1038/nri2569

43.   Reid DM, Gow NA, Brown GD. Pattern recognition: recent insights from Dectin-1. Curr Opin Immunol 2009;21(1):30-7, doi:10.1016/j.coi.2009.01.003

44.   Kerscher B, Willment JA, Brown GD. The Dectin-2 family of C-type lectin-like receptors: an update. Int Immunol 2013;25(5):271-7, doi:10.1093/intimm/dxt006

45.   Pfannkuch L, Hurwitz R, Traulsen J, et al. ADP heptose, a novel pathogen-associated molecular pattern identified in. FASEB J 2019;33(8):9087-9099, doi:10.1096/fj.201802555R

46.   Rosales C, Uribe-Querol E. Phagocytosis: A Fundamental Process in Immunity. Biomed Res Int 2017;2017(9042851, doi:10.1155/2017/9042851

47.   Aderem A, Underhill DM. Mechanisms of phagocytosis in macrophages. Annu Rev Immunol 1999;17(593-623, doi:10.1146/annurev.immunol.17.1.593

48.   Dupré-Crochet S, Erard M, Nüβe O. ROS production in phagocytes: why, when, and where? J Leukoc Biol 2013;94(4):657-70, doi:10.1189/jlb.1012544

49.   Speidl WS, Kastl SP, Huber K, et al. Complement in atherosclerosis: friend or foe? J Thromb Haemost 2011;9(3):428-40, doi:10.1111/j.1538-7836.2010.04172.x

50.   Széplaki G, Varga L, Füst G, et al. Role of complement in the pathomechanism of atherosclerotic vascular diseases. Mol Immunol 2009;46(14):2784-93, doi:10.1016/j.molimm.2009.04.028

51.   Wieczorek M, Abualrous ET, Sticht J, et al. Major Histocompatibility Complex (MHC) Class I and MHC Class II Proteins: Conformational Plasticity in Antigen Presentation. Front Immunol 2017;8(292, doi:10.3389/fimmu.2017.00292

52.   Podojil JR, Miller SD. Molecular mechanisms of T-cell receptor and costimulatory molecule ligation/blockade in autoimmune disease therapy. Immunol Rev 2009;229(1):337-55, doi:10.1111/j.1600-065X.2009.00773.x

53.   Garçon F, Patton DT, Emery JL, et al. CD28 provides T-cell costimulation and enhances PI3K activity at the immune synapse independently of its capacity to interact with the p85/p110 heterodimer. Blood 2008;111(3):1464-71, doi:10.1182/blood-2007-08-108050

54.   Ma SD, Mussbacher M, Galkina EV. Functional Role of B Cells in Atherosclerosis. Cells 2021;10(2), doi:10.3390/cells10020270

55.   Ray M, Autieri MV. Regulation of pro- and anti-atherogenic cytokines. Cytokine 2019;122(154175, doi:10.1016/j.cyto.2017.09.031

56.   Saigusa R, Winkels H, Ley K. T cell subsets and functions in atherosclerosis. Nat Rev Cardiol 2020;17(7):387-401, doi:10.1038/s41569-020-0352-5

57.   Schäfer S, Zernecke A. CD8 + T Cells in Atherosclerosis. Cells 2020;10(1), doi:10.3390/cells10010037

58.   Janeway CAJ, Travers P, Walport M. Immunobiology: The Immune System in Health and Disease. 5th edition. New York: Garland Science; 2001. B-cell activation by armed helper T cells. Available from: https://www.ncbi.nlm.nih.gov/books/NBK27142/. 2001.

59.   Jellusova J, Nitschke L. Regulation of B cell functions by the sialic acid-binding receptors siglec-G and CD22. Front Immunol 2011;2(96, doi:10.3389/fimmu.2011.00096

60.   Tedder TF, Poe JC, Haas KM. CD22: a multifunctional receptor that regulates B lymphocyte survival and signal transduction. Adv Immunol 2005;88(1-50, doi:10.1016/S0065-2776(05)88001-0

61.   Sage AP, Tsiantoulas D, Binder CJ, et al. The role of B cells in atherosclerosis. Nat Rev Cardiol 2019;16(3):180-196, doi:10.1038/s41569-018-0106-9

62.   Sage AP, Mallat Z. Multiple potential roles for B cells in atherosclerosis. Ann Med 2014;46(5):297-303, doi:10.3109/07853890.2014.900272

63.   Hu D, Yin C, Luo S, et al. Vascular Smooth Muscle Cells Contribute to Atherosclerosis Immunity. Front Immunol 2019;10(1101, doi:10.3389/fimmu.2019.01101

64.   Magnusson MK, Mosher DF. Fibronectin: structure, assembly, and cardiovascular implications. Arterioscler Thromb Vasc Biol 1998;18(9):1363-70, doi:10.1161/01.atv.18.9.1363

65.   Rekhter MD. Collagen synthesis in atherosclerosis: too much and not enough. Cardiovasc Res 1999;41(2):376-84, doi:10.1016/s0008-6363(98)00321-6

66.   Sorokin V, Vickneson K, Kofidis T, et al. Role of Vascular Smooth Muscle Cell Plasticity and Interactions in Vessel Wall Inflammation. Front Immunol 2020;11(599415, doi:10.3389/fimmu.2020.599415

67.   Allahverdian S, Chaabane C, Boukais K, et al. Smooth muscle cell fate and plasticity in atherosclerosis. Cardiovasc Res 2018;114(4):540-550, doi:10.1093/cvr/cvy022

68.   Beamish JA, He P, Kottke-Marchant K, et al. Molecular regulation of contractile smooth muscle cell phenotype: implications for vascular tissue engineering. Tissue Eng Part B Rev 2010;16(5):467-91, doi:10.1089/ten.TEB.2009.0630

69.   Swirski FK, Nahrendorf M. Do vascular smooth muscle cells differentiate to macrophages in atherosclerotic lesions? Circ Res 2014;115(7):605-6, doi:10.1161/CIRCRESAHA.114.304925

70.   Vengrenyuk Y, Nishi H, Long X, et al. Cholesterol loading reprograms the microRNA-143/145-myocardin axis to convert aortic smooth muscle cells to a dysfunctional macrophage-like phenotype. Arterioscler Thromb Vasc Biol 2015;35(3):535-46, doi:10.1161/ATVBAHA.114.304029

71.   Shankman LS, Gomez D, Cherepanova OA, et al. KLF4-dependent phenotypic modulation of smooth muscle cells has a key role in atherosclerotic plaque pathogenesis. Nat Med 2015;21(6):628-37, doi:10.1038/nm.3866

72.   Shankman LS, Gomez D, Cherepanova OA, et al. Corrigendum: KLF4-dependent phenotypic modulation of smooth muscle cells has a key role in atherosclerotic plaque pathogenesis. Nat Med 2016;22(2):217, doi:10.1038/nm0216-217a

73.   Allahverdian S, Chehroudi AC, McManus BM, et al. Contribution of intimal smooth muscle cells to cholesterol accumulation and macrophage-like cells in human atherosclerosis. Circulation 2014;129(15):1551-9, doi:10.1161/CIRCULATIONAHA.113.005015

74.   Wang Y, Dubland JA, Allahverdian S, et al. Smooth Muscle Cells Contribute the Majority of Foam Cells in ApoE (Apolipoprotein E)-Deficient Mouse Atherosclerosis. Arterioscler Thromb Vasc Biol 2019;39(5):876-887, doi:10.1161/ATVBAHA.119.312434

75.   Busse R, Fleming I. Vascular endothelium and blood flow. Handb Exp Pharmacol 2006;176 Pt 2):43-78, doi:10.1007/3-540-36028-x_2

76.   Schimmel L, Heemskerk N, van Buul JD. Leukocyte transendothelial migration: A local affair. Small GTPases 2017;8(1):1-15, doi:10.1080/21541248.2016.1197872

77.   Wang S, Li X, Parra M, et al. Control of endothelial cell proliferation and migration by VEGF signaling to histone deacetylase 7. Proc Natl Acad Sci U S A 2008;105(22):7738-43, doi:10.1073/pnas.0802857105

78.   Alberts B, Johnson A, Lewis J. Molecular Biology of the Cell. 4th edition. New York: Garland Science; 2002. Blood Vessels and Endothelial Cells. Available from: https://www.ncbi.nlm.nih.gov/books/NBK26848/.

79.   Alom-Ruiz SP, Anilkumar N, Shah AM. Reactive oxygen species and endothelial activation. Antioxid Redox Signal 2008;10(6):1089-100, doi:10.1089/ars.2007.2007

80.   Pober JS, Sessa WC. Evolving functions of endothelial cells in inflammation. Nat Rev Immunol 2007;7(10):803-15, doi:10.1038/nri2171

81.   Gimbrone MA, García-Cardeña G. Endothelial Cell Dysfunction and the Pathobiology of Atherosclerosis. Circ Res 2016;118(4):620-36, doi:10.1161/CIRCRESAHA.115.306301

82.   Vartanian KB, Kirkpatrick SJ, McCarty OJ, et al. Distinct extracellular matrix microenvironments of progenitor and carotid endothelial cells. J Biomed Mater Res A 2009;91(2):528-39, doi:10.1002/jbm.a.32225

83.   Singh S, Torzewski M. Fibroblasts and Their Pathological Functions in the Fibrosis of Aortic Valve Sclerosis and Atherosclerosis. Biomolecules 2019;9(9), doi:10.3390/biom9090472

84.   Kendall RT, Feghali-Bostwick CA. Fibroblasts in fibrosis: novel roles and mediators. Front Pharmacol 2014;5(123, doi:10.3389/fphar.2014.00123

85.   Tillie RJHA, van Kuijk K, Sluimer JC. Fibroblasts in atherosclerosis: heterogeneous and plastic participants. Curr Opin Lipidol 2020;31(5):273-278, doi:10.1097/MOL.0000000000000700

86.   Kuret T, Sodin-Semrl S. The Role of Fibroblasts in Atherosclerosis Progression. In: Bertoncelj, M. F. , Lakota, K. , editors. Fibroblasts - Advances in Inflammation, Autoimmunity and Cancer [Internet]. London: IntechOpen; 2021 [cited 2022 Dec 23]. Available from: https://www.intechopen.com/chapters/77138 doi: 10.5772/intechopen.98546.

87.   Todua F, Gachechiladze D. Structural Characteristics of Atherosclerotic Plaque. In: Noninvasive Radiologic Diagnosis of Extracranial Vascular Pathologies. Springer, Cham. 2018. https://doi.org/10.1007/978-3-319-91367-4_12.

88.   Seidman MA, Mitchell RN, Stone JR. Chapter 12 - Pathophysiology of Atherosclerosis, Editor(s): Monte S. Willis, Jonathon W. Homeister, James R. Stone, Cellular and Molecular Pathobiology of Cardiovascular Disease, Academic Press, 2014, Pages 221-237, ISBN 9780124052062, https://doi.org/10.1016/B978-0-12-405206-2.00012-0. .

89. Clarke M, Bennett M. The emerging role of vascular smooth muscle cell apoptosis in atherosclerosis and plaque stability. Am J Nephrol 2006;26(6):531-5, doi:10.1159/000097815

90. Sorokin L. The impact of the extracellular matrix on inflammation. Nat Rev Immunol 2010;10(10):712-23, doi:10.1038/nri2852

91. Sayers TJ. Targeting the extrinsic apoptosis signaling pathway for cancer therapy. Cancer Immunol Immunother 2011;60(8):1173-80, doi:10.1007/s00262-011-1008-4

92. Martinet W, Coornaert I, Puylaert P, et al. Macrophage Death as a Pharmacological Target in Atherosclerosis. Front Pharmacol 2019;10(306, doi:10.3389/fphar.2019.00306

93. Elmore S. Apoptosis: a review of programmed cell death. Toxicol Pathol 2007;35(4):495-516, doi:10.1080/01926230701320337

94. Bao Q, Shi Y. Apoptosome: a platform for the activation of initiator caspases. Cell Death Differ 2007;14(1):56-65, doi:10.1038/sj.cdd.4402028

95. Wang L, Li H, Tang Y, et al. Potential Mechanisms and Effects of Efferocytosis in Atherosclerosis. Front Endocrinol (Lausanne) 2020;11(585285, doi:10.3389/fendo.2020.585285

96. Yurdagul A, Doran AC, Cai B, et al. Mechanisms and Consequences of Defective Efferocytosis in Atherosclerosis. Front Cardiovasc Med 2017;4(86, doi:10.3389/fcvm.2017.00086

97. Ge Y, Huang M, Yao YM. Efferocytosis and Its Role in Inflammatory Disorders. Front Cell Dev Biol 2022;10(839248, doi:10.3389/fcell.2022.839248

98. Virmani R, Kolodgie FD, Burke AP, et al. Lessons from sudden coronary death: a comprehensive morphological classification scheme for atherosclerotic lesions. Arterioscler Thromb Vasc Biol 2000;20(5):1262-75, doi:10.1161/01.atv.20.5.1262

99. Yang A, Chen F, He C, et al. The Procoagulant Activity of Apoptotic Cells Is Mediated by Interaction with Factor XII. Front Immunol 2017;8(1188, doi:10.3389/fimmu.2017.01188

100. Vanden Berghe T, Kaiser WJ, Bertrand MJ, et al. Molecular crosstalk between apoptosis, necroptosis, and survival signaling. Mol Cell Oncol 2015;2(4):e975093, doi:10.4161/23723556.2014.975093

101. Karunakaran D, Geoffrion M, Wei L, et al. Targeting macrophage necroptosis for therapeutic and diagnostic interventions in atherosclerosis. Sci Adv 2016;2(7):e1600224, doi:10.1126/sciadv.1600224

102. Cho YS. The role of necroptosis in the treatment of diseases. BMB Rep 2018;51(5):219-224, doi:10.5483/bmbrep.2018.51.5.074

103. Strzyz P. Cell death: Pulling the apoptotic trigger for necrosis. Nat Rev Mol Cell Biol 2017;18(2):72, doi:10.1038/nrm.2017.1

104. Fuster JJ, Fernández P, González-Navarro H, et al. Control of cell proliferation in atherosclerosis: insights from animal models and human studies. Cardiovasc Res 2010;86(2):254-64, doi:10.1093/cvr/cvp363

105. Andrés V, Pello OM, Silvestre-Roig C. Macrophage proliferation and apoptosis in atherosclerosis. Curr Opin Lipidol 2012;23(5):429-38, doi:10.1097/MOL.0b013e328357a379

106. Lamharzi N, Renard CB, Kramer F, et al. Hyperlipidemia in concert with hyperglycemia stimulates the proliferation of macrophages in atherosclerotic lesions: potential role of glucose-oxidized LDL. Diabetes 2004;53(12):3217-25, doi:10.2337/diabetes.53.12.3217

107. Zhang C, Adamos C, Oh MJ, et al. oxLDL induces endothelial cell proliferation via Rho/ROCK/Akt/p27. Am J Physiol Cell Physiol 2017;313(3):C340-C351, doi:10.1152/ajpcell.00249.2016

108. Chisolm GM, Chai Y. Regulation of cell growth by oxidized LDL. Free Radic Biol Med 2000;28(12):1697-707, doi:10.1016/s0891-5849(00)00227-6

109. Braganza DM, Bennett MR. New insights into atherosclerotic plaque rupture. Postgrad Med J 2001;77(904):94-8, doi:10.1136/pmj.77.904.94

110. Andrés V, Castro C, Campistol JM. Potential role of proliferation signal inhibitors on atherosclerosis in renal transplant patients. Nephrol Dial Transplant 2006;21 Suppl 3(iii14-7, doi:10.1093/ndt/gfl296

111. Stefanadis C, Antoniou CK, Tsiachris D, et al. Coronary Atherosclerotic Vulnerable Plaque: Current Perspectives. J Am Heart Assoc 2017;6(3), doi:10.1161/JAHA.117.005543

112. Rey S, Semenza GL. Hypoxia-inducible factor-1-dependent mechanisms of vascularization and vascular remodelling. Cardiovasc Res 2010;86(2):236-42, doi:10.1093/cvr/cvq045

113. Zhou Y, Zhu X, Cui H, et al. The Role of the VEGF Family in Coronary Heart Disease. Front Cardiovasc Med 2021;8(738325, doi:10.3389/fcvm.2021.738325

114. Camaré C, Pucelle M, Nègre-Salvayre A, et al. Angiogenesis in the atherosclerotic plaque. Redox Biol 2017;12(18-34, doi:10.1016/j.redox.2017.01.007

115. Namba T, Koike H, Murakami K, et al. Angiogenesis induced by endothelial nitric oxide synthase gene through vascular endothelial growth factor expression in a rat hindlimb ischemia model. Circulation 2003;108(18):2250-7, doi:10.1161/01.CIR.0000093190.53478.78

116. Chistiakov DA, Orekhov AN, Bobryshev YV. Contribution of neovascularization and intraplaque haemorrhage to atherosclerotic plaque progression and instability. Acta Physiol (Oxf) 2015;213(3):539-53, doi:10.1111/apha.12438

117. Abela GS, Aziz K. Cholesterol crystals rupture biological membranes and human plaques during acute cardiovascular events--a novel insight into plaque rupture by scanning electron microscopy. Scanning 2006;28(1):1-10, doi:10.1002/sca.4950280101

118.   Frink R. Inflammatory Atherosclerosis: Characteristics of the Injurious Agent. Sacramento (CA): Heart Research Foundation; 2002. Chapter 2, The Smooth Muscle Cell. The Pivot in Atherosclerosis. Available from: https://www.ncbi.nlm.nih.gov/books/NBK2018/.

119.   Gomez D, Owens GK. Smooth muscle cell phenotypic switching in atherosclerosis. Cardiovasc Res 2012;95(2):156-64, doi:10.1093/cvr/cvs115

120.   Fishbein MC. The vulnerable and unstable atherosclerotic plaque. Cardiovasc Pathol 2010;19(1):6-11, doi:10.1016/j.carpath.2008.08.004

121.   Loftus I. Mechanisms of Plaque Rupture. In: Fitridge R, Thompson M, editors. Mechanisms of Vascular Disease: A Reference Book for Vascular Specialists [Internet]. Adelaide (AU): University of Adelaide Press; 2011. 4. Available from: https://www.ncbi.nlm.nih.gov/books/NBK534259/.

122.   Owens AP, Mackman N. Role of tissue factor in atherothrombosis. Curr Atheroscler Rep 2012;14(5):394-401, doi:10.1007/s11883-012-0269-5

123.   Bentzon JF, Otsuka F, Virmani R, et al. Mechanisms of plaque formation and rupture. Circ Res 2014;114(12):1852-66, doi:10.1161/CIRCRESAHA.114.302721

124.   Willich SN, Löwel H, Lewis M, et al. Weekly variation of acute myocardial infarction. Increased Monday risk in the working population. Circulation 1994;90(1):87-93, doi:10.1161/01.cir.90.1.87

125.   Kim HO, Kim JM, Woo JS, et al. Circadian Distribution of Acute Myocardial Infarction in Different Age Groups. Am J Cardiol 2018;121(11):1279-1284, doi:10.1016/j.amjcard.2018.02.006

126.   Doherty CJ, Kay SA. Circadian control of global gene expression patterns. Annu Rev Genet 2010;44(419-44, doi:10.1146/annurev-genet-102209-163432

127.   Pickel L, Sung HK. Feeding Rhythms and the Circadian Regulation of Metabolism. Front Nutr 2020;7(39, doi:10.3389/fnut.2020.00039

128.   Refinetti R. Circadian rhythmicity of body temperature and metabolism. Temperature (Austin) 2020;7(4):321-362, doi:10.1080/23328940.2020.1743605

129.   Kuhlman SJ, Craig LM, Duffy JF. Introduction to Chronobiology. Cold Spring Harb Perspect Biol 2018;10(9), doi:10.1101/cshperspect.a033613

130.   Vitaterna MH, Takahashi JS, Turek FW. Overview of circadian rhythms. Alcohol Res Health 2001;25(2):85-93

131.   Astiz M, Heyde I, Oster H. Mechanisms of Communication in the Mammalian Circadian Timing System. Int J Mol Sci 2019;20(2), doi:10.3390/ijms20020343

132.   Hastings MH, Maywood ES, Brancaccio M. Generation of circadian rhythms in the suprachiasmatic nucleus. Nat Rev Neurosci 2018;19(8):453-469, doi:10.1038/s41583-018-0026-z

133.   Varadarajan S, Tajiri M, Jain R, et al. Connectome of the Suprachiasmatic Nucleus: New Evidence of the Core-Shell Relationship. eNeuro 2018;5(5), doi:10.1523/ENEURO.0205-18.2018

134. Saper CB. The central circadian timing system. Curr Opin Neurobiol 2013;23(5):747-51, doi:10.1016/j.conb.2013.04.004

135. Scheiermann C, Kunisaki Y, Frenette PS. Circadian control of the immune system. Nat Rev Immunol 2013;13(3):190-8, doi:10.1038/nri3386

136. Sheng JA, Bales NJ, Myers SA, et al. The Hypothalamic-Pituitary-Adrenal Axis: Development, Programming Actions of Hormones, and Maternal-Fetal Interactions. Front Behav Neurosci 2020;14(601939, doi:10.3389/fnbeh.2020.601939

137. Reilly DF, Curtis AM, Cheng Y, et al. Peripheral circadian clock rhythmicity is retained in the absence of adrenergic signaling. Arterioscler Thromb Vasc Biol 2008;28(1):121-6, doi:10.1161/ATVBAHA.107.152538

138. Dickmeis T. Glucocorticoids and the circadian clock. J Endocrinol 2009;200(1):3-22, doi:10.1677/JOE-08-0415

139. Partch CL, Green CB, Takahashi JS. Molecular architecture of the mammalian circadian clock. Trends Cell Biol 2014;24(2):90-9, doi:10.1016/j.tcb.2013.07.002

140. Cox KH, Takahashi JS. Circadian clock genes and the transcriptional architecture of the clock mechanism. J Mol Endocrinol 2019;63(4):R93-R102, doi:10.1530/JME-19-0153

141. Zhang Y, Fang B, Emmett MJ, et al. GENE REGULATION. Discrete functions of nuclear receptor Rev-erbα couple metabolism to the clock. Science 2015;348(6242):1488-92, doi:10.1126/science.aab3021

142. Chaix A, Zarrinpar A, Panda S. The circadian coordination of cell biology. J Cell Biol 2016;215(1):15-25, doi:10.1083/jcb.201603076

143. Lamia KA, Papp SJ, Yu RT, et al. Cryptochromes mediate rhythmic repression of the glucocorticoid receptor. Nature 2011;480(7378):552-6, doi:10.1038/nature10700

144. Yang X, Wood PA, Ansell CM, et al. The circadian clock gene Per1 suppresses cancer cell proliferation and tumor growth at specific times of day. Chronobiol Int 2009;26(7):1323-39, doi:10.3109/07420520903431301

145. Cal-Kayitmazbatir S, Kulkoyluoglu-Cotul E, Growe J, et al. CRY1-CBS binding regulates circadian clock function and metabolism. FEBS J 2021;288(2):614-639, doi:10.1111/febs.15360

146. Trott AJ, Menet JS. Regulation of circadian clock transcriptional output by CLOCK:BMAL1. PLoS Genet 2018;14(1):e1007156, doi:10.1371/journal.pgen.1007156

147. Zhang R, Lahens NF, Ballance HI, et al. A circadian gene expression atlas in mammals: implications for biology and medicine. Proc Natl Acad Sci U S A 2014;111(45):16219-24, doi:10.1073/pnas.1408886111

148. Mure LS, Le HD, Benegiamo G, et al. Diurnal transcriptome atlas of a primate across major neural and peripheral tissues. Science 2018;359(6381), doi:10.1126/science.aao0318

149. McGlincy NJ, Valomon A, Chesham JE, et al. Regulation of alternative splicing by the circadian clock and food related cues. Genome Biol 2012;13(6):R54, doi:10.1186/gb-2012-13-6-r54

150. Kalliolias GD, Ivashkiv LB. TNF biology, pathogenic mechanisms and emerging therapeutic strategies. Nat Rev Rheumatol 2016;12(1):49-62, doi:10.1038/nrrheum.2015.169

151. Rabinovich-Nikitin I, Lieberman B, Martino TA, et al. Circadian-Regulated Cell Death in Cardiovascular Diseases. Circulation 2019;139(7):965-980, doi:10.1161/CIRCULATIONAHA.118.036550

152. Biaggioni I. Circadian clocks, autonomic rhythms, and blood pressure dipping. Hypertension 2008;52(5):797-8, doi:10.1161/HYPERTENSIONAHA.108.117234

153. Degaute JP, van de Borne P, Linkowski P, et al. Quantitative analysis of the 24-hour blood pressure and heart rate patterns in young men. Hypertension 1991;18(2):199-210, doi:10.1161/01.hyp.18.2.199

154. Scheiermann C, Kunisaki Y, Lucas D, et al. Adrenergic nerves govern circadian leukocyte recruitment to tissues. Immunity 2012;37(2):290-301, doi:10.1016/j.immuni.2012.05.021

155. Pick R, He W, Chen CS, et al. Time-of-Day-Dependent Trafficking and Function of Leukocyte Subsets. Trends Immunol 2019;40(6):524-537, doi:10.1016/j.it.2019.03.010

156. Gschwandtner M, Derler R, Midwood KS. More Than Just Attractive: How CCL2 Influences Myeloid Cell Behavior Beyond Chemotaxis. Front Immunol 2019;10(2759, doi:10.3389/fimmu.2019.02759

157. Shi C, Pamer EG. Monocyte recruitment during infection and inflammation. Nat Rev Immunol 2011;11(11):762-74, doi:10.1038/nri3070

158. Winter C, Silvestre-Roig C, Ortega-Gomez A, et al. Chrono-pharmacological Targeting of the CCL2-CCR2 Axis Ameliorates Atherosclerosis. Cell Metab 2018;28(1):175-182.e5, doi:10.1016/j.cmet.2018.05.002

159. He W, Holtkamp S, Hergenhan SM, et al. Circadian Expression of Migratory Factors Establishes Lineage-Specific Signatures that Guide the Homing of Leukocyte Subsets to Tissues. Immunity 2018;49(6):1175-1190.e7, doi:10.1016/j.immuni.2018.10.007

160. Mitroulis I, Alexaki VI, Kourtzelis I, et al. Leukocyte integrins: role in leukocyte recruitment and as therapeutic targets in inflammatory disease. Pharmacol Ther 2015;147(123-135, doi:10.1016/j.pharmthera.2014.11.008

161. Herbin O, Regelmann AG, Ramkhelawon B, et al. Monocyte Adhesion and Plaque Recruitment During Atherosclerosis Development Is Regulated by the Adapter Protein Chat-H/SHEP1. Arterioscler Thromb Vasc Biol 2016;36(9):1791-801, doi:10.1161/ATVBAHA.116.308014

162. Khismatullin DB, Truskey GA. Leukocyte rolling on P-selectin: a three-dimensional numerical study of the effect of cytoplasmic viscosity. Biophys J 2012;102(8):1757-66, doi:10.1016/j.bpj.2012.03.018

163. McAlpine CS, Swirski FK. Circadian Influence on Metabolism and Inflammation in Atherosclerosis. Circ Res 2016;119(1):131-41, doi:10.1161/CIRCRESAHA.116.308034

164.   Niehaus GD, Ervin E, Patel A, et al. Circadian variation in cell-adhesion molecule expression by normal human leukocytes. Can J Physiol Pharmacol 2002;80(10):935-40, doi:10.1139/y02-121

165.   Yuan Y, Wu S, Li W, et al. A Tissue-Specific Rhythmic Recruitment Pattern of Leukocyte Subsets. Front Immunol 2020;11(102, doi:10.3389/fimmu.2020.00102

166.   Muller JE, Stone PH, Turi ZG, et al. Circadian variation in the frequency of onset of acute myocardial infarction. N Engl J Med 1985;313(21):1315-22, doi:10.1056/NEJM198511213132103

167.   Thosar SS, Butler MP, Shea SA. Role of the circadian system in cardiovascular disease. J Clin Invest 2018;128(6):2157-2167, doi:10.1172/JCI80590

168.   Reinberg AE. Concepts in chronopharmacology. Annu Rev Pharmacol Toxicol 1992;32(51-66, doi:10.1146/annurev.pa.32.040192.000411

169.   Dallmann R, Brown SA, Gachon F. Chronopharmacology: new insights and therapeutic implications. Annu Rev Pharmacol Toxicol 2014;54(339-61, doi:10.1146/annurev-pharmtox-011613-135923

170.   Gachon F, Firsov D. The role of circadian timing system on drug metabolism and detoxification. Expert Opin Drug Metab Toxicol 2011;7(2):147-58, doi:10.1517/17425255.2011.544251

171.   Musiek ES, Fitzgerald GA. Molecular clocks in pharmacology. Handb Exp Pharmacol 2013;217(217):243-60, doi:10.1007/978-3-642-25950-0_10

172.   Chen M, Zhou C, Zhang T, et al. Identification of rhythmic human CYPs and their circadian regulators using synchronized hepatoma cells. Xenobiotica 2020;50(9):1052-1063, doi:10.1080/00498254.2020.1737890

173.   Koopman MG, Koomen GC, Krediet RT, et al. Circadian rhythm of glomerular filtration rate in normal individuals. Clin Sci (Lond) 1989;77(1):105-11, doi:10.1042/cs0770105

174.   Eckerbom P, Hansell P, Cox E, et al. Circadian variation in renal blood flow and kidney function in healthy volunteers monitored with noninvasive magnetic resonance imaging. Am J Physiol Renal Physiol 2020;319(6):F966-F978, doi:10.1152/ajprenal.00311.2020

175.   Baraldo M. The influence of circadian rhythms on the kinetics of drugs in humans. Expert Opin Drug Metab Toxicol 2008;4(2):175-92, doi:10.1517/17425255.4.2.175

176.   Ahuja A, Varshney M, Rathore G. A Review on Chronopharmacology-Cycle of Circadian Rhythms. J Pharmacy and Drug Innovations 2021;2(5)(doi:http://doi.org/03.2020/1.1033

177.   Marino M, Jamal Z, Zito PM. Pharmacodynamics. [Updated 2022 Jan 11]. In: StatPearls [Internet]. Treasure Island (FL): StatPearls Publishing; 2022 Jan-. Available from: https://www.ncbi.nlm.nih.gov/books/NBK507791/.

178.   Scheiermann C, Gibbs J, Ince L, et al. Clocking in to immunity. Nat Rev Immunol 2018;18(7):423-437, doi:10.1038/s41577-018-0008-4

179.   He B, Nohara K, Park N, et al. The Small Molecule Nobiletin Targets the Molecular Oscillator to Enhance Circadian Rhythms and Protect against Metabolic Syndrome. Cell Metab 2016;23(4):610-21, doi:10.1016/j.cmet.2016.03.007

180.   Lemmer B, Scheidel B, Behne S. Chronopharmacokinetics and chronopharmacodynamics of cardiovascular active drugs. Propranolol, organic nitrates, nifedipine. Ann N Y Acad Sci 1991;618(166-81, doi:10.1111/j.1749-6632.1991.tb27245.x

181.   Ruben MD, Smith DF, FitzGerald GA, et al. Dosing time matters. Science 2019;365(6453):547-549, doi:10.1126/science.aax7621

182.   Junqueira LC, Bignolas G, Brentani RR. Picrosirius staining plus polarization microscopy, a specific method for collagen detection in tissue sections. Histochem J 1979;11(4):447-55, doi:10.1007/BF01002772

183.   Lattouf R, Younes R, Lutomski D, et al. Picrosirius red staining: a useful tool to appraise collagen networks in normal and pathological tissues. J Histochem Cytochem 2014;62(10):751-8, doi:10.1369/0022155414545787

184.   Wingett SW, Andrews S. FastQ Screen: A tool for multi-genome mapping and quality control. F1000Res 2018;7(1338, doi:10.12688/f1000research.15931.2

185.   Dobin A, Davis CA, Schlesinger F, et al. STAR: ultrafast universal RNA-seq aligner. Bioinformatics 2013;29(1):15-21, doi:10.1093/bioinformatics/bts635

186.   Ziemann M. Accuracy, speed and error tolerance of short DNA sequence aligners. bioRxiv 2016;053686, doi:10.1101/053686

187.   Bioinformatics E. Best RNA-Seq Aligner: A comparison of mapping tools. 2017. Available from: https://www.ecseq.com/support/ngs/best-RNA-seq-aligner-comparison-of-mapping-tools.

188.   Li H, Handsaker B, Wysoker A, et al. The Sequence Alignment/Map format and SAMtools. Bioinformatics 2009;25(16):2078-9, doi:10.1093/bioinformatics/btp352

189.   Liao Y, Smyth GK, Shi W. The R package Rsubread is easier, faster, cheaper and better for alignment and quantification of RNA sequencing reads. Nucleic Acids Res 2019;47(8):e47, doi:10.1093/nar/gkz114

190.   Wu G, Anafi RC, Hughes ME, et al. MetaCycle: an integrated R package to evaluate periodicity in large scale data. Bioinformatics 2016;32(21):3351-3353, doi:10.1093/bioinformatics/btw405

191.   Carlucci M, Kriščiūnas A, Li H, et al. DiscoRhythm: an easy-to-use web application and R package for discovering rhythmicity. Bioinformatics 2019, doi:10.1093/bioinformatics/btz834

192.   Yang R, Su Z. Analyzing circadian expression data by harmonic regression based on autoregressive spectral estimation. Bioinformatics 2010;26(12):i168-74, doi:10.1093/bioinformatics/btq189

193.   Hughes ME, Hogenesch JB, Kornacker K. JTK_CYCLE: an efficient nonparametric algorithm for detecting rhythmic components in genome-scale data sets. J Biol Rhythms 2010;25(5):372-80, doi:10.1177/0748730410379711

194. Glynn EF, Chen J, Mushegian AR. Detecting periodic patterns in unevenly spaced gene expression time series using Lomb-Scargle periodograms. Bioinformatics 2006;22(3):310-6, doi:10.1093/bioinformatics/bti789

195. Cornelissen G. Cosinor-based rhythmometry. Theor Biol Med Model 2014;11(16, doi:10.1186/1742-4682-11-16

196. Zhang R, Podtelezhnikov AA, Hogenesch JB, et al. Discovering Biology in Periodic Data through Phase Set Enrichment Analysis (PSEA). J Biol Rhythms 2016;31(3):244-57, doi:10.1177/0748730416631895

197. Kuleshov MV, Jones MR, Rouillard AD, et al. Enrichr: a comprehensive gene set enrichment analysis web server 2016 update. Nucleic Acids Res 2016;44(W1):W90-7, doi:10.1093/nar/gkw377

198. Chen EY, Tan CM, Kou Y, et al. Enrichr: interactive and collaborative HTML5 gene list enrichment analysis tool. BMC Bioinformatics 2013;14(128, doi:10.1186/1471-2105-14-128

199. Humphrey SJ, Karayel O, James DE, et al. High-throughput and high-sensitivity phosphoproteomics with the EasyPhos platform. Nat Protoc 2018;13(9):1897-1916, doi:10.1038/s41596-018-0014-9

200. Zhang X, Smits AH, van Tilburg GB, et al. Proteome-wide identification of ubiquitin interactions using UbIA-MS. Nat Protoc 2018;13(3):530-550, doi:10.1038/nprot.2017.147

201. Stoeckius M, Zheng S, Houck-Loomis B, et al. Cell Hashing with barcoded antibodies enables multiplexing and doublet detection for single cell genomics. Genome Biol 2018;19(1):224, doi:10.1186/s13059-018-1603-1

202. Lun AT, McCarthy DJ, Marioni JC. A step-by-step workflow for low-level analysis of single-cell RNA-seq data with Bioconductor. F1000Res 2016;5(2122, doi:10.12688/f1000research.9501.2

203. Landgraf D, Neumann AM, Oster H. Circadian clock-gastrointestinal peptide interaction in peripheral tissues and the brain. Best Pract Res Clin Endocrinol Metab 2017;31(6):561-571, doi:10.1016/j.beem.2017.10.007

204. de Assis LVM, Oster H. The circadian clock and metabolic homeostasis: entangled networks. Cell Mol Life Sci 2021;78(10):4563-4587, doi:10.1007/s00018-021-03800-2

205. Casula M, Colpani O, Xie S, et al. HDL in Atherosclerotic Cardiovascular Disease: In Search of a Role. Cells 2021;10(8), doi:10.3390/cells10081869

206. Shachter NS. Apolipoproteins C-I and C-III as important modulators of lipoprotein metabolism. Curr Opin Lipidol 2001;12(3):297-304, doi:10.1097/00041433-200106000-00009

207. Chan L, Chang BH, Nakamuta M, et al. Apobec-1 and apolipoprotein B mRNA editing. Biochim Biophys Acta 1997;1345(1):11-26, doi:10.1016/s0005-2760(96)00156-7

208. Fitzgerald ML, Mujawar Z, Tamehiro N. ABC transporters, atherosclerosis and inflammation. Atherosclerosis 2010;211(2):361-70, doi:10.1016/j.atherosclerosis.2010.01.011

209. Weber LW, Boll M, Stampfl A. Maintaining cholesterol homeostasis: sterol regulatory element-binding proteins. World J Gastroenterol 2004;10(21):3081-7, doi:10.3748/wjg.v10.i21.3081

210. Eberlé D, Hegarty B, Bossard P, et al. SREBP transcription factors: master regulators of lipid homeostasis. Biochimie 2004;86(11):839-48, doi:10.1016/j.biochi.2004.09.018

211. Caster SZ, Castillo K, Sachs MS, et al. Circadian clock regulation of mRNA translation through eukaryotic elongation factor eEF-2. Proc Natl Acad Sci U S A 2016;113(34):9605-10, doi:10.1073/pnas.1525268113

212. Torres M, Becquet D, Franc JL, et al. Circadian processes in the RNA life cycle. Wiley Interdiscip Rev RNA 2018;9(3):e1467, doi:10.1002/wrna.1467

213. Parnell AA, De Nobrega AK, Lyons LC. Translating around the clock: Multi-level regulation of post-transcriptional processes by the circadian clock. Cell Signal 2021;80(109904, doi:10.1016/j.cellsig.2020.109904

214. Staller P, Peukert K, Kiermaier A, et al. Repression of p15INK4b expression by Myc through association with Miz-1. Nat Cell Biol 2001;3(4):392-9, doi:10.1038/35070076

215. Morgan DO. The Cell Cycle: Principles of Control. New Science Press: 2007.

216. Monte M, Benetti R, Buscemi G, et al. The cell cycle-regulated protein human GTSE-1 controls DNA damage-induced apoptosis by affecting p53 function. J Biol Chem 2003;278(32):30356-64, doi:10.1074/jbc.M302902200

217. Macůrek L, Lindqvist A, Lim D, et al. Polo-like kinase-1 is activated by aurora A to promote checkpoint recovery. Nature 2008;455(7209):119-23, doi:10.1038/nature07185

218. Sun M, Jia M, Ren H, et al. NuMA regulates mitotic spindle assembly, structural dynamics and function via phase separation. Nat Commun 2021;12(1):7157, doi:10.1038/s41467-021-27528-6

219. Gaglio T, Saredi A, Compton DA. NuMA is required for the organization of microtubules into aster-like mitotic arrays. J Cell Biol 1995;131(3):693-708, doi:10.1083/jcb.131.3.693

220. Alvord VM, Kantra EJ, Pendergast JS. Estrogens and the circadian system. Semin Cell Dev Biol 2022;126(56-65, doi:10.1016/j.semcdb.2021.04.010

221. Wu S, Huang J, Dong J, et al. hippo encodes a Ste-20 family protein kinase that restricts cell proliferation and promotes apoptosis in conjunction with salvador and warts. Cell 2003;114(4):445-56, doi:10.1016/s0092-8674(03)00549-x

222. Aubrey BJ, Kelly GL, Janic A, et al. How does p53 induce apoptosis and how does this relate to p53-mediated tumour suppression? Cell Death Differ 2018;25(1):104-113, doi:10.1038/cdd.2017.169

223. Rath PC, Aggarwal BB. TNF-induced signaling in apoptosis. J Clin Immunol 1999;19(6):350-64, doi:10.1023/a:1020546615229

224. Greijer AE, van der Wall E. The role of hypoxia inducible factor 1 (HIF-1) in hypoxia induced apoptosis. J Clin Pathol 2004;57(10):1009-14, doi:10.1136/jcp.2003.015032

225. Goodridge HS, Wolf AJ, Underhill DM. Beta-glucan recognition by the innate immune system. Immunol Rev 2009;230(1):38-50, doi:10.1111/j.1600-065X.2009.00793.x

226. Pedro ARV, Lima T, Fróis-Martins R, et al. Dectin-1-Mediated Production of Pro-Inflammatory Cytokines Induced by Yeast β-Glucans in Bovine Monocytes. Front Immunol 2021;12(689879, doi:10.3389/fimmu.2021.689879

227. Panopoulos AD, Watowich SS. Granulocyte colony-stimulating factor: molecular mechanisms of action during steady state and 'emergency' hematopoiesis. Cytokine 2008;42(3):277-88, doi:10.1016/j.cyto.2008.03.002

228. Xie CB, Jane-Wit D, Pober JS. Complement Membrane Attack Complex: New Roles, Mechanisms of Action, and Therapeutic Targets. Am J Pathol 2020;190(6):1138-1150, doi:10.1016/j.ajpath.2020.02.006

229. Nakao A, Imamura T, Souchelnytskyi S, et al. TGF-beta receptor-mediated signalling through Smad2, Smad3 and Smad4. EMBO J 1997;16(17):5353-62, doi:10.1093/emboj/16.17.5353

230. Toma I, McCaffrey TA. Transforming growth factor-β and atherosclerosis: interwoven atherogenic and atheroprotective aspects. Cell Tissue Res 2012;347(1):155-75, doi:10.1007/s00441-011-1189-3

231. Abdelaziz MH, Abdelwahab SF, Wan J, et al. Alternatively activated macrophages; a double-edged sword in allergic asthma. J Transl Med 2020;18(1):58, doi:10.1186/s12967-020-02251-w

232. Liu N, Luo J, Kuang D, et al. Lactate inhibits ATP6V0d2 expression in tumor-associated macrophages to promote HIF-2α-mediated tumor progression. J Clin Invest 2019;129(2):631-646, doi:10.1172/JCI123027

233. Huynh KK, Eskelinen EL, Scott CC, et al. LAMP proteins are required for fusion of lysosomes with phagosomes. EMBO J 2007;26(2):313-24, doi:10.1038/sj.emboj.7601511

234. Dheilly E, Battistello E, Katanayeva N, et al. Cathepsin S Regulates Antigen Processing and T Cell Activity in Non-Hodgkin Lymphoma. Cancer Cell 2020;37(5):674-689.e12, doi:10.1016/j.ccell.2020.03.016

235. York IA, Chang SC, Saric T, et al. The ER aminopeptidase ERAP1 enhances or limits antigen presentation by trimming epitopes to 8-9 residues. Nat Immunol 2002;3(12):1177-84, doi:10.1038/ni860

236. Yanai H, Chiba S, Hangai S, et al. Revisiting the role of IRF3 in inflammation and immunity by conditional and specifically targeted gene ablation in mice. Proc Natl Acad Sci U S A 2018;115(20):5253-5258, doi:10.1073/pnas.1803936115

237.   Jin Z, Xu L, Zhang L, et al. Interleukin enhancer binding factor 2 is a prognostic biomarker for breast cancer that also predicts neoadjuvant chemotherapy responses. Am J Transl Res 2018;10(6):1677-1689

238.   Salinas RE, Ogohara C, Thomas MI, et al. A cellular genome-wide association study reveals human variation in microtubule stability and a role in inflammatory cell death. Mol Biol Cell 2014;25(1):76-86, doi:10.1091/mbc.E13-06-0294

239.   Moritz M, Braunfeld MB, Guénebaut V, et al. Structure of the gamma-tubulin ring complex: a template for microtubule nucleation. Nat Cell Biol 2000;2(6):365-70, doi:10.1038/35014058

240.   Maiato H, DeLuca J, Salmon ED, et al. The dynamic kinetochore-microtubule interface. J Cell Sci 2004;117(Pt 23):5461-77, doi:10.1242/jcs.01536

241.   Chu X, Chen X, Wan Q, et al. Nuclear Mitotic Apparatus (NuMA) Interacts with and Regulates Astrin at the Mitotic Spindle. J Biol Chem 2016;291(38):20055-67, doi:10.1074/jbc.M116.724831

242.   Bai C, Sen P, Hofmann K, et al. SKP1 connects cell cycle regulators to the ubiquitin proteolysis machinery through a novel motif, the F-box. Cell 1996;86(2):263-74, doi:10.1016/s0092-8674(00)80098-7

243.   Möröy T, Geisen C. Cyclin E. Int J Biochem Cell Biol 2004;36(8):1424-39, doi:10.1016/j.biocel.2003.12.005

244.   Wakana Y, Takai S, Nakajima K, et al. Bap31 is an itinerant protein that moves between the peripheral endoplasmic reticulum (ER) and a juxtanuclear compartment related to ER-associated Degradation. Mol Biol Cell 2008;19(5):1825-36, doi:10.1091/mbc.e07-08-0781

245.   Sano R, Reed JC. ER stress-induced cell death mechanisms. Biochim Biophys Acta 2013;1833(12):3460-3470, doi:10.1016/j.bbamcr.2013.06.028

246.   Guo X, Sesaki H, Qi X. Drp1 stabilizes p53 on the mitochondria to trigger necrosis under oxidative stress conditions in vitro and in vivo. Biochem J 2014;461(1):137-46, doi:10.1042/BJ20131438

247.   Nosrati N, Kapoor NR, Kumar V. DNA damage stress induces the expression of ribosomal protein S27a gene in a p53-dependent manner. Gene 2015;559(1):44-51, doi:10.1016/j.gene.2015.01.014

248.   Oberhammer FA, Hochegger K, Fröschl G, et al. Chromatin condensation during apoptosis is accompanied by degradation of lamin A+B, without enhanced activation of cdc2 kinase. J Cell Biol 1994;126(4):827-37, doi:10.1083/jcb.126.4.827

249.   Sahara S, Aoto M, Eguchi Y, et al. Acinus is a caspase-3-activated protein required for apoptotic chromatin condensation. Nature 1999;401(6749):168-73, doi:10.1038/43678

250.   Moriwaki K, Bertin J, Gough PJ, et al. Differential roles of RIPK1 and RIPK3 in TNF-induced necroptosis and chemotherapeutic agent-induced cell death. Cell Death Dis 2015;6(e1636, doi:10.1038/cddis.2015.16

251. Upton JW, Chan FK. Staying alive: cell death in antiviral immunity. Mol Cell 2014;54(2):273-80, doi:10.1016/j.molcel.2014.01.027

252. Chistiakov DA, Sobenin IA, Orekhov AN. Vascular extracellular matrix in atherosclerosis. Cardiol Rev 2013;21(6):270-88, doi:10.1097/CRD.0b013e31828c5ced

253. MacRae LF, Yancey PG, Davies SS, et al. The Role of Lipids and Lipoproteins in Atherosclerosis. [Updated 2019 Jan 3]. In: Feingold KR, Anawalt B, Boyce A, et al., editors. Endotext [Internet]. South Dartmouth (MA): MDText.com, Inc.; 2000-. Available from: https://www.ncbi.nlm.nih.gov/books/NBK343489/.

254. Febbraio M, Silverstein RL. CD36: implications in cardiovascular disease. Int J Biochem Cell Biol 2007;39(11):2012-30, doi:10.1016/j.biocel.2007.03.012

255. Shapiro MD, Fazio S. Apolipoprotein B-containing lipoproteins and atherosclerotic cardiovascular disease. F1000Res 2017;6(134, doi:10.12688/f1000research.9845.1

256. Melton EM, Li H, Benson J, et al. Myeloid. J Biol Chem 2019;294(43):15836-15849, doi:10.1074/jbc.RA119.010564

257. Igarashi M, Osuga J, Uozaki H, et al. The critical role of neutral cholesterol ester hydrolase 1 in cholesterol removal from human macrophages. Circ Res 2010;107(11):1387-95, doi:10.1161/CIRCRESAHA.110.226613

258. van der Leij FR, Cox KB, Jackson VN, et al. Structural and functional genomics of the CPT1B gene for muscle-type carnitine palmitoyltransferase I in mammals. J Biol Chem 2002;277(30):26994-7005, doi:10.1074/jbc.M203189200

259. McGarry JD, Brown NF. The mitochondrial carnitine palmitoyltransferase system. From concept to molecular analysis. Eur J Biochem 1997;244(1):1-14, doi:10.1111/j.1432-1033.1997.00001.x

260. Maier A, Wu H, Cordasic N, et al. Hypoxia-inducible protein 2 Hig2/Hilpda mediates neutral lipid accumulation in macrophages and contributes to atherosclerosis in apolipoprotein E-deficient mice. FASEB J 2017;31(11):4971-4984, doi:10.1096/fj.201700235R

261. Ning H, Liu D, Yu X, et al. Oxidized low-density lipoprotein-induced p62/SQSTM1 accumulation in THP-1-derived macrophages promotes IL-18 secretion and cell death. Exp Ther Med 2017;14(6):5417-5423, doi:10.3892/etm.2017.5221

262. Lin X, Cui M, Xu D, et al. Liver-specific deletion of Eva1a/Tmem166 aggravates acute liver injury by impairing autophagy. Cell Death Dis 2018;9(7):768, doi:10.1038/s41419-018-0800-x

263. Mukaida N, Wang YY, Li YY. Roles of Pim-3, a novel survival kinase, in tumorigenesis. Cancer Sci 2011;102(8):1437-42, doi:10.1111/j.1349-7006.2011.01966.x

264. Schönenberger F, Deutzmann A, Ferrando-May E, et al. Discrimination of cell cycle phases in PCNA-immunolabeled cells. BMC Bioinformatics 2015;16(180, doi:10.1186/s12859-015-0618-9

265.   Jain A, Kaczanowska S, Davila E. IL-1 Receptor-Associated Kinase Signaling and Its Role in Inflammation, Cancer Progression, and Therapy Resistance. Front Immunol 2014;5(553, doi:10.3389/fimmu.2014.00553

266.   Chinnadurai G, Vijayalingam S, Rashmi R. BIK, the founding member of the BH3-only family proteins: mechanisms of cell death and role in cancer and pathogenic processes. Oncogene 2008;27 Suppl 1(Suppl 1):S20-9, doi:10.1038/onc.2009.40

267.   Forghanifard MM, Naeimi Khorasanizadeh P, Abbaszadegan MR, et al. Role of DIDO1 in Progression of Esophageal Squamous Cell Carcinoma. J Gastrointest Cancer 2020;51(1):83-87, doi:10.1007/s12029-019-00212-1

268.   Roth W, Stenner-Liewen F, Pawlowski K, et al. Identification and characterization of DEDD2, a death effector domain-containing protein. J Biol Chem 2002;277(9):7501-8, doi:10.1074/jbc.M110749200

269.   Yasui K, Okamoto H, Arii S, et al. Association of over-expressed TFDP1 with progression of hepatocellular carcinomas. J Hum Genet 2003;48(12):609-613, doi:10.1007/s10038-003-0086-3

270.   de Boer HR, Guerrero Llobet S, van Vugt MA. Controlling the response to DNA damage by the APC/C-Cdh1. Cell Mol Life Sci 2016;73(5):949-60, doi:10.1007/s00018-015-2096-7

271.   Shtivelman E, Sussman J, Stokoe D. A role for PI 3-kinase and PKB activity in the G2/M phase of the cell cycle. Curr Biol 2002;12(11):919-24, doi:10.1016/s0960-9822(02)00843-6

272.   Vázquez-Novelle MD, Mailand N, Ovejero S, et al. Human Cdc14A phosphatase modulates the G2/M transition through Cdc25A and Cdc25B. J Biol Chem 2010;285(52):40544-53, doi:10.1074/jbc.M110.133009

273.   Han Y, Xia G, Tsang BK. Regulation of cyclin D2 expression and degradation by follicle-stimulating hormone during rat granulosa cell proliferation in vitro. Biol Reprod 2013;88(3):57, doi:10.1095/biolreprod.112.105106

274.   Gu Y, Rosenblatt J, Morgan DO. Cell cycle regulation of CDK2 activity by phosphorylation of Thr160 and Tyr15. EMBO J 1992;11(11):3995-4005, doi:10.1002/j.1460-2075.1992.tb05493.x

275.   Ghiselli G. SMC3 knockdown triggers genomic instability and p53-dependent apoptosis in human and zebrafish cells. Mol Cancer 2006;5(52, doi:10.1186/1476-4598-5-52

276.   Chin AI, Shu J, Shan Shi C, et al. TANK potentiates tumor necrosis factor receptor-associated factor-mediated c-Jun N-terminal kinase/stress-activated protein kinase activation through the germinal center kinase pathway. Mol Cell Biol 1999;19(10):6665-72, doi:10.1128/MCB.19.10.6665

277.   Portillo JA, Feliciano LM, Okenka G, et al. CD40 and tumour necrosis factor-α co-operate to up-regulate inducuble nitric oxide synthase expression in macrophages. Immunology 2012;135(2):140-50, doi:10.1111/j.1365-2567.2011.03519.x

278.   Aggarwal BB, Eessalu TE, Hass PE. Characterization of receptors for human tumour necrosis factor and their regulation by gamma-interferon. Nature 1985;318(6047):665-7, doi:10.1038/318665a0

279.   Majoros A, Platanitis E, Kernbauer-Hölzl E, et al. Canonical and Non-Canonical Aspects of JAK-STAT Signaling: Lessons from Interferons for Cytokine Responses. Front Immunol 2017;8(29, doi:10.3389/fimmu.2017.00029

280.   Deguine J, Barton GM. MyD88: a central player in innate immune signaling. F1000Prime Rep 2014;6(97, doi:10.12703/P6-97

281.   Schmid JA, Birbach A. IkappaB kinase beta (IKKbeta/IKK2/IKBKB)--a key molecule in signaling to the transcription factor NF-kappaB. Cytokine Growth Factor Rev 2008;19(2):157-65, doi:10.1016/j.cytogfr.2008.01.006

282.   Weber ANR, Bittner Z, Liu X, et al. Bruton's Tyrosine Kinase: An Emerging Key Player in Innate Immunity. Front Immunol 2017;8(1454, doi:10.3389/fimmu.2017.01454

283.   Zang Y, Chaudhari K, Bashaw GJ. New insights into the molecular mechanisms of axon guidance receptor regulation and signaling. Curr Top Dev Biol 2021;142(147-196, doi:10.1016/bs.ctdb.2020.11.008

284.   Longart M, Liu Y, Karavanova I, et al. Neuregulin-2 is developmentally regulated and targeted to dendrites of central neurons. J Comp Neurol 2004;472(2):156-72, doi:10.1002/cne.20016

285.   Yan L, Gong YZ, Shao MN, et al. Distinct diagnostic and prognostic values of γ-aminobutyric acid type A receptor family genes in patients with colon adenocarcinoma. Oncol Lett 2020;20(1):275-291, doi:10.3892/ol.2020.11573

286.   Ruben MD, Wu G, Smith DF, et al. A database of tissue-specific rhythmically expressed human genes has potential applications in circadian medicine. Sci Transl Med 2018;10(458), doi:10.1126/scitranslmed.aat8806

287.   Khelifi AF, D'Alcontres MS, Salomoni P. Daxx is required for stress-induced cell death and JNK activation. Cell Death Differ 2005;12(7):724-33, doi:10.1038/sj.cdd.4401559

288.   Baksh S, Tommasi S, Fenton S, et al. The tumor suppressor RASSF1A and MAP-1 link death receptor signaling to Bax conformational change and cell death. Mol Cell 2005;18(6):637-50, doi:10.1016/j.molcel.2005.05.010

289.   Atzei P, Gargan S, Curran N, et al. Cactin targets the MHC class III protein IkappaB-like (IkappaBL) and inhibits NF-kappaB and interferon-regulatory factor signaling pathways. J Biol Chem 2010;285(47):36804-17, doi:10.1074/jbc.M110.139113

290.   Bulwin GC, Heinemann T, Bugge V, et al. TIRC7 inhibits T cell proliferation by modulation of CTLA-4 expression. J Immunol 2006;177(10):6833-41, doi:10.4049/jimmunol.177.10.6833

291.   Iwasaki A, Medzhitov R. Control of adaptive immunity by the innate immune system. Nat Immunol 2015;16(4):343-53, doi:10.1038/ni.3123

292.   Wu Q, Fu C, Li M, et al. CINP is a novel cofactor of KLF5 required for its role in the promotion of cell proliferation, survival and tumor growth. Int J Cancer 2019;144(3):582-594, doi:10.1002/ijc.31908

293.   Hsu J, Arand J, Chaikovsky A, et al. E2F4 regulates transcriptional activation in mouse embryonic stem cells independently of the RB family. Nat Commun 2019;10(1):2939, doi:10.1038/s41467-019-10901-x

294.   Rodier G, Kirsh O, Baraibar M, et al. The transcription factor E4F1 coordinates CHK1-dependent checkpoint and mitochondrial functions. Cell Rep 2015;11(2):220-33, doi:10.1016/j.celrep.2015.03.024

295.   Guo N, Chen Y, Zhang Y, et al. Potential Role of APEX1 During Ferroptosis. Front Oncol 2022;12(798304, doi:10.3389/fonc.2022.798304

296.   Ahn SG, Thiele DJ. Redox regulation of mammalian heat shock factor 1 is essential for Hsp gene activation and protection from stress. Genes Dev 2003;17(4):516-28, doi:10.1101/gad.1044503

297.   Finan C, Gaulton A, Kruger FA, et al. The druggable genome and support for target identification and validation in drug development. Sci Transl Med 2017;9(383), doi:10.1126/scitranslmed.aag1166

298.   Eliopoulos AG, Wang CC, Dumitru CD, et al. Tpl2 transduces CD40 and TNF signals that activate ERK and regulates IgE induction by CD40. EMBO J 2003;22(15):3855-64, doi:10.1093/emboj/cdg386

299.   Brecker M, Khakhina S, Schubert TJ, et al. The Probable, Possible, and Novel Functions of ERp29. Front Physiol 2020;11(574339, doi:10.3389/fphys.2020.574339

300.   Olivari S, Molinari M. Glycoprotein folding and the role of EDEM1, EDEM2 and EDEM3 in degradation of folding-defective glycoproteins. FEBS Lett 2007;581(19):3658-64, doi:10.1016/j.febslet.2007.04.070

301.   Yu Y, Liu DY, Chen XS, et al. MANF: A Novel Endoplasmic Reticulum Stress Response Protein-The Role in Neurological and Metabolic Disorders. Oxid Med Cell Longev 2021;2021(6467679, doi:10.1155/2021/6467679

302.   Garg B, Pathria G, Wagner C, et al. Signal Sequence Receptor 2 is required for survival of human melanoma cells as part of an unfolded protein response to endoplasmic reticulum stress. Mutagenesis 2016;31(5):573-82, doi:10.1093/mutage/gew023

303.   Iannotti MJ, Figard L, Sokac AM, et al. A Golgi-localized mannosidase (MAN1B1) plays a non-enzymatic gatekeeper role in protein biosynthetic quality control. J Biol Chem 2014;289(17):11844-11858, doi:10.1074/jbc.M114.552091

304.   Maity S, Das F, Kasinath BS, et al. TGFβ acts through PDGFRβ to activate mTORC1 via the Akt/PRAS40 axis and causes glomerular mesangial cell hypertrophy and matrix protein expression. J Biol Chem 2020;295(42):14262-14278, doi:10.1074/jbc.RA120.014994

305. Zhang T, Wang Y, Yu H, et al. PGK1 represses autophagy-mediated cell death to promote the proliferation of liver cancer cells by phosphorylating PRAS40. Cell Death Dis 2022;13(1):68, doi:10.1038/s41419-022-04499-0

306. Organization WH. 2021. Available from: https://www.who.int/news-room/fact-sheets/detail/cardiovascular-diseases-(cvds).

307. Hong YM. Atherosclerotic cardiovascular disease beginning in childhood. Korean Circ J 2010;40(1):1-9, doi:10.4070/kcj.2010.40.1.1

308. Birger M, Kaldjian AS, Roth GA, et al. Spending on Cardiovascular Disease and Cardiovascular Risk Factors in the United States: 1996 to 2016. Circulation 2021;144(4):271-282, doi:10.1161/CIRCULATIONAHA.120.053216

309. Allam AH, Thompson RC, Wann LS, et al. Atherosclerosis in ancient Egyptian mummies: the Horus study. JACC Cardiovasc Imaging 2011;4(4):315-27, doi:10.1016/j.jcmg.2011.02.002

310. Gluba-Brzózka A, Franczyk B, Rysz-Górzyńska M, et al. Emerging Anti-Atherosclerotic Therapies. Int J Mol Sci 2021;22(22), doi:10.3390/ijms222212109

311. Jamkhande PG, Chandak PG, Dhawale SC, et al. Therapeutic approaches to drug targets in atherosclerosis. Saudi Pharm J 2014;22(3):179-90, doi:10.1016/j.jsps.2013.04.005

312. Pedro-Botet J, Climent E, Benaiges D. Atherosclerosis and inflammation. New therapeutic approaches. Med Clin (Barc) 2020;155(6):256-262, doi:10.1016/j.medcli.2020.04.024

313. Lévi FA, Zidani R, Vannetzel JM, et al. Chronomodulated versus fixed-infusion-rate delivery of ambulatory chemotherapy with oxaliplatin, fluorouracil, and folinic acid (leucovorin) in patients with colorectal cancer metastases: a randomized multi-institutional trial. J Natl Cancer Inst 1994;86(21):1608-17, doi:10.1093/jnci/86.21.1608

314. Izquierdo-Palomares JM, Fernandez-Tabera JM, Plana MN, et al. Chronotherapy versus conventional statins therapy for the treatment of hyperlipidaemia. Cochrane Database Syst Rev 2016;11(CD009462, doi:10.1002/14651858.CD009462.pub2

315. Johnstone MT, Mittleman M, Tofler G, et al. The pathophysiology of the onset of morning cardiovascular events. Am J Hypertens 1996;9(4 Pt 3):22S-28S, doi:10.1016/0895-7061(95)00403-3

316. Méndez-Ferrer S, Chow A, Merad M, et al. Circadian rhythms influence hematopoietic stem cells. Curr Opin Hematol 2009;16(4):235-42, doi:10.1097/MOH.0b013e32832bd0f5

317. Chakrabarti S, Michor F. Circadian clock effects on cellular proliferation: Insights from theory and experiments. Curr Opin Cell Biol 2020;67(17-26, doi:10.1016/j.ceb.2020.07.003

318. Takaguri A, Sasano J, Akihiro O, et al. The role of circadian clock gene BMAL1 in vascular proliferation. Eur J Pharmacol 2020;872(172924, doi:10.1016/j.ejphar.2020.172924

319. Rekhter MD, Gordon D. Active proliferation of different cell types, including lymphocytes, in human atherosclerotic plaques. Am J Pathol 1995;147(3):668-77

320. Rosenfeld ME. Macrophage proliferation in atherosclerosis: an historical perspective. Arterioscler Thromb Vasc Biol 2014;34(10):e21-2, doi:10.1161/ATVBAHA.114.303379

321. Gerlach BD, Ampomah PB, Yurdagul A, et al. Efferocytosis induces macrophage proliferation to help resolve tissue injury. Cell Metab 2021;33(12):2445-2463.e8, doi:10.1016/j.cmet.2021.10.015

322. Dzau VJ, Braun-Dullaeus RC, Sedding DG. Vascular proliferation and atherosclerosis: new perspectives and therapeutic strategies. Nat Med 2002;8(11):1249-56, doi:10.1038/nm1102-1249

323. Härdtner C, Kornemann J, Krebs K, et al. Inhibition of macrophage proliferation dominates plaque regression in response to cholesterol lowering. Basic Res Cardiol 2020;115(6):78, doi:10.1007/s00395-020-00838-4

324. Bennett MR, Sinha S, Owens GK. Vascular Smooth Muscle Cells in Atherosclerosis. Circ Res 2016;118(4):692-702, doi:10.1161/CIRCRESAHA.115.306361

325. Mallat Z, Tedgui A. Apoptosis in the vasculature: mechanisms and functional importance. Br J Pharmacol 2000;130(5):947-62, doi:10.1038/sj.bjp.0703407

326. Guicciardi ME, Gores GJ. Life and death by death receptors. FASEB J 2009;23(6):1625-37, doi:10.1096/fj.08-111005

327. Pan L, Hong Z, Yu L, et al. Shear stress induces human aortic endothelial cell apoptosis via interleukin-1 receptor-associated kinase 2-induced endoplasmic reticulum stress. Mol Med Rep 2017;16(5):7205-7212, doi:10.3892/mmr.2017.7524

328. Yang S, Wu M, Li X, et al. Role of Endoplasmic Reticulum Stress in Atherosclerosis and Its Potential as a Therapeutic Target. Oxid Med Cell Longev 2020;2020(9270107, doi:10.1155/2020/9270107

329. Bombeli T, Karsan A, Tait JF, et al. Apoptotic vascular endothelial cells become procoagulant. Blood 1997;89(7):2429-42

330. Proudfoot D, Skepper JN, Hegyi L, et al. Apoptosis regulates human vascular calcification in vitro: evidence for initiation of vascular calcification by apoptotic bodies. Circ Res 2000;87(11):1055-62, doi:10.1161/01.res.87.11.1055

331. Tabas I. Apoptosis and plaque destabilization in atherosclerosis: the role of macrophage apoptosis induced by cholesterol. Cell Death Differ 2004;11 Suppl 1(S12-6, doi:10.1038/sj.cdd.4401444

332. Wang Q, Ji J, Hao S, et al. Iron Together with Lipid Downregulates Protein Levels of Ceruloplasmin in Macrophages Associated with Rapid Foam Cell Formation. J Atheroscler Thromb 2016;23(10):1201-1211, doi:10.5551/jat.32292

333. Kojima Y, Weissman IL, Leeper NJ. The Role of Efferocytosis in Atherosclerosis. Circulation 2017;135(5):476-489, doi:10.1161/CIRCULATIONAHA.116.025684

334. Sohrabi Y, Reinecke H, Soehnlein O. Trilateral interaction between innervation, leukocyte, and adventitia: a new driver of atherosclerotic plaque formation. Signal Transduct Target Ther 2022;7(1):249, doi:10.1038/s41392-022-01121-9

335. Hu S, Zhu L. Semaphorins and Their Receptors: From Axonal Guidance to Atherosclerosis. Front Physiol 2018;9(1236, doi:10.3389/fphys.2018.01236

336. Mohanta SK, Peng L, Li Y, et al. Neuroimmune cardiovascular interfaces control atherosclerosis. Nature 2022;605(7908):152-159, doi:10.1038/s41586-022-04673-6

337. Vieira E, Ruano E, Figueroa AL, et al. Altered clock gene expression in obese visceral adipose tissue is associated with metabolic syndrome. PLoS One 2014;9(11):e111678, doi:10.1371/journal.pone.0111678

338. Hatori M, Vollmers C, Zarrinpar A, et al. Time-restricted feeding without reducing caloric intake prevents metabolic diseases in mice fed a high-fat diet. Cell Metab 2012;15(6):848-60, doi:10.1016/j.cmet.2012.04.019

339. Cunningham PS, Ahern SA, Smith LC, et al. Targeting of the circadian clock via CK1δ/ε to improve glucose homeostasis in obesity. Sci Rep 2016;6(29983, doi:10.1038/srep29983

340. Sundaram S, Johnson LK, Yan L. High-Fat Diet Alters Circadian Rhythms in Mammary Glands of Pubertal Mice. Front Endocrinol (Lausanne) 2020;11(349, doi:10.3389/fendo.2020.00349

341. Kohsaka A, Laposky AD, Ramsey KM, et al. High-fat diet disrupts behavioral and molecular circadian rhythms in mice. Cell Metab 2007;6(5):414-21, doi:10.1016/j.cmet.2007.09.006

342. Prasai MJ, Mughal RS, Wheatcroft SB, et al. Diurnal variation in vascular and metabolic function in diet-induced obesity: divergence of insulin resistance and loss of clock rhythm. Diabetes 2013;62(6):1981-9, doi:10.2337/db11-1740

343. Duan Y, Zeng L, Zheng C, et al. Inflammatory Links Between High Fat Diets and Diseases. Front Immunol 2018;9(2649, doi:10.3389/fimmu.2018.02649

344. Kiran S, Rakib A, Kodidela S, et al. High-Fat Diet-Induced Dysregulation of Immune Cells Correlates with Macrophage Phenotypes and Chronic Inflammation in Adipose Tissue. Cells 2022;11(8), doi:10.3390/cells11081327

345. Haque S, Morris JC. Transforming growth factor-β: A therapeutic target for cancer. Hum Vaccin Immunother 2017;13(8):1741-1750, doi:10.1080/21645515.2017.1327107

346. Zhao L, Zou Y, Liu F. Transforming Growth Factor-Beta1 in Diabetic Kidney Disease. Front Cell Dev Biol 2020;8(187, doi:10.3389/fcell.2020.00187

347. Shi Y, Chen X, Huang C, et al. RIPK3: A New Player in Renal Fibrosis. Front Cell Dev Biol 2020;8(502, doi:10.3389/fcell.2020.00502

348. Zhang Y, Yang X. The Roles of TGF-β Signaling in Cerebrovascular Diseases. Front Cell Dev Biol 2020;8(567682, doi:10.3389/fcell.2020.567682

349. Ismaeel A, Kim JS, Kirk JS, et al. Role of Transforming Growth Factor-β in Skeletal Muscle Fibrosis: A Review. Int J Mol Sci 2019;20(10), doi:10.3390/ijms20102446

350. Teixeira AF, Ten Dijke P, Zhu HJ. On-Target Anti-TGF-β Therapies Are Not Succeeding in Clinical Cancer Treatments: What Are Remaining Challenges? Front Cell Dev Biol 2020;8(605, doi:10.3389/fcell.2020.00605

351. Grainger DJ. Transforming growth factor beta and atherosclerosis: so far, so good for the protective cytokine hypothesis. Arterioscler Thromb Vasc Biol 2004;24(3):399-404, doi:10.1161/01.ATV.0000114567.76772.33

352. Petr Nachtigal and Jana Rathouska and Lenka Vecerova and Zbynek S. The Role of TGF-β and TGF-β Receptors in Atherosclerosis. In: Atherogenesis. (Sampath P. ed.) IntechOpen: Rijeka; 2012.

353. Nachtigal P, Rathouska J, Vecerova L, et al. The Role of TGF-β and TGF-β Receptors in Atherosclerosis. 2012.

354. Fernández-Ruiz I. Promising anti-IL-6 therapy for atherosclerosis. Nat Rev Cardiol 2021;18(8):544, doi:10.1038/s41569-021-00575-8

355. Ma J, Chen X. Anti-inflammatory Therapy for Coronary Atherosclerotic Heart Disease: Unanswered Questions Behind Existing Successes. Front Cardiovasc Med 2020;7(631398, doi:10.3389/fcvm.2020.631398

356. Soehnlein O, Tall AR. AIMing 2 treat atherosclerosis. Nat Rev Cardiol 2022;19(9):567-568, doi:10.1038/s41569-022-00755-0

357. Joffre J, Potteaux S, Zeboudj L, et al. Genetic and Pharmacological Inhibition of TREM-1 Limits the Development of Experimental Atherosclerosis. J Am Coll Cardiol 2016;68(25):2776-2793, doi:10.1016/j.jacc.2016.10.015

358. Zeng W, Wu D, Sun Y, et al. The selective NLRP3 inhibitor MCC950 hinders atherosclerosis development by attenuating inflammation and pyroptosis in macrophages. Sci Rep 2021;11(1):19305, doi:10.1038/s41598-021-98437-3

359. Qian Z, Zhao Y, Wan C, et al. Pyroptosis in the Initiation and Progression of Atherosclerosis. Front Pharmacol 2021;12(652963, doi:10.3389/fphar.2021.652963

360. Challet E. Minireview: Entrainment of the suprachiasmatic clockwork in diurnal and nocturnal mammals. Endocrinology 2007;148(12):5648-55, doi:10.1210/en.2007-0804

361. Fernandez DM, Rahman AH, Fernandez NF, et al. Single-cell immune landscape of human atherosclerotic plaques. Nat Med 2019;25(10):1576-1588, doi:10.1038/s41591-019-0590-4

362. Bray MS, Young ME. Diurnal variations in myocardial metabolism. Cardiovasc Res 2008;79(2):228-37, doi:10.1093/cvr/cvn054

363. Yanagihara H, Ando H, Hayashi Y, et al. High-fat feeding exerts minimal effects on rhythmic mRNA expression of clock genes in mouse peripheral tissues. Chronobiol Int 2006;23(5):905-14, doi:10.1080/07420520600827103

364. Oishi K, Uchida D, Itoh N. Low-carbohydrate, high-protein diet affects rhythmic expression of gluconeogenic regulatory and circadian clock genes in mouse peripheral tissues. Chronobiol Int 2012;29(7):799-809, doi:10.3109/07420528.2012.699127

365. Huang S, Jiao X, Lu D, et al. Recent advances in modulators of circadian rhythms: an update and perspective. J Enzyme Inhib Med Chem 2020;35(1):1267-1286, doi:10.1080/14756366.2020.1772249

366. Scherholz ML, Schlesinger N, Androulakis IP. Chronopharmacology of glucocorticoids. Adv Drug Deliv Rev 2019;151-152(245-261, doi:10.1016/j.addr.2019.02.004

Acknowledgements

This thesis couldn't have been done without the guidance and input of my Thesis director and boss, Prof. Dr. Dr. med. Oliver Soehnlein and my supervisor, Prof. Carlos Silvestre-Roig. Thanks a lot for believing in me, for the scientific guidance and for allowing me to grow professionally and personally by your side.

Furthermore, I'd like to thank all the members in the laboratories in the IPEK and in ExPat for your help and advice. Sanne, Laura, PC, thanks for your patience and your support during the long 24h experiments and for giving me the best start in my PhD that I could ask for.

And thanks to the people outside the lab that were by my side during this long 4 years. Thanks for standing me even when I couldn't stand myself.

Annex 1

Buffers prepared

Buffer name	Content
HANKs Buffer	1x Hank´s buffered salt solution (HBSS, Gibco) 0.06% BSA, 0.5 mM EDTA
Lysis buffer	150 mM NH4Cl, 10Mm KHCO3, 0.1 Mm EDTA. pH at 7.4
Digestion buffer	RPMI, 10% FBS (Thermo Fisher Scientific), 1.25 mg/mL liberase (Roche)
Blocking solution	6 ml PBS, 1% BSA + 3 drops horse serum (VECTA laboratories)

Enrichment analysis of oscillating genes in Apoe$^{-/-}$

Metabolism

Carbohydrates
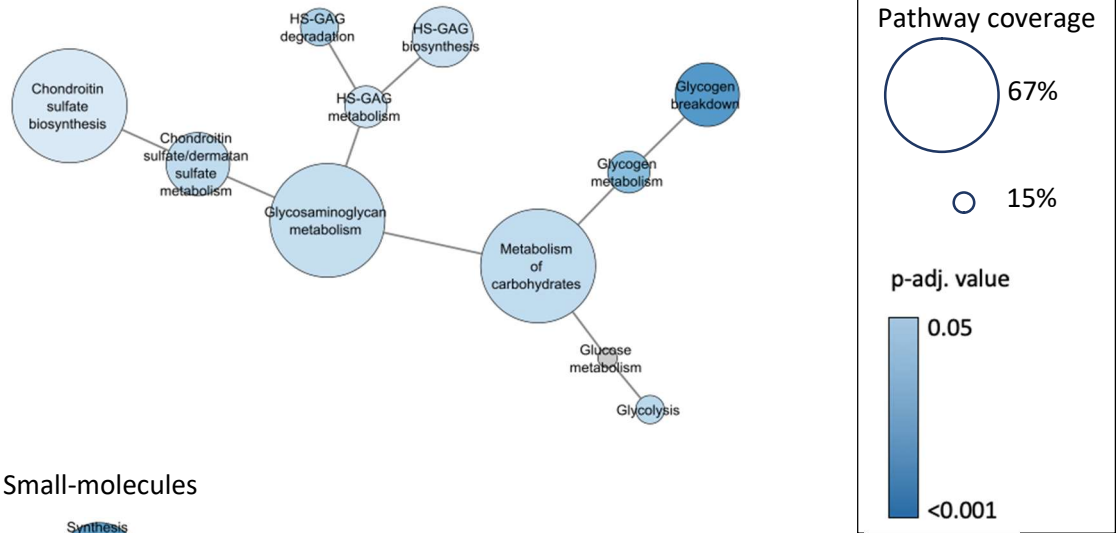
Small-molecules
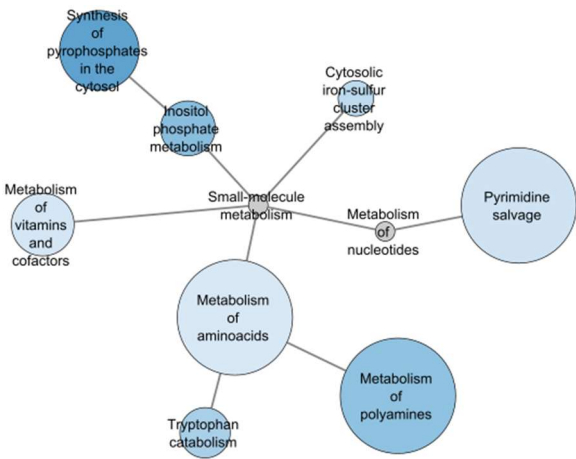
Integration metabolism
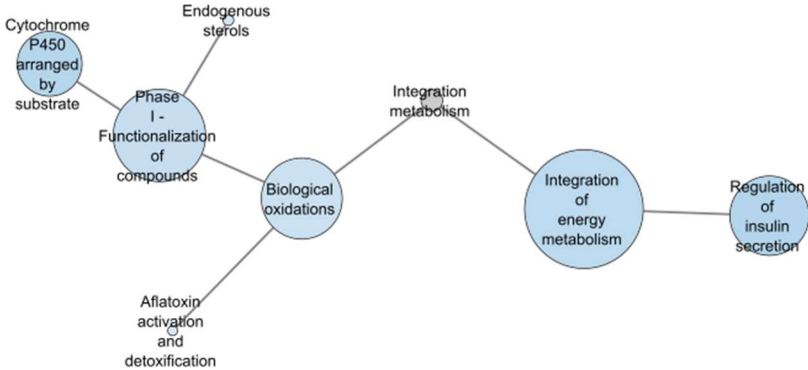
Proteins
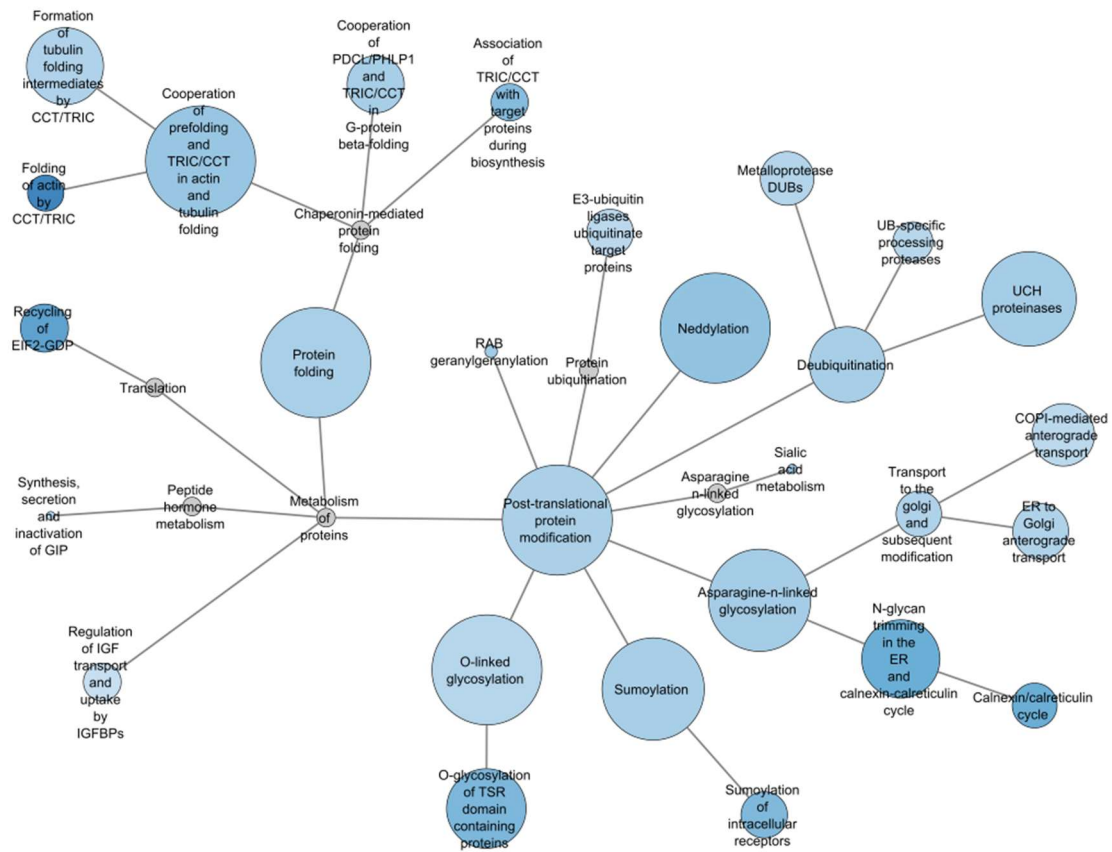
RNA
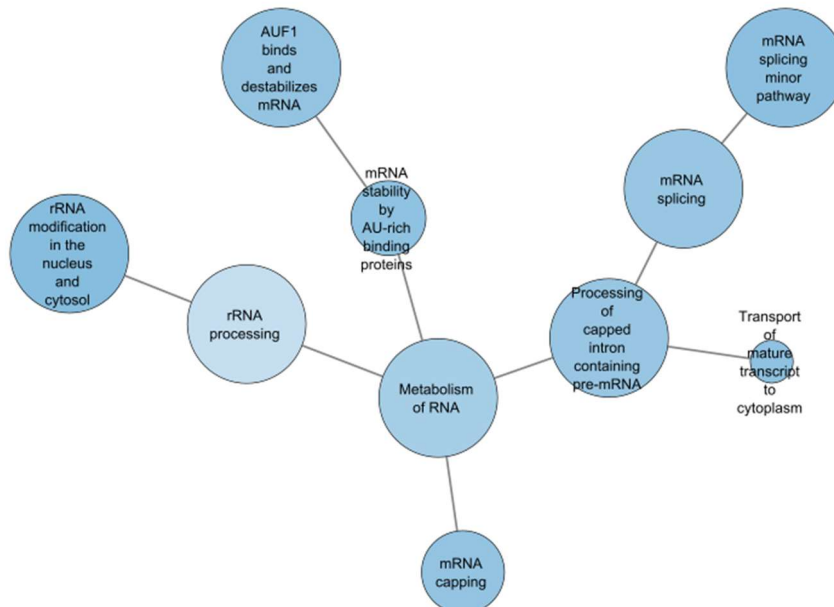
Lipids
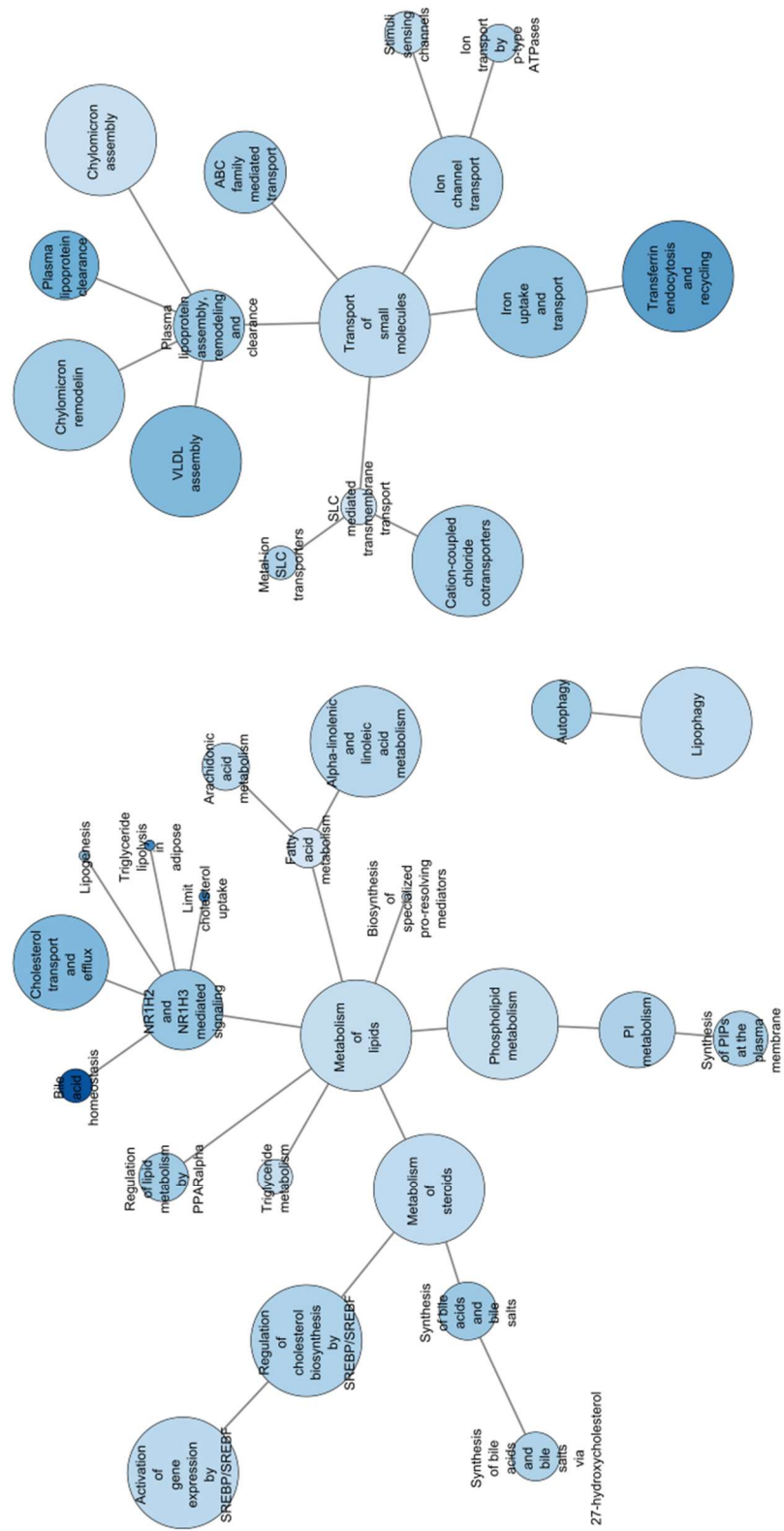
Signal transduction
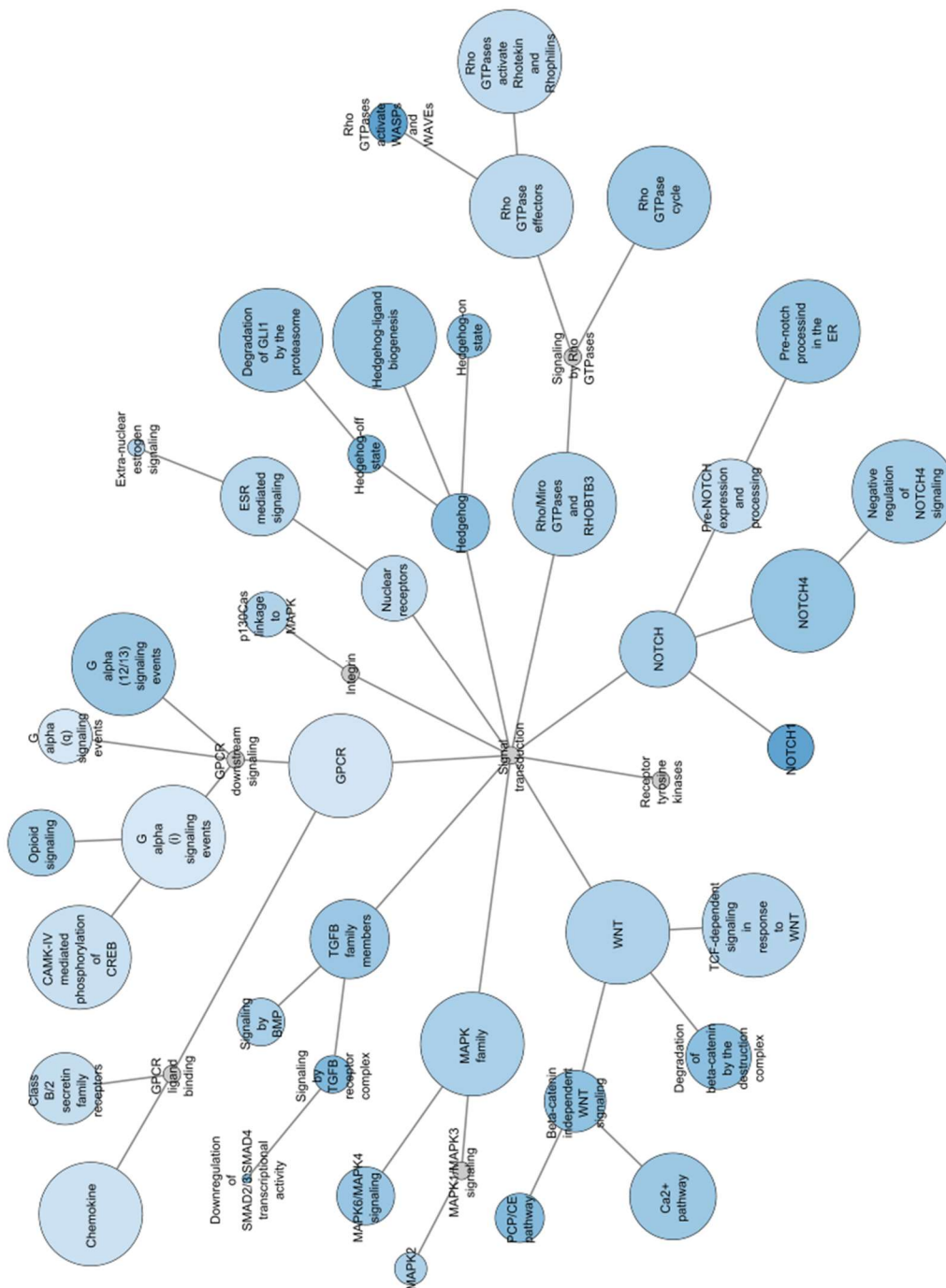
Cell cycle
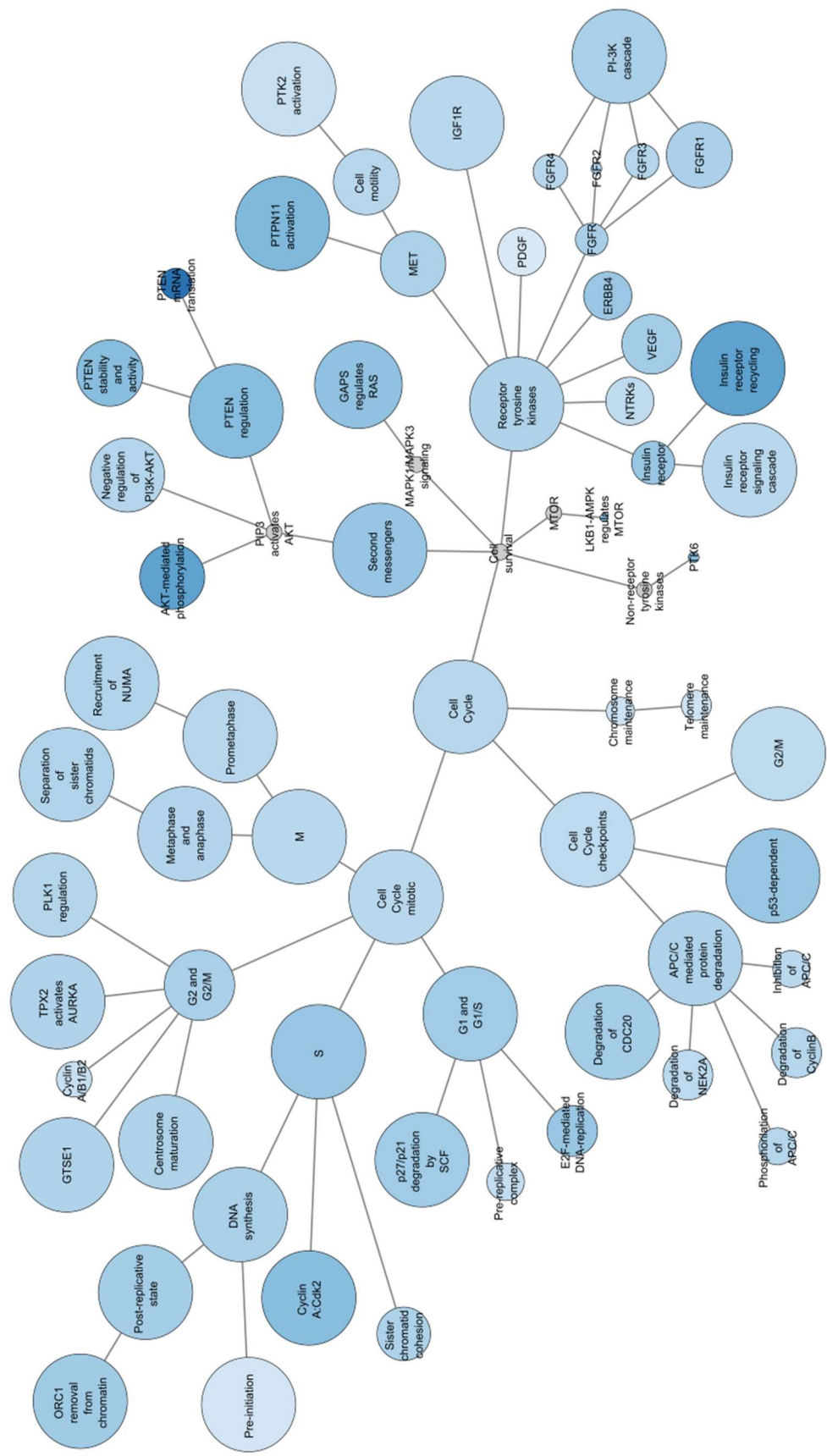
Programmed cell death
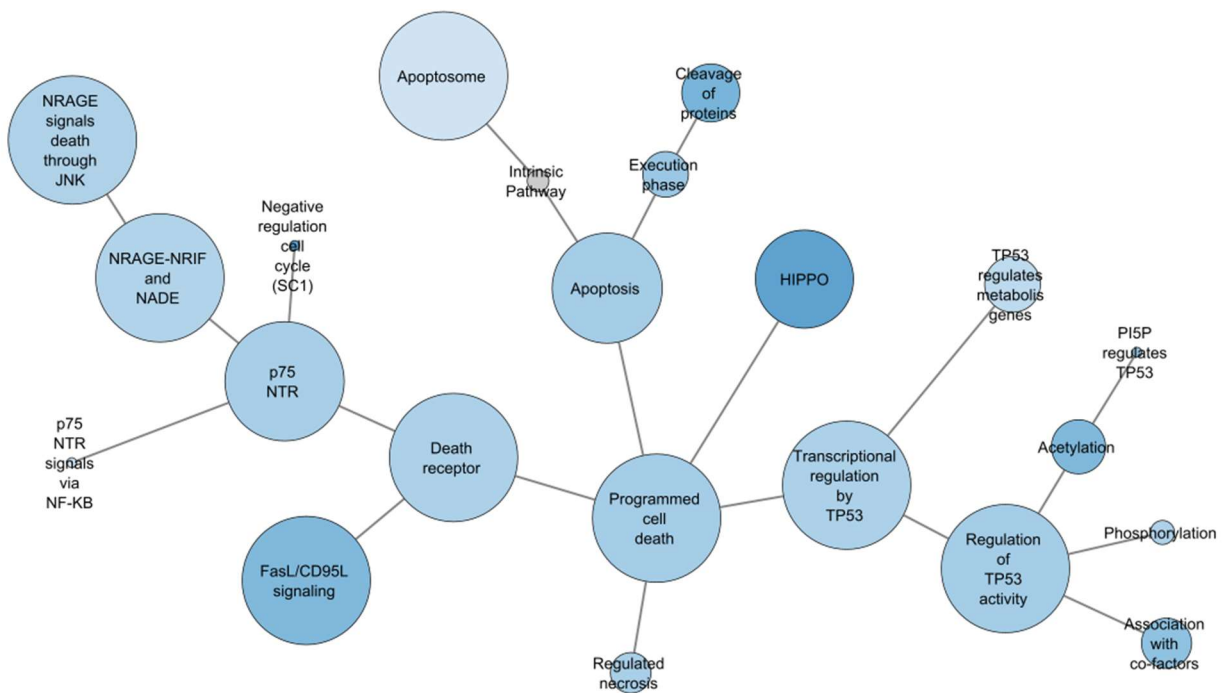
Generic transcription pathway
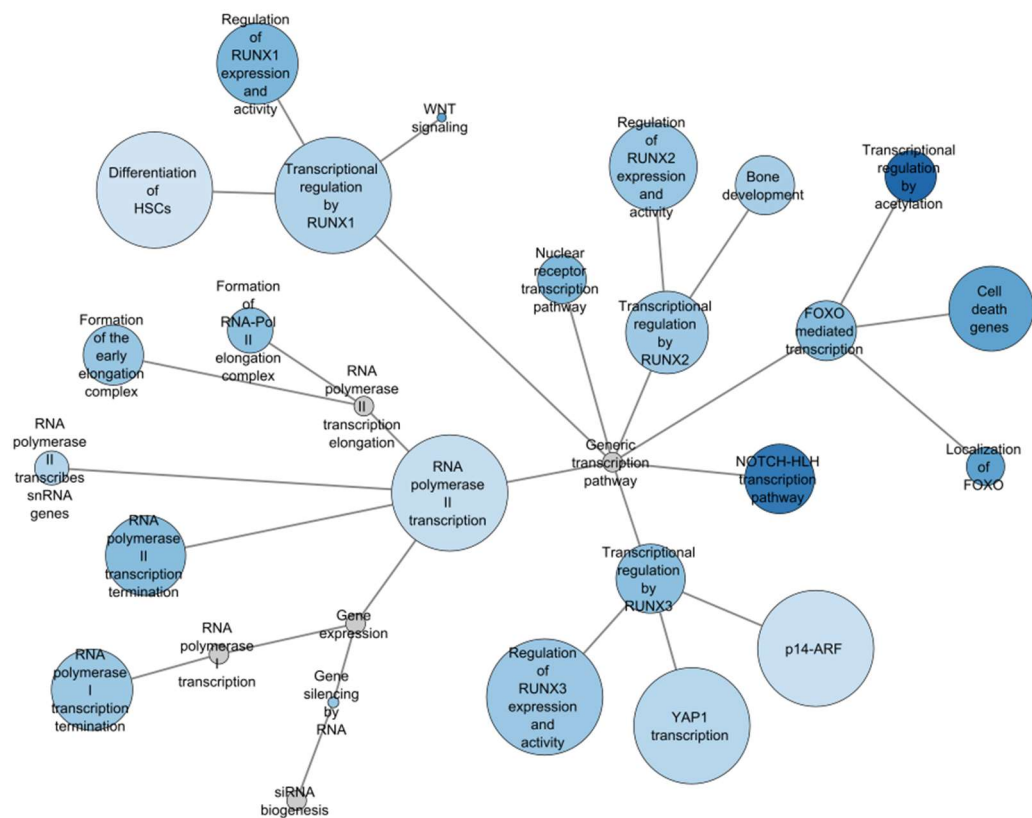
Immune system
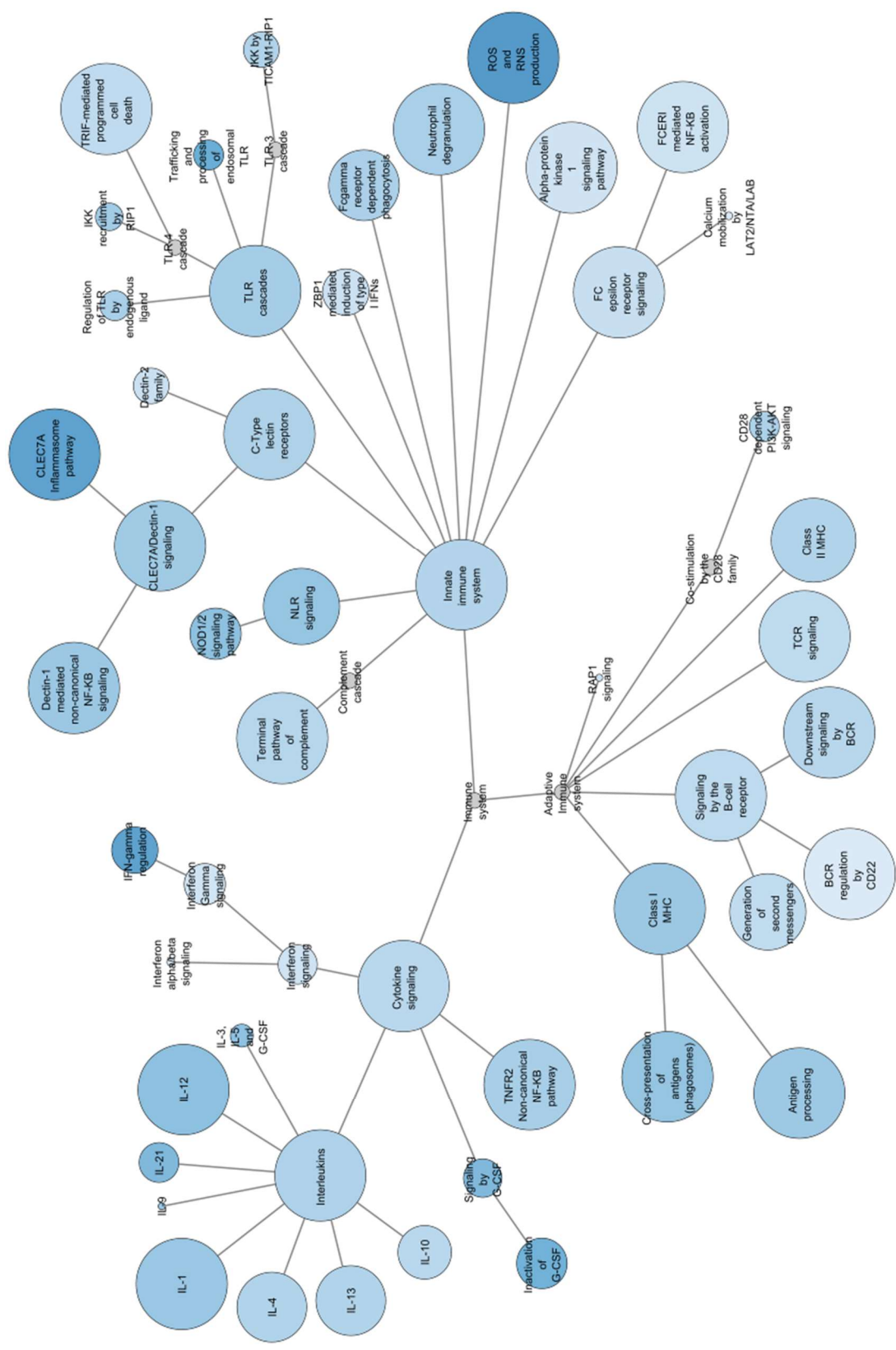
Nervous system

216
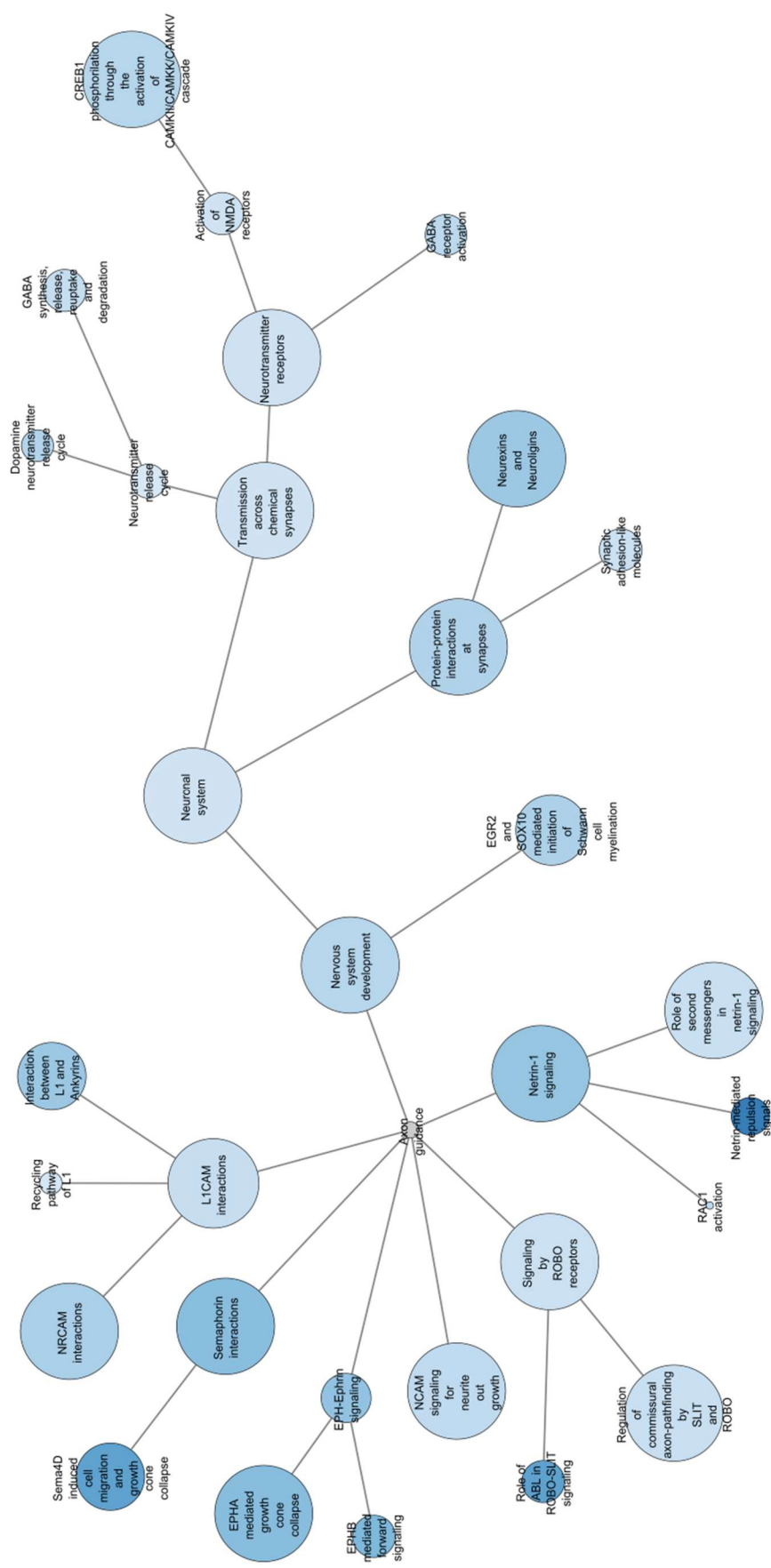
Cellular responses to stress
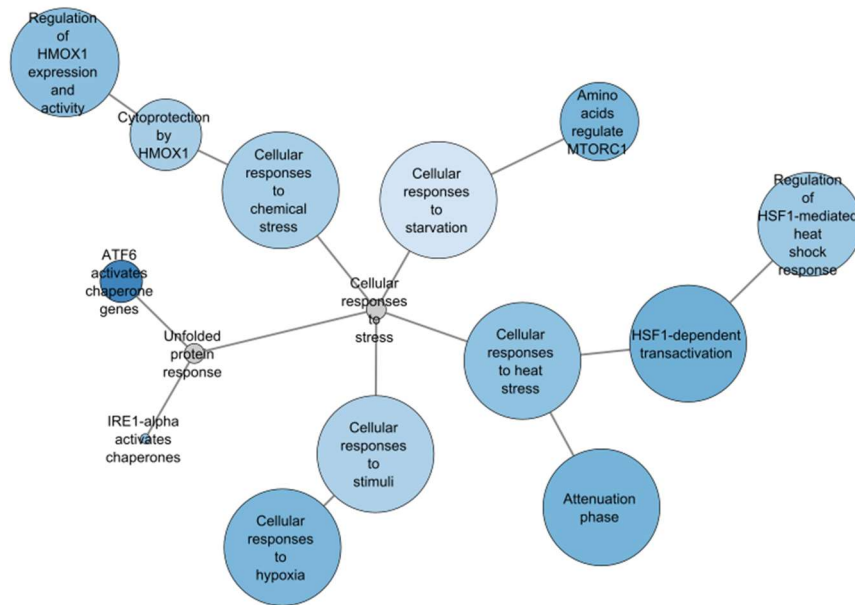
Vesicle-mediated transport
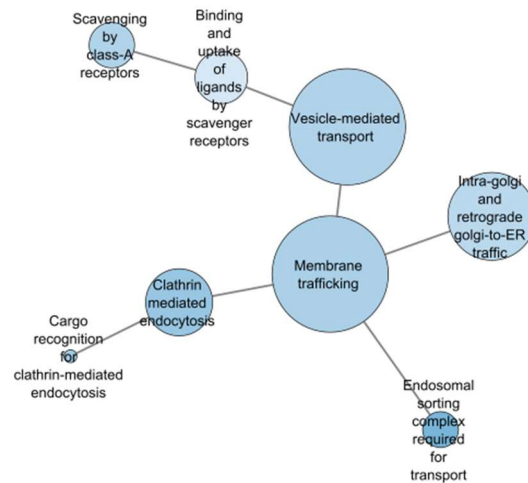
Cell-cell communication
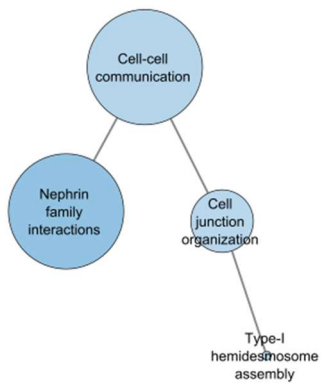
Hemostasis
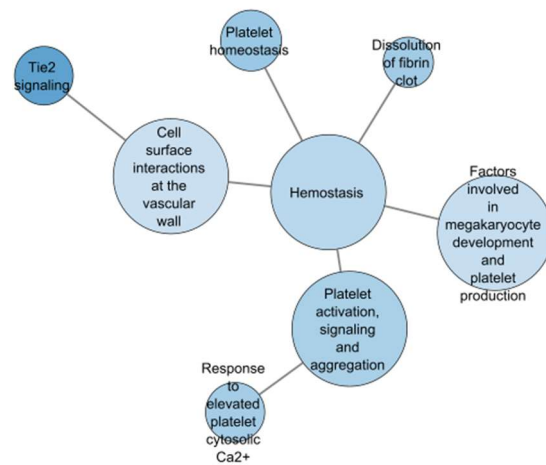
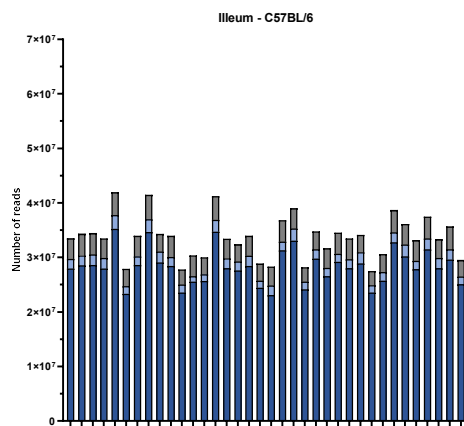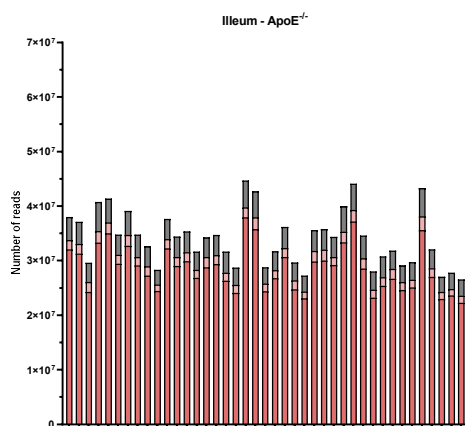**Organelle biogenesis and maintenace**
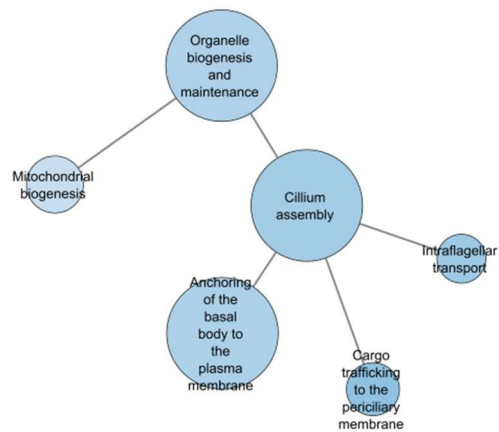
Chromatin organization
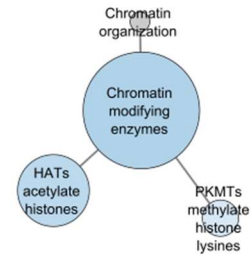
Circadian clock
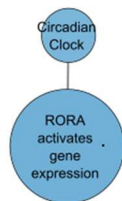
Muscle contraction
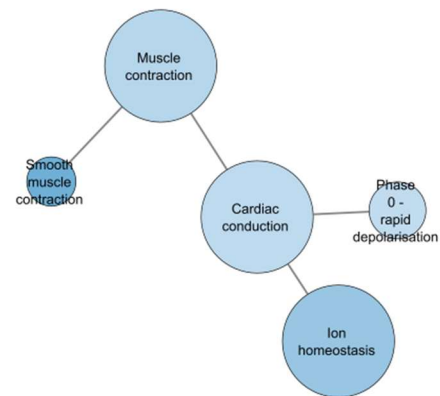
Extracellular matrix organization

RNA sequencing quality

Illeum - ApoE^{-/-}

Illeum - C57BL/6

Kidney - ApoE^{-/-}

Kidney - C57BL/6

Liver - ApoE^{-/-}

Liver - C57BL/6

Lung - ApoE^{-/-}

Lung - C57BL/6

220

Muscle - ApoE$^{-/-}$

Muscle - C57BL/6

Spleen - ApoE$^{-/-}$

Spleen - C57BL/6

WAT - ApoE$^{-/-}$

WAT - C57BL/6
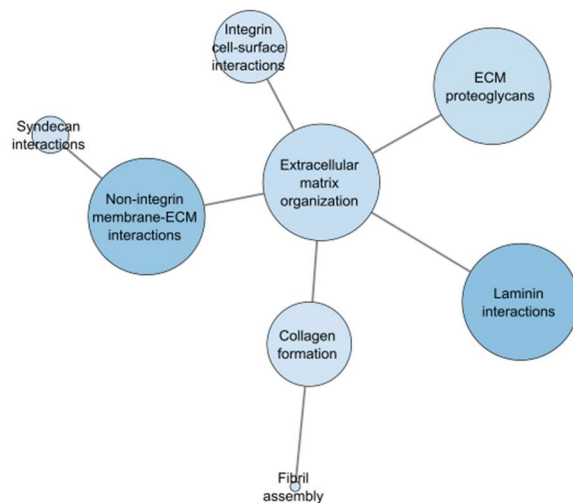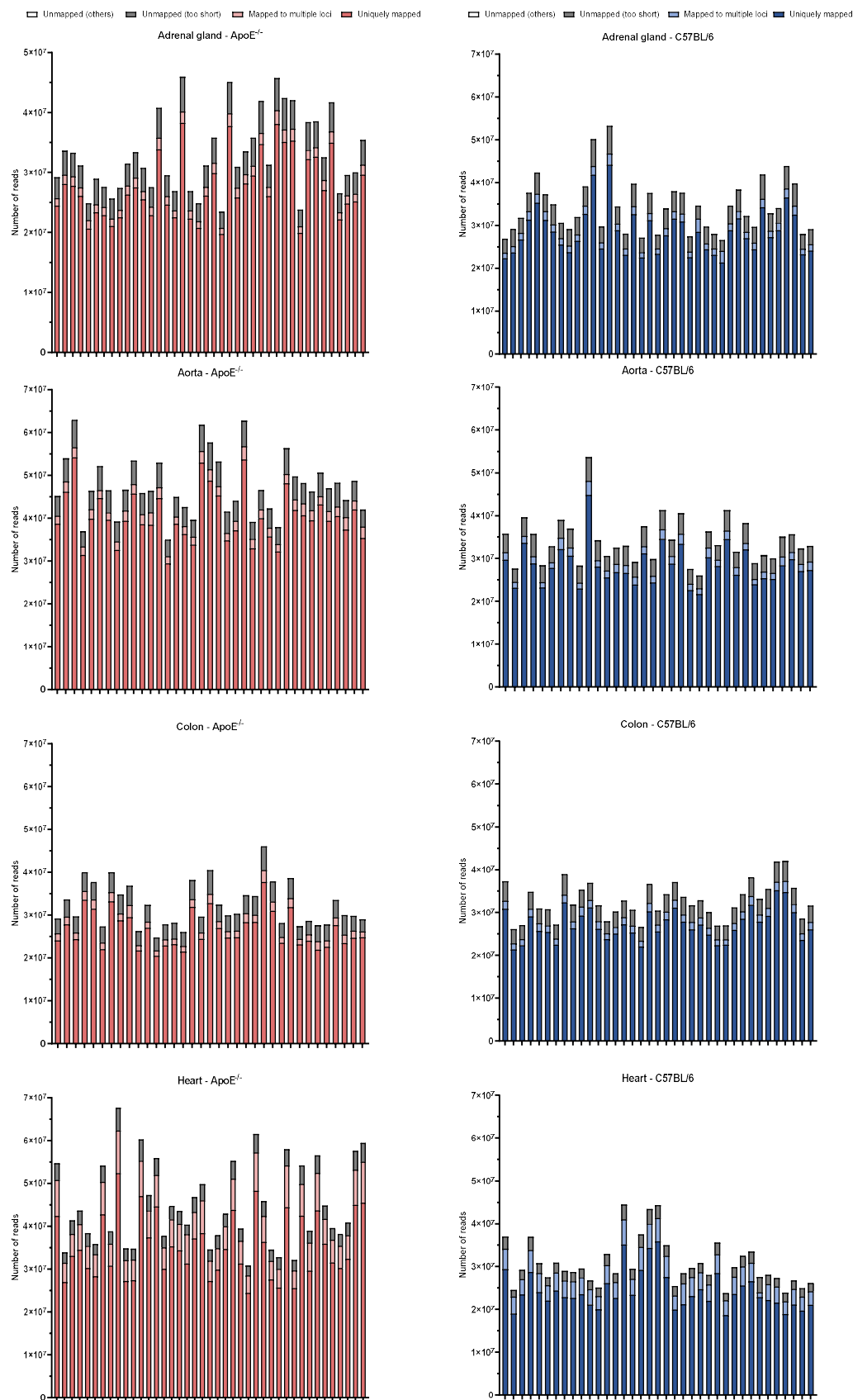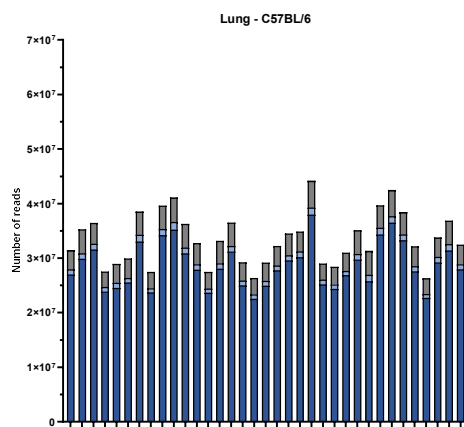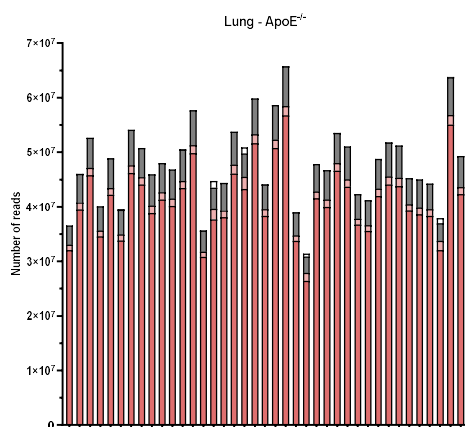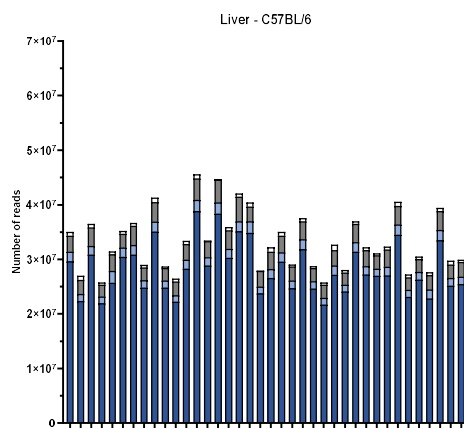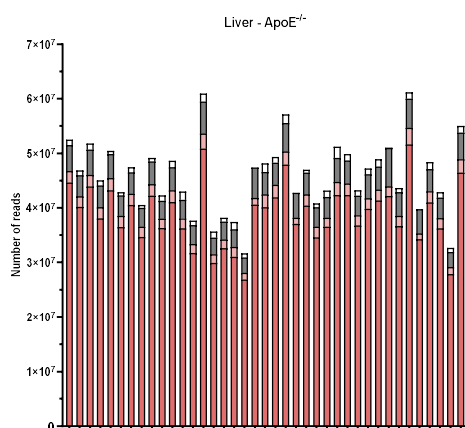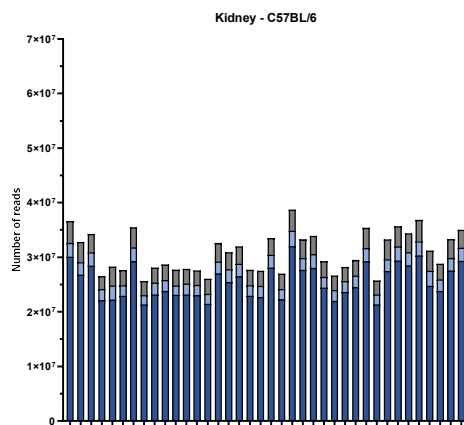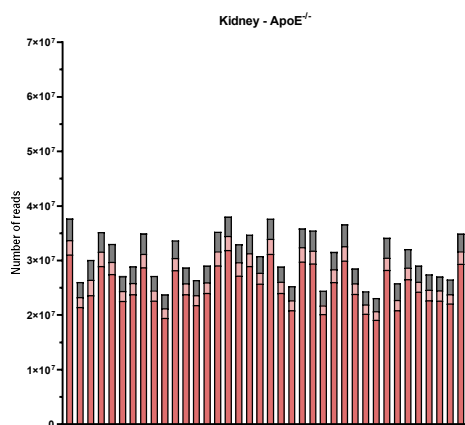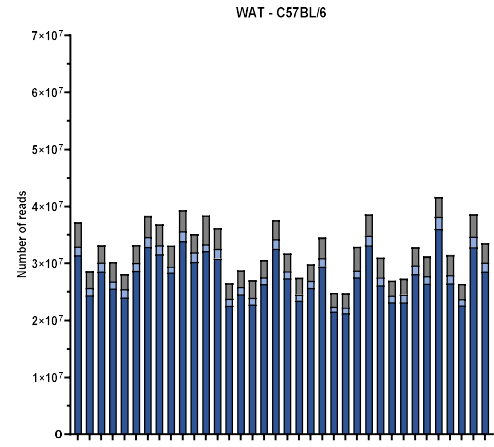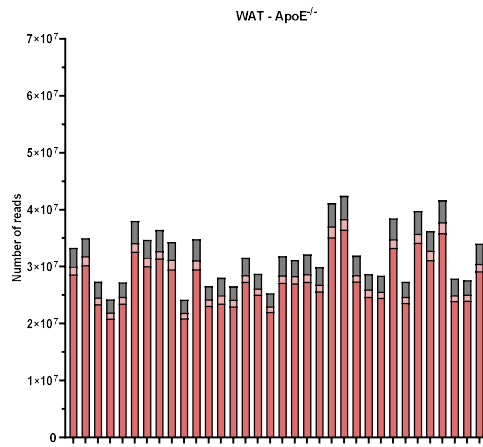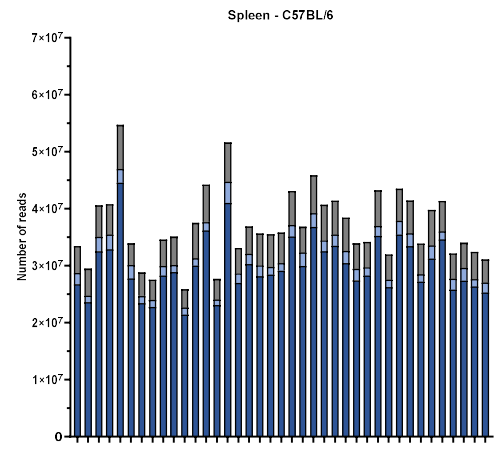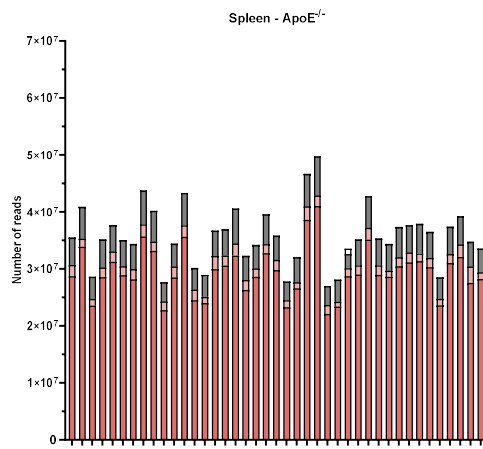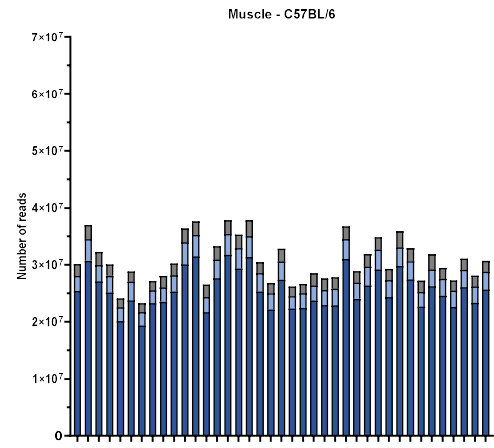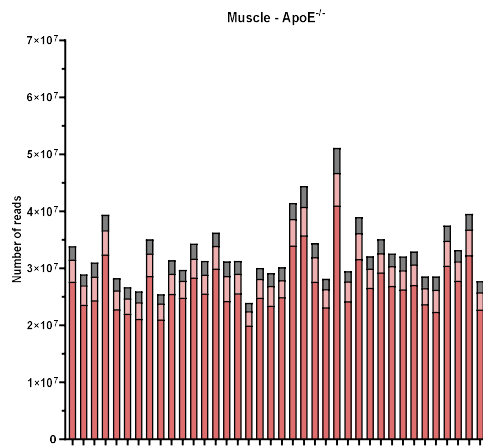
Affidavit

Borja Almarcha, Celia
Surname, first name

Center of Molecular Biology of Inflammation (ZMBE), Von Esmarch Str. 56
Street

48149 Münster Germany
Zip code, town

Germany
Country

I hereby declare, that the submitted thesis entitled

The rhythm of the plaque: Circadian oscillation in the advanced atherosclerotic lesion

is my own work. I have only used the sources indicated and have not made unauthorised use of services of a third party. Where the work of others has been quoted or reproduced, the source is always given.

I further declare that the dissertation presented here has not been submitted in the same or similar form to any other institution for the purpose of obtaining an academic degree.

Steinen, 20 October 2023
Place, date

Celia Borja Almarcha
Signature doctoral candidate

Confirmation of congruency between printed and electronic version of the doctoral thesis

Borja Almarcha, Celia

Surname, first name

Center of Molecular Biology of Inflammation (ZMBE), Von Esmarch Str. 56

Street

48149 Münster Germany

Zip code, town

Germany

Country

I hereby declare that the electronic version of the submitted thesis, entitled

The rhythm of the plaque: Circadian oscillation in the advanced atherosclerotic lesion

is congruent with the printed version both in content and format.

Steinen, 20 October 2023

Place, date

Celia Borja Almarcha

Signature doctoral candidate

Curriculum Vitae

Celia Borja Almarcha

Work experience

02/2019-09/2022	**Scientific Researcher.** Universitätsklinikum Münster, Karolinska Institute Stockholm, Ludwig-Maximilians-Universität München.
06/2018-12/2018	**Scientific Researcher.** Technical University of Munich
06/2017-02/2018	**Scientific Coordinator.** Bemygene Health Company
03/2017-06/2017	**Bioinformatics Intern.** Centro de Investigación Príncipe Felipe
07/2016-12/2016	**Internship Santander in SME.** Bemygene Health Company
01/2016-07/2016	**Academic program intern.** Instituto de investigación Sanitaria INCLIVA

Academy track

02/2019-	**PhD in Medical Research.** Ludwig-Maximilians-Universität München
11/2021-12/2022	**Master in Clinical Assays (M.Sc).** University of Sevilla
09/2016-06/2018	**Master in Bioinformatics (M.Sc).** University of Valencia
09/2012-06/2016	**Bachelor in Biology (B.Sc).** University of Valencia

List of publications

Pan C, Herrero-Fernandez B, **Borja Almarcha C**, et al.

Time-restricted feeding enhances early atherosclerosis in hypercholesterolemic mice.

Circulation (accepted for publication)